GDANSK UNIVERSITY OF TECHNOLOGY
FACULTY OF OCEAN ENGINEERING AND SHIP TECHNOLOGY
SECTION OF TRANSPORT TECHNICAL MEANS
OF TRANSPORT COMMITEE OF POLISH ACADEMY OF SCIENCES
UTILITY FOUNDATIONS SECTION
OF MECHANICAL ENGINEERING COMMITTEE OF POLISH ACADEMY OF SCIENCE

ISSN 1231 – 3998
ISBN 83 – 900666 – 2 – 9

Journal of

POLISH CIMAC

DIAGNOSTIC, RELIABILITY AND SAFETY

Vol. 3 **No. 2**

Gdansk, 2008

Science publication of Editorial Advisory Board of POLISH CIMAC

Editorial Office:

GDANSK UNIVERSITY OF TECHNOLOGY
Faculty of Ocean Engineering and Ship Technology
Department of Ship Power Plants
G. Narutowicza 11/12 80-952 GDANSK POLAND
tel. +48 58 347 29 73, e – mail: sek4oce@pg.gda.pl

This journal is devoted to designing of diesel engines, gas turbines and ships' power transmission systems containing these engines and also machines and other appliances necessary to keep these engines in movement with special regard to their energetic and pro-ecological properties and also their durability, reliability, diagnostics and safety of their work and operation of diesel engines, gas turbines and also machines and other appliances necessary to keep these engines in movement with special regard to their energetic and pro-ecological properties, their durability, reliability, diagnostics and safety of their work, and, above all, rational (and optimal) control of the processes of their operation and specially rational service works (including control and diagnosing systems), analysing of properties and treatment of liquid fuels and lubricating oils, etc.

All papers have been reviewed

ISSN 1231 – 3998
ISBN 83 – 900666 – 2 – 9

Printed in Poland

CONTENTS

Journal of POLISH CIMAC
Faculty of Ocean Engineering & Ship Technology
GDAŃSK UNIVERSITY OF TECHNOLOGY

EFFECT OF THE WORKING TIME OF COMRESSION-IGNITION ENGINE ON CHARGE LOSS

Karol Franciszek Abramek

Szczecin University of Technology
al. Piastów 19, 70-310 Szczecin, Poland
tel.: +48 91 4494811, fax.: +48 91 4494820
e-mail: karol.abramek@ps.pl

Summary

In the paper is presented a statistical analysis of the effect of compression-ignition engine working time on the phenomenon of exhaust gas scavenging into crankcase. Characteristics of the crankcase scavenging and pressure variations were made for the start-up speed of SB-3.1 one-cylinder compression-ignition engine as well as micrometric measurements of the cylinder liner were performed after a run of 549 hours of operation on engine test bed. Basing on the analysis of obtained measuring results, it was showed that measurement of exhaust gas scavenging and exhaust gas pressure in crankcase may be used for determination of engine run and life.

Key words: *scavenging, wear, piston, rings, cylinder*

1. Introduction

Piston with rings is a sliding seal of piston combustion engine working space. As the operational run increases, its units and cooperating parts are getting worn out. This wear brings about worsening of engine technical and operational indicators, the symptoms of which are: power drop, increase of lubricating oil consumption, increase of smokiness and toxic substance emission in exhaust gases, increase of fuel consumption, increase of noise level, difficulties in engine start-up and a considerable decrease of engine reliability. The most important factors that induce changes in shapes, dimensions, quality and properties of engine parts as well as worsening of engine operation properties are first of all tribological processes (friction and accompanying processes), considerable dynamic and heat loads of engine parts and corrosion, erosion and cavitation phenomena. Elements of the piston-rings-cylinder (PRC) system operate in particularly difficult conditions [1, 2, 7].

Determination of the reasons of most intensive wear in the PRC group has a decisive effect on the prolongation of engine operational time and run. As a rule, the wear of these elements determines the necessity of executing engine repair or taking it out of service. Therefore, this tribological pair is required to ensure failure-free operation of engine in as long time as possible and to not limit its usability by engine performance in this time [9]. The course of wear processes in the PRC group as well as its size and character depend on many factors, which can include physicochemical properties of material, quality of cooperating parts, size of unit pressures, speed of the relative displacement of elements, temperature of elements, quality of oil and thickness of oil film as well as course of combustion processes in the working space over piston.

In the PRC group, wear processes take place that are induced by friction phenomena and processes leading to destruction of the surface layer of frictional pair caused by mechanical

abrasion of surface irregularities, effect of intermolecular forces, local friction welding and disruption of the tops of surface irregularities (type I and II adhesion), micro-cutting, scratching and ridging caused by the presence of wear bodies and products within the areas of cooperating elements which act as abrasive material or clearly harder surface irregularities of one of the fricative bodies.

2. Description of wear processes in the PRC group

The PRC assembly is characterised by a large variation of the mutual speed between cooperating surfaces. Only in one working cycle there are periods when the relative speed of cooperating frictional pairs is too small for the fluid friction to occur. At that time, an interruption of the oil film occurs and it comes to direct contact of friction surfaces. Such a contact is accompanied by mechanical separation of material particles. Such a phenomenon can take place both in case of the dry friction and through a layer of lubricating oil. The friction surfaces contacting with each other get into contact, due to the effect of load, with the tops of surface irregularities which undergo plastic strain and then tacking bridges develop in result of adhesion. Mutual displacement of spot welded surfaces brings about the pulling of metal particles out of the bottom of metal surface layer with lower strength and their translocation onto the cooperating surface [6].

Separate group is the wear connected with material fatigue due to variable mechanical or heat loads. A result of the fatigue wear is surface layer flaking.

The PRC group is also exposed to corrosive destruction (chemical and electrochemical corrosion as well). Chemical corrosion occurs first of all in exhaust gas atmosphere, in particular at raised temperatures and in fluids, which can be fuels. In practice, a fuel composed of organic compounds containing carbon and hydrogen is applied to all engines with internal combustion. In this connection, a basic combustion product is water and carbon dioxide. In case of normal operation conditions, water vapour produced in combustion is condensed on very effectively cooled cylinder parts only. Condensation can occur only where the partial pressure of water vapour is higher from the saturation pressure, i.e. in places where the dew-point has been reached. In case of combustion products which do not contain sulphur, the dew-point at a pressure of 0.2 MPa is between 323 and 333 K and increases together with pressure buildup [8]. Decrease of the temperature of combustion products being found on cylinder walls or in piston ring ducts below the dew-point exerts a considerable influence on corrosive wear of all PRC assembly elements. Particularly large influence on the wear is exerted by sulphur contained in fuel and air. This sulphur undergoes combustion producing sulphur dioxide SO_2, with part of SO_2 undergoing subsequently a change into SO_3. Sulphur compounds can work corrosively in different way. Three temperature areas of the effect of sulphur compounds produced during fuel combustion are conventionally accepted. The first zone corresponds to intensive electrolytic corrosion occurring at water vapour condensation. The second zone is characterised by the lowest wear and corresponds to temperatures at which water vapour condensation does no longer occur. The third zone corresponds to high-temperature corrosion. Intensive increase of high-temperature corrosion occurs only when temperature of the surface of elements exceeds 573 K. Since such high temperatures do not occur in piston engines on friction surfaces, therefore this corrosion is of minimal importance. Out of the PRC group, only some areas of the piston head can be subject to it. The presence of sulphur compounds, SO_2 and SO_3, in combustion products increases the dew-point by 80 to 115 K above the dew-point of pure water vapour. This is why sulphurous acid H_2SO_3 and sulphuric acid H_2SO_4 are formed due to dissolution of SO_2 and SO_3 in condensate. The corrosive effect of sulphuric acid depends on its concentration. The most dangerous is its concentration ranging from 20 to 60%. Attention should be paid to the fact that corrosive wear is also dependent on engine high-speed because water vapour condensation process takes place not

immediately but requires some time. This causes that considerably less condensate is formed in high-speed engines than in low-speed ones, where in addition it stays considerably longer.

With the intensive flow of fluids or exhaust gases in the form of scavenging through clearances in the PRC system, also erosion processes take place that leave marks on metal surfaces [6].

3. Formulation of research problem

The presented wear processes occurring in the PRC assembly are inevitable. Nevertheless, the most intensive is the wear induced by friction phenomena and processes [5]. Material losses in the cooperating parts cause development of greater and greater clearances between PRC elements. This favours an increase of the exhaust gas scavenging into crankcase, destruction of oil film layer and development of more intensive erosion processes. Therefore, there is a large probability of the intensification of wear phenomena.

In principle, many authors have been examining wear processes in the PRC group [4, 6, 7, 8, 9, 12]. However, there is not much studies directly connected with the loss of medium in the form of exhaust gas scavenging into crankcase through ring sealing assembly [1, 5, 12], hence follows the interest of the author in statistical description of the effect of wear processes and cylinder liner wear size on the value of exhaust gas scavenging intensity. In particular, there are not any results of scavenging tests for the speed of engine crankshaft during start-up. Also an attempt was taken up to explain whether measurements of exhaust gas scavenging into crankcase could be used for evaluation of the technical condition of the PRC kinematic pair and, in particular, whether they are correlated with cylinder liner wear and engine operational run.

In order to evaluate and examine changes in the course of wear intensity in the PRC group and their effect on the loss of medium, studies were carried out consisting in measurement of the intensity of exhaust gas scavenging into crankcase for the start-up speed for a warm (lubricating oil temperature of 333 K) and cold engine (285 K), every ninth hour after replacement of cylinder liner, piston and rings, and for a worn-out SB-3.1 engine. Measurement of the diameters of piston, cylinder liner and rings for new and worn-out elements after the service life eliminates an undesirable effect of the measurements of these values during the service life which can affect engine operation parameters and medium loss. The scavenging values given are arithmetic mean from three measurements. Diameter measurements were taken with an inside micrometer caliper in horizontal planes being distant from cylinder liner end face by 20 mm, which corresponded to the piston position in the upper dead centre (UDC). It is well-known that circularity of cylinder becomes deteriorated in result of wear and resembles an oval. Its larger diameter (measured in the B-B plane) corresponds to a plane perpendicular to the axis of engine crankshaft (it results from the dynamics of crankshaft-pistons-connecting rods system), while a smaller one (measured in the A-A plane) occurs in a plane parallel to the axis of engine crankshaft. A clearance that develops then between a piston and rings is the main reason of scavenging.

4. Test results

Test results for cylinder liner micrometric measurements in the function of operational run for a run of 549 hours worked in engine test bed are presented in Table 1.

Tab. 1. Test results of micrometric measurements for SB-3.1 engine

Measurement direction	l_1=20 [mm]		
	Before test	After test	Wear [μm]
A-A	-4	+21	25
B-B	-2	+39	41

It can be seen that cylinder liner wear processes are not the same in each plane. Larger wear occurs in the plane perpendicular to the axis of engine crankshaft since there are larger normal strengths occurring in this plane that have effect on cylinder liner and induce larger unit pressures and more intensive action of wear processes through friction.

Examination of the scavenging characteristics for the start-up speed (i.e. for engine crankshaft speeds obtained with starter drive) was performed for lubricating oil temperature of 333 K, determining it as a warm engine, and for temperature of 285 K, determining it as a cold engine. Dependence of the scavenging intensity on engine operational run, expressed in operation hours on engine test bed, was obtained using a scavenging intensity test bench presented on Fig. 1 designed and made at the Department of Automotive Vehicle Operation of the Szczecin University of Technology.

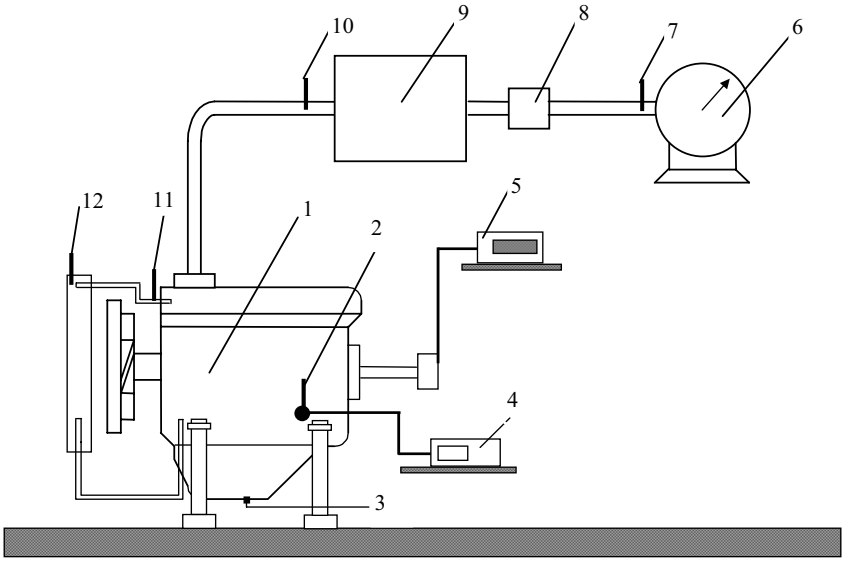

Fig. 1. Diagram of a test bench for examining exhaust gas scavenging into crankcase [3]
1 – tested engine, 2 – crankcase exhaust gas concentration pressure meter, 3 – oil temperature meter, 4 – oil pressure meter, 5 – engine-speed meter, 6 – laboratory gas meter, 7 – exhaust gas temperature meter, 8 – filter, 9 – equalising tank, 10 – exhaust gas temperature meter, 11 – engine port water temperature mete, 12 – cooler water temperature meter

Measurement of the scavenging intensity consisted in that that measuring instrument (6) was connected to the crankcase of tested engine (1) by means of a rubber hose inserted into the oil inlet hole. The pressure produced in crankcase during engine operation induced a flow of exhaust gases into the equalising tank (9), which was filled with steel chips in order to eliminate pulsation and pre-treat exhaust gases from oil mist. Thereafter, exhaust gases went through a filter (8) where they were thoroughly cleaned and went into a laboratory gas meter (6). Additional device, i.e. crankcase exhaust gas concentration pressure meter (2), served as control of the resistance of exhaust gas flow, showing the value of pressure concentration in crankcase [3].

Figure 2 presents the characteristics of exhaust gas scavenging in the function of operational run expressed in operation hours on engine test bed for warm engine, while that for cold engine is presented on Fig. 4.

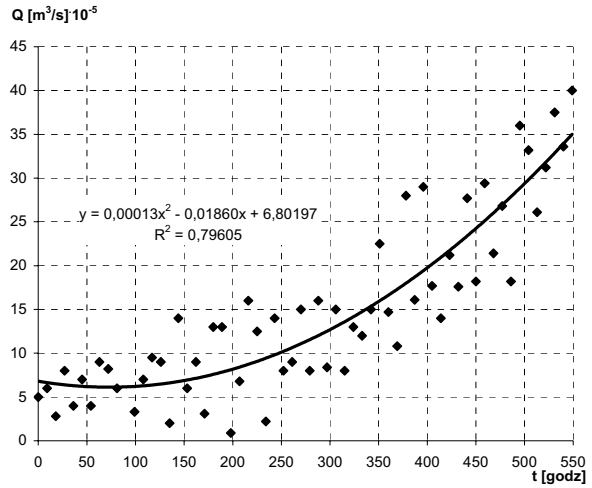

Fig. 2. Dependence of the intensity of exhaust gas scavenging into crankcase on the operational run of warm engine SB-3.1 operated on engine test bed for the start-up speed

Figures 3 and 5 present the dependencies of exhaust gas pressure in crankcase on the operational run of engine SB-3.1 for warm and cold engine, respectively.

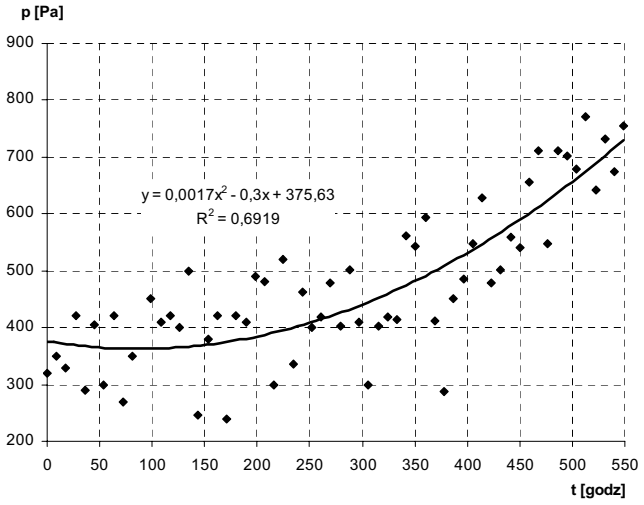

Fig. 3. Dependence of the pressure of exhaust gas in crankcase on the operational run of warm engine SB-3.1 operated on engine test bed for the start-up speed

It can be seen that the value of lost charge intensity in the form of exhaust gas scavenging into crankcase and of exhaust gas concentration changes and increases in result of operational wear (run). This is caused by that that during operation the wear of piston-rings-cylinder group elements increases and a free section, through which a loss of charge takes place in the form of exhaust scavenging, enlarges. The diameter of cylinder section increases, as well as clearances in the joints of respective piston rings (piston packing rings and piston oil control ring) [12].

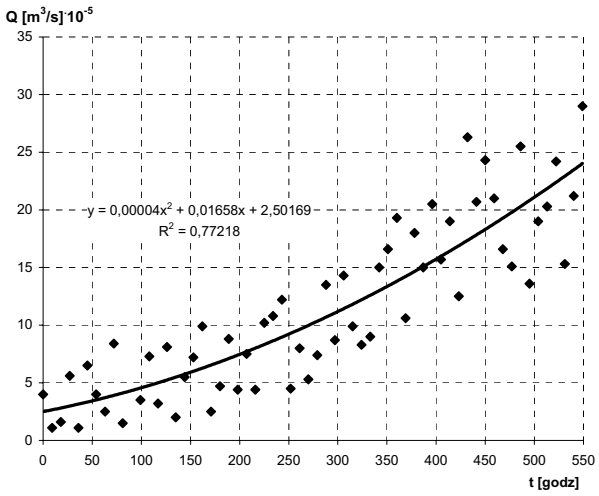

Fig. 4. Dependence of the intensity of exhaust gas scavenging into crankcase on the operational run of cold engine SB-3.1 operated on engine test bed for the start-up speed

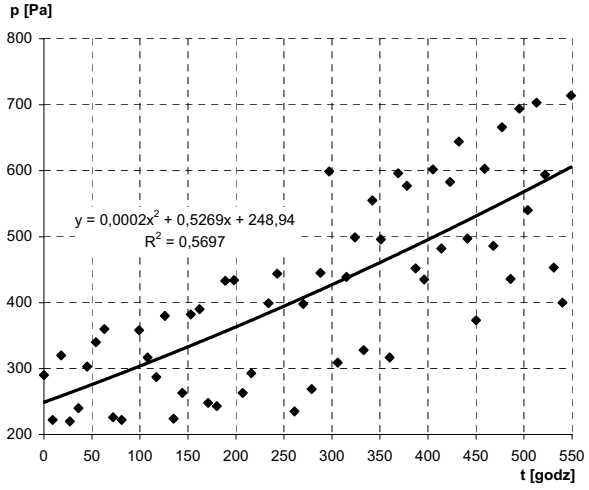

Fig. 5. Dependence of the pressure of exhaust gas in crankcase on the operational run of cold engine SB-3.1 operated on engine test bed for the start-up speed

When analysing the obtained results of exhaust gas scavenging measurements for the start-up speed and cylinder liner wears due to operation of SB-3.1 engine on engine test bed, it can be observed that the amount [quantity] of exhaust gases scavenged into crankcase increases in result of the PRC system wear. The study showed that evaluation of the technical condition of piston engine, in particular of the PRC kinematic pair, can be accomplished by measuring the intensity of exhaust gas scavenging into engine crankcase for the start-up speed. It was observed that characteristics of the intensity of exhaust gas scavenging for warm engine reaches larger values. This is due to the effect of changes in lubricating oil density and its effect on the caulking of the PRC space [2, 5].

Conclusions

When evaluating the usefulness of exhaust gas scavenging measurements for forecasting the service life, the fact should be taken into consideration that examination of medium losses ought to be correlated with operational run. The following coefficients of correlation were obtained: r^2=0.796 for warm engine and r^2=0.772 for cold one. It is well-known by experience that achievement of such an appreciable value of the coefficient of correlation in case of diagnostic tests is rather difficult and requires great repeatability of measurements conditions. Slightly worse were measurements of the concentration of exhaust gases in crankcase. The following results were obtained for exhaust gas concentration: r^2=0.691 for warm engine and r^2=0.569 for cold one. In both cases, it is better to carry out examinations for warm engine because coefficient of correlation reaches then higher values. Taking into account difficulties connected with taking measurements of exhaust gas scavenging in relation to those of exhaust gas pressure in crankcase, the pressure measurement itself seems to be reasonable as well. However, it has been observed by experience that all leaks have greater effect on measurement "falsification" and error as far as the pressure in crankcase is concerned than on exhaust gas scavenging intensity error.

The presented dependencies of exhaust gas scavenging intensity (Figs 2 and 4) are a second order polynomial and a change in the value of exhaust gas scavenging illustrates the 2nd period of changes (normal wear period) being described by the Lorenz curve.

Also the dynamics of signal change in both cases is possibly large and can be calculated from the following formula [4]:

$$d_p = \frac{X_m - X_o}{X_o} \tag{1}$$

where:
X_m – signal boundary value, indicating the necessity of performing a repair or taking the object out of service; in our case it is a run of 549 hours on engine test bed,
X_o – signal initial value, characterising a new object after termination of the running-in period.

For exhaust gas scavenging measurements, the value of signal change dynamics for warm engine is $d_p = \frac{40-5}{5} = 7$, whereas for cold one $d_p = \frac{25-2.5}{2.5} = 9$.

Slightly lower values are reached by signal change dynamics for the measurements of exhaust gas pressure in crankcase. They are as follows: for warm engine $d_p = \frac{750-350}{350} = 1.1$, whereas for cold one $d_p = \frac{600-250}{250} = 1.4$.

Summing up, it is possible to conclude about wear [and tear] degree, and the same about the run of piston combustion compression-ignition [Diesel] engine, basing on the examination of exhaust gas pressure in crankcase. The advantage of measurements of exhaust gas scavenging into crankcase is that that they are carried out on actually operating engine as well as that they can be performed within the whole range of engine crankshaft rotational speed. This gives the full picture of PRC assembly cooperation quality and may serve as indication of leak-tightness loss for a specific range of engine rotational speed.

References

[1] Abramek, K. F., *Wpływ warunków pracy pierścieni tłokowych na ilość gazów przedostających się do skrzyni korbowej, Zeszyt naukowy nr 1: Eksploatacja Silników Spalinowych,* Wydawnictwo Katedry Eksploatacji Pojazdów Samochodowych Politechniki Szczecińskiej, Szczecin 2000.

[2] Abramek, K. F., *Effect of scavenging of gases to crankcase on actual compression ratio during start-up,* Problems of Applied Mechanics International Scientific Journal, Georgian Committee of The International Federation For The Promotion of Mechanism And Machine Science, Tbilisi, Nr 2(19)/2005.

[3] Abramek, K. F., *Effect of modification of sealing rings on starting properties of compression-ignition engines,* Международный Сборник Научных Трудов, Издательство Калининградский Государственный Технический Университет, Kaliningrad 2005.

[4] Abramek, K. F., *An attempt at an analytical description of blow-by intensity to a crankcase,* Teka Komisji Motoryzacji i Energetyki Rolnictwa Polskiej Akademii Nauk Oddział w Lublinie, Lublin, Vol. VII, 2007.

[5] Abramek, K. F., *The study of crankcase exhaust gas blow-up phenomenon,* Silniki Spalinowe, SC1 2007.

[6] Janecki, J., Gołąbek S., *Zużycie części i zespołów pojazdów samochodowych,* Wydawnictwa Komunikacji i Łączności, Warszawa 1974.

[7] Kozaczewski, W., *Konstrukcja grupy tłokowo-cylindrowej silników spalinowych,* Wydawnictwa Komunikacji i Łączności, Warszawa 2004.

[8] Merkisz, J., Tomaszewski, F., Ignatow, O., *Trwałość i diagnostyka węzła tłokowego silników spalinowych, wybrane zagadnienia,* Wydawnictwo Politechniki Poznańskiej, Poznań 1995.

[9] Niewczas, A., *Trwałość zespołu tłok-pierścienie tłokowe-cylinder silnika spalinowego,* Wydawnictwo Naukowo-Techniczne, Warszawa 1998.

[10] Serdecki, W., *Wpływ pierścieni uszczelniających na kształtowanie filmu olejowego na gładzi cylindrowej silnika spalinowego,* Wydawnictwo Politechniki Poznańskiej, Poznań 1990.

[11] Smoczyński, M., Sygniewicz, J., *Przemieszczenia uszczelniającego pierścienia tłokowego w rowku pierścieniowym tłoka,* Journal of KONES Vol. 2, No 1, Warszawa-Poznań 1995.

[12] Telatyński, R., *Diagnozowanie zużycia silników z zapłonem samoczynnym na podstawie pomiaru intensywności przedmuchów spalin do skrzyni korbowej,* Prace Naukowe Politechniki Szczecińskiej, Zeszyt nr 439, Szczecin 1991.

Journal of POLISH CIMAC

Faculty of Ocean Engineering & Ship Technology
GDAŃSK UNIVERSITY OF TECHNOLOGY

APPLICATION OF AN EXHAUST SIGNAL FOR DIAGNOSING A SHIP BOILER

Andrzej Adamkiewicz

Szczecin Maritime Academy
Faculty of Mechanical Engineering
Institute of Technical Operation of Marine Power Plants
Wały Chrobrego 1-2, 70-500 Szczecin, Poland
e-mail: andrzej.adamkiewicz@am.szczecin.pl

Janusz Fydrych

Euro Africa Shipping Lines Co Ltd., Szczecin

Abstract

This study presents causes of faults and break-downs of ship steam boilers. The so-far used methods of their operation control based ona thermal-flow diagnostic signal have been discussed. The need to apply an exhaust signal for boiler diagnosing has been justified. A method of determining its parameters has been described. Thermal-flow clues indicating the need to start the boiler diagnosing process and an example of operational decision making based on the measured parameters of the exhaust signal (practical algorithm for a chosen boiler) has been presented. Utilitarian role of this signal in ship steam boiler operation, not only due to its pro- ecological value, has been indicated.

Keywords:. *steam boiler, diagnostic signal, fault, emission, technical condition*

1. Introduction

Auxiliary ship boilers produce steam to feed all other receivers apart from the main power system. They are installed both on motor ships and on steam ships. Contemporary auxiliary ship boilers run solely on liquid fuels, products of petroleum distillation. Boiler fuels contain: carbon< (85-90)%, hydrogen (10 –12)%, sulphur (0.6-2)%, oxygen and nitrogen 0.5% and other impurities.

In the process of complete fuel burning, oxidation of combustible particles takes place, and as a result of an exothermic reaction the following are emitted: from carbon – CO2 (carbon dioxide), from hydrogen – H2O (water), from sulphur – SO2 (sulphur dioxide), in the gas form or as smoke. The residuals as sediments, which can be corrosive and may retard heat penetration, may partly remain in the boiler. Nitrogen and oxygen in the exhaust come from the air supplied to the furnace and also to a small extent from the fuel. [4,6,7].

When fuel burns with insufficient amount of supplied air the exhaust apart from CO2 contains also CO and unburned carbohydrates, which could be still oxidized However, burning process outside the combustion chamber is more difficult due to too low temperatures and insufficient amount of oxygen or/and insufficient amount of combustible components in the mixture.

Noxious exhaust products from auxiliary ship boilers present a real threat to maritime environment (especially when the ship is in harbours, shipyards or sailing in coastal waters) and for the boilers themselves. Exhaust from ship fuels i.e. CO, SOx and NOx have a destructive influence on the technical condition of ship boilers [1].

Some compounds from the exhaust, during operation, bring about typical destructive effects on the boiler technical condition. A characteristic one is a degradation of the technical condition of the heat exchange surface (heated) of boilers both on the side of exhaust and water. It is the consequence of corrosive processes and formation of sediments on surfaces in contact with exhaust products and with water from the boiler [1]. A specific quality of boilers as technical objects is the occurrence of faults of the same type simultaneously in several elements. There are the following, listed in the order of frequency of their appearance:

– formation of sediments impairing heat exchange and consequently the efficiency of the boiler;
– erosion, corrosion and cavitation being the result of water impurity, non-designed operation states and non-ideal construction of boiler elements;
– leakages;
– insulation faults;
– faults of oil and water pumps.

So far ship steam boilers have operated according to the scheduled-preventive (statistic) strategy, where the dates of servicing are fixed for certain points of their operation. Observation of these dates is supervised by classification societies. However, this strategy does not take into account non-scheduled servicing being the consequence of haphazard events, faults and break-downs [2].

This situation favours the application of two differing operational tactics: finding the faults and later their origins and a way to remove them.

2. Thermal-flow diagnostics in recognizing boiler faults

Sediment formation, soot on the exhaust side and scale on the water side is a particular fault which develops evolutionally and it results in a significant number of boiler faults and break-downs. Thus, an early recognition of too intensive sedimentation of exhaust products and scale is very important. It is also crucial to have reliable diagnostic methods which do not require interrupting boiler operation.

The sediments forming on heat exchange surfaces create an additional thermal resistance. It is due to low heat conductivity of oil layers, scale and exhaust sediments (in comparison to conductivity of metals). [4,6,7]. Deterioration of heat conductivity may be quantitatively determined using heat balance relations, however this method requires apart from heat measurements also measuring water fluxes which is not usually done in boiler installations.

Corrosion itself does not directly influence flow resistance in pipes, however sediments and especially impurities and scale lead to a significant increase in flow resistance. That is why it is possible to diagnose a boiler through measuring the difference in pressures [6,7]. It can be done on a ship and the stated pressure difference can be treated as a measurement of sediment formation. This method can be used to localize impurities in the air heater ducts appearing mainly on the exhaust side. For this purpose standard boiler control equipment can be used.

Detecting sediments inside and outside tubes and also on the boiler drum using the method of heat balance requires special measurement techniques. It is not a standard for ship steam boilers to measure the mass flux of exhaust gases.

To evaluate the correct functioning of an auxiliary boiler and burner, total boiler efficiency η_B defined as

$$\eta_B = \frac{\dot{m}_1 (i_1 - i_w)}{\dot{m}_{fuel} HV + \dot{m}_{air} i_{air\ amb}} \tag{1}$$

is used, where:

$\dot{m}_1, i_1$ – mass flux and enthalpy of overheated steam leaving the boiler

i_w – enthalpy of water feeding the boiler at the inside boiler water heater

$\dot{m}_{fuel}$ – mass flux of fuel (required) feeding the boiler

$\dot{m}_{air}, i_{air\ amb}$ – mass flux and enthalpy of atmospheric air feeding the boiler at temperature $T_{amb} = T_0$ in Fig 1,2,3

HV – fuel quality – the amount of energy emitted during complete combustion of 1 kilogram of fuel.

Boiler efficiency relation (1) can be used if only overheated steam is produced. However, as some of the steam is cooled in the cooler and the air feeding the boiler goes through an inside boiler heater, another relation (5) should be used in the boiler diagnostic model. It can be done when additional diagnostic information i.e. exhaust signal parameters are available. To measure them, in the presented boiler diagnosing, exhaust analyzer Madur Electronics GA-20 plus was used.

3. Methodology of exhaust signal parameters determination

The GA-20 *plus* is a multi-functional flow gas analyzer. Electrochemical sensors are used for the measurement of gas concentration. The instrument can be fitted with 2 or 3 of these sensors. All analyzers are fitted with O2 and CO sensors, a third gas cell may be chosen as optional when the instrument is ordered. The following description is based on an analyzer containing 3 cells, the third one being a NO sensor [5]:

– Oxygen O_2
– Carbon monoxide CO
– Nitric oxide NO
– Carbon dioxide CO_2
– Nitrogen oxides NO_x

The first three gases (O2, CO, NO) are measured directly using electrochemical cells. The remaining components are calculated. The concentrations of oxygen and carbon dioxide are shown in percentage The concentrations of the remaining gases is are shown as follows:

– volume concentration in [ppm],
– absolute mass concentration in [mg/m^3],
– mass concentration relative to the oxygen content in [mg/m^3].

In addition, the air inlet or ambient temperature and flow gas temperature are measured. Using the measured temperatures, gas concentrations and the known fuel parameters the analyzer calculates a variety of combustion parameters such as Stack Loss - SL, Efficiency - η, Excess Air - λ, Loss through Incomplete Combustion - IL.

Temperature values and also concentration of those gas elements which are detected by independent electrochemical sensors are obtained in direct measurements. The electrochemical cell indications are proportional to the volume concentration of the detected elements expressed in [ppm] (parts per million). The following quantities are obtained by means of direct measurement:

– flow gas temperature T gas and ambient temperature, expressed in [^{o}C]
– volume concentration of CO [ppm]
– volume concentration of NO [ppm]
– volume concentration of SO_2 (or any other optional cell) [ppm]
– volume concentration of O_2 [%].

3.1. Calculating the concentration of carbon dioxide

The volume concentration of carbon dioxide (expressed in [% vol]) is not obtained by direct measurement, but is calculated on the basis of measured oxygen concentration and the CO_{2max}

parameter, characteristic for a given fuel. Formula 2 shows the formula according to which the analyzer calculates the volume concentration of CO_2 [5]:

$$CO_2 = CO_{2\max}\left(1 - \frac{O_{2meas}[\%]}{20{,}95[\%]}\right), \tag{2}$$

where:

20,95% – volume concentration of O_2 [%] in clean air.

3.2. Calculating the concentration of nitrogen oxides NOx

In addition to nitric oxide NO, combustion gases contain also higher oxides of nitrogen (mainly NO_2). GA-20 *plus* does not have the nitrogen dioxide sensor in its basic version, only the nitric oxide sensor NO. But it is possible to calculate the NO_2 contents on the basis of the measured NO. It is generally assumed that nitric oxide NO contained in combustion gases makes up about 95% of the total amount of nitrogen oxides NO_x. GA-20 *plus* calculates the total concentration of nitrogen oxides NO_x according to the following formula:

$$NO_x[ppm] = \frac{NO[ppm]}{0{,}95} \tag{3}$$

The optional sensor of the GA-20 *plus* analyzer has not got the NO sensor.

3.3. Concentration of "undiluted" carbon monoxide CO_{undil}

To calculate carbon monoxide concentration in combustion gases independent of excess air with which the combustion process is conducted, the idea of "undiluted" carbon monoxide COundil was introduced (it is also called the CO concentration calculated for 0% O_2). The value of CO_{undil} is calculated according to the formula below:

$$CO_{undil} = CO\,\lambda \tag{4}$$

where:

CO – volume concentration CO[ppm],

λ – excess air number.

As can be seen, the concentration of "undiluted" CO is the hypothetical concentration that would have been formed if the same amount of carbon monoxide had appeared in combustion gases when burning without excess air (where λ = 1, so O_2 = 0%).

3.4. Calculating combustion parameters

Besides calculating gas component concentrations the analyzer calculates some parameters describing the combustion process. The formulas for calculating combustion parameters are empirical ones. GA-20 *plus* analyzer calculates the parameters of the combustion process according to the principles predicted by DIN standards. The most important parameter is the amount of heat convected by combustion gases to the environment – the so-called chimney loss (stack loss) SL. Chimney loss is calculated on the basis of empirical formula known as Siegert's formula [4, 5]:

$$S_L[\%] = \left(T_{gas}\left[^{o}C\right] - T_{amb}\left[^{o}C\right]\right)\left(\frac{A_1}{CO_2[\%]} + B\right) \quad (5)$$

where:

S_L – chimney loss - the percentage of heat produced in combustion process, which is convected with the combustion gases,
T_{gas} – flow gas temperature,
T_{amb} – the temperature of the boiler inlet air (it is assumed by the analyzer to be the ambient temperature)
CO_2 – the calculated (on the basis of oxygen concentration and CO2max) amount of CO_2 in combustion gases, expressed in [% vol]
A1, B – factors characteristic for a given fuel type [5].

Based on the calculated chimney loss the analyzer estimates the efficiency of the combustion process h (don't confuse it with boiler efficiency)

$$\eta = 100\% - S_L \quad (6)$$

The above formula assumes that the only quantity decreasing combustion efficiency is chimney loss. Thus, it omits incomplete combustion losses, radiation losses etc. Such a simplification is a result of the inability to measure the size of other losses with the gas analyzer. Because of this gross simplification in the formula above, it should be remembered that the efficiency calculated in this way can not be treated as precise. However, efficiency calculated like this is very convenient as a comparable parameter when regulating the furnace. The formula, though simplified, reflects precisely the tendencies of efficiency change, thus it is possible to observe whether the efficiency increases or decreases. It is sufficient information for the regulation process. It is possible to take into account the efficiency reduction caused by incomplete combustion. This loss is represented by a quantity called the loss by incomplete combustion IL. It determines the percentage of energy loss caused by the presence of flammable gases (in this case mainly CO) in the combustion gases. The loss caused by incomplete combustion is calculated on the basis of measured CO concentration in the combustion gases according to the following formula:

$$I_L = \frac{\alpha\, CO[\%]}{CO[\%] + CO_2[\%]} \quad (7)$$

where:
CO, CO_2 – volume concentrations of CO and CO_2 in the combustion gases,
α – the factor specific for a given fuel.

Calculating I_L enables a correction of the previously calculated (formula 6) combustion efficiency. Then the so-called corrected efficiency η^* is calculated:

$$\eta^* = \eta - I_L \quad (8)$$

The last combustion parameter calculated by GA-20 *plus* is the excess air factor l. This factor expresses how many times the amount of air supplied to the boiler is larger than the minimum amount which is necessary to burn the fuel completely. The system calculates the l factor on the basis of the known CO_{2max} value for the given fuel and the calculated concentration of CO_2 in the combustion gases using the formula:

$$\lambda = \frac{CO_{2\max}}{CO_{2mierz}} \quad (9)$$

The above formula may be transformed with the use of formula (2) into the form:

$$\lambda = \frac{20{,}95\%}{20{,}95\% - O_2[\%]} \tag{10}$$

The basis for correct determination of the quantities describing the combustion process is the knowledge of fuel parameters.

4. Operational clues for starting the process of boiler diagnosis

At a voyage incorrect operation of an auxiliary boiler was stated. The analysis of the object was the quality of heat exchange in a boiler of the DJ 1250 type manufactured by Termo Trading AS [3]. Tube boiler with forced circulation installed on a container ship had the following operation parameters: operating steam pressure 0.5 MPa- set by the classificator Germanischer Lloyd for that particular boiler (maximum 0.9 MPa), temperature 180 ^{o}C, maximum steam output 1250 kg/h, heated surface 26.4 m^2. The boiler ran on L oil with the Dumphy TL burner 24 YHL did not reach the operation steam pressure (even about 0.5 MPa) and the acceptable exhaust temperature was exceeded. With the steam pressure even lower than 0.5 MPa, the boiler in a daily cycle operated in total 18-20 hours, longer than it was designed to operate in temperate climatic zone i.e.8-12 hours (it was switched on more frequently by the system of automatic regulation). At the same time excessive consumption of fuel (1.2 – 1.6 t/day) was observed, when it should have been only 0.8T/day. Steam-water installation did not show any leakages or faults. The temperature of water supplying the boiler (in the thermal box) was 75-80 ^{o}C, boiler water pH was equal to 8.3, the content of chlorides 20 ppm (all parameters were correct). On the basis of such symptoms, the boiler was stated to be unfit for further operation and the decision on the need to start diagnosing process was taken.

5.Realization of the diagnosing algorithm

Due to ambiguous symptoms of boiler faultiness additional source of diagnostic information had to be found. Besides thermal-flow parameters to check the diagnosing of the current boiler operation, exhaust signal parameters were used. Exhaust parameters are shown in Fig 1 (Fig 1a shows the situation for two operating burner nozzles, Fig 1b when only one nozzle operates, Fig 1c shows gas temperature in the outlet collector, when the second nozzle was switched off).

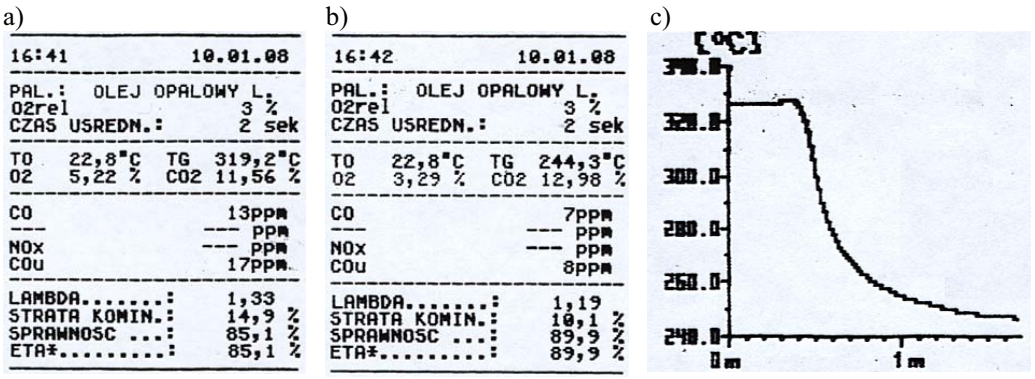

Fig. 1. The results of the first boiler diagnostics:
a – with two operating burner nozzles; b –with only one nozzle; c – gas temperature in the outlet collector (when the second nozzle was switched off) TG [^{o} C] as a function of time [min.]

The presented results showed that exhaust temperature exceeded significantly the accepted values: at two operating nozzles the exhaust temperature was 319 ^{o}C, instead of the accepted 270 ^{o}C, and for one operating nozzle 244 ^{o}C instead of the accepted 180 ^{o}C [3]. The excess air coefficient λ, chimney loss and boiler efficiency were better for the operation with only one nozzle (see recordings in Fig 1). The boiler condition was considered as unfit for further operation and the diagnosing algorithm was started. Within the diagnosing process the following activities connected with fuel mixture preparation were considered necessary:

– mechanism of the air throttling valve regulator ran by a hydraulic servo was regulated (the servo is fed with fuel depending on the number of operating nozzles: one nozzle – fuel pressure at the nozzle should be equal to 0.28 MPa (but it was 0.18 MPa);two nozzles – fuel pressure at the nozzle should be equal to 0.38 MPa (but it was 0.25 MPa);
– cleanliness of the diffuser of the air supplying the boiler combustion chamber was checked, and later a second diagnostic check-up was carried out – exhaust flux parameters at the outlet collector were measured again.

The results were shown in Fig 2 (Fig 2a shows the situationwhen only one nozzle operates, Fig 2b for two operating burner nozzles, Fig 2c shows the runs of temperature changes in the automatic operation cycle-range 1 and with manual burner switching – range 2).

a)

```
16:48                10.01.08
PAL.:  OLEJ OPALOWY L.
O2rel                    3 %
CZAS USREDN.:            2 sek
TO    22,8°C  TG  224,0°C
O2    3,30 %  CO2 12,97 %
CO                      7ppm
---                  --- ppm
NOx                  --- ppm
COu                     8ppm
LAMBDA.....:          1,19
STRATA KOMIN.:        9,2 %
SPRAWNOSC ...:        90,8 %
ETA*.......:          90,8 %
```

b)

```
16:49                10.01.08
PAL.:  OLEJ OPALOWY L.
O2rel                    3 %
CZAS USREDN.:            2 sek
TO    22,9°C  TG  313,0°C
O2    5,25 %  CO2 11,54 %
CO                     13ppm
---                  --- ppm
NOx                  --- ppm
COu                    17ppm
LAMBDA.....:          1,33
STRATA KOMIN.:        14,6 %
SPRAWNOSC ...:        85,4 %
ETA*.......:          85,4 %
```

c)

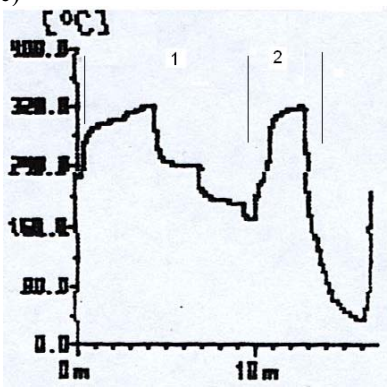

Fig. 2. The results of the second boiler diagnostics after regulating the supplying fuel system, cleaning the ventilator and the diffuser of the air supplying the boiler combustion chamber
a – with one operating burner nozzle; b –with two operating nozzles; c – gas temperature in the outlet collector TG [° C] : range 1 – in the automatic operation cycle, at the moment when the second nozzle was switched on and the cycle of boiler switching off by the automatic system; range 2 – manual regulation – the increase of temperature of gases as a result of manual switching on of the burner, and the decrease of temperature as a result of burner switching off

After the regulation of the supplying system, cleaning of ventilator flow ducts and the diffuser of the air feeding the boiler combustion chamber, it was stated that:

– outlet gas temperature in comparison with the first control measurements decreased only slightly by 20 K at one operating nozzle, and by 6 K at two operating nozzles,
– chimney losses also decreased only slightly, for example at one operating nozzle from10.1% to 9.2%,
– total boiler efficiency, calculated from (8) remained at approximately the same level (85.1%/85.4% at two operating nozzles, and 89.9%/90.8% at one operating nozzle)

The above indicates that after the servicing activities the burner of the boiler operates correctly, but the values of boiler efficiency, longer operation time (more frequent turning-on) and the

remaining still relatively high temperatures of exhaust gases indicate deterioration of thermal conductivity of heated surfaces of the boiler.
That is why, according to the second servicing diagnosis water compartments and boiler furnace and smoke chambers were opened. A significant amounts of sediments on the surfaces of heat exchange were observed with scale on the water side and the remains of incomplete combustion of fuel (soot)on the flame side. Mechanical cleaning of fire compartment and combustion tubes was carried out, from the water side it was only washing with water under pressure without chemical treatment. After the start-up of the boiler the third diagnostics was carried out whose results are shown in Fig 3. They showed that:
– operation time of the burner in the automatic cycle decreased,
– the boiler reached a higher efficiency, closer to the designed one,
– the outlet gas temperature decreased,
– the value of the excess air coefficient decreased,
– carbon oxides content increased

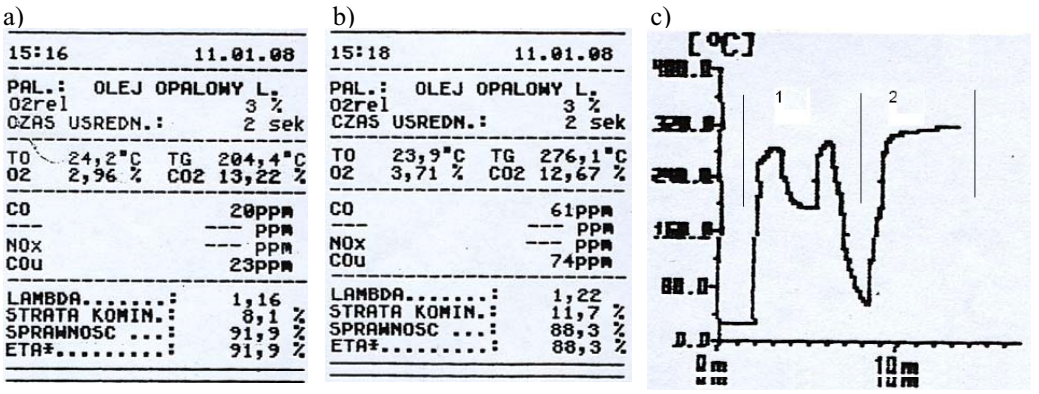

Fig. 3. The results of the second boiler diagnostics after cleaning the flame and smoke side and pressure washing of the water side of the boiler
a – with one operating burner nozzle; b –with two operating nozzles; c – gas temperature in the outlet collector TG [^{o} C] : range 1 – in the automatic operation cycle, at the moment when the second nozzle was switched on and the cycle of boiler switching off by the automatic system; range 2 – manual regulation – the result of manual turning on of the burner to check the increase of temperature of gases

The obtained results justified the crew's decision to turn on the boiler o make it operate in the ship power system.

5. Conclusions and summery

In boiler operation control detection and location of faults in most cases takes place on the basis of thermal-flow diagnostic signals and thanks to visual methods. Using only these methods it is not possible to find quite a big number of faults.

The presented in this paper algorithm of ship boiler diagnosing with two diagnostic signals: thermal –flow and exhaust gases proved to be a very practical method of combining several signals for boiler diagnosing and servicing.

The process of realization of diagnostic algorithm confirmed that the cleanliness of heat exchange surfaces is reflected in different diagnostic parameters. Sediments and impurities of the boiler significantly influence the quality of heat reception, whereas the burner regulation affects the process of fuel combustion. Therefore relation (1) should be used, in the thermal-flow diagnostics and it should be verified by the results of calculations obtained from relation (5) based

on the measurements from exhaust analyzer. In the case of boiler diagnostics based on two diagnostic signals measurement possibilities can be optionally extended (in comparison to the presented ones) with the measurements of the temperature and pressure of exhaust and content of toxic compounds (e.g. nitrogen oxides) in exhaust gases.
Application of exhaust emission signal parameters for boiler diagnostics requires a particularly careful estimation of measurement and calculation precision both for the verification of thermal-flow parameters and to meet the requirements of the MARPOL Convention.

The choice of a diagnostic algorithm will always depend on the measurement availability of the boiler (its kind, construction and type) and measurement possibilities of the possessed diagnostic system.

References

[1] Adamkiewicz, A., Kołwzan K**.,** *Influence of Combustion Products on Faults in Ship Auxiliary Boilers.* Materials from the XXVIII Symposium of Ship Power Plants, Akademia Morska Gdynia, 15 – 16 listopada 2007, Gdynia 2007.

[2] Adamkiewicz A., Tomaszewski F., *Analysis Of Possibilities Of Applying Ship Boiler Maintenance Strategies With Quasidynamic Diagnostics.* 27 th International scientific conference DIAGO® 2008. Technical diagnostics of machines and Manufacturing equipment. Vysoká škola báňská - Technická univerzita Ostrava. Asociace technických diagnostiků ČR o.s., 5. - 6. February 2008, Rožnov pod Radhoštěm.

[3] Technical-operational files of a steam boiler run on liquid fuel Boiler of the *DJ 1250 type Termo Trading AS, Dunphy burner of the TL 24 YH typeL.*

[4] Kruczek S., *Boilers Construction and calculations.* Oficyna wydawnicza Politechniki Wrocławskiej. Wrocław 2001.

[5] *Flue Gas Analyzer GA-20 plus.* Operating manual 01/2003. ®MADUR Electronics. *01/2003.*

[6] Perepeczko, A., Staliński, J., *Ship boilers and steam engines*. Wydawnictwo Morskie, Gdańsk 1971.

[7] Pronobis M., Modernisation of power boilers Wydawnictwa Naukowo-Techniczne. Warszawa 2002

Journal of POLISH CIMAC
Faculty of Ocean Engineering & Ship Technology
GDAŃSK UNIVERSITY OF TECHNOLOGY

AN ATTEMPT OF EVALUATION OF OVERHEATING OF GAS TURBINE BLADES

Mariusz Bogdan

Białystok Technical University
Wiejska 45c street, 15-351 Białystok, Poland
marbog@doktoranci.pb.edu.pl

Abstract

Increase of sensitivity and reliability of non-destructive diagnosing of condition of gas turbine blades became possible thanks to discovery of relevance and relationship between change of colour of their surface and change of microstructure of material resulting from influence of high temperatures. The data in the form of digital images were obtained in lab conditions with help of a photosensitive element i.e. a CCD matrix (digital camera). Acquired images were split up to main primary colours i.e. red, green and blue. This allowed to obtain information about variations of colour intensity for individual channels of digital images and for various temperatures applied for heating of blades. Thus, from the point of view of diagnostics of technical objects, with help of a non-invasive method obtained was the important diagnostic information, i.e. change of luminance and chrominance resulting from influence of high temperature on blades. Researched was also the microstructure of surface and sub-surface layer (change of thickness of coating, change of distribution and size of excretions of reinforcing phase γ'). Obtained information may be useful for evaluation of microstructure of material in the course of operation of gas turbine blades.

Keywords: *gas turbine blades, evaluation of condition, heat-resistance and creep-resistance, digital image, phase* γ'

1. The matter of considered problem

The object of research considered in the present work is a gas turbine, regarded as rotor flow machine, which transforms the enthalpy of working medium (jet of exhaust gas) into the mechanical work, which causes rotation of the rotor. The work, together with mass flow rate, determines the power of the turbine indispensable for driving of receivers [1]. Gas turbines are used not only in power engineering, but also in such important area of economy as transport: water transport (ocean, sea, river), road transport (road, railway), air transport (turbojet engine, turboprop engine, turboshaft engine). Gas turbines are also applied for: military vehicles (land, water, air vehicles), in auxiliary devices: turbochargers for piston engines, main starters of aircraft engines; gas electric power stations based upon gas turbines may be fitted with sets of a few gas turbines.

Thus, the reliability of operation of a gas turbine is limited by proper operation of power receivers. The elements, which have essential influence on reliable operation of a gas turbine are the blades of nozzle unit and rotor blades. The evaluation of condition of gas turbine blades under thermal load is carried out in the course of operation with visual method on the basis of surface image and comparison of this view with standard blade surface. Such criteria of condition assessment are very subjective, because they depend on skills and vision of the person which performs diagnostics. The verification of decision of diagnostics technician is realised with destructive methods i.e. with metallographic examinations. Thus far there is no non-destructive method of examination of grade of blade material overheating based on objective criteria. With regard to important role played by gas turbines the problem of credible evaluation of condition of blades seems to be fully justified [2].

Thermal efficiency of gas turbine circulation cycle, hence the efficiency of real installation, depends significantly on exhaust gas temperature at the turbine inlet. The higher is the temperature

the higher is the efficiency of conversion of fuel chemical energy within the system. The upper temperature limit depends on creep resistance of blade material. In the course of operation of turbine engines of all types (aircraft, traction and ship engines) appear various defects of turbine units. The most frequent cause of defects is overheating of material, as well as thermal fatigue of blades of nozzle unit and rotor caused by both excessive temperature and its duration as well as by chemical activity of exhaust gas [3]. Overheating of blades results from excess of admissible average temperature of exhaust gas as well as from irregular distribution of temperature on the perimeter. Fig. 1 shows exemplary momentary distribution of temperature T_4 of exhaust gas measured after the turbine and measured with help of 8 thermocouples. The operator obtains only the average temperature value for given rotational speed, but has no knowledge about appearing fluctuations and deviations from the average value (supercritical temperature).

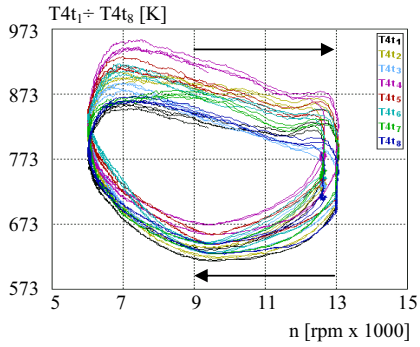

Fig. 1. Exemplary momentary distribution of temperature measured with thermocouples installed after the turbine [4]

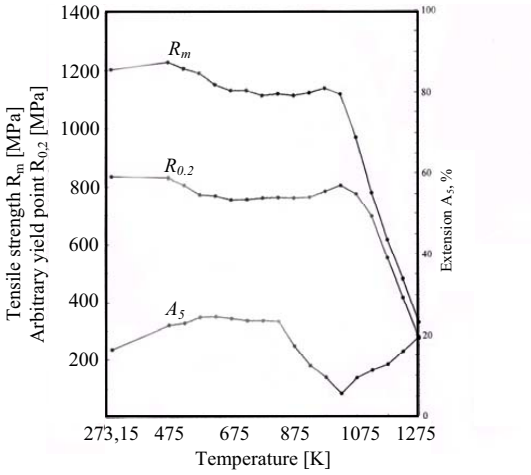

Fig. 2. Mechanical properties of alloy EI-867 as a function of temperature [5]

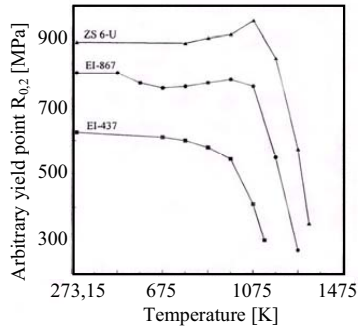

Fig. 3. Influence of temperature on yield point $R_{0.2}$ of selected superalloys [5]

Influence of temperature on mechanical properties (R_m, $R_{0.2}$, A_5) of a gas turbine blade made of alloy EI-867 is shown on the Fig. 2. The change of strength properties $R_{0.2}$ and R_m for various temperatures is of similar character. Observed is slight change of these two parameters below 473 K. Below 673 K observed are minor decrease of value; small fluctuations variations appear below 1023 K. Above 1023 K visible is distinctive drop of tensile strength and arbitrary yield point with simultaneous increase of extension. Similar phenomenon occurs for various alloys (Fig. 3), where

the arbitrary yield point $R_{0.2}$ for the superalloy ŻS 6-U drops violently at 1223 K. Discussed functions for individual superalloys depend on content and properties of the phase γ'. The alloy ŻS 6-U has the greatest relative volume of reinforcing phase (ca. 56% of phase γ'), the alloy EI-867 ca. 32% of phase γ' and the alloy EI-437 ca. 13% of phase γ'. Thus, together with increase of relative volume of the phase γ' the maximum $R_{0.2}$ is the greater, the more phase contains the alloy (Fig. 3).

Increase of reliability and operational durability of turbine blades depends on many factors, but the essential criterion are the material properties (size and distribution of reinforcing phase γ' determines heat and creep resistance).

Development of non-destructive, based on objective criteria diagnostic method (computer-aided) of this machine element will contribute to improvement of reliability of gas turbines. To make the evaluation of blades condition more objective proposed is the method of acquisition of information about grade of overheating of blade microstructure through analysis of surface images recorded with help of an optoelectronic system together with photosensitive detector – a CCD matrix. Acquired data in the form of digital images describe the condition of given surface (the grade of overheating). The information about surface condition is stored in the form of digital images and perceived as change of luminance (brightness) and chrominance (hue) of gas turbine blades. The histogram parameter (distribution of brightness of coloured images) is correlated with results of metallographic examinations (modification of the phase γ') in connection with heating temperature [6, 7].

2. Characteristics of materials applied for gas turbine blades

The temperature increase at the turbine inlet is limited by material problems i.e. creep resistance, thermal fatigue, sulphur high-temperature corrosion (so-called hot corrosion) and erosion. Each gas turbine used in e.g. aircraft turbojet engine consists of three units differing with character of thermal and mechanical loads:

1. Compressor, where aspirated air is compressed and heated;
2. Combustion chamber, where the air-fuel mixture is combusted;
3. Turbine, where high-temperature exhaust gas meets vanes and rotor blades and drives the compressor.

Basic materials for gas turbine blades are metal alloys (hest- and creep-resistant), mainly nickel and cobalt alloys. Requirements for these materials are as below [8, 9]:

1. High long-term creep resistance;
2. High yield point and tensile strength;
3. Good plasticity, ductility and brittle fracture resistance;
4. High thermal and thermal/mechanical fatigue resistance in the course of operation;
5. Stable structure and properties, low susceptibility for reinforcement decrease and reinforcement increase and brittleness in the course of operation;
6. Favourable physical properties – possibly high thermal conductivity and low thermal expansion;
7. Good heat resistance in exhaust gas environment.

Crucial influence on properties of an alloy has the intermetallic phase γ' described with the formula Ni_3 (Al, Ti). Chemical composition, morphology, and distribution of the phase within the structure have crucial influence on creep resistance of the alloy. Additionally, the volume fraction of the phase influences mechanical properties (fig. 3). It has been assumed that the optimum quantity of dispersion particles of intermetallic phases within the volume of grain of alloy should amount to 40-60% [5]. As a result of alloy processing the phase γ' is very comminuted. The phase results from the process of constant extraction from a disordered solid solution and is a

intermetallic compound-like superstructure of A1 lattice. The fact that the phase γ' retains the lattice of matrix γ guarantees coherence of both these phases. The chemical composition of the phase γ' influences significantly the value of lattice parameter and resulting grade of mismatch to the matrix lattice. This affects the morphology of γ' phase excretions and its durability. In multicomponent alloys alloying additions are selected in such way that lattice parameters of both phases are similar. It appears that the grade of mismatch of phase lattice parameters is the function of temperature. The increase of lattice mismatch from 0,16 to 0,80 % in alloys containing niobium and tantalum causes growth of tensile strength at 1033 K by more than 200MPa [10].

3. Analysis of surface image of gas turbine blade

Fragments of gas turbine blades made of EI-867 alloy were heated in a vacuum stove (three samples at once) at five temperature values from 1023 K every 100 K (heating time one hour, cooling in the stove to the environment temperature). As a result of stove heating of blades observed was change of their surface colour (Fig. 4).

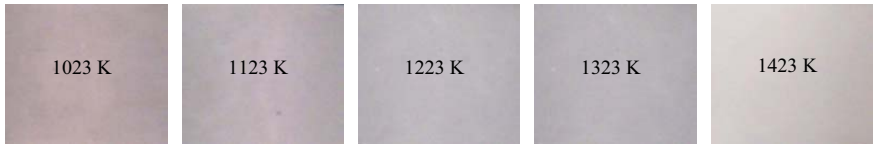

Fig. 4. Images of surface of samples heated at various temperatures

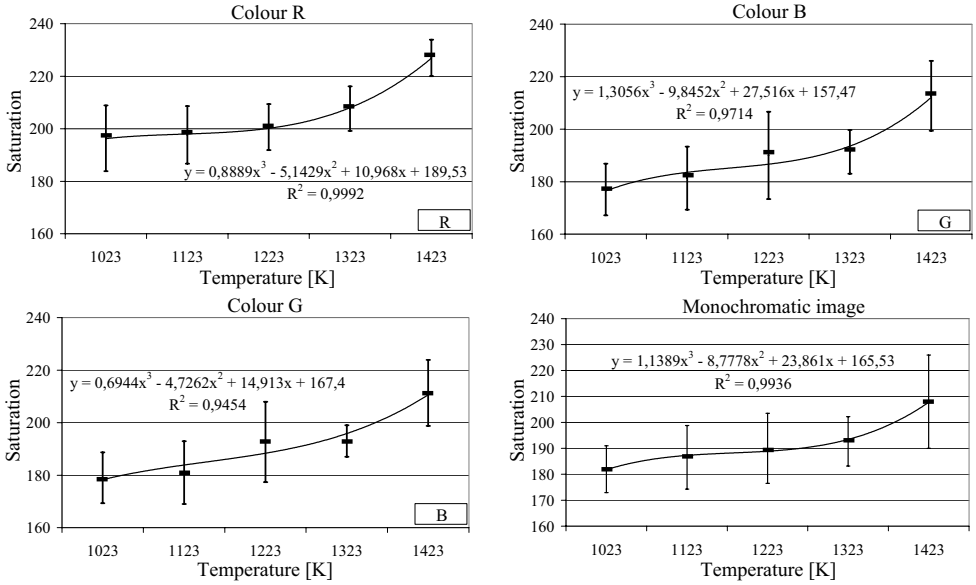

Fig. 5. Change of value of position of maximum amplitude of image saturation with RGB components and grey tones for various heating temperatures of samples

On heated surfaces separated were regions of interest of 24-bit colour depth and dimensions 200x200 pixels. Images were recorded at special stand [6], which ensured repeatability and accuracy of detection.

To determine parameters which enable description of microstructure changes (overheating) of examined surfaces used was image analysis through splitting of image to primary colours, i.e. **R**ed,

Green and **B**lue – RGB and analysis of grey tones of individual surfaces (fig. 5). Due to character of researched phenomenon considered were only changes of position of maximum saturation amplitude (histogram of brightness distribution of digital image).

4. Metallographic examination of gas turbine blades

Application of scanning microscope allowed analysis of microstructure changes resulting from high temperature. Fig. 6 shows that at 1023 K and 1123 K detected was preliminary stadium of coagulation of excretions of reinforcing phase γ', which was characterised with relative regularity and very high density.

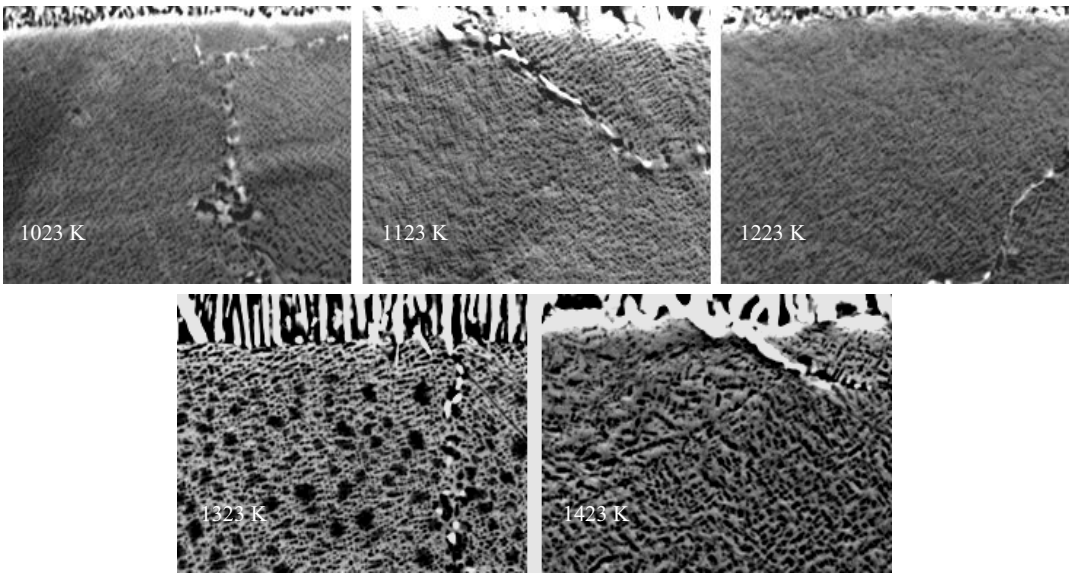

Fig. 6. Subsurface structures for individual temperatures of heating, scanning microscope (x 4500)

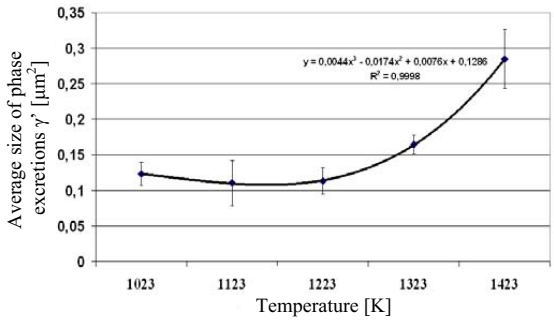

Fig. 7. Modification of reinforcing phase γ' as a function of temperature

Together with increase of temperature of examined blades the structure of the phase γ' became less regular with simultaneous change of grain size (rys 7).

The examination of microstructure proved proper structure below 1223 K. At 1323 K detected was growth and coagulation of excretions of reinforcing phase γ', and then its coagulation within solid solution. Together with temperature increase the effects of coagulation and dissolution of

these excretions in solid solution become stronger. The morphology of phase γ' proves that above 1223 K the alloy EI – 867 becomes overheated, and the examined blade is no more useful. According to A. Dudziński [11] and A. Poznańska [5] growth and coagulation of of excretions of reinforcing phase γ' proves susceptibility for brittle fracture. Additionally, A. Dudziński in his work [3] states that a blade made of similar alloy EI - 929 examined for creeping above 1188 K can be assumed as overheated. Acquired images of microstructure of the alloy EI - 867 heated in higher and higher temperatures can make base for evaluation of grade of overheating of gas turbine blades.

4. Nomogram for evaluation of condition of gas turbine blade

To combine change of colour of blade surface with temperature influence on its microstructure elaborated was the nomogram (Fig. 8) for evaluation of condition. The evaluation of blade condition is based on colour analysis of surface image and is connected with material criterion (modification of excretions of reinforcing phase γ'), worsening properties of thermal resistance – creep resistance and heat resistance.

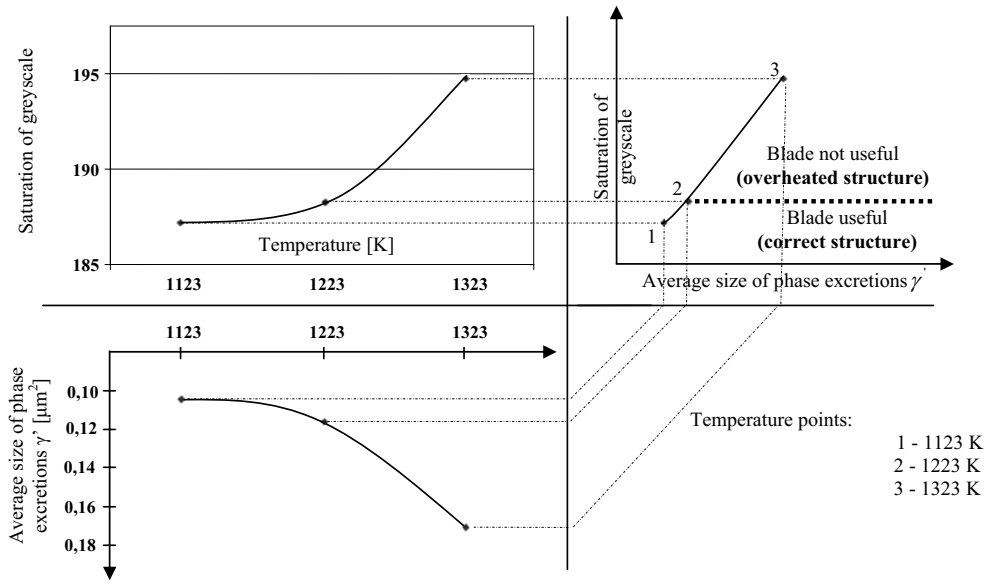

Fig. 8. Nomogram for evaluation of condition of gas turbine blades based on relation between change of grey tones of examined surface and change of size of phase excretions γ' for various heating temperatures

On the basis of the nomogram, which shows relation of hue change (greyscale) as a function of heating temperature of blades, can be evaluated the change of microstructure of the alloy EI – 867. High temperature influences both change of thickness of aluminium surface layer (variable surface which reflects the light) and modification of structure of the phase γ'. Practically, changes of aluminium coating cause change of luminance and chrominance recorded by the optoelectronic system together with photosensitive detector, a CCD matrix. Examined microstructure of subsurface layer reflects changes of the alloy EI – 867 and proves overheating of structure of this alloy (Fig. 6 and 8) after heating of fragments of the blade in temperatures above 1223 K. Taking the material criterion i.e. change of size of phase excretions γ', as the criterion allowing further use of a blade, it is possible to determine the limit of usefulness for further operation.

5. Conclusions

Depreciation of microstructure of blade material consists in growth of intermetallic phase γ'(Fig. 6). The phase has crucial influence on properties of nickel alloys. In special cases the growth of the phase γ' leads to coagulation of excretions and their further dissolution in solid solution. The chemical composition of the phase γ' affects significantly the value of its lattice parameter $a\gamma'$ and correlated grade of mismatch Δa with matrix lattice $a\gamma$, where $\Delta a = (a\gamma - a\gamma') / a\gamma$. This influences the morphology of excretions of the phase γ' and its durability. It appears that the grade of mismatch of lattice parameters is the function of temperature.

Proved was the correlation between heating temperature (change of grey tones of examined surface) and changes of microstructure of the alloy EI-867 (growth and coagulation of excretions of reinforcing phase γ'). Proposed was the methodology of evaluation of usefulness of blades heated in high temperatures on the base of developed nomogram. With help of non-invasive methods used for diagnostics of technical objects efforts were made to acquire important cognitive information, which in practice can be used for evaluation of microstructure changes i.e. state of overheating, as well as thermal fatigue of elements and components of technical objects being subject of variable thermal loads. In next research works will be analysed the problem of credibility (errors) of developed methodology.

References

[1] Dżygadło, Z., and others, *Zespoły wirnikowe silników turbinowych*, WKŁ, Warsaw, 1982.

[2] Błachnio, J., *Non-destructive testing methods as applied to the diagnosing of turbine engines*, EXPLO-DIESEL & GAS TURBINE'05, IV International Scientific – Technical Conference, Gdańsk - Kopenhaga 2005.

[3] Bojar Z., and others, *Zmiany mikrostruktury łopatek ze stopu ŁK-4 w warunkach długotrwałej eksploatacji turbiny silnika lotniczego*, Military University of Technology Bulletin, No. 12, pp 51-64, Warsaw 1988.

[4] Pawlak, W. I., and others, *Identyfikacja wpływu stanu technicznego turbinowych silników odrzutowych na rozkład pola temperatury przed turbiną*, Report KBN no. 8T12D0142, July 2003.

[5] Poznańska, A., *Żywotność łopatek silników lotniczych ze stopu EI-867 w aspekcie odkształcenia niejednorodnego i zmian strukturalnych*, Doctor`s thesis, Rzeszow University of Technology, Rzeszów 2000.

[6] Bogdan, M., *Computer processing of some surface images of technical objects after influence of the high temperature conditions*, 4th International Conference „Mechatronic Systems and Materials 2008", Białystok, Poland 2008 – in print.

[7] Błachnio, J., *The effect of high temperature on the degradation of heat-resistant and high-temperature alloys*, 4th International Conference „Mechatronic Systems and Materials 2008", Białystok, Poland 2008 – in print.

[8] Paton, B., *Żaroprocznost litiejnych nikieliewych spławow i zaszczita ich ot okislienija*, Naukowa Dumka, Kiev 1997.

[9] Tajra, S., Otani, R., *Tieorija wysokotiempieraturnoj procznosti matieriałow*, Mietałurgija, Moscow 1986.

[10] Hernas, A., *Żarowytrzymałość stali i stopów,* Part I, Silesian University of Technology, Gliwice 1999.

[11] Dudziński, A., *Analiza rentgenostrukturalna stopu EI-929 poddanego długotrwałemu wygrzewaniu*. Doctor`s thesis, Military University of Technology, Warsaw 1987.

Praca naukowa finansowana ze środków na naukę w latach 2008-2010 jako projekt badawczy

Journal of POLISH CIMAC
Faculty of Ocean Engineering & Ship Technology
GDAŃSK UNIVERSITY OF TECHNOLOGY

THE USE OF SPECTROMETRIC DIAGNOSTICS IN IDENTIFICATION OF THE TECHNICAL CONDITION OF TRIBOLOGICAL SYSTEMS

Piotr Bzura

Gdansk Uniwersity of Technology
ul. Narutowicza 11/12, 80-952 Gdansk, Poland
tel. +48583472573

Abstract

The paper presents, as an effect of the analysis of investigation results, a possibility of using the spectrometric diagnostics in the tribological system technical condition supervision arrangement.

A model, based on the emission of solid particles in tribological system operation, allows to identify the system technical condition. After the analysis of tests carried out with the use of that model, it has been found that the content of elementary substances in the lubricating oil may be considered a tribological system condition parameter.

Key words: tribological system, spectrometer, correlation

1. Introduction

Correct running of an internal combustion engine requires the knowledge of the current technical condition of all its tribological systems. That allows to take proper decisions on further running, shut-down, repair or other appropriate actions. Fig. 1 below shows that the pre-failure period begins at moment I, then symptoms appear that an admissible value [1] of the engine tribological system has been exceeded.

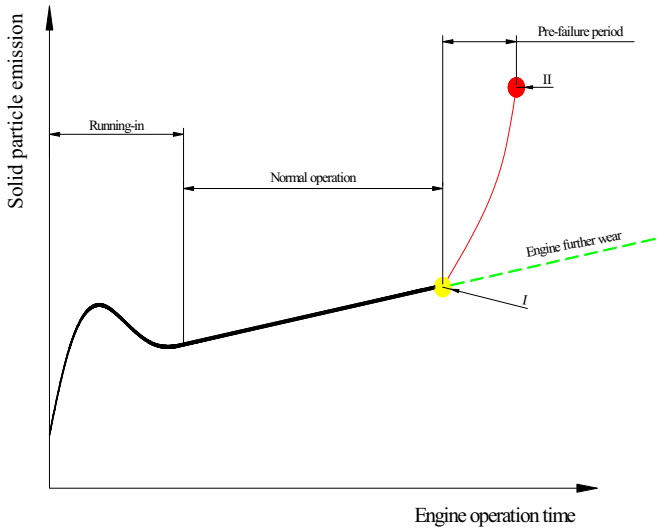

Fig.1. Changes of the wear product emission [4], where:
I – excessive wear (problem appears), II – failure (engine shut-down)

The engine may continue to perform the functions but its technical and operational properties do not meet the requirements (e.g. excessive wear of piston rings causes increased fuel consumption). This type of a symptom may be e.g. an increased content of metals in the lubricating oil. An effect of the missed or disregarded pre-failure period symptoms is cumulation of changes in the engine technical condition and ensuing engine failure.

Further wear of the engine, if the failure has been prevented, is marked with broken line.

The lubricating oil, as one of the tribological system elements, is also subject to qualitative changes and it reflects the technical condition of tribological system. Taking that into account, a model has been developed allowing to identify the tribological system technical condition from the spectrometric diagnostics.

The work is aimed at investigating to what extent the content of elementary substances in the lubricating oil may be treated as a parameter evaluating the technical condition of a tribological system.

2. Methodology of investigations

The content of elementary substances, such as iron (Fe), copper (Cu), zinc (Zn), nickel (Ni) and calcium (Ca), in the lubricating oil is determined by the X-ray fluorescence method on a Philips X-Met920 spectrometer.

The investigated sample is irradiated by primary rays (from an X-ray tube). Atoms of the sample absorb photons, disposing of electrons from the internal orbitals. A "vacuum" that is created in that way will be filled by transferring another electron from an external orbital and a difference of energy between the two orbitals will cause emission of fluorescent X-radiation.

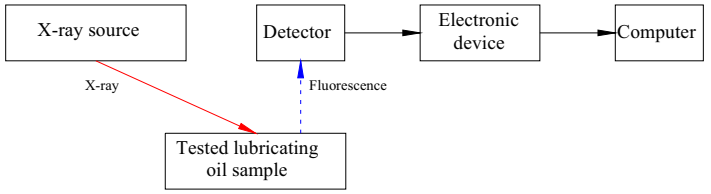

Fig. 2. Schematic diagram of the XRF spectrometer

The XRF method is based on the phenomenon that each elementary substance contained in the tested sample emits, under the X-ray excitation, a characteristic spectrum subject to a qualitative and quantitative analysis.

The investigation model allowing to use the spectrometric diagnostics for identification of the technical condition of a tribological system analyses results of two stages of investigations.

The first stage consists in testing the content of elementary substances in an oil sample taken from a running engine or immediately after the engine stoppage, before the filter (e.g. the LUBIANA [4] system).

Next, a test is carried out on a T-02 four-ball extreme pressure tester (made by ITeE in Radom [3]), with linear increase of the friction node load in any temperature range. The friction node consisted of dia. 12.7 mm ball bearing balls made from the LH15 steel (an iron Fe alloy with average content of 1% C, 0.02% S, 0.3% Ni, 0.3% Cu) in the accuracy class 16 in accordance with the PN-83/M-86452 standard, lubricated with the oil tested on the spectrometer at the first stage. The friction node linear increase of load to 7.4 kN led to the ball seizure, which caused change of the elementary substance content in the lubricating oil. After completion of each test (lasting 18 seconds) the lubricating oil was poured from the friction node pocket to the spectrometer sampler in order to check the solid particle emission.

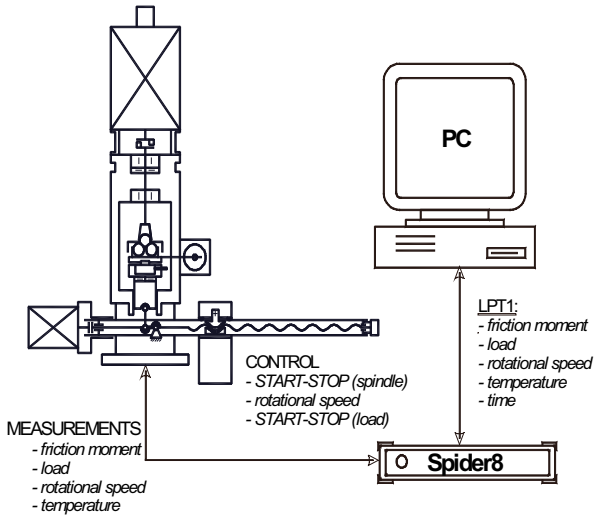

Fig. 3. Schematic diagram of the T-02 [3] four-ball extreme pressure tester measurement and control system

In the second stage the content of elementary substances, such as iron (Fe), copper (Cu), zinc (Zn), nickel (Ni) and calcium (Ca), in the lubricating oil is determined again on a Philips X-Met920 spectrometer.

3. Analysis of the investigation results

Analysis of the investigation results was carried out on the Daewoo API SJ 5W-30 lubricating oil samples taken from a LANOS 1,5 DOHC engine in the 2005 to 2008 operation period.

3.1 First stage of investigations

From the spectrometer measurement results of the lubricating oil samples (Table 1), an analysis (Fig. 4) was performed in order to determine which initial parameter may be considered a diagnostic parameter of the tribological system technical condition.

Table 1. Elementary substance content

Type of lubricating oil Daewoo API SJ 5W-30	Initial parameters - elementary substance content [ppm]				
	IRON	ZINC	COPPER	NICKEL	CALCIUM
Clean - unused	61,2 ±1,5	514,7 ±8,8	863 ±11,9	647,1 ±11,4	3788,7 ±191,8
After one year of use from 2005 to 2006	87,0 ±2,6	453,7 ±8,3	811 ±72,3	577 ±10,8	2807,1 ±168,8
After one year of use from 2006 to 2007	92,4 ±2,7	491,7 ±8,6	828 ±58,5	647,6 ±11,4	3491,7 ±185,5
After one year of use from 2007 to 2008	116 ±3,0	536,7 ±9	925 ±12,3	692,3 ±11,8	3366,1 ±182,7

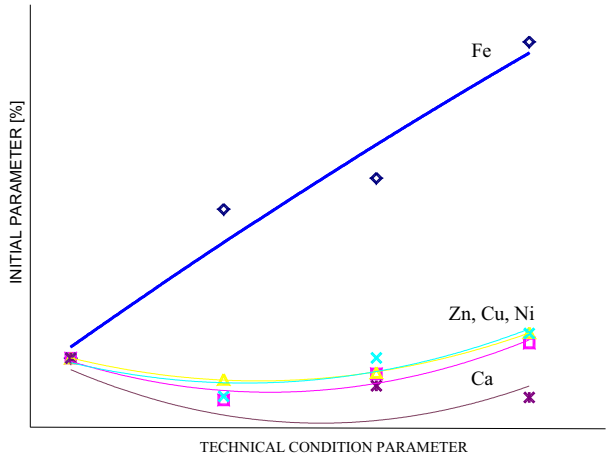

Fig. 4. Graphical illustration of variants of the technical condition [2]

An initial parameter (e.g. content of an elementary substance in the lubricating oil) may be considered a tribological system technical condition diagnostic parameter if it meets the following requirements:

- uniqueness (i.e. each value of the technical condition parameter corresponds with only one determined amount of the elementary substance),
- sufficient range of the parameter values (i.e. better is the initial parameter with greater change of value for a given change of the technical condition parameter),
- availability (easy measurement of the elementary substance content).

Fig. 4, presenting the first stage measurement analysis, indicates that the most unique parameter, with the widest range of values, is the content of iron. The availability requirement will be verified in the analysis of the second stage measurements.

3.2 Second stage of investigations

After the test of oil samples (at 80°C - oil temperature during the engine run) in the T-02 four-ball extreme pressure tester, the elementary substance content was measured (Table II). Then an analysis of initial parameters was performed in connection with the T-02 apparatus ball seizure (Fig. 5).

Table II. Elementary substance content

Type of lubricating oil Daewoo API SJ 5W-30	Elementary substance content [ppm]				
	IRON	ZINC	COPPER	NICKEL	CALCIUM
Clean - unused	102 ±2,8	519,8 ±8,9	900 ±12,1	667,2 ±11,6	3666,9 ±189,6
After one year of use from 2005 to 2006	147 ±3,3	473,4 ±8,5	805 ±11,5	599,6 ±11	3150,5 ±178,1
After one year of use from 2006 to 2007	161 ±3,4	505 ±8,7	891 ±12,6	670,3 ±11,6	3308,3 ±181,5

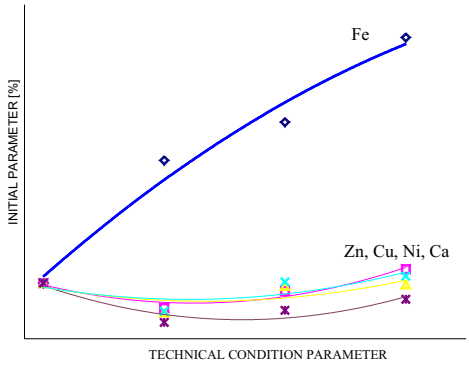

Fig. 5. Graphical illustration of variants of the technical condition [2]

An additional conclusion drawn from the second stage measurement analysis (Fig. 5) is that the iron content in lubricating oil is the easiest available initial parameter (the ball wear clearly increases the iron content in the lubricating oil).

3.3 Identification of the tribological system technical condition

The graphical illustrations (Fig. 4 and 5) indicate that the iron content may be considered a diagnostic parameter of any tribological system technical condition. Additionally, worth mentioning is the high value of the correlation coefficient (Table III) between the seizure load P_t (determined in the four-ball extereme pressure tester - Fig. 6) and the iron emission during the ball seizure.

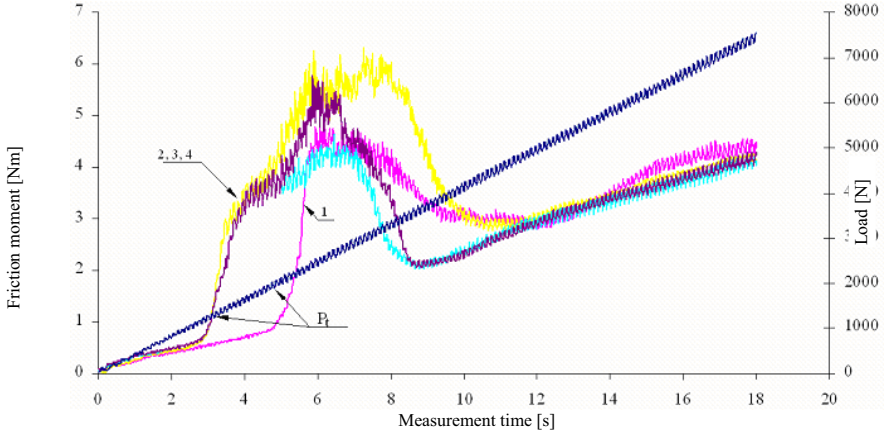

Fig. 6. Friction moment curves obtained in the constant load increase conditions, where:
1- clean unused oil, 2 – oil after one year of use from 2005 to 2006, 3 – oil after one year of use from 2006 to 2007, 4 – oil after one year of use from 2007 to 2008, P_t – seizing load

Table III. Correlation coefficient

P_t [N]	Fe[ppm]	Correlation coefficient r
2119,2	102 - 61,2 =40,8	-0,92456
1350	147 - 87 =60	
1305	161 - 92,4 =68,6	
1297	192 - 116 =76	

The high value of the correlation coefficient of the lubricating oil random samples from normal distribution sets allowed also to check whether there was correlation of those two parameters in the set (i.e. the lubricating oil installation) where the random sample had been taken from. Checked is then the zero hypothesis: H_O: $\rho = 0$ assuming that there is no correlation in the set between those two parameters.

The t Student test is used for the purpose [2]:

$$t = \frac{r}{\sqrt{1-r^2}} \cdot \sqrt{n-2} = \frac{0{,}92456}{\sqrt{1-(0{,}92456)^2}} \cdot \sqrt{4-2} = 4{,}85281$$

where: r – correlation coefficient calculated from the sample data;
n – sample size.

With the significance level 0.05 and n-2 = 2 degrees of freedom, the value read out from the t Student distribution: $t_{0.05} = 4.303 < t = 4.85281$ – therefore the zero hypothesis may be rejected and conclusion may be drawn that correlation exists in the whole lubricating oil set between the seizure load and the iron content.

4. Final remarks and conclusions

- The presented investigation results have shown that emission of elementary substances may be considered a symptom of wear of the investigated tribological systems.
- The quantity of iron in the lubricating oil has an impact on the seizure load.
- The presented identification model of a tribological system technical condition may be included in a tribological system supervision arrangement, which is confirmed by rejection of the zero hypothesis H_O.
- The applied measurement method of the iron content in lubricating oil may be used to determine the oil temperature, which may prove useful for the EA registration and analysis in investigating the surface and the lubricating oil interaction.
- The scope of measurements performed with the apparatus may be extended by:
    - change of the bearing ball material (now it is the LH15 bearing steel) so that its surface structure is similar to that of the slide bearing liner,
    - wider range of different elementary substances measured in the lubricating oil.

References:

[1] M.Hebda, T.Mazur, H.Pelc, *Theory of vehicle operation*, (in Polish) Wydawnictwo Komunikacji i Łączności, Warszawa 1978
[2] T.Puchalski, *Elements of the statistical control of production quality*, (in Polish) Państwowe Wydawnictwo Naukowe, Warszawa 1970
[3] M. Szczerek, W. Muszyński, *Tribological investigations. Seizure*. (in Polish) Radom: Biblioteka Problemów Eksploatacyjnych 2000
[4] *Industrial lubricating materials. Handbook*, (in Polish) Wydawnictwo TOTAL Polska Sp.z o.o., Warszawa 2003

Journal of POLISH CIMAC

Faculty of Ocean Engineering & Ship Technology
GDAŃSK UNIVERSITY OF TECHNOLOGY

THE INFLUENCE OF TREATMENT PARAMETERS ON THE QUALITY OF MMC COATINGS SURFACES APPLIED TO RECONDITION PARTS OF SHIP MACHINERY

Tomasz Dyl. Robert Starosta

Gdynia Maritime University, The Faculty of Marine Engineering, Department of Marine Maintenance, ul. Morska 81-87, 81-225 Gdynia,
dylu@am.gdynia.pl , starosta@am.gdynia.pl

Abstract

During voyage lots of repairs are carried out onboard vessels. It is quite frequent to recondition cylindrical surfaces (for example torque pump shaft neck). The welding technology of applying alloy and composite coatings is very common. In this paper the technology of infrasound thermal spraying of composite metal-ceramic coatings was presented. It is a simple technology and a very useful one in ship machinery repairs during voyage (e.g. internal combustion engines, torque pumps, separators). The MMC coatings must undergo finishing treatment due to high surface roughness after application. The most popular is machining (e.g. lathing or grinding). The authors also propose the application of plastic treatment. In the paper the influence of treatment parameters as well as plastic treatment on the treated surface quality of cylinders made of C45 steel with Ni-Al alloy coating and Ni-Al-Al_2O_3 was defined.

Key words*: composite MMC coatings, roughness reduction, strain hardening, finishing of coating.*

1. Introduction

Materials of new or improved qualities are widely used in such fields of technology as for example cosmonautics, electronics, energetics, armaments industry, automotive industry, aviation, shipping etc. Composite materials are divided according to the matrix: metal, polymer or ceramic. The choice of matrix for composite material depends on the required output qualities, whose aim is for instance to decrease material weight, to achieve appropriate thermal expansion or lubricating ability, rigidity, proper thermal conductivity, hardness, resistance to abrasion, radiation, raised temperature, chemical media, corrosion etc [1]. Composite materials of metal MMC matrix are often used for coatings. Composite coatings of metal matrix with disperse intrusions of non-metal phase are characterised by high resistance to tribologic wear. Technologies used to obtain disperse coatings are the following: galvanic methods, plasma and infrasound spraying HVOF. However, they require high financial support and special skills for equipment operation. Therefore they can not be utilised on board ships for reconditioning parts of machinery during voyage [2,3,4]. The determination of the influence of disperse phase Al_2O_3 on the potential properties of composite coatings of nickel matrix, applied by the use of infrasound flame thermal spraying, enables preliminary examination of the usefulness of this method in acquiring composite coatings. When choosing this technology the following factors were taken into account: simplicity of technology, usefulness for ship torque pumps repair during voyage, low costs of material and equipment. Composite coatings on nickel matrix obtained by thermal spraying have high values of surface roughness [5]. That is why the coatings must undergo finishing machining treatment. However, in spite of machining treatment, alloy coatings flame sprayed were very rough depending on the

method of application and the speed of machining, and the R_a parameter was ranging from 2,55 to 7,79 μm [6]. In order to determine the technology of finishing treatment that would improve the surface quality of composite coatings – the usage of proper treatment parameters for grinding and machining were suggested together with proper machining tools of a negative clearance angle , made of sintered carbides which are recommended for heat-resistant supper alloy and titanium alloys treatment. These alloys have high resistance to thermal and mechanical stresses during continuous or interrupted treatment. After carrying out experimental research , the influence of lathing and grinding on the roughness of composite Ni-Al-Al_2O_3 coatings thermally sprayed was defined. Then the cold rolling trials of composite MMC coatings were performed to estimate the possibility of applying plastic treatment to shape stereometric structure of composite Ni-Al-Al_2O_3 coatings sprayed thermally.

2. Research metod

Experimental research was carried out in the Department of Marine Maintenance, at the Faculty of Marine Engineering at Gdynia Maritime University. In order to define the influence of finishing treatment parameters on the treated surface quality of shaft neck in torque pumps, the following range of research was determined: two types of coatings Ni-Al alloy and composite Ni-Al-Al_2O_3 were sprayed and subjected to machine treatment (lathing and grinding) as well as plastic treatment.

Lathing was performed at three machining speeds. Grinding alloy and composite surfaces were operated for constant machining parameters. Rolling was carried out at two real deformations φ_h 0,06;0,12. The surface that was covered with alloy and composite coatings was prepared in an appropriate way by rough lathing, then prime layers were applied, and finally it was degreased and cleaned of the oxidation products.

Infrasound flame powder spraying of alloy and composite coatings was performed at the assumed parameters: flame gas pressure - acetylene : 0,,7MPa, oxygen pressure : 0,4 MPa, burner distance from the sprayed surface: 150 mm , the number of layers sprayed : 12, achieved thickness of coatings : h_p=0,6÷,2 mm [5, 6]. Prior to applying Ni-Al and Ni-Al-Al_2O_3 layers by "cold" infrasound flame powder coating (where the base was preheated to the temperature of about 100℃, and after spraying the sample temperature did not exceed 250℃) and by "hot" coating (where the base was heated to about 250℃, and then the coating was performed while the object temperature reached 500-600℃) – the roughness measurements were taken on the rollers surface. Rollers surface roughness R_a before spraying coatings was 8 to 16 μm, whereas average arithmetic roughness profile for the layer obtained by "cold" and "hot" thermal spraying was about 13 μm.

The finishing lathing treatment of alloy and composite sprayed coatings was performed on a universal lathe TU 1000. During treatment of both types of coatings the following machining parameters were applied: rate of feed f_n =0,08 mm/turn; depth of machining a_p =0,05 mm; machining speed V_{c1}=21 m/min, V_{c2}= 66 m/min, V_{c3}= 105 m/min. Multi blade plates TNMG 16 04 08-23 H10F of a negative angle made by Sandvik Coromant and consisting of sintered carbides were utilised. Such plates are recommended for super alloys and titanium alloys treatment at low machining speeds, as they are characterised by good resistance to thermal and mechanical shocks during continuous as well as interrupted treatment which do not require greasing. A regular T-Max P handle with a fixed plate clamp ,symbol DTGNR 2020 K16 was used for securing the plate in a tool post. Abrasive treatment of alloy and composite coatings was carried out on a centre-type grinder for rollers. The rotational speed of the grinding wheel was V=42m/s.

3. Experiments results

The finishing treatment of Ni-Al alloy and composite Ni-Al-Al_2O_3 coatings was performed by means of chip, grind and plastic treatment.

The "cold" thermally sprayed Ni-Al alloy co ating was lathed without cooling-greasing medium. While treating the "cold" thermally sprayed Ni-Al coating , the multiblade plate was behaving properly. The coating showed good machining quality. No visible defects or damages appeared on the plate.

The "hot" thermally sprayed Ni -Al coating underwent the same finishing treatment as the "cold" thermally sprayed Ni-Al coating at the same machining parameters. The latter coating showed similar good machining quality and sustained no damage.

The process of lathing the composite "hot" sprayed Ni-Al-Al $_2O_3$ coating was performed without cooling-greasing medium. At the lowest assumed machining speed V_{c1}=21 m/min the plate underwent damage and quick wear appeared on the surface of application, while the coating was slightly lathed with a low quality lathing surface. Then the coating was lathed at the speed of V_{c2} =66 m/min but this attempt showed the increase of the previous result and finally the plate was completely damaged , having thermal cracks perpendicular to the machining edge.

For the next finishing treatment test of "hot" sprayed composite Ni-Al-Al $_2O_3$ coating, a cooling-greasing solution in the form of emulsifying oil Emulgol ES-12 was utilized which improved the machining process. However, in spite of using the greasing oil, the plate surface of application was worn. The lowest roughness values (Tab.1.) were achieved at the highest machining speed V_{c3}=105 m/min.

After machining treatment the treated surface of the alloy Ni-Al coating was perfectly smooth and showed metallic lustre. Composite Ni-Al-Al_2O_3 coating showed poorer grinding quality. The treated surface had visible surface defects which could have resulted from tearing particles of a coating surface. Moreover, while treating the composite coating, the grinding wheel showed signs of bluntness and it had to be sharpened frequently.

The process of rolling alloy and composite coatings was carried out in the Laboratory of Plastic Treatment at the Department of Machine Materials Technology and Welding at the University of Technology in Gdańsk [7]. "Cold" rolling was performe d at the ambient temperature in the laboratory rolling mill duo with the rollers diameter of ϕ 200 mm and the roll face length 250 mm for the real rolling reduction φ_h =0,06; 0,12. It was estimated that the surface of alloy and composite coatings possesses considerably better quality in comparison with the coatings that were chip treated. The lowest values for roughness parameters after rolling with real rolling reduction φ_h =0,12 are shown in Table 1.

The assessment of adherence of alloy and composite coatings to the base was carried out before and after the chip, abrasive and plastic treatment, according to norm PN-79/H-04607. Two methods were used: scratch method and temperature changes method. The coating was examined under the stereoscopic microscope MBC-9 being magnified five times. The coating adherence was considered good if no shells, no blow holes or exfoliations were observed. The quality assessment methods applied for evaluating coating properties did not show negative influence of the finishing treatment on the coating adherence to steel base.

Surface roughness was measured after the finishing treatment by a profile meter HOMMEL TESTER T1000.

The measuring length was 4.8 mm, and the sampling length was 0.8 mm. On the basis of average arithmetic roughness profile (parameter R_a) - the surface roughness decrease factor was determined:

$$K_{Ra} = \frac{R_a'}{R_a} \tag{1}$$

where: R_a– average arithmetic roughness profile before finishing treatment,
R_a – average arithmetic roughness profile after finishing treatment

Figure 1 presents examples of composite MMC coatings surface profilogram that underwent finishing treatment for the lowest value of average arithmetic roughness profile.

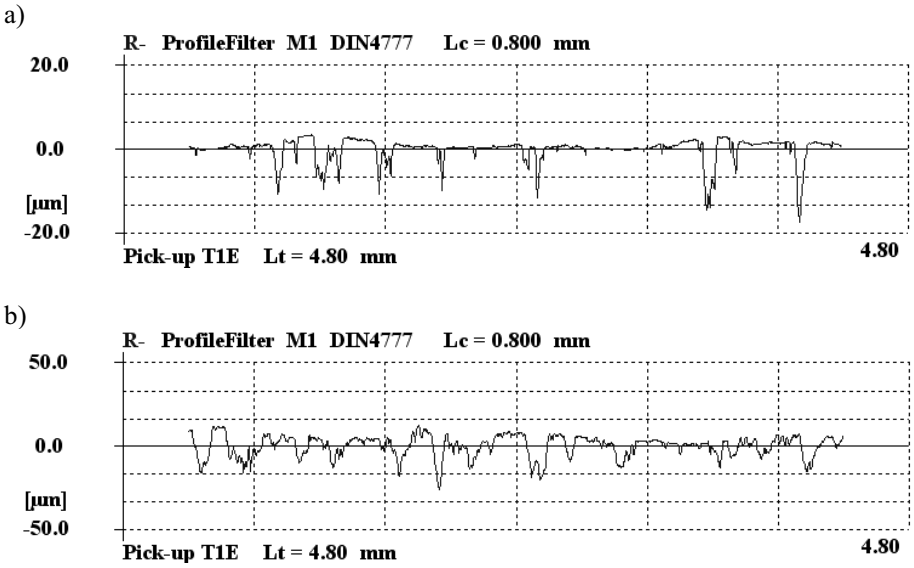

Fig.1. Roughness profilogram after finishing treatment:
a) after grinding, R_a = 1,72 µm, b) after rolling, R_a = 5,23 µm

Figure 2 presents surface roughness decrease factor after application of finishing treatment by means of lathing, grinding and rolling of alloy and composite coatings on metal matrix MMC.

Surface roughness has decreased most after grinding and the least after lathing. After rolling, composite layers gained surface roughness that was comparable to that after grinding, but the surface roughness decreased after rolling . Moreover, the plastic treatment being a chipless treatment does not cause surface material decrement. The technological process of plastic formation of composite MMC coatings, both "cold" and "hot" sprayed went well and without any significant difficulties, however during abrasive treatment particles of layer material were torn out and it was necessary to sharpen the grinding wheel quite often. That is why, from the technological and economical points of view, it seems appropriate to utilize plastic treatment to form stereometric properties of composite coatings. In order to obtain better quality of treated composite MMC coatings surface – another type of treatment that is burnishing treatment ,based on surface plastic deformation has been put forward.

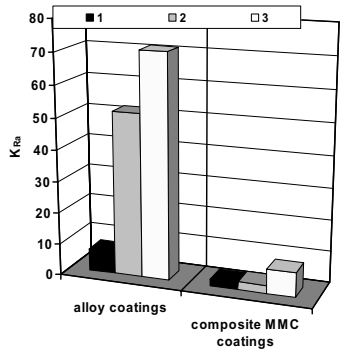

Fig.2. Roughness decrease factor (K_{Ra}) of alloy and composite MMC coatings: 1-after lathing, 2- after rolling, 3- after grinding.

Table 1 shows the measurements results related to load curve of the alloy and composite roughness profile that underwent finishing treatment.

Tab.1. Parameters measurements results related to load curve of the roughness profile

Treatment type	coating type	R_a , μm	R_k , μm	R_{pk}, μm	R_{vk} , μm
lathing	composite	6,20	20,07	5,36	13,27
	alloy	1,95	6,12	1,38	3,27
grinding	composite	1,72	1,14	0,83	9,42
	alloy	0,19	0,56	0,36	0,28
rolling	composite	5,23	10,38	2,92	12,21
	alloy	0,26	0,53	0,20	0,98

On the basis of the data included in table 1 it is possible to state that the reduced depth of valleys (R_{vk}) defined for composite coatings reaches high values after grinding and rolling, compared to parameters values : depth of roughness core (R_k) and reduced height of elevations (R_{pk}).

This may reflect high load share of composite coatings undergoing finishing treatment by grinding and rolling.

Figures 3 and 4 present load curves of the roughness profile of composite and alloy coatings subjected to finishing treatment by finishing lathing, grinding and rolling. It can be observed (Fig.3.) that the highest load share is characteristic for composite coatings after grinding and rolling.

So the most favourable finishing treatment for composite Ni-Al-Al_2O_3 coatings would be grinding and rolling, due to the possibility of obtaining proper tribological properties of the reconditioned parts of ship machinery. It can also be noticed (Fig.4) that in case of alloy coatings , the highest load share occurs for the coatings subjected to plastic treatment by means of rolling. That is why plastic treatment seems to be the best finishing treatment for alloy coatings Ni-Al, taking into account the fact that the squeezing self stress condition is achieved in the coatings which in turn may affect the increase of the durability of ship machinery components.

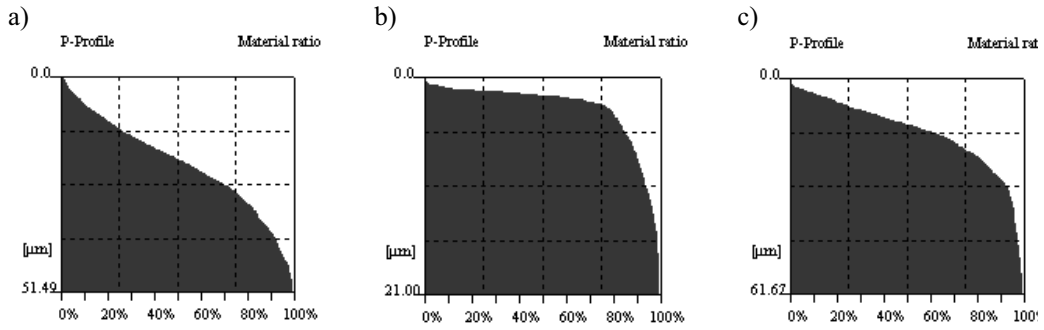

Fig.3. Load curve of the composite coating roughness profile after finishing treatment: a) after lathing, B) after grinding, c) after rolling

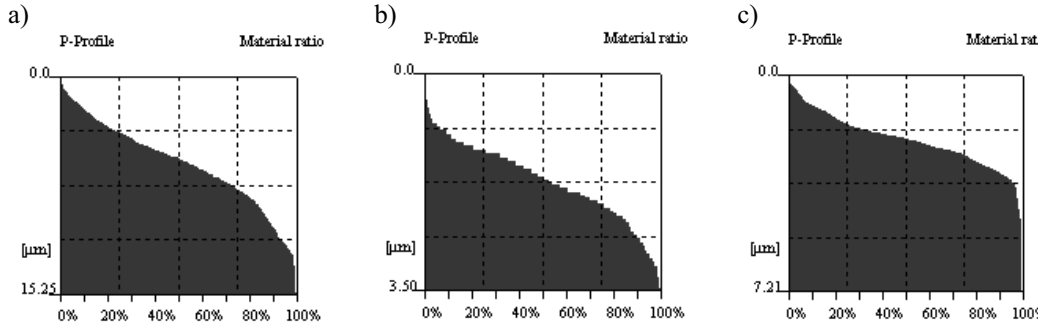

Fig.4. Load curve of the alloy coating roughness profile after finishing treatment: a) after lathing, B) after grinding, c) after rolling

The micro hardness measurement was carried out by means of hardness meter Vickers type with the use of a H type device secured to the handle of metallographic microscope Vertival at the load of 0,4N. To evaluate the influence of the technological process parameters on the micro hardness of the coating treated, the rate of relative consolidation of the surface treated was determined from the following formula:

$$S_u = \frac{\mu HV_2 - \mu HV_1}{\mu HV_1} \cdot 100\% \qquad (2)$$

where: μHV_1 – micro hardness of coating matrix before finishing treatment,
μHV_2 – micro hardness of coating matrix after finishing treatment.

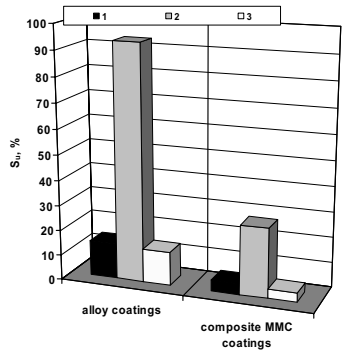

Fig.5. The rate of relative surface consolidation (S_u) of alloy and composite MMC coatings: 1- after lathing, 2- after rolling, 3-after grinding

Figure 5 presents the rate of relative surface consolidation of the treated surface after lathing, grinding and plastic treatment of Ni-Al alloy and composite Ni-Al-Al_2O_3 coatings. It can be observed that the consolidation of composite and alloy coatings as a result of machining treatment was quite insignificant. However, considerable increase of alloy and composite coatings consolidation occurred after plastic treatment by means of rolling. Therefore the squeezing self stress condition was achieved in the coatings which will undoubtedly affect the durability increase of the reconditioned and generated machinery parts.

The process of lathing alloy coatings that were "hot" or "cold" sprayed went well and the machining plate did not undergo any damage, but the Ni-Al coating itself, showed great smoothness. When lathing Ni-Al-Al_2O_3 coatings that were "hot" sprayed , the plate used was damaged. After lathing it was observed that the coating showed signs of "tearing" particles out of the coating stereometric structure. The Ni-Al-Al_2O_3 coating that was "cold" sprayed, was greased with emulsifying oil Emulgol ES-12, and in spite of that showed low susceptibility to lathing treatment. During that process the plates also got damaged. The grinding treatment of alloy and composite coatings sprayed in both methods was performed at fixed machining parameters. The Ni-Al coating showed metallic lustre after the treatment and high smoothness which could indicate a considerable improvement of R_a parameter compared to the condition before treatment. The coating had no signs of tearing particles out of coating stereometric structure. The Ni-Al-Al_2O_3 coatings were ground, however the grinding wheel got blunt and it was necessary to sharpen the wheel during the treatment.

4. Summary

On the basis of the results obtained from experimental research it is possible to state the following:

- the decrease of surface roughness of composite MMC coatings can be observed after machining treatment (lathing and grinding) as well as after plastic treatment,,
- Ni-Al alloy coatings showed lower roughness than composite Ni-Al-Al_2O_3 coatings after machining treatment and plastic treatment,,
- , considerable decrease of surface roughness occurred at higher speeds of lathing,
- for alloy coatings thermally sprayed, the average arithmetic roughness profile showed low values (R_a=0,26 μm for φ_h=0,12, R_a =0,33 μm for φ_h=0,06) after rolling, compared to surface roughness profile after lathing,
- Ni-Al and Ni-Al-Al_2O_3 coatings that were "hot" sprayed demonstrated lower roughness R_a after grinding , compared to Ni-Al and Ni-Al-Al_2O_3 coatings that were "cold" sprayed,
- the highest load share is characteristic for composite coatings after grinding and rolling, and that is why it seems that the most appropriate finishing treatment for composite Ni-Al-Al_2O_3 coatings would be grinding or plastic treatment, due to the possibility of achieving proper tribilogic properties of the reconditioned ship machinery parts,
- composite MMC coatings were characterised by low surface roughness, considerable consolidation, more uniform structure (most pores created after thermal spraying were closed) after plastic treatment compared to coatings that were ground.

Composite coating underwent a finishing treatment by means of lathing and grinding. However the technology developed did not come up to the expectations, which can be proved by the difficulties that occurred during machining treatment (quick wear of grinding tools) or tearing particles out of the stereometric coating structure. As a result it seems advisable to improve the technology of finishing treatment for Ni-Al-Al_2O_3 coatings. Composite coatings

that were rolled showed roughness values similar to those after grinding, however the rate of relative consolidation gained much higher values. So, taking into consideration technological as well as economical factors, the plastic treatment seems to be appropriate for shaping stereometric properties of composite coatings. Consequently, the surface plastic treatment is suggested as an alternative finishing treatment, in order to achieve better quality of the treated surface in composite MMC coatings thermally sprayed.

Literatura

[1] Dobrzański L.A., *Podstawy nauki o materiałach i metaloznawstwo. Materiały inżynierskie z podstawami projektowania materiałowego*. Wydawnictwo Naukowo – Techniczne, Gliwice – Warszawa 2002.

[2] Piaseczny L., *Technologia naprawy okrętowych silników spalinowych*. Wydawnictwo Morskie, Gdańsk 1992.

[3] Klimpel A., *Technologie napawania i natryskiwania cieplnego*. Wyd. Politechniki Śląskiej. Gliwice 1999.

[4] Starosta R., Zieliński A. *Effect of chemical composition on corrosion and wear behaviour of the composite Ni-Fe-Al_2O_3 coating*. Journal of Materials Processing Technology, No 157 – 158 (2004), 434-441

[5] Starosta R., Klatt K., *Ocena podatności technologii natryskiwania płomieniowego ROTO-TECK do nakładania powłok kompozytowych Ni-Al_2O_3*. Materiały i Technologie, Roczniki Naukowe Pomorskiego Oddziału PTM, nr 2 (2004) s. 191-194.

[6] Starosta R., Dyl T., *Obróbka wykańczająca powłok Ni-Al oraz Ni-Al-Al_2O_3, natryskiwanych płomieniowo, Materiały i Technologie*, Roczniki Naukowe Pomorskiego Oddziału PTM, nr 4 (2006) s. 260 – 263

[7] Skoblik R., Starosta R., Dyl T., *The influence of dispersion phase on composite coating properties after cold working, Monograph, Developments in mechanical engineering*, Gdańsk University of Technology Publisher, Part III, Chapter 13, Volume 2, Gdańsk 2008, s. 119-125

Journal of POLISH CIMAC
Faculty of Ocean Engineering & Ship Technology
GDAŃSK UNIVERSITY OF TECHNOLOGY

STOCHASTIC MODEL OF THE PROCESS OF STARTING COMBUSTION ENGINES AND PRACTICAL APPLICATION OF THE PROCESS

Jerzy Girtler

Gdansk University of Technology
Faculty of Ocean Engineering & Ship Technology
Department of Ship Power Plants
tel. (+48 58) 347-24-30; fax (+48 58) 347-19-81
e-mail: jgirtl@pg.gda.pl

Abstract

The paper presents a proposal of a model of diesel engine (or gas turbine engine) starting process as semi-Markov process which is discreet in states and continuous during operation. States of the process are the following: cold engine state (s_1), warm engine state (s_2) and hot engine state (s_3). Idea of using the model for determining a quantity of harmful substances emitted in exhaust gases during starting of engine, has also been proposed herein. Moreover, the paper provides a possibility of considering in researches on the quantity of harmful substances contained in exhaust gases, a mass of harmful substances as a random variable. For the considerations it has been accepted that statistics of the random variable has got asymptotically normal distribution. The presented stochastic model of self-ignition engines starting process enables deriving the limiting distribution of the process, being the probabilities of occurring the mentioned states (s_1), (s_2) and (s_3) one by one. The distribution is indispensable to determine the expected value of the mass of harmful substances emitted in time of successive re-starts of engine performed during long operation. The second approach to estimation of the mentioned mass considered as a random variable enables estimating its expected value in time of long-term work of engines till the first failure or in the period between two successive preventive maintenances. Estimation of the expected value of the masses of harmful substances emitted during long operation of engine, can be made by applying point or interval estimation. The paper proposes the interval estimation because it makes possible to assess accuracy of the estimation. In this case the mentioned value is determined in the form of interval with random edges (limits), which comprises unknown value of the mass of harmful substances emitted by engine, at the probability called confidence level.

Keywords: *diesel engine, semi-Markov process, toxic substance*

1. Introduction

Considerations in the phases of combustion engines (diesel engines or gas turbine engines) designing and operating, include not only parameters characterizing the energy conversion, like [2, 14, 15, 17, 18]: general ability of engine, heat emission rate, heat usage rate, heat evolution rate, pressure escalation rate, etc. Emission (Fig. 1.) content should also be submitted to analysis for such toxic compounds as carbon monoxide (CO), hydrocarbons (C_nH_m), nitric oxide (NO_x), particulate solid (PM- Particulate Matte) and sulfur compounds (SiO_2, SiO_3, H_2SO_3, H_2SO_4), aldehydes and others [1, 12]. From researches on fuel combustion processes results that physical (not chemical) processes have great influence on the quantity of emission of particular toxic compounds included in exhaust gases. The other issue from the researches is that their emission is closely connected with each other and possibility of reduction of one of them can cause increase of emission of another one. Therefore, any action to reduce the content of toxic compounds in exhaust gases must be followed by a compromise ensuring minimization of harmful impact of toxic exhaust compounds on natural environment.

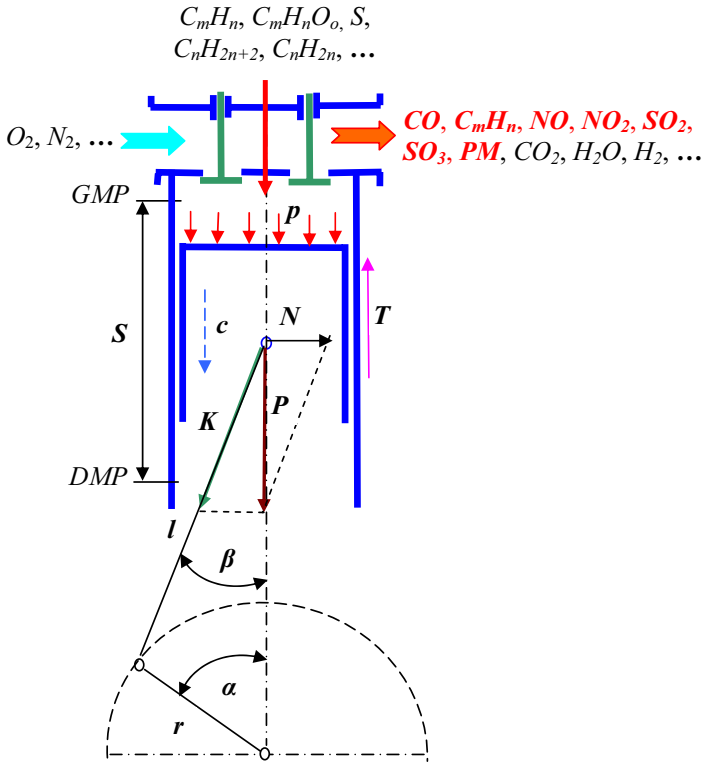

Fig. 1. Toxic compounds as carbon monoxide (CO), hydrocarbons (C_nH_m), nitric oxide (NO_x), particulate solid (PM-Particulate Matte) and sulfur compounds (SiO_2, SiO_3): GMP – top dead centre, DMP – bottom dead centre, p – exhaust gas pressure, S – piston stroke, c – piston speed, N – piston-side-thrust force, T – friction-force, P – piston force, K – connecting-rod force, l – connecting-rod length, r – crank radius, α – crank angle, β - connecting-road deflexion angle

Emission of the toxic compounds depends among others on engine thermal state, especially while starting engine. Thus, this paper provides a proposal of an original method to determine the mass of toxic compounds emitted by self-ignition or spark-ignition engine during starting. The method considers the stochastic model of starting engines of this kind. It has been shown that the model can be presented in the form of semi-Markov process.

Professional literature proves that the most toxic compounds are formed in exhaust gases during so called "cold engine star ting", so when the engine is started after not sufficient pre-warming phase [1, 9, 11, 19]. From this reason there is a need to create a model of engine starting process considering at least three states of engine: cold, warm (up-warm) and hot.

2. Model of self-ignition engine starting process

Considering the process of starting a combustion engine (diesel engine or gas turbine engine), at least three thermal states of it, which exist directly before starting, can be distinguished, i.e. *cold state* (s_1), *warm state* (s_2), and *hot state* (s_3). The states may be values of the process $\{U(t): t \in T\}$ being a real model of the engine starting process. The model can be presented in the form of semi-Markov process having the set of states [5]:

$$S = \{s_1, s_2, s_3\} \tag{1}$$

with the following interpretation of the states:

- s_1 cold state which enables starting the engine in ambient conditions (conditions of ship power plant) with typical low temperatures (T) not higher than 290 K;
- s_2 warm state which enables starting the engine in conditions of pre-warming (T >300 K) performed on it in state s_1 before starting;
- s_3 hot state which enables starting the engine in its operating (working) conditions following from the need of stopping the engine work under even large load and then re-starting.

Thus, the process is a three-state one with continuous realizations (time-continuous process). It is a semi-Markov process [4, 5, 6, 7] and, as a model of changes of the states of combustion engine starting, is the simplest model which can be of practical significance.

In this relation the set of states of starting self-ignition engines $S = \{ s_1, s_2, s_3\}$ can be considered as a set of values of the stochastic process $\{U(t)\colon t \in T\}$ with constant intervals and right-side continuous realizations.

Initial distribution of the process $\{U(t)\colon t \in T\}$ of any combustion engine is defined by the formula [5]:

$$P_i = P\{U(0) = s_i\} = \begin{cases} 1 & dla \quad i = 1 \\ & \\ 0 & dla \quad i = 2,3 \end{cases}. \tag{2}$$

Functional matrix of the process is as follows:

$$\mathbf{Q(t)} = \begin{bmatrix} 0 & Q_{12}(t) & Q_{13}(t) \\ Q_{21}(t) & 0 & Q_{23}(t) \\ Q_{31}(t) & Q_{32}(t) & 0 \end{bmatrix}. \tag{3}$$

Thus, for the presented process $\{U(t)\colon t \in T\}$ with functional matrix expressed by the formula (3), the following limiting distribution can be determined:

$$P_1 = \frac{\pi_1 E(T_1)}{H}, \quad P_2 = \frac{\pi_2 E(T_2)}{H}, \quad P_3 = \frac{\pi_3 E(T_3)}{H} \tag{4}$$

at:

$$\pi_1 = \frac{p_{31} + p_{12}p_{32}}{2 + p_{12}p_{23}p_{31} + p_{13}p_{21}p_{32}}, \quad \pi_2 = \frac{p_{32} + p_{12}p_{31}}{2 + p_{12}p_{23}p_{31} + p_{13}p_{21}p_{32}},$$

$$\pi_3 = \frac{1 - p_{12}p_{21}}{2 + p_{12}p_{23}p_{31} + p_{13}p_{21}p_{32}},$$

$$H = \pi_1 E(T_1) + \pi_2 E(T_2) + \pi_3 E(T_3),$$

where:

P_1, P_2, P_3 – probability that combustion engine is started from the states accordingly: s_1, s_2, s_3,

π_j – limiting probability of the embedded Markov chain of the process $\{U(t)\colon t \in T\}$ describing the possibility of occurring the state $s_j, j = 1, 2, 3$,

p_{ij} – probability of the process $\{U(t)\colon t \in T\}$ transition from the state s_i to the state s_j;

$E(T_j)$ – expected value of duration of the state s_j, ($j = 1, 2, 3$).

The presented states of starting any combustion engine are connected with particular thermal states of the engine. They reflect states existing in practice. Therefore, the proposed model can be employed for determining the mass of toxic compounds.

3. Determination of toxic compounds mass during the phase of engine starting.

Analysis of research results on the combustion process run, shows that during combustion there are different conditions for toxic compounds to form in emission. The most significant of them are: carbon monoxide (CO), hydrocarbons (C_nH_m), nitric oxide (NO_x), particulate solid and substances in very little amounts (forming low concentrations) like sulfur compounds (SiO_2, SiO_3, H_2SO_3 and H_2SO_4), aldehydes and others [1, 12, 14, 18]. In practice there is a need to control emission of the mentioned substances.

Emission of toxic substances can be determined from the following formula [1]:

$$e_k = \frac{v_{mix}\rho_k K_H c_k}{s} 10^{-6} \tag{5}$$

at $k = 1, 2, ..., n$ – type (number) of the given toxic substance,

where:

e_k – mass of toxic substance [g/km],
v_{mix} – volume of dilute emission in normal conditions [dm^3/test],
ρ_k – density of toxic substance in normal conditions [g/dm^3],
K_M – correction rate of humidity of nitric oxide mass,
c_k – concentration of the substance toxic for surroundings [ppm],
s – road traveled by a transport mean (car, sea-going ship) during testing [km].

Emission e_k ($k = 1, 2, ..., n$) differs depending on whether the starting of engine runs from the cold state (s_1), warm state (s_2) or hot state (s_3). During test performance, on the road (s) traveled by the given transport mean (car, sea-going ship), engine can be started several times from its different states mentioned above. The emission will be also different for the engine depending on the technical state of its fuel system and the fuel quality. Ambient conditions in which the engine is started are important, as well. Therefore, the emission value of toxic substances, determined from the formula (5) may be accepted as emission realization considered as a random variable. Hence, taking into account the dependence (4), the mass of toxic substances can be expressed by the following formula:

$$\mathrm{E}(E_k) = \frac{(p_{31} + p_{12}p_{32})E(T_1)}{M} e_{1k} + \frac{(p_{32} + p_{12}p_{31}E(T_2)}{M} e_{2k} + \frac{(1 - p_{12}p_{21})E(T_3)}{M} e_{3k} \tag{6}$$

at:

$$M = E(T_1) + p_{12}E(T_2) + (1 - p_{12}p_{23})E(T_3),$$

where:

e_k – mass of the substance toxic for the natural environment ($k = 1, 2, ..., n$),
p_{ij} – probability of transition of the engine starting process $\{U(t): t \in T\}$ from the state s_i to the state s_j, $i \neq j$; $i, j = 1, 2, 3$,

$E(T_j)$ – expected value of state s_j (j = 1, 2, 3) duration.

The formula (6) follows from consideration of all dependences provided in the formula (4) which determines the probabilities P_1, P_2 i P_3.

The mentioned toxic substances contained in emission like: carbon monoxide (CO), nitric oxides (NO_x), the most of all NO, hydrocarbons (C_nH_m), particulate solid (PM) and sulfur compounds, as sulfur dioxide (SO_2), sulfur trioxide (SO_3), sulfurous acid (H_2SO_3), sulfuric acid (H_2SO_4), can be and should be considered as random variables. That is because these characteristics are such variables which, in the result of successive measures, take different numerical values with determined probability. So, the mass e_k of the mentioned toxic substances in emission, calculated from the formula (5), can be considered as realization of random variable E_k, where k = CO, NO, C_nH_m, PM, SO_2, SO_3, H_2SO_3, H_2SO_4. That means that determined probability is assigned to each possible value of any random variable E_k,. This fact can be described in the following form [3, 13]:

$$P(E_k = e_{ki}) = p_{ki} \ (i = 1, 2, ..., \ n). \tag{7}$$

The formula shows that probability p_{ki} is a function of the values which can be taken by a random variable E_k. So, for any random variable E_k the following description can be made:

$$p_{ki} = f(e_{ki}). \tag{8}$$

The characteristic of the function is that the sum of probabilities determined by the dependence (8) is equal to 1, what can be described as follows:

$$\sum_{i=1}^{n} p(e_{ki}) = 1 . \tag{9}$$

Analyzing the toxic substances contained in the emission as random variables E_k and making the successive measures of their mass values, the average mass value (arithmetic average) can be determined from the formula [3, 8, 10, 16]:

$$\bar{e}_k = \frac{1}{n}\sum_{i=1}^{n} e_{ki} , \tag{10}$$

where:

e_{ki} – value of the analyzed characteristic (random variable) E_k .

Average value $\bar{e}_k$, determined from the formula (10) is the observed value of statistics $\overline{E}_k$. The statistics is a random variable [3]

$$\overline{E}_{kn} = \frac{1}{n}\sum_{i=1}^{n} E_{ki} , \tag{11}$$

where E_{ki} – random variable with the same (arbitrary) distribution of a common expected value $E(E_{ki}) = m_{1k}$ and variation $D^2(E_{ki}) = \sigma_k^2 \neq 0$.

Thus, random variable $\overline{E}_k$ is an arithmetic average with n independent random variables E_{ki} of identical distribution. Expected value and variation of random variable $\overline{E}_k$ are defined in the form of dependences [3, 8]:

$$\mathrm{E}(\overline{E}_{kn}) = \mathrm{E}(E_{ki}) = m_{1k}\,, \qquad \mathrm{D}^2(E_{kn}) = \frac{1}{n}\mathrm{D}^2(E_{ki}) = \frac{\delta_k^2}{n}\,. \tag{12}$$

From the Lindeberg-Levy theorem follows [3] that the random variable $\overline{E}_k$ (statistics) has got asymptotically normal distribution N(m_{1k}, $\frac{\sigma_k}{\sqrt{n}}$) regardless of the character of the random variable E_k. That means that the arithmetic average with n independent random variables E_{ki}, arbitrary but identical distribution, common expected value $\mathrm{E}(E_{ki}) = m_{1k}$ and variation $\mathrm{D}^2(E_{ki}) = \sigma_k^2$, has got asymptotically normal distribution N(m_{1k}, $\frac{\sigma_k}{\sqrt{n}}$).

Analysis of toxic substances contained in emission according to the presented proposal is interesting in the aspect that convergence of the statistics $\overline{E}_k$ distribution to the normal distribution N(m_{1k}, $\frac{\sigma_k}{\sqrt{n}}$) is so quick that it can be used for all $n \geq 4$, so almost always.

When the value σ is known and the distribution N(m_{1k}, $\frac{\sigma_k}{\sqrt{n}}$) of the statistics $\overline{E}_k$ is considered, it is possible to determine a confidence interval for unknown expected value $m_{k1} = \mathrm{E}(E_k)$ from the formula [3, 8, 10]:

$$P\left\{\overline{e}_k - y_\alpha \frac{\sigma_k}{\sqrt{n}} \leq \mathrm{E}(E_k) \leq \overline{e}_k + y_\alpha \frac{\sigma_k}{\sqrt{n}}\right\} = \beta\,, \tag{13}$$

where:

β – confidence level,
y_α – standardized variable of normal distribution, meeting the confidence level $\beta = 1 - \alpha$ (α – significance level).

In research practice the value σ is, as a rule, unknown and for its evaluation the following formula [3, 16] is applied:

$$s_k = \sqrt{\frac{1}{n-1}\sum_{i=1}^{n}(e_{ki} - \overline{e}_k)^2}\,. \tag{14}$$

Because the statistics $\overline{E}_k$ has always got asymptotically normal distribution N(m_{1k}, $\frac{\sigma_k}{\sqrt{n}}$), and its convergence to normal distribution N(m_1, σ) is very quick, so practically it can be accepted that the analyzed characteristic E_k of emission, being a content of k toxic substance, has a normal distribution N(m_{1k}, σ_k). Hereby, it has to be pointed out that acceptance of the assumption that the mentioned characteristic E_k has a normal distribution N(m_{1k}, σ_k) is not a limitation in the research practice because the statistics $\overline{E}_k$ has always got asymptotically normal distribution N(m_{1k}, $\frac{\sigma_k}{\sqrt{n}}$). Additionally, convergence of this distribution to normal distribution is very quick [3]. Thus, the random variable $\frac{\overline{E}_k - \mathrm{E}(E_k)}{s_k}\sqrt{n-1}$ has distribution t-Student with $k = n - 1$ degrees of freedom.

That means that confidence interval for unknown expected value $E(E_k)$ of the random variable E_k can be determined from the formula [3, 8]:

$$P\left\{\overline{e}_k - t_{\alpha,n-1}\frac{s_k}{\sqrt{n-1}} \le \mathrm{E}(E_k) \le \overline{e}_k + t_{\alpha,n-1}\frac{s_k}{\sqrt{n-1}}\right\} = \beta. \tag{15}$$

4. Final conclusions

Emission of toxic substances, occurring during operation of combustion engines, depends among others on their thermal states. The highest emission of toxic substances is recorded in time of starting the engines. Starting an engine from its cold state, so the state having an ambient temperature, is particularly unfavourable. Engines in warm state and especially hot state generate smaller amount of toxic substances. Therefore, it is significant to know the probabilities of starting engines from their particular states. For determining the probabilities it has been proposed herein the semi-Markov model of the engine starting three-state process with the following interpretation of the states: cold state (s_1), warm state (s_2), hot state (s_3). It has been shown usability of the model to determine the mass of toxic substances emitted to the surroundings during starting engines. There has also been presented another approach to testing the content of toxic substances in exhaust gases. It consists in considering the mass of any toxic substance as a characteristic of emission, being a random variable. The paper has also shown usability of the Lindeberg-Levy's theorem from which follows that the statistics occurred from test results on determined mass of emitted toxic substance is a random variable with asymptotically normal distribution regardless of the character of the random variable which is the tested mass of the mentioned substance. This enables applying the interval estimation for assessing unknown expected value of a random variable which can be a mass of any toxic substance existing in the exhaust gases.

References

[1] Bielaczyc, P., Merkisz, J., Pielecha, J., *Stan cieplny silnika spalinowego a emisja związków szkodliwych*, Wydawnictwo Politechniki Poznańskiej, Poznań 2001.

[2] Brun, R., *Szybkobieżne silniki wysokoprężne. WKiŁ, Warszawa 1973. Dane o oryginale: Science et Technique du Moteur Diesel Industriel et de Transport*, Copyright by Societe des Editions Technip et Institut Francais du Petrole, Paris 1967.

[3] Firkowicz, S., *Statystyczna ocena jakości i niezawodności lamp elektronowych*, WNT, Warszawa 1963.

[4] Girtler, J., *Stochastic model of the process of starting piston combustion engines and the practical use of the process*, Journal of KONES Powertrain and Transport. Vol 13, No 2, Warsaw 2006, pp.73-79.

[5] Girtler, J., *Semi-Markovian models of the process of technical state changes of technical objects*, Polish Maritime Research No 4/2004. Gdansk.

[6] Girtler, J., *Physical aspects of application and usefulness of semi-Markovian processes for modeling the processes occurring in operational phase of technical objects*. Polish Maritime Research No 3/2004. Gdansk.

[7] Grabski, F., *Teoria semi-markowskich procesów eksploatacji obiektów technicznych*, Zeszyty Naukowe AMW, nr 75 A, Gdynia 1982.

[8] Greń, J., *Modele i zadania statystyki matematycznej*, PWN, Warszawa 1968.

[9] Hglund, P.G., stedt, A., *Reduced Air Pollution and Fuel Consumption with Preheated Car Engines*, Urban Transport and the Environment for the 21st Century, International Conference, Lisbon 1998.

[10] Krzysztofiak, M., Urbanek, D., *Metody statystyczne*, PWN, Warszawa 1979.

[11] Larson, R.E., *Vehicle Emission Characteristics under Cold Ambient Conditions*, SAE Technical Paper 890021.
[12] Lotko, W., *Zasilanie silników spalinowych paliwami alternatywnym,* ITE, Radom 1995.
[13] Pawłow, B., W., *Badania diagnostyczne w technice,* WNT, Warszawa 1967.
[14] Piotrowski, I., *Okrętowe silniki spalinowe,* WM, Gdańsk 1971.
[15] Piotrowski, I., Witkowski, K., *Eksploatacja okrętowych silników spalinowych,* AM, Gdynia 2002.
[16] Volk, W., *Statystyka stosowana dla inżynierów,* WNT, Warszawa 1965.
[17] Wajand, J.A., *Silniki o zapłonie samoczynnym*, WNT, Warszawa 1988.
[18] Zabłocki, M., *Wtrysk i spalanie w silnikach wysokoprężnych,* WKiŁ, Warszawa 1976.
[19] Swedish Environmental Protection Agency and Motortestcenter of the Swedish Motor Vehicle Inspection Company. Cold Climate Emissions 1993.

Journal of POLISH CIMAC

Faculty of Ocean Engineering & Ship Technology
GDAŃSK UNIVERSITY OF TECHNOLOGY

EFFECTS OF UNDERWATER EXPLOSION ON MINEHUNTERS SHAFTS LINES

Andrzej Grządziela

Naval University of Gdynia, Mechanical – Electrical Faculty
uL. Śmidowicza 69, 81-103 Gdynia, Poland,
tel. +48 58 626 27 24
e-mail: agrza@amw.gdynia.pl

Abstract

Ships' propulsion plant usually works in a hard environment caused by static forces and permanent dynamic loads. Exciding of tolerated values of shaft alignments causes a damage of radial and thrust bearings in relative short time. Modeling of dynamical reactions could bring information to the designer for recognizing the level of hazard for propulsion system. A paper presents a proposal of identification of a degree of hazard to ship shaft line due to forces of underwater explosion. A theoretical analysis was made of influence of changes in co-axiality of shafts resulting from elastic deformations of hull structure in vicinity of shaft bearing foundations. The main problem of naval vessels is a lack of dynamical requirements of stiffness of the hull. Modelled signals were recognized within sensitive symptoms of two sub models: model of propulsion system and model of shafts misalignment. Both sub models allow testing forces and their responses in vibration spectrum using SIMULINK software.

Keywords*: ship shaft lines, technical diagnostics, modelling, vibrations, underwater explosion*

1. Introduction

Minehunters propulsion systems are subjected to specific sea loads due to waving and dynamical impacts associated with underwater explosion. Sea waving can be sufficiently exactly modeled by means of statistical methods. Much more problems arise from modeling impacts due to underwater explosion. Knowledge of a character of impulse loading which affects ship shaft line can make it possible to identify potential failures by means of on-line vibration measuring systems.

2. Analysis of forces acting on shaft-line bearings

Ship shaft lines are subjected to loads in the form of forces and moments which generate bending, torsional and axial vibrations. In most cases strength calculations of driving shafts are carried out by using a static method as required by majority of ship classification institutions.

Moreover they require calculations of torsional vibrations which have to comply with permissible values, to be performed. Calculation procedures of ship shaft lines generally amount to determination of reduced stresses and safety factor related to tensile yield strength of material. The above mentioned methods do not model real conditions of shaft-line operation, which is confirmed by the character of ship hull response, i.e. its deformations under dynamic loads. Much more reliable would be to relate results of the calculations to fatigue strength of material instead of its yield strength [5].

In static calculation procedures no analysis of dynamic excitations, except torsional vibrations, is taken into consideration. In certain circumstances the adoption of static load criterion may be disastrous especially in the case of resonance between natural vibration frequencies and those of external forces due to dynamic impacts.

To analyze the dynamic interaction a simplified model of shaft line is presented below, Fig. 1.

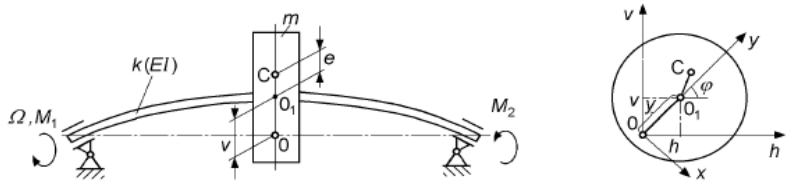

Fig. 1. A simplified shaft-line model for critical speed calculation [4]

Let us note: M_1 - torque, M_2 - anti-torque. The system can be represented by the following set of equations:

$$\begin{aligned} m\ddot{h} + kh &= me(\ddot{\varphi}\sin\varphi + \dot{\varphi}^2\cos\varphi), \\ m\ddot{v} + kh &= me(-\ddot{\varphi}\cos\varphi + \dot{\varphi}^2\sin\varphi), \\ (J + me^2)\ddot{\varphi} &= me(\ddot{h}\sin\varphi - \ddot{v}\cos\varphi) + M_1 - M_2. \end{aligned} \tag{1}$$

The presented form of the equations is non-linear. Considering the third of the equations (1) one can observe that the variables h, v and φ are mutually coupled. It means that any bending vibration would disturb rotational motion of the shaft. The third of the equations (1) can be written also in the equivalent form as follows:

$$J\ddot{\varphi} = ke(v\cos\varphi - h\sin\varphi) + M_1 - M_2 \ . \tag{2}$$

To obtain the shaft angular speed Ω_w constant to use time-variable torque is necessary:

$$M = M_1 - M_2 = ke(h\sin\varphi - v\cos\varphi). \tag{3}$$

Presented theoretical analysis indicates that shaft bending deformation continuously accumulates a part of shaft torque. However the quantity of torque non-uniformity is rather low

since shaft-line eccentricity is low;it results from manufacturing tolerance, non-homogeneity of material, propeller weight and permissible assembling clearances of bearing foundations. For minehunters propulsion system the torque pulsation expressed by means of Fourier series is much more complex. It additionally contains components resulting from number of propeller blades, kinematical features of reduction gear as well as disturbances from main engine and neighbouring devices. In general case occurrence of only one harmonic does not change reasoning logic.

Theoretical analysis of operational conditions of intermediate and propeller shafts indicates that static and dynamic loads appear. In a more detailed analysis of dynamic excitations of all kinds the following factors should be additionally taken into consideration:

- disturbances coming from ship propeller (torsional, bending and compressive stresses);
- disturbances from propulsion engine (torsional and compressive stresses);
- disturbances from reduction gear (torsional stresses);
- disturbances from other sources characteristic for a given propulsion system or ship mission.

3. Underwater explosion

Knowledge of loads determined during simulative explosions is helpful in dimensioning ship's hull scantlings [3]. Another issue is possible quantification of explosion energy as well as current potential hazard to whole ship and its moving system. From the point of view of shock wave impact on shaft line, underwater and over-water explosions should be considered in two situations:

- when shock wave (or its component) impacts screw propeller axially,
- when shock wave (or its component) impacts screw propeller perpendicularly to its rotation axis.

The axial shock-wave component affects thrust bearing and due to its stepwise character it may completely damage sliding thrust bearing. Rolling thrust bearings are more resistant to stepwise loading hence they are commonly used on naval ships [3]. The shock wave component perpendicular to shaft rotation axis is much more endangering. Shock wave can cause: damage of stern tube, brittle cracks in bearing covers and tracks, plastic displacement of shaft supporting elements including transmission gear and main engine, and even permanent deformation of propeller shaft. The problem of influence of sea mine explosion on hull structure is complex and belongs to more difficult issues of ship dynamics. Underwater explosion is meant as a violent upset of balance of a given system due to detonation of explosives in water environment. The process is accompanied with emission of large quantity of energy within a short time, fast running chemical and physical reactions, emission of heat and gas products. The influence of underwater explosion does not constitute a single impulse but a few (2 to 4) large energy pulsations of gas bubbles [2,8,9]. The pulsation process is repeated several times till the instant when the gas bubble surfaces. Hence the number of pulsations depends a.o. on immersion depth of the explosive charge. The character of changes of pressure values in a motionless point of the considered area is shown in Fig. 2. In the subject-matter literature can be found many formulae for determining maximum pressure value, based on results of experiments; however da ta on a character of pulsation and its impact on ship structures are lacking. To identify underwater explosion parameters a pilotage test was performed with the use of the explosive charge having the mass m = 37,5 kg. The schematic diagram of the experiment is shown in Fig. 3.

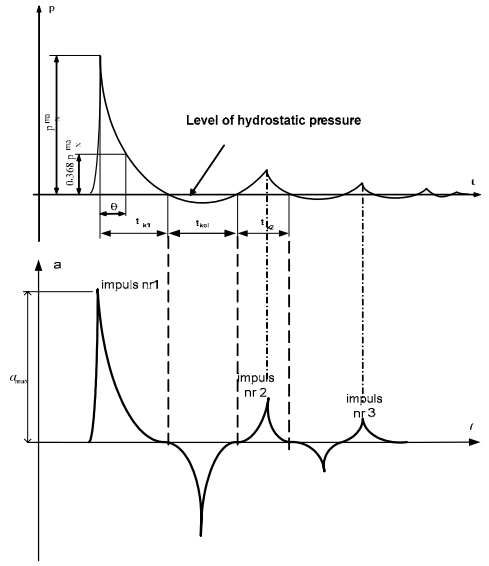

Fig. 2. Run of changes of shock wave pressure and ship hull acceleration measured on hull surface during underwater explosion.

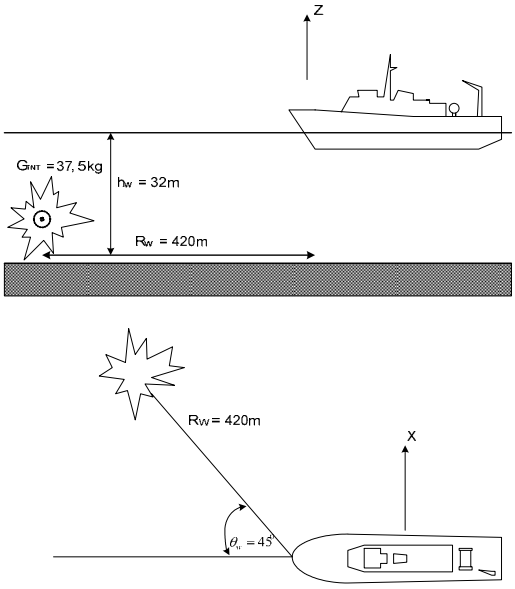

Fig. 3 Schematic diagram of the performed experimental test

During the sea-test were measured vibration accelerations of casings of intermediate and thrust bearings in the thrust direction and that perpendicular to shaft rotation axis. The ship course angle relative to the explosion epicentre was 45^0 and the shaft line rotated with the speed n_{LW}=500 rpm. Ship's distance from the mine and its immersion depth was determined by using

a hydro-location station and ROV underwater vehicle – figure 4. The vibration gauges were fixed over the reduction gear bearing as well as on the intermediate shaft bearing.

Fig. 4. ROV vehicle with TNT charge

The typical measurement record, in the vertical directions, is presented in Fig. 5. The time waveform of acceleration of the recorded signals were the same in all measurement points.

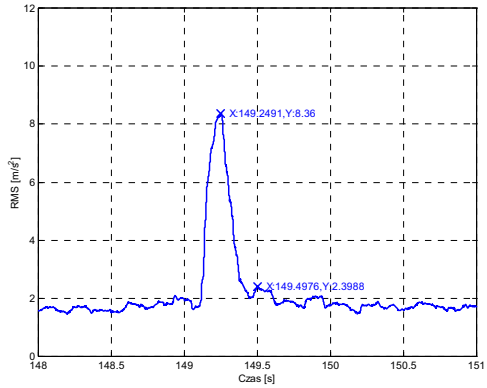

Fig. 5 Explosion, Port side (LB), Thrust bearing, V axis

The performed tests were aimed at achieving information dealing with:

- character of shock wave impact on shaft-line bearings , in the form of recorded vibration parameters;
- assessment of time-run of vibration accelerations with taking into account dynamic features of the signals in set measurement points;
- assessment of possible identification of influence of pulsation of successive gas bubbles during the time-run of vibration accelerations;
- identification of features of the signals by means of spectral analysis.

Since the mass of the explosive charge was small, to reliably identify the effect of only first and second pulsation was possible during the test.

4. Models of excitation due to underwater explosion

Analysis of dynamic impacts including impulse ones should take into account basic parameters which influence character of time-run of a given signal as well as its spectrum. The basic parameters which identify impulse impact resulting from explosion are the following:

- form of impulse which identifies kind of impulse;
- impulse duration time t_I at the ratio A/t_I maintained constant , which identifies explosive charge power (time of propagation of gas bubble);
- influence of damping on spectrum form , which identifies distance from explosion and - simultaneously - epicentre depth
- number of excitation impulses, which informs on distance from explosion, combined with explosive charge mass;
- time between successive impulses , which characterizes explosive charge mass;

The possible recording of measured shock wave pressure and accelerations on intermediate and propeller shaft bearings enables to identify some explosion parameters hence also hazards to power transmission system. Analysing the run of underwater shock wave pressure one is able to assume its time-dependent function (Fig. 6 and Eq. 4):

$$A = at^{kb} \cdot e^{kct} \tag{4}$$

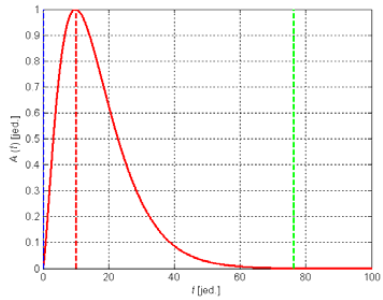

Fig. 6 Example of the function form for b=1,5 , c=-0,15 and k=1

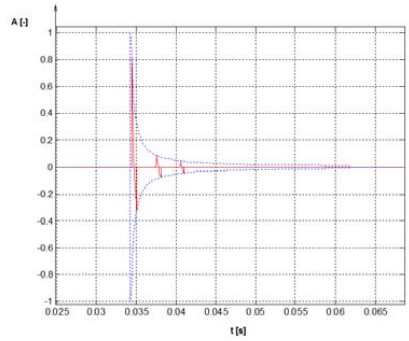

Fig. 7. Run of the assumed unit vibration acceleration model

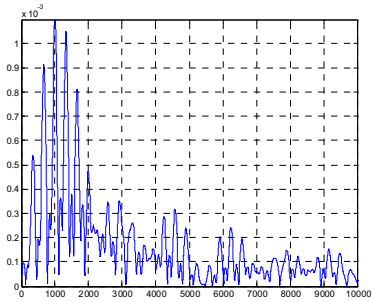

Fig. 8. Spectrum of the assumed vibration acceleration model

For the assumed mathematical model of the first shock wave impulse the run of vibration accelerations recorded on ship hull - for the example function given in Eq. 4 - can be presented as shown in Fig. 7 and 8.

5. Model of shaftline

The proposed model of minehunter shaft line is nonlinear and it is presented in Fig. 9.

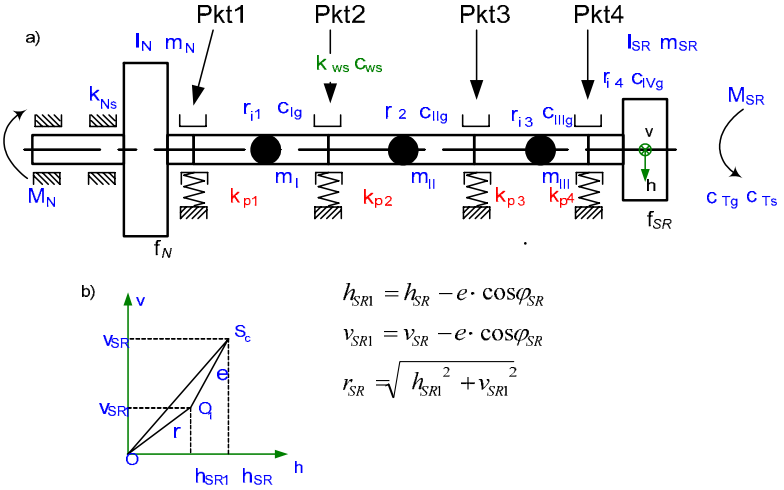

Fig. 9 Scheme of shaft line of minehunter, where:

I_N; m_N - reduced moment of inertia of the propulsion part, I_{SR}; m_{SR} - reduced moment of inertia of the propelled part, M_N; M_{SR} – torque and anti torque - propeller, m_I; m_{II}; m_{III} – reduced mass of shaft between bearings, k_{Ns} - torsional stiffness of propulsion system, r_{i1}; r_{i2}; r_{i3}; r_{i4};- coefficients of bending stiffness elements of shaft between bearings, c_{Ig}; c_{IIg}; c_{IIIg}; c_{IVg} - coefficients of bending damping elements of shaft between bearings, k_{ws}; c_{ws} - coefficients of torsional stiffness and damping of the shaft, φ_N; φ_{SR} – angles of rotation propulsion system and propeller, h_{SR}; v_{SR} – horizontal and vertical coordinates of centre of gravity S_c (after the shaft deflection), h_{SR1}; v_{SR1} - horizontal and vertical coordinates of centre of rotation O_1, h_N; h_I; h_{II}; v_N; v_I; v_{II} - horizontal and vertical coordinates for masses m_N; m_I; m_{II}, c_{Tg}; c_{Ts} - resistance of water bending and torsional damping

The model fulfill following requirements:

- it allows to insert the environmental loads,
- it allows to insert to the model the impulse of underwater explosion,
- the model reacts to changes of rotational speed of shaft line,
- the model reacts for axes misalignment,
- it keeps concordance in spectral and time domains with real object.

The kinetic energy of the model of shaft line can be represented by the following equation:

$$E_k = \frac{1}{2} I_N \dot{\varphi}_N^2 + \frac{1}{2} I_{SR} \dot{\varphi}_{SR}^2 + \frac{1}{2} m_I (\dot{v}_I^2 + \dot{h}_I^2) + \frac{1}{2} m_{II} (\dot{v}_{II}^2 + \dot{h}_{II}^2) + \\ + \frac{1}{2} m_{SR} (\dot{v}_{SR}^2 + \dot{h}_{SR}^2) + \frac{1}{2} m_N (\dot{v}_N^2 + \dot{h}_N^2) \tag{5}$$

The potential energy is written as follows:

$$E_p = \frac{1}{2} k_{NS} \varphi_N^2 + \frac{1}{2} k_{ws} (\varphi_{SR} - \varphi_N)^2 + \frac{1}{2} k_{Ig} (h_I^2 + v_I^2) + \frac{1}{2} k_{IIg} (h_{II}^2 + v_{II}^2) + \\ + \frac{1}{2} k_{IIIg} (h_{III}^2 + v_{III}^2) + \frac{1}{2} k_{IVg} (h_{SR1}^2 + v_{SR1}^2) \tag{6}$$

and the dissipated energy in form:

$$E_R = \frac{1}{2} c_{ws} (\dot{\varphi}_{SR} - \dot{\varphi}_N)^2 + \frac{1}{2} c_{Ts} \dot{\varphi}_{SR}{}^2 + \frac{1}{2} c_{Ig} (\dot{h}_I^2 + \dot{v}_I^2) + \frac{1}{2} c_{IIg} (\dot{h}_{II}^2 + \dot{v}_{II}^2) + \\ + \frac{1}{2} c_{IIIg} (\dot{h}_{III}^2 + \dot{v}_{III}^2) + \frac{1}{2} c_{IVg} (\dot{h}_{SR1}^2 + \dot{v}_{SR1}^2) \tag{7}$$

It allows obtaining the second kind of Lagrange's set of equations which can be represented as follow:

$$\begin{aligned}
&I_N \ddot{\varphi}_N + c_{ws} (\dot{\varphi}_N - \dot{\varphi}_{SR}) + k_{NS} \varphi_N + k_{ws} (\varphi_N - \varphi_{SR}) = M_N \\
&m_I \ddot{h}_I + c_{Ig} \dot{h}_I + r_{11} h_I + r_{12} h_{II} + r_{13} h_{III} + r_{14} h_{SR} = 0 \\
&m_I \ddot{v}_I + c_{Ig} \dot{v}_I + r_{11} v_I + r_{12} v_{II} + r_{13} v_{III} + r_{14} v_{SR} = 0 \\
&m_{II} \ddot{h}_{II} + c_{IIg} \dot{h}_{II} + r_{21} h_I + r_{22} h_{II} + r_{23} h_{III} + r_{24} h_{SR} = 0 \\
&m_{II} \ddot{v}_{II} + c_{IIg} \dot{v}_{II} + r_{21} v_I + r_{22} v_{II} + r_{23} v_{III} + r_{24} v_{SR} = 0 \\
&m_{III} \ddot{h}_{III} + c_{IIIg} \dot{h}_{III} + r_{31} h_I + r_{32} h_{II} + r_{33} h_{III} + r_{34} h_{SR} = 0 \\
&m_{III} \ddot{v}_{III} + c_{IIIg} \dot{v}_{III} + r_{31} v_I + r_{32} v_{II} + r_{33} v_{III} + r_{34} v_{SR} = 0 \\
&I_{SR} \ddot{\varphi}_{SR} + c_{ws} (\dot{\varphi}_{SR} - \dot{\varphi}_N) + c_{Ts} \dot{\varphi}_{SR} + c_{IIIg} (\dot{h}_{SR} e \sin \varphi_{SR} - \\
&\dot{v}_{SR} e \cos \varphi_{SR} + e^2 \dot{\varphi}_{SR}) + k_{ws} (\varphi_{SR} - \varphi_N) + \\
&r_{44} (h_{SR} e \sin \varphi_{SR} - v_{SR} e \cos \varphi_{SR}) = M_{SR} \\
&m_{SR} \ddot{h}_{SR} + c_{IVg} (\dot{h}_{SR} + \dot{\varphi}_{SR} e \sin \varphi_{SR}) + r_{41} h_I + r_{42} h_{II} + r_{43} h_{III} + \\
&r_{44} (h_{SR} - e \cos \varphi_{SR}) = 0 \\
&m_{SR} \ddot{v}_{SR} + c_{IVg} (\dot{v}_{SR} - \dot{\varphi}_{SR} e \cos \varphi_{SR}) + r_{41} v_I + r_{42} v_{II} + \\
&r_{43} v_{III} + r_{44} (v_{SR} - e \sin \varphi_{SR}) = 0
\end{aligned} \tag{8}$$

The model of shaft line is implemented to the MATLAB SIMULINK software with accordance of mentioned requirements – Fig. 10.

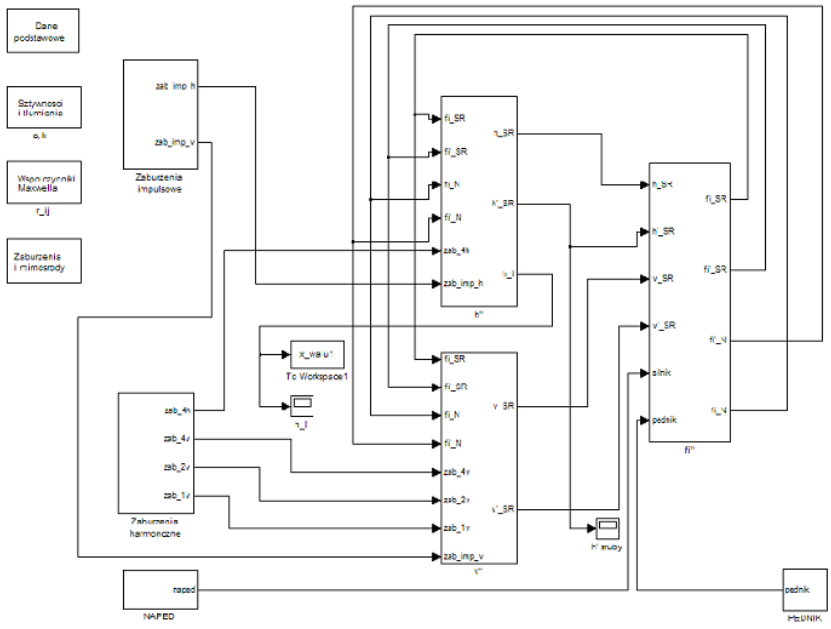

Fig. 10 Scheme of structure shaft line model in the MATLAB SIMULINK

Typical dangers for minhunter propulsion system are stresses coming from underwater explosion. Presented model allows calculating reactions in time and frequency domain. The example of spectrum of vibration acceleration in the point 3 of model (Fig. 9) during the simulated explosion is presented in the Fig. 11.

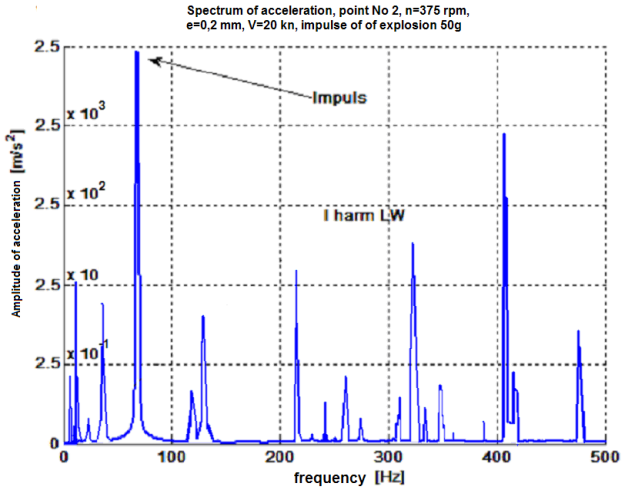

Fig. 11. The spectrum of acceleration with the inserted simulation of underwater explosion

6. Final conclusions

It's common knowledge that failure frequency is the most hazardous factor in marine industry, just after aeronautics. Dynamic reactions which occur on ships in service at sea are rarely able to produce wear sufficient to cause a failure. The possible application of an on-line monitoring system of vibration parameters of the propulsion system of minehunter makes it possible to perform the typical technical diagnostic tests of torque transmission system and to identify possible plastic deformations of hull plating as a result of underwater explosion.

The modelling of impulse impact form and next its identification makes it possible additionally: to identify explosion power by using an analysis of the first vibration impulse amplitude and its duration time, to identify distance from explosion epicentre (hence a degree of hazard) by analysing signal's damping, to identify a kind of explosion and even characteristic features of type of used mine, to select dynamic characteristics of a measuring system which has to comply with requirements for typical technical diagnostics and for a hazard identification system, to identify elastic or plastic deformation of shaft line by using spectral assessment of its characteristic features from before and after underwater explosion.

The presented results of modelling related to the performed experimental test do not make it possible - due to strongly non-linear character of interactions occurring in sea environment – to assign unambiguously the modelled signal features to those of the recorded ones during the real test.

Successive experimental tests will make it possible to verify features of the signals assumed for the analysis, to be able to build reliable models.

The wide range of stochastic dynamic loads acting on ships during its life-time makes that in the nearest future the application of on-line diagnostic techniques to ship propulsion systems, based on analysing vibration signals, will constitute an obvious tactical and technical necessity.

References

[1] Cempel, Cz., Tomaszewski F. (Ed.), *Diagnostics of machines. General principles. Examples of applications,* Publ. MCNEM, Radom 1992.

[2] Cole, R. H., *Underwater Explosions*, Princeton University Press, Princeton 1948.

[3] Cudny, K., Powierża Z., *Selected problems of shock resistance of ships (in Polish)*, Publ. Polish Naval University, Gdynia 1987.

[4] Dąbrowski, Z., *Machine shafts (in Polish),* State Scientific Publishing House (PWN), Warszawa 1999.

[5] Dietrich, I., Kocańda, S., Korewa, W., *Essentials of machine building (in Polish)*, Scientific Technical Publishing House (WNT), Warszawa 1974.

Journal of POLISH CIMAC

Faculty of Ocean Engineering & Ship Technology
GDAŃSK UNIVERSITY OF TECHNOLOGY

INTRODUCTION TO DIAGNOSTIC INVESTIGATION OF MARINE DIESEL ENGINES AT LIMITED MONITORING SUSCEPTIBILITY

Zbigniew Korczewski, Marcin Zacharewicz

The Polish Naval Academy
Ul. Śmidowicza 69, 81-103 Gdynia, Poland
Tel.: +48 58 626 23 82
e-mail: M.Zacharewicz@amw.gdynia.pl

Abstract

There have been presented preliminary assumptions of the new diagnostic method concerning the marine diesel engine's workspace areas, which had been elaborated at the Polish Naval Academy. There is expected that the method will be very useful to diagnose technical shape of marine diesel engines at limited monitoring susceptibility, it means, which are not equipped with the indicator valves. The research problem and main purposes of the research have been formulated. The notion of the workspace areas has been defined, moreover the analysis of factors that have the most decided impact on destruction phenomenon has been carried out. There have been also considered operation strategies applied at present on marine diesel engines: according to the engine installation life, according to the technical shape as well as according to the level of reliability. The mutual interdependences between characteristic technical states of the research object (workspace areas) have been characterized. The conducted research is showed in the background of achievements of foreign and national scientific centres. By this way the research diagram of gasdynamical processes has been precised for diagnostic purposes of marine diesel engines.

Keywords: *Marine diesel engines, diagnostics, workspaces area*

1. Introduction

How to elaborate a diagnostic method that makes it possible to diagnose workspace areas of marine diesel engines, which are not provided with indicator valves, represents the most important research question for diagnostic teams from the Polish Naval Academy nowadays. Such the engines have been recently implemented into the Polish Navy. The main solved problem consists in determination of the relation between gasdynamical parameters of the working medium inside exhaust passages and the alterations within the structure of an engine's workspace areas. The authors estimate that the elaborating diagnostic method makes it possible to introduce the operation system according to technical shape for diagnosing workspace areas of marine diesel engines without indicator valves. It means that in practice all the worship's diesel engines in the Polish Navy will be operated according to their technical state.

2. The reasons of unserviceable states appearance within marine diesel engine's workspace areas

Marine diesel engines are in common usage on boards of the Polish Warships. There are usually high-speed and medium-speed engines equipped with turbochargers [8,17]. The largest number of the turbochargers works in the pulsatory configurations of supercharging systems. Such the engines represent the part of the ship's propulsion system (the main engines) as well as the part of the ship's electric power plant (the auxiliary engines).

Every combustion engine is characterised with a transformation energy process where the chemical energy is transformed into thermal energy that is subsequently transformed into

mechanical work. The production of mechanical work as well as chemical reactions during fuel combustion process in the engine's cylinders are tightly associated with the series of undesirable phenomena that have essential impact on a technical state of the construction structure components and especially their workspace areas. Chemical reactions representing the result of combustion process cause heat and exhaust creation. The exhaust represents a gas mixture, which can be polluted by solid combustion products. The solid components of the burning process can create difficult removable deposits on surfaces of the engine's workspace Futhermore, the hard mineral pieces of and other hard solid body flowing in thermodynamical medium cause erosion processes on surfaces of the workspace areas structure. Moreover, anhydride of sulphurous and hydro sulphuric acids begin to exist as the burning products. The acids represent the reason for chemical corrosion of engine's components (especially in the region of engine's workspace areas) [10,15].

Another reason for appearing diesel engines unserviceable states is a metal fatigue. Periodically changeable mechanical and thermal stresses represent a main reason for the metal fatigue [1,10,15].

All the foregoing specified fatigue processes and phenomena lead to the degradation of construction structure within diesel engine's workspace areas.

The workspace areas of the marine diesel engines are the research objects considered in the paper, as follow:

- cylinder sections, limited by cylinder liner, crowd along with rings and the engine's head,
- air and exhaust passages connecting engine's cylinders with turbocharger,
- compressor's and turbine's internal channel of the turbocharger set.

A schematic diagram of the relation between particular engine's workspace areas is presented in figure 1. There are distinguished in the diagram particular engine's workspace areas and flow directions of the thermodynamical medium. Moreover, influences (feedbacks) between particular flow machines are shown in the figure as well: working periodically – cylinders of the engine and working continuously – turbocharger's rotor.

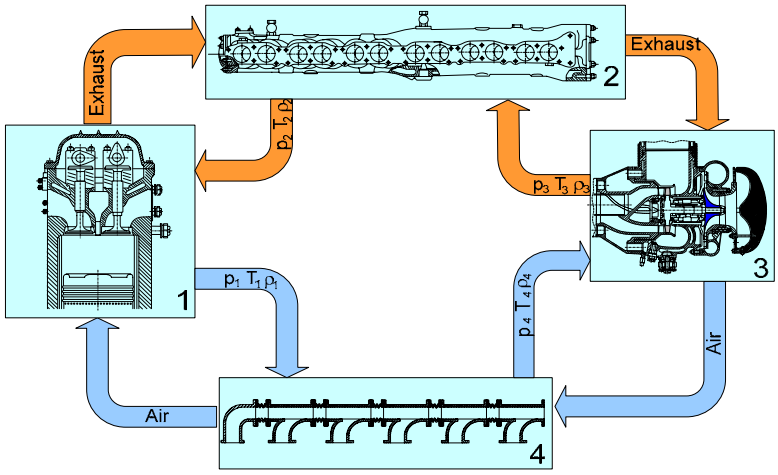

Fig. 1. The relation between particular engine's workspace areas
1 – combustion chamber, 2 – exhaust channel, 3 – turbocharger, 4 – inlet channel

The author's reliability research led to the conclusion that the majority of marine diesel engine's unserviceable states accounts for a consequence of physical and chemical destruction processes [10]. The most often faced failures concern the cylinders sections. They represent the

result of solid burning product's deposits on surfaces of cylinder liners, bottom of crowds and the engine's heads.

The solid burning product's deposits lead to progressive reduction of cylinders volumes. As a consequence a deterioration of engine's running occur (considerable non-uniform loads between the cylinder systems). In other hand, the cylinder volume can increase during engine's operation. The process of volume increasing of the engine's combustion chamber is associated with the increase of bearing clearances between a connecting rod and crowd pin or between a connecting rod and crankshaft. It leads to increase of the load dispersion around the average value as well [12].

The solid burning products can also seat into grooves of piston gas rings. It leads to the loss of leak tightness of the piston-ring-cylinder system (PRC) as well as to leakages of the thermodynamic medium from the combustion chamber [10].

Inlet and outlet valves of the cylinder sections (simultaneously, air and exhaust flow passages). Are another vulnerable components of the engine's workspace areas. Exhaust valves are the most endangered engine's parts with the failures. They work at the severe conditions being flowed by hot, chemical active ("aggressive") exhaust gass es. Such a working environment of the exhaust valves has an essential impact on wear intensity of precision pair: valve stem – guide. In the extreme cases, as a result of forces and torques influences on the valve stem the valve head may "skewed" and the working medium leakage from the combustion chamber may appear [10].

The exhaust channel cooled with sea water represents the next key component of engine's workspace areas. The marine diesel engine's exhaust channels are exposed to degradation of technical structure as a result of operation in unfriendly sea conditions (on the board of worships). Pollutions gathered on channel's interior surfaces, representing solid combustion products, are the reason of failures appearance in the most frequent cases. The pollution process leads to the constant decrease of exhaust channel's face area and decrease of channel's volume. Moreover, the exhaust channel is exposed to activity of aggressive and hot exhaust gasses. Additionally it is exposed to chemical and stress corrosion [1].

Turbocharger's internal passages represent an equally important component of the engine's workspace areas from the reliable functioning point of view. The turbine's internal channels are threaten to solid substance contents in exhaust gases. In the other hand, the compressor is submitted to solid substance contents in the sucked air (especially mineral particles). The solid particles which flow through turbine and compressor's internal channels form deposits on the surface of turbocharger's rotor. The solid deposits cause mass growth of turbocharger's rotor and diminish its rotational speed. As a consequence of this process compression ratio and mass flow rate of the compressor decrease and an efficiency of turbine and compressor are fallen. The decrease of mass flow rate leads to deterioration of the combustion air factor. This process makes the burning process poor and solid particles emission increases. Moreover, the polluted compressor works without a stability margin of the flow process [10, 15].

The turbocharger's rotor might also lost a mechanical stability as a result of the turbocharger's internal passages pollution. The loss of turbocharger's rotor stability leads to mechanical vibration and finally leads to the mechanical resonance phenomenon that causes an accelerated wear process of turbocharger's bearing nodes and fatigue cracks of the rotor's blades [1, 10].

Erosion phenomenon represents a different consequence of turbocharger's internal passages pollution. The phenomenon usually leads to the growth of passages' surface roughness and to the changes of profile geometry of turbine's and compressor's blades [10, 15].

3. The operation strategies of marine diesel engines

Destruction processes worked out inside marine diesel engine's workspace areas are unavoidable and continuous and always associated with the engines' operation in sea conditions.

Searching optimum strategy of the engine's operation represents the only way for minimization of the occurrence probability of primary or secondary failures. The optimal strategy of engine's operation should secure maximum time extension of the failure-free operation. Moreover, the engine should be efficient enough and should assure high dynamic and static performance. The strategy of marine diesel engine's operation should also take into account functioning the diagnostic system, which gives possibilities to detect initial stages of developed states of operational unfitness. The following operating decisions are undertaken on the basis of formulated diagnosis about the engine's technical state: further running without any limits, introduced limitations of permissible engine's loads, mending or cleaning workspace areas. The earlier will be detection and unfitness states removal the cheaper will be costs of damages' repair. Moreover, the precise and early unfitness detection allows shortening the repair time [7, 9].

Three different operation strategies could be distinguished as a result of searching the most efficient operation strategy:

1. Operation according to the overhaul life – assumes the exchange of particular engine's elements after strictly defined period called the overhaul life. This strategy is useful enough in the cases when the engine's elements are characterized with visible dependence between intensity of the defect appearance and the time of the engine's running. This relation should involve a short interval of time. Moreover, this method could be put into practise when the elements have limited monitoring susceptibility and designing the diagnostic system is not remunerative. A typical function course of failures' intensity is shown in figure 2 – curves 1. The overhaul life strategy is effective for the engine's elements, which are endangered for cyclically changing stresses. They drive to the material fatigue, especially within mechanical systems.
2. Operation according to technical state – consist in a periodical control of the technical state of engine's elements which are involve with the diagnostic system. The strategy proves its usability for those construction elements which unfitness dispersion spreads in wide interval of the time and failures develop very slowly. Moreover, the diagnostic system should assure the unfitness's localisation, precision estimation of technical state tendency and should give precision prognosis about the time of correct engine's running. The operation strategy according to the technical state leads to increase of average working time without any damages. It directly drives to diminishing operation costs. This strategy allows short time engine's operation with a slight unfitness it means at slightly lower engine's efficiency. A typical course of the density of engine's elements damages probability function is shown in figure 2 – curves 2. The operation experiences of the engines applied in the Polish Navy warships clearly show that such a strategy could be very useful for the engine's workspace areas.
3. Operation according to the level of reliability concerns the engine's functional systems, for which the time of correct functioning has exponential schedule or when there is not existing a dependence between an intensity of damages occurrence and the working time (there is a random damages occurrence that is independent of the time). The engine's elements are operated up to the damages uprising. The operation system permits the failure's existence which is not dangerous for the engine's reliability and when it could be quickly removed. The technical services are carried out only when they are absolutely necessity and intended unfitness can't be identified with diagnostic activities. A typical course of the density of engine's elements damages probability function is shown in figure 2 – curves 3 end 4. The operation strategy according to the level of reliability is effective enough for electronic components of the engines' control systems.

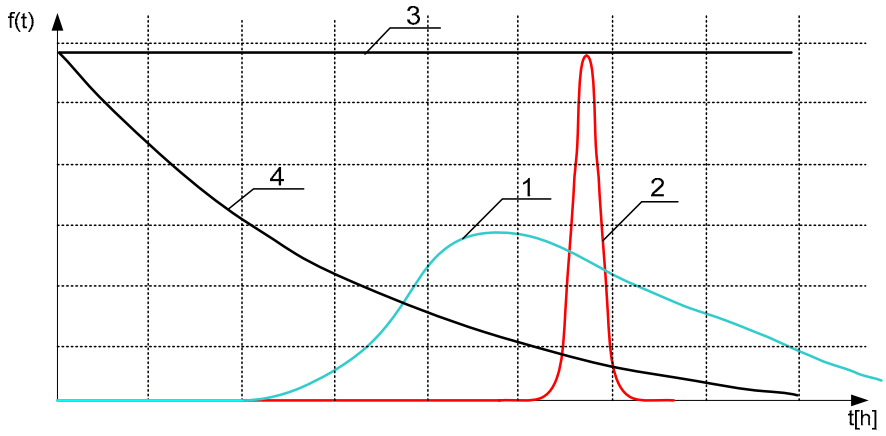

Fig. 2. Time courses of a density of the engine's elements damages probability function while the engine is operated according to: 1- overhaul life, 2- technical state, 3 and 4 - level of reliability

As far as the evaluation of the working spaces technical shape is concerned a proper qualification of the limiting engine's technical states and their classes represents the most important, key diagnostic problem. The example dependences between the states of an engine's efficiency and the states of an engine's technical fitness in an aspect of the parameters of construction structure within exhaust channel are showed in figure 3. The figure 3 takes into account two different cases of the failure's occurrence: natural and sudden [20]. Curves 1 represents a natural case of the failure, curves 2 represents a sudden case of the failure. The natural cases of the failure are typical for the dirt of workspaces areas. The sudden cases of the failure are typical for material fatigues of the engine's elements, for example, like the failure presented in figure 4. There is presented in figure 4 compressor's stator blades with stuck a broken metal piece of the exhaust manifold.

The majority of warship's engines are subject to the operation according to their technical state. Diagnostic tests of the workspace areas base on the results of measurements of intracylindrical pressures. The diagnostic measurements are performed by means of highly specialized pressure recorders equipped with pressure sensors for example OPTRAND type sensors. But there is still an unsolved problem concerning the diagnosing engine's workspace areas while there are no possibilities to measure intracylindrical pressures. In such a situation, while the engine is not equipped with the indicator valves, the workspace areas are only diagnosed with the use of endoscopies. The diagnostic endoscopic tests make it possible to assess the state of visible surfaces limiting workspaces areas [10].

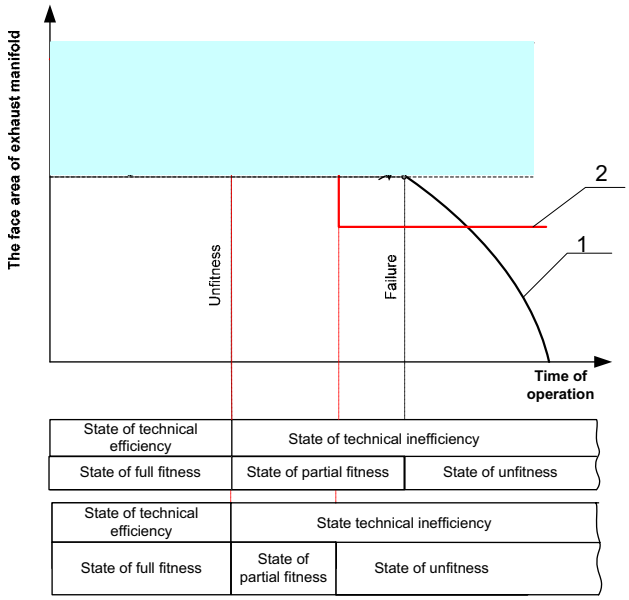

Fig. 3. Dependences between the characteristic states of workspaces areas, for which the technical state can be defined by only one parameter of constructional structure – the face area of exhaust manifold
1 - natural failure, 2 - sudden failure.

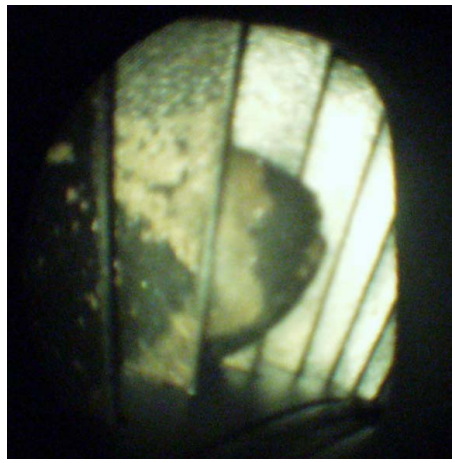

Fig. 4. A metal piece of exhaust manifold stuck into the stator blade cascade of a turbocharger's turbine

The problem „how to diagnose workspace areas of the engines without indicator valves" has become recently very important for the diagnostic team from the Polish Naval Academy [2, 13]. This is a fundamental diagnostic issue because nowadays such engines are in common operation in the Polish Navy. The following engine constructions represent mentioned above a type of the engine:

- main engines ZWIEZDA M520 and ZWIEZDA M520 type, applied on warships 205 and 660 type,

- main engines ZWIEZDA M401A1/A2 type, applied on warships 607 type,
- auxiliary engines DETROIT DIESEL DDA149TI type, applied on warships Oliver Hazard Perry type.

Low diagnostic susceptibility and common application the foregoing mentioned engines enforces the necessity of searching new alternative methods, which make it possible to conduct a parametric evaluation of the engine's workspace areas technical state. The author's scientific experiences, confirmed by results gathered during engines' operation enable formulating the conclusion that the analyze of time pressure courses along the exhaust passages could represent one of the most promising diagnostic method.

An idea of engine's diagnostic tests on the basis of the observation of exhaust pressure's alterations in outlet passages of the working medium is original. So far, gasdynamical processes inside exhaust manifold were analysed only for construction purposes. A wide variety of bibliography clearly shows that a number of polish and foreign researchers specialised with IC engine construction have dealt with gasdynamical processes in the exhaust passages. Many of them can be also very useful in our research, for example publications like [4,5,11,14,19].

Many accessible publications within the scope of diagnostics of marine diesel engines stand for the results of research worked out mainly on automotive engines. Majority of the publications where the authors describe methods of automotive engine's technical state evaluation is directed to construction elements that has the most essential impact on the engine's efficiency, performance and intensity of harmful chemical emission in the exhaust [6]. Only few research teams deal with diagnostic issue of the engines that have different assignment like marine engines. The issue of diagnosing the IC engine's construction modules has been also considered in other publication that was very useful for the authors [1, 2, 3, 10, 13, 16, 18].

4. The research problem

The literature review, author's experiences in marine diesel engines' operation and diagnosing as well as results of diagnostic examinations worked out by the scientific centres in the country and abroad make it possible to formulate a research problem, as follow:

How to conduct diagnostic research aimed an evaluation of the technical shape of marine diesel engines' workspace while the engines are not equipped with the indicator valves in current operation?

The immediate, quantitative and qualitative assessment of cylinders processes is not possible for the engines mentioned above hence the diagnostic problem how to diagnose diesel engines without indicator valves" become an essential operation problem. It results from the fact that those type of engines are in common use in the Polish Navy warships. In the light of the conducted analysis on the possibilities of diagnosing the considered engines there has been formulated a following thesis:

The alterations of the technical state of engine's workspace areas generate deformations within the courses of pressure waves along the exhaust manifold powered a turbine of the turbocharger. Such alterations determine an energy flux of the exhaust in front of the turbine and in the same way – turbine's power, delivery of the supercharged compressor, in general the engine's performance and efficiency. That's why there is possible to distinguish adequate diagnostic parameters from the file of gasdynamical parameters which characterize pulsation flow of exhaust gasses discharging the engine's cylinders .

5. Main purposes of the research

An elaboration of the diagnostic method of the engine's workspace areas on the basis of the exhaust pressure measurements in the channels connecting the engine cylinders and turbocharger's turbine represents the main aim of the research works undertaken. The elaborated methodology of the diagnostic research enables:

- estimation of the load inequality among the cylinder sets,
- identification of those cylinders the working process of which are significantly different from the remaining ones,
- identification of unserviceable operation states of the functional engine subsystems that have an impact on the course of the fuel burning process inside the combustion chambers.

6. The fundamental assumptions of the research methodology

A consideration of gasdynamical phenomena in exhaust manifolds of marine diesel engines enforces an elaboration of a research realisation scheme. The research's scheme (figure 5) consists of classical (according to Cannon's theory) approach to gasdynamical processes in diesel engines, like: a physical model, mathematical model, simulating experiments on the real object and on the elaborated mathematical model. Diagnostic blocks like: alterations of the research object's structure parameters and gathering results of research in data base "unfitness – symptoms" represent the innovated elements in an issue of processes' mathematical modelling called "simulating diagnostics". A scheme of the re search performance is presented in figure 5.

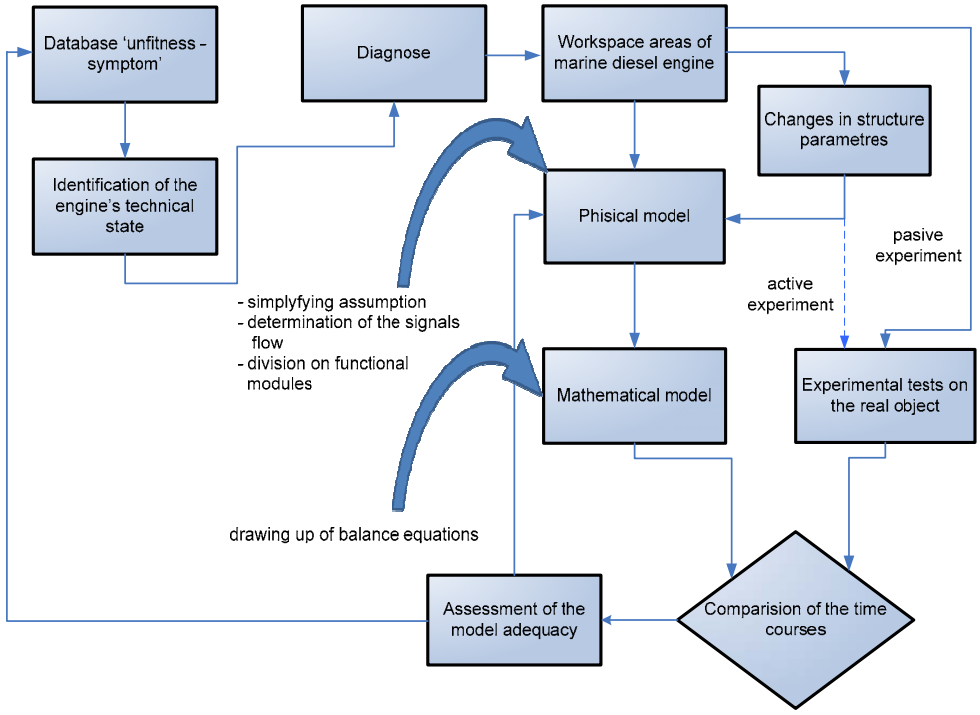

Fig. 5. The research scheme of gasdynamical processes examinations for diagnostic purposes of marine diesel engines

According to the introduced algorithm of the research conduction, investigations on real objects and the mathematical model elaboration have been worked out simultaneously. The time courses of the observed gasdynamical parameters represent the result of conducted measurements. During the realization of investigations on laboratory SULZER engine 6 AL 20/24 type a possibility of modifying constructional structure of its working spaces was foreseen. However in case of ZWIEZDA engine M401 type and DETROIT DIESEL engine DDA 149 TI type a passive experiment on large population of operated engines was assumed. A necessity of the passive experiment application results from the lack of possibility in introducing alterations into the constructional structure of working spaces of engines being currently operated.

7. Conclusion

Considerations presented in this article stand for an introduction to the elaboration of diagnostic method of marine diesel engines working spaces having low supervisory susceptibility. It results from non providing of them in indicator valve. A lack of indicating possibility of the engine's cylinders excludes the possibility of an accomplishment of the quantitative and qualitative comparative analysis of the changeability of intracylindrical pressures courses. By this way a qualification of the technical state of the engine's working spaces could not be done during engine's operation.

As a result of the analysis of accessible professional literature as well as the conducted preliminary investigations the thesis, aims and basic assumptions of the methodology concerning an investigation of the processes worked out in working spaces of the marine diesel engine for diagnostic purposes were formulated.

It is expected that the worked out methodology of diagnostic investigations makes it possible to implement the strategy of engines' operation according to their technical state into operation system of the Polish Navy warships. It will contribute to enlargement of their reliability and durability.

Bibliography

[1] Girtler, J., i inni, *Identyfikacja stanu technicznego układów korbowo – tłokowych silników o zapłonie samoczynnym, ze szczególnym uwzględnieniem emisji akustycznej jako sygnału diagnostycznego*, Opracowanie w ramach projektu badawczego MNiSW nr: N504 043 31/3480.

[2] Bruski, S., *Zastosowanie metod analizy częstotliwościowej drgań skrętnych wału napędowego do identyfikacji stanu technicznego wtryskiwaczy paliwa średnioobrotowego silnika okrętowego w eksploatacji*, Rozprawa Doktorska, AMW, Gdynia 2005.

[3] Czajgucki, Z., *Niezawodność spalinowych siłowni okrętowych*, WM, Gdańsk 1984.

[4] Dornseifer, T., Grobel, M., Neunhoeffer, T., *Numerical simulation in fluid dynamics*, SIAM, Philadelphia 1981.

[5] Dzierżanowski, P., Łyżwiński, M., Szczeciński S., *Silniki Tłokowe*, WKŁ, Warszawa 1981,

[6] Güther, H., *Diagnozowanie silników wysokoprężnych*, WKŁ, Warszawa 2002.

[7] Hebda, M., Mazur, T., Pelc, H., *Teoria eksploatacji pojazdów*, WKŁ, Warszawa 1978.

[8] *Jane's Fighting Ships 2005-2006*, jfs.janes.com, GB 2005.

[9] Kluj, S., *Diagnostyka urządzeń okrętowych*, WSM, Gdynia 2000.

[10] Korczewski, Z., *Endoskopia silników okrętowych*, AMW, Gdynia 2008.

[11] Kordziński, C., Środulski, T., *Silniki spalinowe z turbodoładowaniem, WKŁ, Warszawa 1970.*

[12] Lus, T., *Historia jednej niesprawności silnika okrętowego 6TD48*, Wydawnictwo Uczelniane Politechniki Szczecińskiej, Szczecin 2006.

[13] Łutowicz, M., *Identyfikacja procesu sprężania okrętowego tłokowego silnika spalinowego dla potrzeb diagnostyki jego przestrzeni roboczych*, Rozprawa Doktorska, AMW, Gdynia 2006.
[14] Szczeciński, S., *Lotnicze silniki tłokowe*, MON, Warszawa 1969.
[15] Piaseczny, L., *Technologia naprawy okrętowych silników spalinowych*, WM, Gdańsk 1992.
[16] Tomczak, J., L., *Metodyka bezpośredniego określania położenia kątowego wału korbowego silnika okrętowego i jej wykorzystania w indykatorze elektronicznym*, Rozprawa Doktorska, PG, Gdańsk 2001.
[17] Wajand, J.A., Wajand, J. T., *Tłokowe silniki spalinowe średnio i szybkoobrotowe*, WNT, Warszawa 2005.
[18] Wisłocki, K., *Studium wykorzystania badań optycznych do analizy procesów wtryski i spalania w silnikach o zapłonie samoczynnym*, WPP, Poznań 2004.
[19] Wiśniewski, S., *Obciążenia cieplne silników tłokowych*, WKŁ, Warszawa 1972.
[20] Żółtowski, B., Ćwik, Z., *Leksykon diagnostyki technicznej*, ATR, Bydgoszcz 1996.

Journal of POLISH CIMAC

Faculty of Ocean Engineering & Ship Technology
GDAŃSK UNIVERSITY OF TECHNOLOGY

EXPERIMENTAL DETERMINATION OF LOW SPEED DIESEL ENGINE CRANKSHAFT TWISTING

Przemysław Kowalak

Maritime University of Szczecin – Department of Engineering
70-500 Szczecin, Waly Chrobrego 1-2
tel: +48 91 4809400, fax: +48 91 4809575
e-mail: pkowalak@am.szczecin.pl,

Abstract

The exhaust gas emission control, together with the demand for specific fuel oil consumption reduction, poses a challenge for constructors. As a possible solution a very accurate fuel injection and combustion process control is considered. Such a control needs a precise timing and synchronization with every piston movement. The understanding of crankshaft deformation phenomena seems to be essential. In this work the experimental methodology of the crankshaft twist angle determination has been presented. The method is based on the cylinder pressure signal and an incremental encoder signal analysis. The presented results show the mean value of crankshaft twist angle under load. The momentary values are presented, too.

Keywords: *transport, marine diesel engines, engine control TDC determination, torsional vibration*

1. Introduction

Today's marine engines face the need of a very accurate control. The latest exhaust gas emission restrictions together with high demands for low specific fuel consumption force constructors to a very fine tuning of the combustion process. Such a tuning is impossible without a very exact control of fuel injection and the exhaust valve timing.

As today's marine engines are characterized by a very high power per cylinder the performance verification by means of cylinder indication becomes of utmost importance. In his work Polanowski [8] recognized a set of error sources of mean indicating pressure determination. Like other authors [2, 3, 6, 8, 10, 11] he defined the TDC determination error as the highest source among others.

The latest marine engines constructions based on the common rail idea (Wärtsilä), or electro-hydraulic camshaft (MAN diesel A/G) utilize a precise crankshaft positioning for correct timing of fuel injection and valves timing and for engine's cylinder indication [7]. The positioning sensor is placed on one side of the crankshaft only, usually on its free end. It can be adjusted only when the engine is stopped to indicate static position of the crankshaft. The typical static crankshaft positioning process is done for one cylinder unit only. The other unit positions are calculated based on the shaft geometry and engine's firing order. Such a procedure has some disadvantages as the crankshaft twist due to loading torque and torsional vibration deformation are not taken into account [5].

The crankshaft deformation under load can be estimated with the aid of finite elements method [4]. However it is difficult to calculate it for a real ships' sea-going condition. The verification of calculations by means of experiment results is essential to obtain a correct mathematical model.

The experiment which should allow such verification was carried out on board an ocean going vessel. On the basis of the experiment the following assumptions were made:

- For every cylinder unit the thermodynamic loss angle between the real and thermodynamic TDC is identical under the same load condition,
- The crankshaft rotation speed within the revolution angle less or equal to 1 degree is constant.

The experiment consists in the comparison of the TDC indication read from the sensor mounted on the crankshaft's free end with the thermodynamic TDC read from the cylinder pressure course of every cylinder unit. As the thermodynamic loss angle [10, 11] was assumed constant, the systematic error should be identical for every cylinder unit and should not have influence on the results.

2. The propulsion plant and the measurement conditions

On board of the 1719 TEU container ship, a long stroke low speed MAN 6L70ME-C engine was installed as the prime move. The engine drives the ship's constant pitch propeller directly. The diagram of the propulsion plant is shown on Fig. 1a and its basic technical data are collected in Table 1.

Tab. 1. Basic technical data of the propulsion plant

denomination	value
Engine's nominal power	16980 kW
Engine's nominal speed	98.3 min^{-1}
Engine's firing order	1-5-3-4-2-6
Propeller's shaft diameter	579 mm
Propeller diameter	6700 mm

To eliminate the sea condition influence on the measurement results the experiment was conducted at the calm sea state. A full set of engine working parameters was collected during indication. An extract of the most important is presented in Table 2. The engine torque was measured with the aid of the Maridis torque meter and effective power was given by a genuine MAN digital indicator of PMI type.

Tab. 2. Engines working parameters during measurement

denomination	value
Engine's effective power	8044 kW (47.4%of MCR)
Engine's speed	77 min^{-1}
Engine's torque	997 kNm
Scavenge air pressure	2.12 bar abs
Fuel index	59%

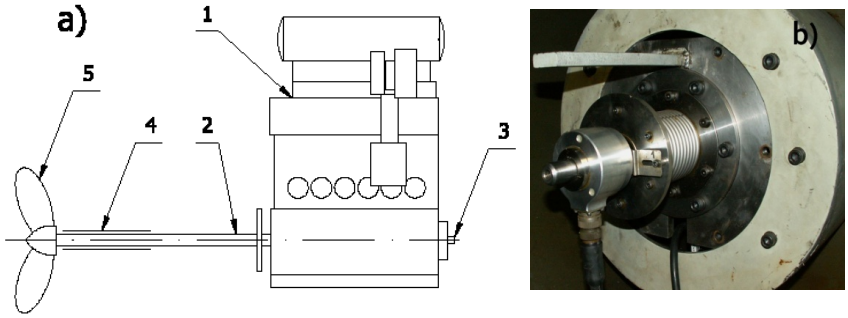

Fig. 1. The propulsion plant: a) Schematic diagram; 1-Main engine; 2-Propulsion shaft; .3-Rotary incremental encoder; 4-Stern tube with stern bearings; 5-Propeller; b) Encoder attached to the crankshaft

The main engine is of the electronic control type. Every fuel injection pump and exhaust valve are hydraulically actuated and controlled by designated digital multipurpose controller (MPC). The MPCs utilize the signal from an incremental encoder for a crankshaft positioning. The encoder is attached to the crankshaft's free end by means of bellows clutch (Fig.1b). The encoder's channel A generates 360 pulses of TTL standard per revolution and the Index channel generates one TTL pulse per revolution. The index pulse is shaped in such a way that it gives low signal for 180 degrees during the 1st unit's compression stroke and a high signal for 180 degrees during the 1st unit's compression expansion stroke. There was not available calibration data of the utilized encoder, so the assessment of the measurement accuracy was rather difficult. However there was made a test of accuracy for another model of incremental encoder of similar standard. On the basis of that test, one can assume that the utilized encoder generates pulses every 1 degree with a standard uncertainty of 0.0032 degree [9]. In Table 3 the utilized measuring instrumentation is presented.

Tab. 3. Measurement instrumentation data

Instrument	type
Measurement board	NI USB-6221, National Instruments, with counter input gate
Encoder	Incremental encoder ITD. 44 A 4 Y34, MAN B&W
Cylinder pressure sensor	F532A8-ACu, Optrand Inc.

During the experiment a simultaneous reading of two described channels from the encoder and in cylinder pressure was carried out. Every cylinder was scanned one by one in stationary working conditions.

3. Methodology

The collected data were processed in two steps. First the pressure signal was prepared, and then the signals were compared in the time domain.

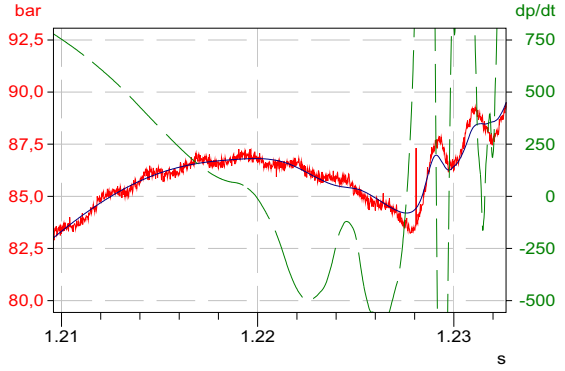

Fig. 2. The denoised signal(solid smooth line) and its differential (dashed line) compared to the raw signal (solid rough line).

Determination of the thermodynamic TDC was carried out by means of differentiation of the cylinder pressure signal. It was assumed that the zeroing of the first derivative of the pressure course reflects the thermodynamic TDC. As the raw cylinder pressure signal is disturbed by a noise of a different origin, the procedure of filtration had to be implemented. As the application of digital low pass filters causes shifting of the processed signal, a wavelet denoising procedure was applied. The Daubechies wavelet of the 7th order was chosen and a

decomposition of the original signal into 8 levels was done [1]. On Figure 2 the results of denoising procedure compared to the original signal have been presented. The accuracy of the thermodynamic TDC determination should be no less that 0.05 degree. That could be obtained at a high sampling rate of the pressure signal and after processing with wavelet denoising procedure.

To calculate the angle between the encoder's TDC signal and the thermodynamic TDC the assumption was made that within 1degree of revolution the rotational speed of the crankshaft is constant. Then the number *n* of encoder's channel A full cycles between time t_3 and t_4 was determined (Fig. 3). As the time between consecutive pulses from channel A corresponds to 1 degree of crankshaft revolution, the fractional angle α_1 between the time t_2 and t_3 as well as fractional angle α_2 between the time t_4 and t_5 were calculated:

$$\alpha_1 = \frac{t_3 - t_2}{t_3 - t_1} \tag{1}$$

$$\alpha_2 = \frac{t_5 - t_4}{t_6 - t_4} \tag{2}$$

Then the angle α between encoder's TDC signal and the thermodynamic TDC is equal to:

$$\alpha = \alpha_1 + n + \alpha_2 \tag{3}$$

However the theoretical angle between the crank arms has to be taken into account:

$$\alpha_f = \alpha_1 + n + \alpha_2 - \delta_i \tag{4}$$

Based on the presented methodology the angle α_f for 7 to 9 cycles for every cylinder unit was calculated. The results are presented on Fig. 4.

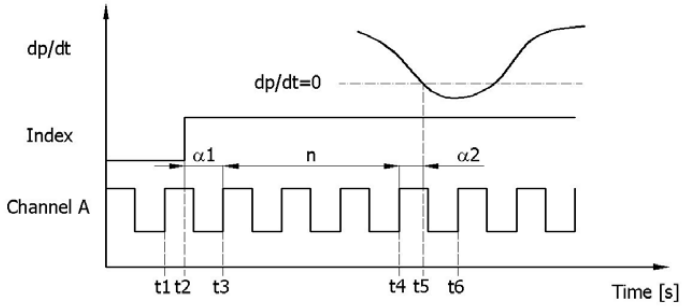

Fig. 3. The principle of data analysis; determination of the angle between encoder's index signal and thermodynamic TDC.

4. Conclusion

One can observe that the thermodynamic TDC mainly delays in relation to the encoder's indication. The mean delay is higher for the units which are placed further from the encoder – units 5 and 6 (Fig. 5). As the engine load during experiment was less than 50% the mean values of the shaft twist reach 0.2ºonly. However, the momentar y values can reach close to 0.5º(Fig. 4). One can presume that according to the mechanics of materials theory the angle should be higher for the engine loaded with higher torque.

Tab. 4. Calculated correction factors for encoder's TDC signal for every cylinder unit at 50% engine load

Cylinder number	Factor value
1	-0.0353º
2	-0.0713º
3	-0.1073º
4	-0.1433º
5	-0.1793º
6	-0.2153º

The experiment shows that the momentary angle between the static and thermodynamic TDC is variable (Fig. 4). As the reason, the torsional vibration of the shaft can mostly be considered. However, the methodology of the thermodynamic TDC determination definitely influences the results, too. In the analyzed engine at 50% load the mean correction factors for the encoders TDC indication can be considered (Table 4). However, it should be kept in mind that the mean values solve the problem only partially. The method for correction of instant angle would be rather more suitable.

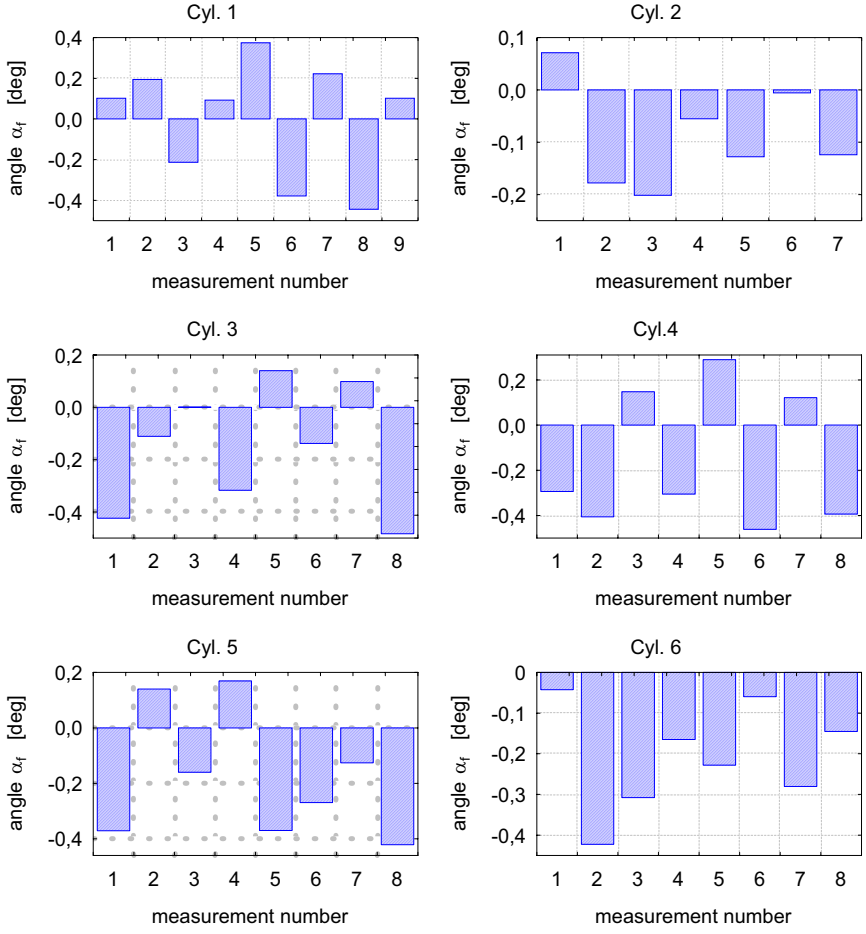

Fig. 4. The results of angle calculation. The values of the individual thermodynamic TDC and encoder's TDC differences in degrees.

The used wavelet denoising procedure has a great advantage compared to the typical low pass filters. The signal suffers no or minimal deformation what is of the uppermost

importance when the signal is going to be differentiated. However the use of wavelets is usually time consuming and may be difficult to use for real time calculations.

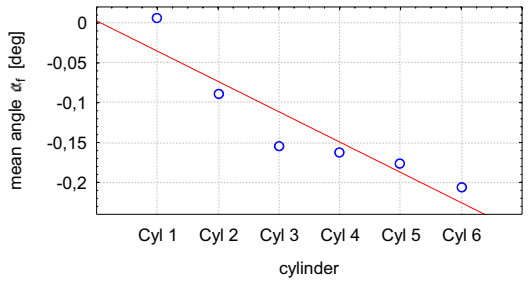

Fig. 5. The mean values of delay angle between the encoder's and thermodynamic TDC and their linear approximation.

Nomenclature

α_1 – fractional angle between the encoder's TDC signal and first rising edge from encoder's channel A

α_2 – fractional angle between the last rising edge from encoder's channel A and determined thermodynamic TDC

α_f – the resulting angle of thermodynamic TDC difference related to encoder's TDC

n – Number of encoder's channel A full cycles between time t_3 and t_4

t_1 – time when the last rising edge from encoder's channel A occurs before encoder's TDC signal.

t_2 – time when encoder's TDC signal occurs.

t_3 – time when the first rising edge from encoder's channel A occurs after encoder's TDC signal.

t_4 – time when the last rising edge from encoder's channel A occurs before thermodynamic TDC.

t_5 – time when the thermodynamic TDC occurs.

t_6 – time when the first rising edge from encoder's channel A occurs after thermodynamic TDC.

δ_i – theoretical angle between first cylinder crank arm and cylinder i, calculated from the firing order ($\delta_1$0º, $\delta_2$240º, $\delta_3$120º, $\delta_4$180º, $\delta_5$60º, $\delta_6$300º)

References

[1] Białasiewicz, J., T., *Falki i aproksymacje,* Wydawnictwo Naukowo-Techniczne, Warszawa 2004

[2] Gałecki, W., Tomczak, L., *Przenośne systemy diagnostyczne dla procesu spalania w okrętowych silnikach wysokoprężnych*, XVIII Międzynarodowe Sympozjum Siłowni Okrętowych, pp. 315-322, Gdynia 1996.

[3] Heywood, J. B., *Internal Combustion Engines Fundamentals,* McGraw-Hill International Editions, Singapore 1988.

[4] Jun, S., Changlin, G., Study on Crankshaft Strength of Engines with Multi-academic Subject, CIMAC Congress, Vienna 2007

[5] Larsen, O.C., Sørtvedt, T., *Prevention of Harmful Engine – and Propeller – Induced Vibrations in the Afterbody of Ships*., Det Norske Veritas Information No. 9, Oslo, August 1972.

[6] Lehmann & Michels GmbH, *Premet Type L, LS, and XL Electronic Indicators*. Rellingen, April 2006 [cited 20 June 2007;14:43 EST]. Available from Internet: <http://www.lemag.de/fileadmin/user_upload/PREMET_liste_10042006.pdf>
[7] MAN B&W Diesel A/S, *PMI System Pressure Analyser*. Holeby, June 2000 [cited 20 June 2007;14:26 EST]. Available from In ternet: <http://www.manbw.com/files/news/filesof2051/pmi.pdf>
[8] Polanowski, S., Błędy pomiaru średniego ciśnienia indykowanego metodami cyfrowymi silników okrętowych w warunkach eksploatacji, Explo-Diesel, Gdańsk-Gdynia-Szczecin 1998.
[9] Praca zbiorowa, *Wyrażanie niepewności pomiaru.* Przewodnik, Główny urząd Miar, Warszawa 1999.
[10] Tazerout M., Le Corre O., Rousseau S. TDC Determination in IC Engines Based on the Thermodynamic Analysis of the Temperature-Entropy Diagram, SAE 1999-01-1489, 1-10, ISBN 0148-7191.
[11] Wimmer, A., Glaser, J., *Indykowanie silnika,* Instytut Zastosowań Techniki, Warszawa 2004.

Journal of POLISH CIMAC
Faculty of Ocean Engineering & Ship Technology
GDAŃSK UNIVERSITY OF TECHNOLOGY

THE ARTIFICIAL NEURAL NETWORK: A TOOL FOR NOx EMISSION ESTIMATION FROM MARINE ENGINE

Jerzy Kowalski

Gdynia Maritime University
Department of Engineering Sciences
Morska Street 81-87, 81-225 Gdynia, Poland
tel.+48 58 6901484, fax: +48 58 6901399
e-mail: jerzy95@am.gdynia.pl

Abstract

The paper presents the preliminary investigations of nitric oxides (NOx) estimation from marine two-stroke engines. The Annex VI to Marpol Convention enforce to ship-owners necessity of periodical direct measurements of the NOx emission from the ship engines. It is very expensive procedure but with a low accuracy. Presented investigations show the possibility of estimation the NOx emission without direct measurements but using the artificial neural network (ANN). The paper presents method of choice the input data influenced on NOx emission and configuration of ANN and effects of calculations. The input data poses 15 parameters of engine working, influencing on NOx emission. The output data, necessary to learning the network, were NOx concentration in engine exhaust gases. We take into account two types of ANN; the 3-layer perceptron (MLP) with number of neurons in the hidden layer from 10 to 20 and the radial basis function neural network (RBF) with number of neurons in the hidden layer from 10 to 80. The input, validation and verification data was obtained from laboratory tests. After procedure of network configuration, the chosen ANN was learned by back propagation and conjugate gradient methods. During this operation the weights of neurons were changed to minimize the root mean square error. We obtained four ANN's, which allow us to estimate the NOx emission from laboratory engine with accuracy, comparable with Annex VI regulations.

Keywords: *emission, NOx, Artificial Neural Network, Marpol Convention, marine diesel engine*

1. Introduction

The nitric oxides (NOx) contained in exhaust gases, emitted from ship engines causes' high level of health hazard. To prevent of sea environment from this pollutant International Maritime Organization introduced Annex VI to MARPOL 73/78 convention in 1997. This Annex forces ship owners to limit nitric oxides emission from ship engines. The allowable level of this emission is defined in NOx Technical Code [11]. According to this Code, every introduced to operation onboard engines above 130 [kW] are obligated to have the valid certificate confirming the acceptable NOx emission. If ship engines are subjected some alterations during their operation period, they will have to extend such a certificate. Its prolonging consists in checking of parameters and structural parts of the engine influencing the NOx emission. Changes of engine structural parameters could entail the necessity of carrying out the direct onboard measurements of the NOx emission. Usually, the standard equipped engine rooms have not installed any appropriate analyzer of exhaust gases. Therefore, such direct measurements lead to significant expenses for ship owners. Moreover, these measurements have to be carried out for strictly determined points of engine load. Such situation can also cause to withdrawing the ship with operation in order to perform these measurements, which are additionally not precise. According to the NOx Technical Code regulations, we can apply the simplified method during the onboard measurements. These regulations allow us to overcome the acceptable levels of emission even about 10% comparing

with methods using on the shore. For the heavy fuel, these regulations allow to exceed this limit even up to 15%.

In order to make these regulations more applicable, many research centers work on alternative methods of nitric oxides estimations from onboard operated diesel engines. Kyrtatos et al. [16] proposes the "*software sensor for exhaust emissions estimation"* based on multi-zone thermochemical model of nitric oxides formation in combustion chamber of the engine. This sensor includes only Zeldovicz's model [10] of nitric oxides creation. Developing this method of nitric oxides estimation the mono-zone multi-component, thermochemical model was proposed [14]. It's based on Konnov's model [13] and consists of 724 reactions between 83 chemical species. The conclusions formulated after researches on this model, shows enough accuracy of nitric oxides estimation only for one engine. Moreover, the complexity of nitric oxides formation in combustion chamber of engine required very expensive computational power, not onboard accessible. According to this, it's necessary finding of the appropriate method, allowing to the lowering of the costs of modeling without limiting her accuracy. Such method can be an approximation of the NOx composition model, possible to calculation by the PC class computer. The useful and universal approximator, being suitable to this aim, is the artificial neuronal network (ANN). Proposed by Werbos method of ANN learning [29], called the back propagation method, allows using the ANN in the various fields of knowledge. Wang et al. [28], Oladsine et al. [20] and Hafner et al. [8] uses ANN to control parameters of the piston engines and Stephan et al. [25] to control the power plant. Yang et al. [30] and Ramadhas et al. [22] proposes use ANNs to modeling of cetane number for blended fuels and Lee et al. [17] use ANN to modeling of fuel spray penetration in combustion chamber of the engine. The ANN was also applied to the lowering of the costs of the modeling of the combustion process reactions [3], [5], [12], [24], [26] specific fuel consumptions of the engine [23] and the temperature of the combustion process [21].

Presented works shows, that using the ANNs is effective and not expensive alternative to modeling of the combustion process parameters. According to this situation we would like to propose a method of the NOx estimation from the onboard diesel engine based on the measurements of working engine parameters like pressures, temperatures, etc. Moreover, we assume that these parameters measured in the standard equipped engine room are sufficient for developing the mentioned method. This, in turn, requires developing the appropriate model connecting these parameters into a function allowing for assessing a level of the NOx emission. In order to reduce the high cost of modeling the artificial neural network is proposed.

2. Formation of the NOx in combustion chamber of the engine

The main reason of nitric oxides formation is reactions of the nitrogen oxidization in environment of high temperature and high pressure in a combustion chamber. The nitrogen oxidized in these reactions comes from air and fuel injected to a cylinder. The process of the nitrogen oxidation is reversible. Unfortunately, the quickness of reactions opposite to the oxidation is too low in conditions of the combustion chamber. It causes to release some parts of the nitric oxides to atmosphere during the scavenging process of a cylinder. Long-term investigations of the NOx formation carried out during a combustion process of various flammable mixtures bring into being many mechanisms allowing for estimating the amount of the emitted NOx. Basing on thermal mechanism [9], we can state that the most important parameter of this process is its temperature. This statement is supported by results of experimental investigations presented in [2]. According to conclusions contained in [7], the second important parameter is pressure of causing for decreasing of NOx molar concentration. Investigations of Lyle and al. [18], shows us the considerable influence of relation between the molar concentration of fuel and air on the NOx emission level. According to results of these studies, the prompt mechanism predominates in rich mixtures. After exceeding a stoichiometric air concentration in a mixture, the rapid growth of the

NOx concentration occurs due to a thermal mechanism domination. However, the further increase of the air concentration causes for decreasing of the NOx concentration due to decreasing the combustion process temperature. Kuo [15] gives also dependences between the fuel composition and burning velocity, and the NOx concentration. According to results, a fuel molecular structure depends on burning the velocity and NOx concentration, but this dependence is ambiguous.

According to these considerations the most important parameters influenced on NOx formation are:

- Composition of burned mixture in the combustion chamber,
- Time of combustion,
- Pressure of combustion,
- Temperature of combustion.

Values of these parameters are changed during the combustion process in the engine cylinder. Moreover, presented parameters couldn't be measured during sea operation of the engine. It means that estimation of the NOx emission requires measurement some another parameters of the engine working influencing on temperature, pressure, time of combustion and composition of the combusted mixture. The author's research demonstrates [14], that measurement of the engine parameters during the sea operation conditions, are enough to the NOx emission estimation. The prediction of NOx emission by the direct calculation of NOx formation during combustion process is very expensive and difficult process [1] [4] [6], [13], requiring large computational power not attainable onboard. In this situation the direct calculation of the NOx formation to estimation of the level of the emission onboard is problematic. On the other hand properly learned neural network, may be sufficient tool to assess the level of the NOx emissions.

3. The preparing of the ANN's

According to the ANN theory [19] the enter data inserted to the ANN model has to comply appropriate requirements. The most important is the mutual independence of the enter data. It means that chosen entered data couldn't influence each other.

The earlier considerations show that the enter data to the ANN must represent the parameters influenced on NOx formation in the combustion chamber. The composition of the burned mixture in the combustion chamber may to be estimated by the parameters of the air and fuel at the inlet to the engine and the parameters of the injection system. We choose the following parameters: temperature and humidity of the scavenging air and a fuel consumption of the engine. Dependence between quantity of fuel and air in the combustion chamber is represented by an air/fuel ratio. Time of combustion is represented in enter data by speed of the engine and pressure of combustion is represented by the mean cylinder pressure, the maximum cylinder pressure and the crankshaft position at the maximum cylinder pressure. Temperature of the combustion process is represented in enter data by parameters of the injection process; the maximum injection pressure, the crankshaft position at the maximum injection pressure and temperature of the fuel before the injecting pump and temperature of the exhaust gas. The cooling system of the engine influences on temperature of combustion process that has way the pressure and temperatures in the inlet and outlet of the cooling system were added to the enter data. According to these considerations 15 independent parameters of the combustion process are taken like the enter data to ANN.

The problem of NOx emission estimation from the diesel engine is classified as regressive problem. General two types of ANN may to be used to solve this class of problems. The first, most popular, network is multilayer perceptron (MLP) [23] and the second the radial basis function network (RBF) [27].

During the investigations both, the MLP and RBF networks are considered. The networks consist of 15 input neurons in input layer for 15 enter data, one neuron in output layer for NOx emission estimation and neurons in one hidden layer. The number of neurons in the hidden layer

was changed from 10 to 20 for MLP network and from 10 to 80 in RBF network. The input, validate, and the test data were collected during direct measurements on two stroke, one cylinder, loop scavenged, laboratory engine. The 212 sets of data are collected to teaching the networks after measurements. The cross validation was used because of a small quantity of the data sets. During the teaching process 162 data sets was randomly assigned as the teaching data, 20 to validation the networks, while the remaining 30 was employed for verification the performance of the ANN prediction. The logistic function as an activation function was used and the data sets before using were standardized to values from 0 to 1. The learning rate was set on 0,1.

The teaching process for all considered ANNs consists of few stages:

- weights of all neurons were randomly assigned,
- inputs were presented to the input layer, and the output was calculated,
- weights were calculated by minimizing the error in back propagation process, this process was repeated to assign all data sets,
- data sets were mixed and the second epoch was started,
- after 200 epochs weights were calculated by minimizing the error in the conjugate gradient method by 500 epochs,
- the cross validation was used and repeated 5 times,

4. The description of the laboratory test

We have carried out the laboratory test using the engine L-22 installed in Gdynia Maritime University laboratory. It is a crosshead, single-cylinder, and two-stroke diesel engine with loop scavenging. Roots' blower driven independently by an electric motor with an infinitely variable adjustment of rotational speed charges this engine. The tested engine is loaded by a water brake. Basic parameters of the L-22 engine are presented in Tab.1. and a schematic diagram of the laboratory stand is presented in Fig.1.

The measuring equipment installed on the tested engine permitted on the continuous recording of the considered parameters of the engine with approximately 0,5 second samplings.

Tab.1. Parameters of the test engine

Nominal Power [kW]	73,5
Rotational Speed [rpm]	600
Cylinder bore [mm]	220
Piston Stroke [mm]	350
Compression Ratio [-]	18,5
Fuel consumption at maximum load* [kg/h]	7,33
Specific fuel consumption at maximum load* [g/kWh]	277,6

* – maximum load considered during laboratory tests (see description below)

The fundamental stage of our research consists of 10 observations. We loaded the tested engine in a range from 25% to 65% of its nominal load with two rotational speeds namely 200 and 360 rpm. The larger load of the engine was not possible because of the admissible load of the used water brake and too small efficiency of the Roots' blower. The measurements have been carried out for the working engine with:

- its constant rotational speed and changeable loads for a constant value of air/fuel equivalence ratio,
- its constant rotational speed and load for changeable values of air/fuel equivalence ratio.

In this research, the air/fuel equivalence ratio [9] was understood as a ratio of a mass amount of air delivered to a cylinder to amount of air necessary to combustion of a fuel dose injected to this cylinder whereas the changeable loads realized by means of using a water brake. Values of the

engine loads (*M*) described like percent of nominal momentum M_n and rotational speeds (*n*) are presented in Tab.2.

During our research, the engine has been supplied by the diesel fuel with its known specification obtained from its producer (Lotos EuroDiesel EKO Z with density at 15ºC equal 829,6 kg/m^3).

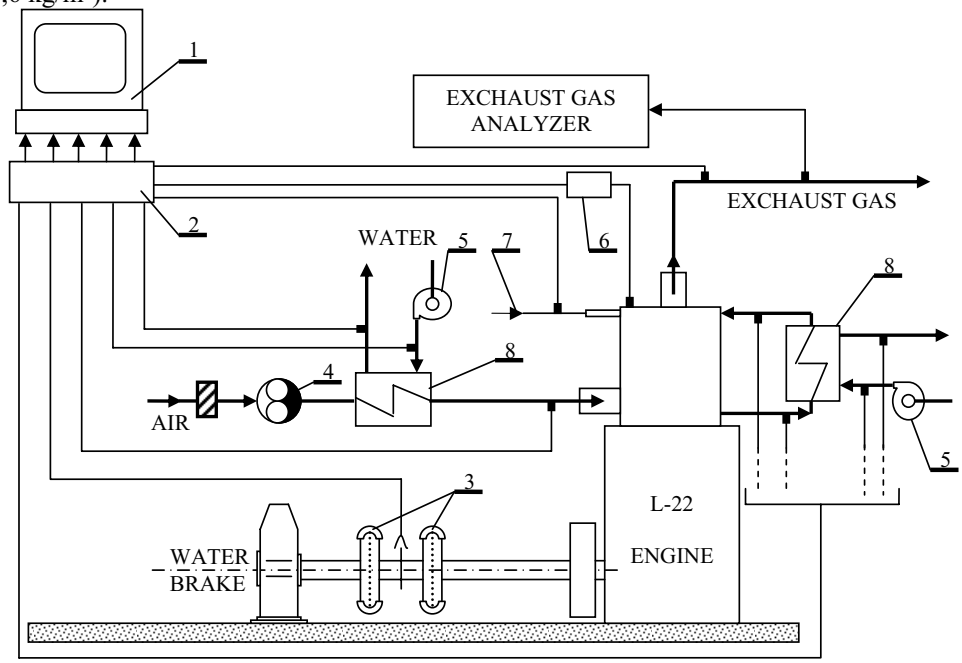

Fig.1. A schematic diagram of the laboratory stand: 1 – a recording computer, 2 – A/C converter, 3 – rubber flexible couplings, 4 – Roots' blower, 5 – a fresh water pump, 6 – an electronic indicator of pressure, 7 – fuel installation, 8 – a heat exchanger

Tab.2. Values of the tested engine loads and rotational speeds

No.	1	2	3	4	5	6	7	8	9
M [% of M_n]	65	60	55	50	45	40	35	30	25
n [rpm]	200								
No.	10	11	12	13	14	15	16	17	18
M [% of M_n]	65	60	55	50	45	40	35	30	25
n [rpm]	360								

5. The results of the investigations

The learning processes of ANNs were prepared in STATISTICA 7.1 computer code. The root mean square errors for best ANNs after cross validation for all considered networks were presented in Fig.2.

According to presented in Fig.2 results, the MLP networks have littlest root mean square errors than RBF networks. Increasing of number of neurons in hidden layer cause decrease considered error, but increasing number of neurons in the hidden layer of RBF network over 70 neurons decreases the error only imperceptibly. The changing of the neurons number in the MLP hidden layer between 10 and 20 neurons doesn't influence improvement of the quality of modeling significantly. The values of the maximum errors for all considered ANNs are presented in Fig.3.

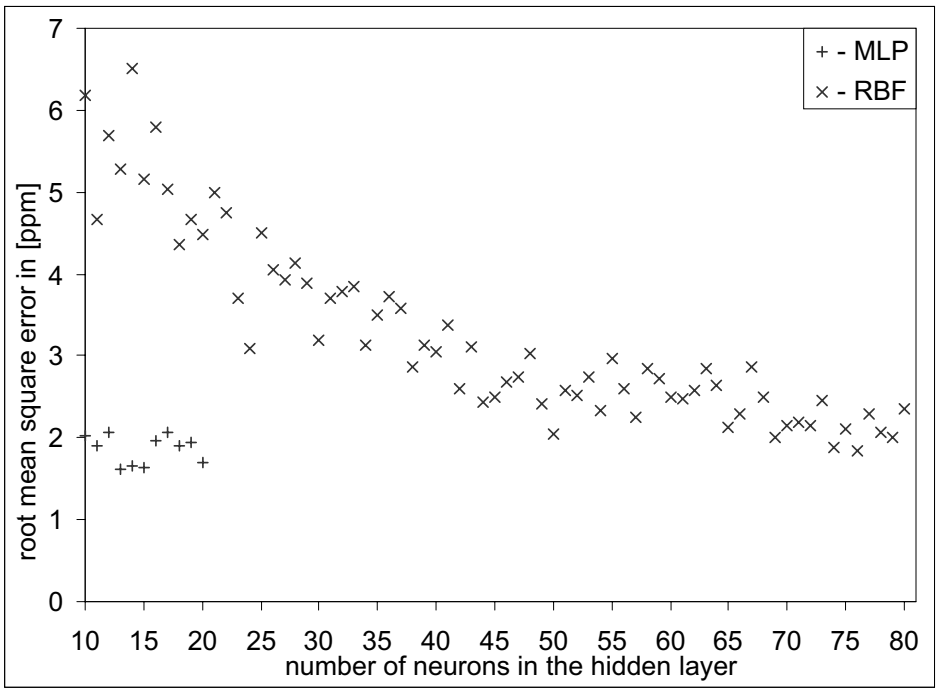

Fig.2. the root mean square error for all considered ANNs

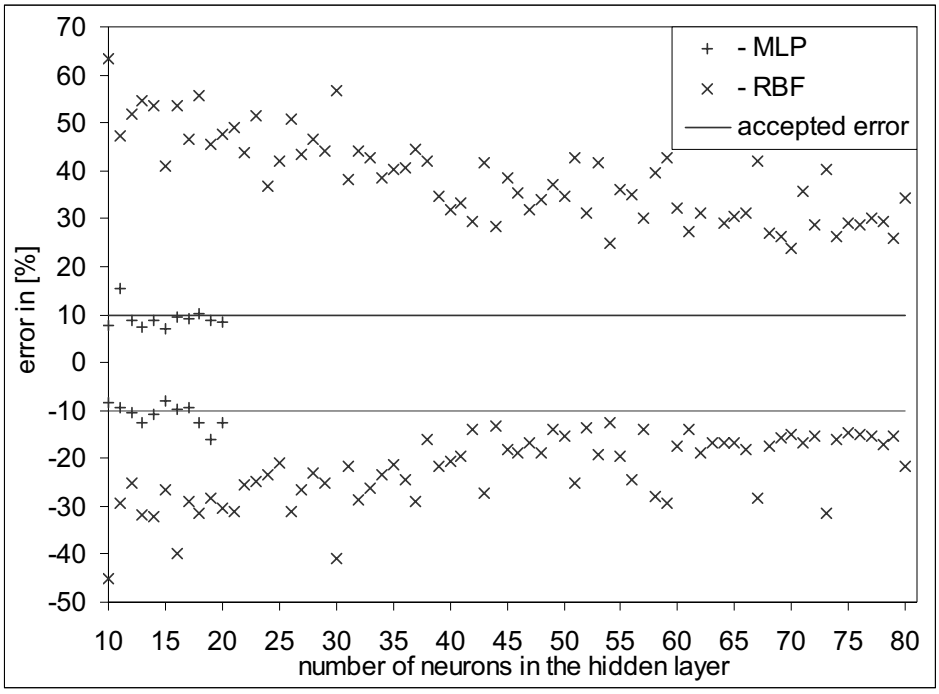

Fig.3. the values of maximum errors for all considered ANNs

Results, presented in Fig.3. shows, that only four MLP networks estimate the NOx emission in errors not excided 10% for all considered points of load the engine. There are the MLP networks with 10, 15, 16, and 17 neurons in the hidden layer. According to these considerations the presented MLP networks are sufficient to NOx emission from engine with accuracy specified in Technical Code.

5. Conclusions

This paper describes the method of ANN preparing to NOx emission estimation from the ship diesel engine during onboard working. The presented results of this work enable the following conclusions to be drawn:

- The possibility of the enter data collecting to the NOx formation model in the ship engine exists without the installation of the additional measuring equipment in the engine room.
- Four MLP networks with 10, 15, 16, and 17 neurons in the hidden layer successful estimate the NOx emission with error not exceeded 10% for all considered points of the engine load.
- The preparing of artificial neural network with considered enter data is sufficient to NOx emission estimation from the ship diesel engine. However the network was learned only for one engine and more studies are necessary.

References

[1] Barlow, R. S., Karpetis, A. N., Frank, J. H., *Scalar profiles and no formation in laminar opposed-flow partially premixed methane/air flames,* Combustion and Flame No. 127/2001, pp. 2102–2118, Elsevier Science Inc. 2001.

[2] Bebara, L., Kermesa, V., Stehlika, P., Canekb, J., Oralc, J., *Low NOx burners—prediction of emissions concentration based on design, measurements and modeling,* Waste Management No. 22/2002, pp. 443–451, Elsevier Science Inc. 2002.

[3] Blasco, J. A., Fueyo, N., Dopazo, C., Ballester, J., *Modelling the temporal evolution of a reduced combustion chemical system with an artificial neural network,* Combustion anf Flame, Vol 113, Elsevier, 1998.

[4] Bowman, C. T, Hanson, R. K., Gardiner, W. C., Lissianski, V., Frenklach, M., Goldenberg, M., Smith, G. P., Crosley, D. R., Golden, D. M., *GRI-Mech 2.11 An optimized detailed chemical reaction mechanism for methane combustion and NO formation and re-burning,* Topical Report Gas Research Institute 6/94 - 2/96.

[5] Cerri, G., Michelassi, V., Monacchia, S., Pica S., *Kinetic combustion neural modelling integrated into computational fluid dynamics,* Proc. Instn. Mech. Engrs. Vol. 217 Part A, IMechE, 2003.

[6] Curran, H. J., Gaffuri, P., Pitz, W. J., Westbrook, C. K., *A comprehensive modeling study of n-heptane oxidation,* Combustion and Flame No. 114/1998, pp. 149-177, Elsevier Science Inc. 1998.

[7] Egolfopoulos, F. N., *Validation of nitrogen kinetics in high pressure fames,* Energy Conversion & Management No. 42/2001, pp. 21-34, Elsevier Science Inc. 2001.

[8] Hafner, M., Schuler, M., Nelles, O., Isermann, R., *Fast neural networks for diesel engine control design,* Control Engineering Practice, Vol. 8, Pergamon 2000.

[9] Heywood, J. B., *Internal Combustion Engine Fundamentals*, McGraw-Hill 1988.

[10] Heywood, J. B., *Sher E., The Two-Stroke Cycle Engine. Its Development, Operation, and Design*, Taylor&Francis N. Y. 1999.

[11] *Interim Guidelines for the Application of the NOx Technical Code*, IMO News, No. 1. 2000. pp. 6.

[12] Kesgin, U., *Genetic algorithm and artificial neural network for engine optimisation of efficiency and NOx emission,* Fuel Vol. 83, Elsevier, 2004.
[13] Konnov, A. A., *Development and validation of a detailed reaction mechanism for the combustion of small hydrocarbons*, 28-th Symposium (Int.) on Combustion. Abstr. Symp. Pap. p. 317. Edinburgh 2000.
[14] Kowalski, J., Tarelko, W., *Nitric Oxides emission estimation based on measuring of work parameters of ship two-stroke engine*, Proceedings of 2nd International Conference on Marine Research and Transportation. Ischia Naples Italy. 2007. Session C.
[15] Kuo, K. K., *Principles of combustion,* Wiley. New Jersey 2005.
[16] Kyrtatos, N. P., Dimopoulos, G. G., Theotokatos, G. P., Tzanos, E. I., Xiros, N. I., *NOx-box: A software sensor for real-time exhaust emissions estimation in marine engine,* Proceedings of IMAM 2002, Athens 2002.
[17] Lee, S. H., Howlett, R. J., Crua, C., Walters, S. D., *Fuzzy logic and neuro-fuzzy modelling of diesel spray penetration: A comparative study,* J. Intel. Fuz. Sys. Vol. 18, IOS Press, 2007.
[18] Lyle, K. H., Tseng, K. L., Gore, J. P., Laurendeau, N. M., *A study of pollutant emission characteristics of partially premixed turbulent jet flames,* Combustion and Flame No. 116/1999, pp. 627-639, Elsevier Science Inc. 1999.
[19] Masters, T., *Practical neural network recipes in C++,* Academic Press Inc., 1993.
[20] Oladsine, M., Bloch, G., Dovifaaz, X., *Neural modelling and control of a diesel engine with pollution constrains,* J. Intel. Robotic Systems, Vol. 41, Kluwer Academic Publishers, 2004,
[21] Parlak, A., Islamoglu, Y., Yasar, H., Egrisogut, A., *Application of artificial neural network to predict fuel consumption and temperature for a diesel engine,* Applied Thermal Engineering Vol. 26, Elsevier, 2006.
[22] Ramadhas, A. S., Jayaraj, S., Muraleedharan, C., Padmakumari, K., *Artificial neural networks used for the prediction of the cetane number of biodiesel,* Renewable Energy Vol. 31, Elsevier, 2006.
[23] Sayin, C., Ertunc, H. M., Hosoz, M., Kilicaslan, I., Canakci, M., *Performance and exhaust emissions of a gasoline engine using artificial neural network,* Applied Thermal Engineering Vol. 27, Elsevier, 2007,
[24] Shenvi, N., Geremia, J. M., Rabitz, H., *Efficient chemical kinetic modelling through neural network maps,* Journal of Chemical Phisics Vol. 120, No 21, American Institute of Physics, 2004.
[25] Stephan, V., Debes, K., Gross, H-M., Wintrich, F. Wintrich, H., *A new control scheme for combustion processes using reinforcement learning based on neural networks,* Int. J. Comput. Intel. Appl. Vol. 1, No 2, Imperial College Press, 2001.
[26] Thompson, G. J., Atkinson, C. M., Clark, N. N., Long, T. W., Hanzevack, E., *Neutal network modelling of the emissions and performance of heavy-duty diesel engine,* Proc. Instn. Mech. Engrs. Vol. 214 Part D, IMechE, 2000.
[27] Wang, S., Yu, D.L., *Adaptive RBF network for parameter estimation and stable air–fuel ratio control,* Neural Networks No 21/2008, pp. 102-112, Elsevier Science Inc. 2008.
[28] Wang, W., Chirwa, E. C., Zhou, E., Holmes, K., Nwagboso C., *Fuzzy neural ignition timing control for a natural gas fuelled spark ignition engine,* Proc. Instn. Mech. Engrs. Vol. 215 Part D, IMechE 2001.
[29] Werbos, P., *Beyond regression: New tools for prediction and analysis in the behavioural sciences,* Ph.D. Thesis, Harvard University 1974.
[30] Yang, H., Ring, Z., Briker, Y., McLean, N., Friesen, W., Fairbridge, C., *Neural network prediction of cetane number and density of diesel fuel from its chemical composition determined by LC and GC-MS,* Fuel Vol. 81, Elsevier, 2002.

Journal of POLISH CIMAC

Faculty of Ocean Engineering & Ship Technology
GDAŃSK UNIVERSITY OF TECHNOLOGY

PRESSURE AND CAPACITY FORCES IN SLIDE JOURNAL PLANE BEARING BY LAMINAR UNSTEADY LUBRICATION

Paweł Krasowski

Gdynia Maritime University
Morska Street 83-87, 81-225 Gdynia, Poland
tel.:+48 58 6901331, fax: +48 58 6901399
e-mail: pawkras@am. gdynia.pl

Abstract

This paper shows results of numerical solutions an modified Reynolds equations for laminar unsteady oil flow in slide journal bearing with planar linear gap. This solution example apply to isothermal bearing model with infinity breadth. Lubricating oil used in this model has Newtonian properties and dynamic viscosity in dependence on pressure. It shows a preliminary analysis change of pressure and capacity forces in the bearing by laminar, unsteady lubrication caused by velocity perturbations of oil flow in the longitudinal direction of a bearing. Described effect can be used as an example of modeling the bearing friction node operations in reciprocating movement during exploitation of engines and machines. Plane crossbar journal bearing occur in ship combustion engine as a crosshead bearing. Results are presented in the dimensionless hydrodynamic pressure and capacity force diagrams.

Keywords: *journal plane bearing, lubrication, unsteady laminar oil flow, pressure distribution, capacity forces*

1. Introduction

Presented subject matter apply to unsteady laminar flows [1],[4],[5] where modified Reynolds number Re*is smaller or equal to 2. This flow s are also determine by Taylor number Ty which is smaller or equal to 41,1. Laminar and unsteady flow of lubricant factor may occur during periodic or randomness non-periodic load perturbation. This kind of perturbation can occur during transient states of machines, but mostly during starts and stops. Presented work analyse change of oil lubricating flow perturbation in longitudinal direction on the slide plane and on the radial race of slide bearing. Plane bearing can be used as a work model of bearing friction node in kinematic pair in translational motion. As an example the crosshead bearing of slow-speed engine. Reynolds equation system for unsteady, laminar Newtonian oil flow in the cylinder radial bearing is presented in work [1] and in the plane slide bearing in work [3]. Stationary model of plane journal bearing lubrication is presented in work [2]. Velocity flow perturbations of lubricating oil on the slide can be caused by longitudinal vibrations during of reciprocating slide motion. Axial vibrations overlay on slide motion and this causes oil velocity perturbation on the slide bearing surface. Values of the perturbation are proportional to the longitudinal amplitude of perturbation and to forced frequency. Longitudinal vibration in the slide bearing elements can be caused by torsional vibration of the crankshaft. Oil flow velocity perturbations in the longitudinal direction on the bearing race can be caused by axial vibration of the race coming from vertical vibration of the engine. Isothermal bearing model can act as work model of bearing friction node by steady-state conditions of thermal load.

2. Modified Reynolds Equation

Lubricating gap is characterize by following geometric parameters: maximal gap height h_o, minimal gap height h_e , gap length L and gap width b (Fig.1). In presented model the following assumption were made: lubricating gap dimensions along it's width of mating surfaces remain identical. Lubricating gap height after gap length was described in cartesian co-ordinate system by the following dimensionless form:

$$h_1(x_1) = \varepsilon - (\varepsilon - 1)x_1 \qquad \text{for} \quad 0 \le x_1 \le 1 \tag{1}$$

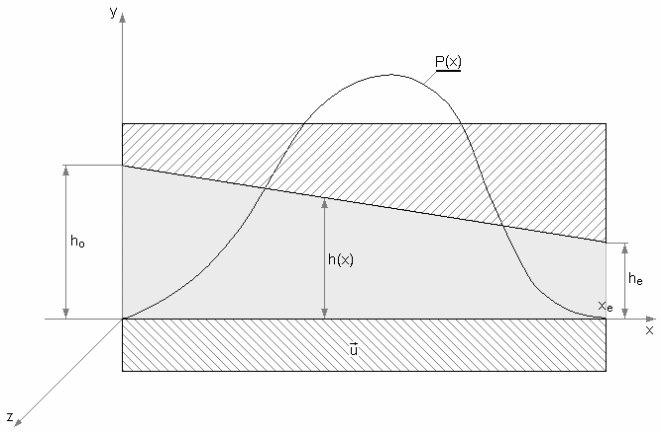

Fig.1. Geometry schema of the slide journal plate bearing gap

Dimensionless values [2],[3] that characterize lubricating gap are: length coordinate x_1 , gap height coordinate h_1 and gap convergence coefficient ε :

$$h_1 = \frac{h}{h_e}; \quad x_1 = \frac{x}{L}; \quad \varepsilon = \frac{h_0}{h_e} \tag{2}$$

In considered model we assume small unsteady disturbances and in order to maintain the laminar flow, oil velocity V_i^* and pressure p_1^* are total of dependent quantities $\widetilde{V}_i$; $\widetilde{p}_1$ and independent quantities V_i; p_1 from time [3],[5] according to equation (3).

$$\begin{aligned} V_i^* &= V_i + \widetilde{V}_i \qquad i = 1,2,3 \\ p_1^* &= p_1 + \widetilde{p}_1 \end{aligned} \tag{3}$$

Unsteady components of dimensionless oil velocity and pressure we [4] in following form of infinite series :

$$\widetilde{V}_i(x_1; y_1; z_1; t_1) = \sum_{k=1}^{\infty} V_i^{(k)}(x_1; y_1; z_1) \exp(j k \omega_0 t_0 t_1) \qquad \text{i}\mp,2,3$$

$$\widetilde{p}_1(x_1; z_1; t_1) = \sum_{k=1}^{\infty} p_1^{(k)}(x_1; z_1) \exp(j k \omega_0 t_0 t_1) \tag{4}$$

where:
ω_0 – angular velocity perturbations in unsteady flow,
j - imaginary unit $j = \sqrt{-1}$.

Reynolds equation describing dimensionless total pressure p_1^* in the lubricating gap of a plane journal bearing [3] by unsteady, laminar, isothermal, Newtonian flow. Together with longitudinal velocity perturbations V_{10} on the race surface and V_{1h} on the slide. Velocity perturbation V_{30} along bearing width on the race and V_{3h} on the slide also occur in this model, as follows:

$$\begin{aligned}
&\frac{\partial}{\partial x_1}\left\{\frac{h_1^3}{\eta_{1B}e^{Kp_1}}\left[\frac{\partial p_1^*}{\partial x_1}-K\left(p_1^*-p_1\right)\frac{\partial p_1}{\partial x_1}\right]\right\}+\frac{1}{L_1^2}\frac{\partial}{\partial z_1}\left\{\frac{h_1^3}{\eta_{1B}e^{Kp_1}}\left[\frac{\partial p_1^*}{\partial z_1}-K\left(p_1^*-p_1\right)\frac{\partial p_1}{\partial z_1}\right]\right\}= \\
&=6\frac{\partial h_1}{\partial x_1}+\frac{1}{2}\rho_1\,\mathrm{Re}^*\,n\left\{\frac{\partial}{\partial x_1}\left[\frac{h_1^3}{\eta_{1B}e^{Kp_1}}\left(V_{10}+V_{1h}\right)\right]+\frac{1}{L_1^2}\frac{\partial}{\partial z_1}\left[\frac{h_1^3}{\eta_{1B}e^{Kp_1}}\left(V_{30}+V_{3h}\right)\right]\right\}\sum_{k=1}^{\infty}A_k+ \\
&-6\left\{\frac{\partial}{\partial x_1}\left[h_1\left(V_{10}+V_{1h}\right)\right]+\frac{1}{L_1^2}\frac{\partial}{\partial z_1}\left[h_1\left(V_{30}+V_{3h}\right)\right]-2\left(V_{1h}\frac{\partial h_1}{\partial x_1}+\frac{1}{L_1^2}V_{3h}\frac{\partial h_1}{\partial z_1}\right)\right\}\sum_{k=1}^{\infty}B_k
\end{aligned} \tag{5}$$

for $0 \le x_1 \le 1;\ 0 \le y_1 \le h_1\ ;-1 \le z_1 \le 1;\ 0 \le t_1 \le t_k\ ;\ p_1^* = p_1^*(x_1; z_1; t_1)$

Oil vector velocity components in dimension form V_x, V_y, V_z and in dimensionless form V_1, V_2, V_3 are described as follows:

$$V_x = UV_1 \qquad V_y = \psi UV_2 \qquad V_z = \frac{U}{L_1}V_3 \tag{6}$$

where:
U – linear velocity of slide bearing,
ψ – relative dimensionless clearance of bearing $(10^{-4} \le \psi \le 10^{-3})$,
b – bearing breadth,
L_1 – relative bearing breadth:

$$\psi = \frac{h_e}{L}\ ; \qquad L_1 = \frac{b}{L} \tag{7}$$

Oil dynamic viscosity η in dependence on pressure was taken according to the Barrus formula [5] and presented [1] in the dimension form η and in dimensionless form η_1:

$$\eta = \eta_0 e^{\alpha(p-p_a)} \approx \eta_0 e^{\alpha p}\ ; \qquad \eta_1 = \frac{\eta}{\eta_0} = \exp(\alpha p) \tag{8}$$

where:
η_o- oil dynamic viscosity by atmospheric pressure $p=p_a \approx 0$,
α – piezocoefficient taking into account viscosity changes in dependence on pressure.

Additional assumptions were made [2]: the dimensionless value for density ρ_1, pressure p_1, time t_1 and for remaining coordinates y_1 and z_1 according to the following designation:

$$\begin{aligned}
\rho = \rho_0\,\rho_1\,, \quad & p = p_0\,p_1\,, \quad & t = t_0\,t_1 \\
z = b\,z_1\,, \quad & y = h_e y_1\,, \quad & K = \alpha p_0
\end{aligned} \tag{9}$$

Density, pressure and time values with zero index are equivalent to basic sizes. Constant value K characterize dynamic viscosity in dependence on pressure. Pressure p_0 , Reynolds number Re, modified Reynolds number Re^* has the following form [2]:

$$p_0 = \frac{U\eta_0}{\psi^2 L} \; ; \qquad Re = \frac{U\rho_0 h_e}{\eta_0} \; ; \qquad Re^* = \psi Re \tag{10}$$

Sums of a series $\sum_{k=1}^{\infty} A_k$ and $\sum_{k=1}^{\infty} B_k$ in Reynolds equation (5) were defined in works [1],[3], has form

$$\sum_{k=1}^{\infty} A_k = \sum_{k=1}^{\infty} \frac{\sin(k\omega_0 t_0 t_1)}{k} = \begin{cases} \dfrac{\pi - \omega_0 t_0 t_1}{2} & 0 < t_1 < 1 \\ 0 & t_1 = 0;1 \end{cases} \tag{11}$$

$$\sum_{k=1}^{\infty} B_k = \sum_{k=1}^{\infty} \frac{\cos(k\omega_0 t_0 t_1)}{k^2} = \frac{1}{4}\left[(\pi - \omega_0 t_0 t_1)^2 - \frac{\pi^2}{3} \right] \quad \text{dla} \quad 0 \le t_1 \le 1$$

In the further numerical analysis relation time was taken into account as a propagation period of axial velocity perturbation of lubricating oil. In case where oil velocity perturbations are caused by forced vibrations of engine then the number n in equation (5) define multiplication of perturbation frequency ω_0 to angular velocity of engine crankshaft ω.

3. Hydrodynamic pressure

Equation solution (3) for infinity breadth bearing with assumption that velocity perturbation does not depend on coordinate x_1 can be present [3] in total dimensionless hydrodynamic pressure p_1^* .

$$\begin{aligned} p_1^*(x_1) = p_{1K} - \frac{p_{10}}{1 - Kp_{10}}(V_{10} - V_{1h}) \sum_{k=1}^{\infty} B_k + \frac{x_1}{4\varepsilon^2} \frac{\rho_1 \mathrm{Re}^* n}{1 - Kp_{10}} (V_{10} + V_{1h}) \left(\varepsilon + 1 - \frac{\varepsilon + h_1}{h_1^2} \right) \sum_{k=1}^{\infty} A_k + \\ + \frac{3K}{(\varepsilon - 1)^2} \frac{\rho_1 \mathrm{Re}^* n}{1 - Kp_{10}} (V_{10} + V_{1h}) \left\{ (x_1 - 1)\ln\varepsilon - \ln h_1 + \frac{1}{\varepsilon + 1} \left[(\varepsilon - 1)(1 - 2x_1) + \frac{\varepsilon}{h_1} - h_1 \right] \right\} \sum_{k=1}^{\infty} A_k \end{aligned} \tag{12}$$

The p_{10} value is a pressure value in the disccused lubricating gap by the steady flow with the constant lubricating oil dynamic viscosity. On the other hand p_{1K} value is a stationary pressure value for viscosity, in dependence on pressure and for discussed form of lubricating gap it was mentioned in work [2]:

$$p_{10} = \frac{6(\varepsilon - 1)(1 - x_1)x_1}{(\varepsilon + 1)(\varepsilon - \varepsilon x_1 + x_1)^2} \; ; \qquad p_{1K} = -\frac{1}{K}\ln\left|1 - Kp_{10}\right| \tag{13}$$

Perturbation pressure $\tilde{p}_1$ in the unsteady part of the flow can be presented as a difference of total pressure p_1^* and stationary pressure p_{1K}.

On the basis of presented dependences for isothermal bearing model with infinity width, the calculations of hydrodynamic pressure distribution in the lubricating gap were made. In the example calculations the following assumption were made: oil with constant density and value of the expression $n\rho_1 Re^* \ddagger 2$, which approximately comply to longitudinal velocity perturbation function in the engine crosshead bearing after the first frequency force from two-stroke, six cylinder engine crankshaft torsional vibration. Hydrodynamic pressure distribution and other pressure parameters are in dependence on lubricating gap convergence coefficient ε [2]. Optimum

gap convergence $\varepsilon_{opt} \neq \sqrt{2}$ comply to maximal hydrodynamic pressure. Pressure in the optional point of lubricating gap changes due the perturbation time and its distribution along the gap length reach the maximal and minimum values. On the Fig.2 example of the hydrodynamic total pressure distribution along the gap length for bearing with the optimal convergence ε_{opt} and for the

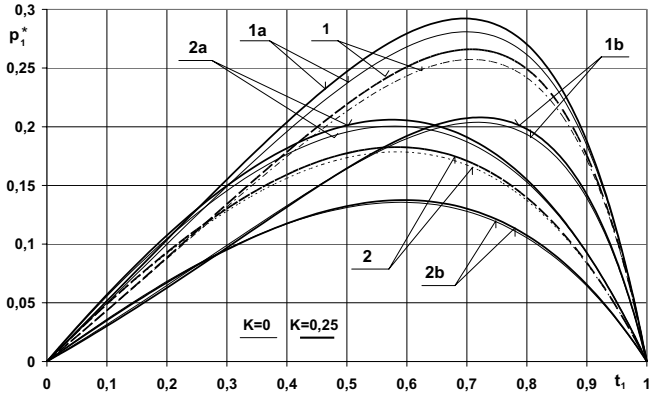

Fig.2 Total maximal (a) and minimal (b) pressure distributions p_1^* in direction x_1 for ε: 1) $\varepsilon = \varepsilon_{opt}$; 2) ε=1,4 by velocity perturbations: V_{10}=0,05

convergence ε≠,4 marked with numbers 1 and 2 by the constant viscosity (Kθ) in dependence on pressure (Kθ,25) marked with thin and th ick lines. Maximal pressure distribution were marked with symbols a and the minimal pressure distribution were marked with b. Pressure quantities by stationary flow were marked with broken line. Unsteady flow on the Fig.2 is caused by longitudinal velocity perturbation only on the bearing race V_{10}θ,05. In the case where oil dynamic viscosity depends on pressure then pressure perturbations are higher than in the case where oil has constant viscosity. Pressure perturbation quantity depends on lubricating oil

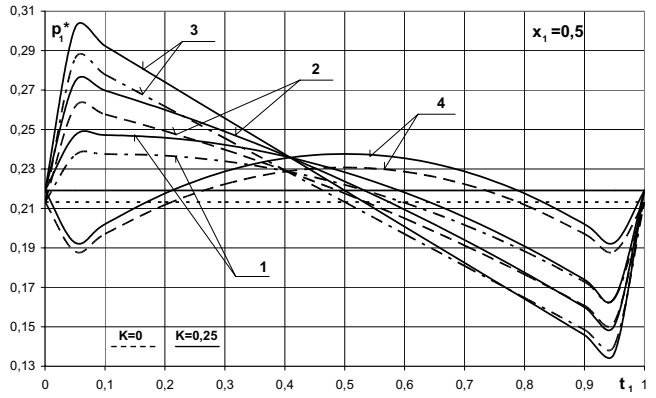

Fig.3 Pressure distributions p_1^* in place x_1=0,5 in the time t_1 by velocity perturbations: 1)V_{10}=0,05; V_{1h}=0; 2) V_{10}=0,05; V_{1h}=0,025;3) V_{10}=0,05; V_{1h}=0,05;4) V_{10}=0,05; V_{1h}=-0,05

convergence ε and is the maximum for optimal convergence. It apply also to stationary pressure increase in the lubricating gap. Further analysis of pressure distribution were made for gap with optima convergence ($\varepsilon=\varepsilon_{opt}$).

Total pressure distribution along the bearing gap and perturbation pressure distribution in the time function in the optional point on the race surface were analyzed. Numerical calculation results were presented by following longitudinal velocity perturbations: 1) V_{10}θ,05, V_{1h}θ,2) V_{10}θ,05,

V_{1h}=0,025;3) V_{10}=0,05, V_{1h}=0,05;4) V_{10}=0,05, V_{1h}=0,05. Unsteady pressure is changing at the time of velocity perturbation and its course is a function of time and its location along the bearing length. It is the temporary function of a period of velocity perturbation. Total pressure course p_1* in the point located in the half way of bearing length x_1=0,5 on the surface of the race in dimensionless time function is presented on the Fig. 3 for fourth different velocity perturbation. Steady pressure is marked with the misfiring line. When the velocity perturbation of oil on the race is harmonious with the slide velocity, the perturbation pressure increases. In the opposite situation it decreases and the drop is much higher than the rise. It lasts shorter than the half perturbation period. The opposite case is when velocity perturbation takes place on the slide. This case has not been presented on the figure. The periods of drop and rise of pressure are asymmetric in the case of different levels of velocity perturbation (Fig. 3). The level of velocity perturbation is higher for both options when the viscosity depends on the pressure.

4. Capacity forces

Hydrodynamic capacity force in the bearing comes from the hydrodynamic pressure integral on bearing surface slide. In dimensionless form:

$$W_1^* = \frac{W^*}{W_0} = \int_0^1 p_1^*(x_1)dx_1 \; ; \qquad W_0 = bLp_0 \tag{14}$$

where:
W_0 – characteristic value of capacity force

Capacity load changes during the time of velocity perturbation. Capacity load change $\widetilde{W}_{1K}$ is calculated as a difference between capacity in unsteady flow W_1^* and stationary flow W_{1K}:

$$\widetilde{W}_{1K} = W_1^* - W_{1K} \; ; \qquad W_{1K} = \int_0^1 p_{1K}(x_1)\,dx_1 \tag{15}$$

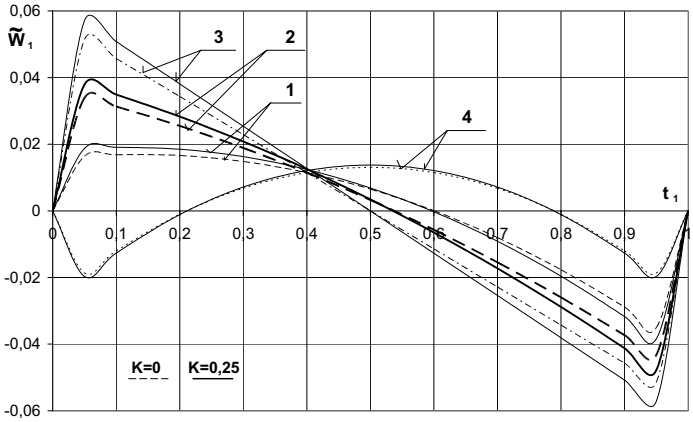

Fig. 4 The capacity forces $\widetilde{W}_1$ *of slide journal bearing in the time* t_1 *by velocity perturbations: 1)* V_{10}*=0,05;* V_{1h}*=0; 2)* V_{10}*=0,05;* V_{1h}*=0,025;3)* V_{10}*=0,05;* V_{1h}*=0,05;4)* V_{10}*=0,05;* V_{1h}*=-0,05*

In case of lubricating oil flow with constant viscosity independent from pressure (K=0), the capacity load by stationary flow W_{10} is determined [2] by equation:

$$W_{10} = \frac{6}{(\varepsilon-1)^2}\left(\ln\varepsilon - 2\frac{\varepsilon-1}{\varepsilon+1}\right) \tag{16}$$

Fig.4 presents hydrodynamic capacity change of plain bearing during the viscosity perturbation time for both considered perturbation alternatives. Capacity load change is similar to total pressure change resulting from Fig. 3. Capacity force decrease caused by velocity perturbations is greater than capacity force increase and it depends on perturbation variant.
Pressure perturbation and capacity load drop and is caused by appearance of counter flow velocity to the direction of stationary flow. In case of oil dynamic viscosity depends on pressure, capacity load by stationary condition is greater than by constant viscosity.

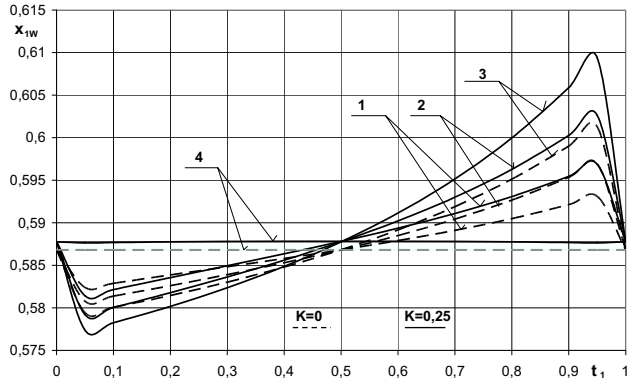

Fig. 5 Coordinate x_{1W} situated capacity force W_1^* in the time t_1 by perturbations:
1) V_{10}=0,05; V_{1h}=0; 2) V_{10}=0,05; V_{1h}=0,025;3) V_{10}=0,05; V_{1h}=0,05;4) V_{10}=0,05; V_{1h}=-0,05

In that case this lubricating oil quality causes that capacity load decrease as a result of velocity perturbation gives greater capacity load margin in both velocity perturbation cases. Capacity load position on the bearing lengthwise can be specified with coordinate – coordinate of centre elementary hydrodynamic pressure surface forces.

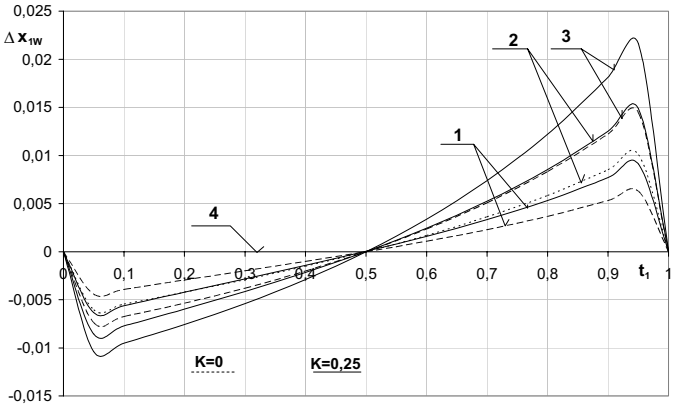

Fig. 6 Change of coordinate Δx_{1W} situated capacity force W_1^* in the time t_1 by perturbations:
1) V_{10}=0,05; V_{1h}=0; 2) V_{10}=0,05; V_{1h}=0,025;3) V_{10}=0,05; V_{1h}=0,05;4) V_{10}=0,05; V_{1h}=-0,05

This coordinate changes the position during velocity perturbation of oil flow. Capacity load diagrams for both considered velocity perturbation are presented on Fig. 5 and Fig. 6. Position

change of capacity force is symmetrical in time, that is it crosses through stationary position by $t_1\theta$,5 in spite of that ca pacity force is not achieving by stationary flow (Fig. 5). Capacity force shift is greater in the end of the bearing direction and occurs when the bearing load capacity decrease according to stationary flow. The capacity force coordinate by stationary flow, and all the coordinate changes in perturbation flow is greater in case when oil dynamic viscosity depends on pressure.

4. Conclusions

Discussed case of the solution to the Reynolds equation for the unsteady laminar Newtonian flow of lubricating factor allows initial estimation of hydrodynamic pressure distribution and its capacity as a basic operational parameter slide bearing. Unsteady axial velocity perturbation on the race surface and slide has influence on the hydrodynamic pressure distribution of the capacity of the lubricated gap. Pressure changes in the bearing are seasonal and equal to the lasting period of velocity perturbation. The level of changes and its nature depends on the kind of perturbation. The author bears in mind of the number of simplifying assumptions used in the presented model of bearing node and applying to the acceptance of Newtonian oil as well as examining isothermal model of bearing. The presented analytical example applies to the bearing of infinite length, however, the conclusions can be useful for the estimation of the pressure distribution and force with laminar, unsteady lubrication of slide nodes of the finished length. Presented results can be used as the comparative values in the case of numerical modeling of laminar, unsteady flows of liquids non-Newtonian in lubricating gaps slide journal bearings.

References

[1] Krasowski P., *Laminar, unsteady lubrication of slide journal bearing in magnetic field with dynamic viscosity depended on pressure*, (in Polish), Tribologia 4/2002 (184), pp. 1189-1200.

[2] Krasowski P., *Hydrodynamic pressure and capacity force in slide journal bearing with linear contracting gap.* (in Polish) Technical University Press, ZN Budownictwo Okrętowe Nr 65, Gdańsk 2004, pp.105 – 112.

[3] Krasowski P., *Modelling of laminar unsteady and unsymmetrical flow in slide journal bearing with linear contracting gap*. (in Polish) Maritime University of Gdynia, Faculty of Marine Engeeniering,,(non publish)

[4] Wierzcholski K., *Mathematical methods in hydrodynamic theory of lubrication,* Technical University Press, Szczecin 1993.

[5] Wierzcholski K., *Theory unconventional lubricant slide journal bearing*, Technical University Press, Szczecin 1995.

Journal of POLISH CIMAC

Faculty of Ocean Engineering & Ship Technology
GDAŃSK UNIVERSITY OF TECHNOLOGY

PRESSURE IN SLIDE JOURNAL BEARING LUBRICATED OIL WITH MICROPOLAR STRUCTURE

Paweł Krasowski

Gdynia Maritime University
ul. Morska 81-87,81-225 Gdynia, Poland
tel.:+48 58 6901331, fax:+48 58 6901399
e-mail:pawkras@am.gdynia.pl

Abstract

Present paper shows the results of numerical solution Reynolds equation for laminar, steady oil flow in slide bearing gap. Lubrication oil is fluid with micropolar structure. Properties of oil lubrication as of liquid with micropolar structure in comparison with Newtonian liquid, characterized are in respect of dynamic viscosity additionally dynamic couple viscosity and three dynamic rotation viscosity. Under regard of build structural element of liquid characterized is additionally microinertia coefficient. In modeling properties and structures of micropolar liquid one introduced dimensionless parameter with in terminal chance conversion micropolar liquid to Newtonian liquid. The results shown on diagrams of hydrodynamic pressure in dimensionless form in dependence on coupling number N^2 and characteristic dimensionless length of micropolar fluid Λ_1. Presented calculations are limited to isothermal models of bearing with infinite length.

Keywords: *micropolar lubrication, journal bearing, hydrodynamic pressure*

1. Introduction

Presented article take into consideration the laminar, steady flow in the crosswise cylindrical slide bearing gap. Non-Newtonian fluid with the micropolar structure is a lubricating factor. Materials engineering and tribology development helps to introduce oils with the compound structure (together with micropolar structure) as a lubricating factors. Exploitation requirements incline designers to use special oil refining additives, to change viscosity properties. As a experimental studies shows, most of the refining lubricating fluids, can be included as fluids of non-Newtonian properties with microstructure [3],[4],[6]. They belong to a class of fluids with symmetric stress tensor that we shall call polar fluids, and include, as a special case, the well known Navier-Stokes model. Physically, the micropolar fluids may represent fluids consisting rigid randomly orientated spherical particles suspended in a viscous medium, where the deformation of fluid particles is neglected [3]. Presented work dynamic viscosity of isotropic micropolar fluid is characterized by five viscosities: shearing viscosity η (known at the Newtonian fluids), micropolar coupling viscosity κ and by three rotational viscosities α, β, γ bounded with rotation around the coordinate axes. This kind of micropolar fluid viscosity characteristic is a result of essential compounds discussed in works [3] and [4]. Regarding of limited article capacity please read above works. In difference to classical oil with Newtonian properties, micropolar fluid is characterized by microinertia of the fluid part and by microrotation velocity field $\vec{\Omega}$. This fact determine the additional system of equation development describing micropolar fluid flow which is described by moment of momentum equation. In result of the above, the conjugation between fluid flow field and the microrotation velocity field. In presented flow, the

influence of lubricating fluid inertia force and the external elementary body force field were omit [3],[4].

2. Basic equations

Basic equation set defining isotropic micropolar fluid flow are describe following equations [2],[3],[4]: momentum equation, moment of momentum equation, energy equation, equation of flow continuity. Incompressible fluid flow is taken into consideration with constant density skipping the body force. We assume also, that dynamic viscosity coefficients which characterize micropolar fluid are constant. According to above velocity flow field is independent from temperature field and the momentum equation, moment of momentum equation and equation of flow continuity are part of closed system of motion equations. Equation of conservation momentum for above assumptions is:

$$\rho\frac{d\vec{V}}{dt} = -\text{grad}\, p + \kappa\, \text{rot}\vec{\Omega} + (\eta + \kappa)\,\text{rot}\left(\text{rot}\,\vec{V}\right) \tag{1}$$

Angular momentum equation in:

$$\rho\, J\frac{d\vec{\Omega}}{dt} = -2\kappa\vec{\Omega} + \kappa\,\text{rot}\,\vec{V} - \gamma\,\text{rot}\left(\text{rot}\,\vec{\Omega}\right) + (\alpha+\beta+\gamma)\,\text{grad}\left(\text{div}\,\vec{\Omega}\right) \tag{2}$$

Equation of flow continuity for incompressible fluid with constant density:

$$\text{div}\vec{V} = 0 \tag{3}$$

Above equation are derive from and described in details in [2],[3]. Further equation analysis were taken in rolling co-ordinate system, where the wrapping coordinate φ describes the wrapping angle of the bearing, the coordinate r describes radial direction from the journal to the bearing, the coordinate z describes longitudinal direction of crosswise bearing. In order to make the analysis of basic equations in dimensionless form [6], we input dimensionless quantities characterizing individual physical quantities. Oil velocity vector components are:

$$V_\varphi = UV_1 \qquad V_r = \psi UV_2 \qquad V_z = \frac{U}{L_1}V_3 \tag{4}$$

Reference pressure p_o caused by journal rotation with the angular velocity ω was assumed in (7) taking into consideration dynamic viscosity of shearing η and the lubricating gap height h_1 at the wrapping angle φ was taken in relative eccentricity function λ :

$$p_0 = \frac{\omega\eta}{\psi^2} \quad ; \quad h_1(\varphi,\lambda) = 1 + \lambda\cos\varphi \tag{5}$$

The constant viscosity of micropolar oil, independent from thermal and pressure condition in the bearing. Quantity of viscosity coefficient depend on shearing dynamic viscosity η, which is decisive viscosity in case of Newtonian fluids. Reference pressure p_0 is also described with this viscosity, in order to compare micropolar oils results with Newtonian oil results. In micropolar oils decisive impact has quantity of dynamic coupling viscosity κ [1],[3]. In some works concerning bearing lubrication with micropolar oil, it's possible to find the sum of the viscosities as a micropolar dynamic viscosity efficiency. In presented article coupling viscosity was characterized with coupling number N^2, which is equal to zero for Newtonian oil:

$$N = \sqrt{\frac{\kappa}{\eta + \kappa}} \qquad 0 \le N < 1 \tag{6}$$

Quantity N^2 in case of micropolar fluid, define a dynamic viscosity of coupling share in the oil dynamic viscosity efficiency. From the coupling number N^2 we can determine both dynamic viscosity ratio, which is dimensionless micropolar coupling viscosity:

$$\kappa_1 = \frac{\kappa}{\eta} = \frac{N^2}{1 - N^2} \qquad \kappa_1 \ge 0 \tag{7}$$

From the dynamic rotational viscosities α, β, γ at the laminar lubrication, individual viscosities are compared to viscosity γ, which is known as the most important and it ratio to shearing viscosity η is bounded to characteristic flow length Λ, which in case of Newtonian flow assume the zero quantity. Dimensionless quantity of micropolar length Λ_1 and micropolar length Λ are defined:

$$\Lambda = \sqrt{\frac{\gamma}{\eta}}; \qquad \Lambda\Lambda_1 = \varepsilon \tag{8}$$

Dimensionless micropolar length Λ_1 in case of Newtonian oil approach infinity. Equations (1),(2) and (3) after writing out in cylindrical coordinates are presented in article [2], where individual phases leading to Reynolds equation for laminar, stationary lubricating process in dimensionless form are mentioned.

3. Reynolds equation and hydrodynamic pressure

Reynolds equation for stationary flow of laminar micropolar fluid in the crosswise, cylindrical, slide bearing gap can be present [1],[2],[7] in dimensional form:

$$\frac{\partial}{\partial \varphi}\left(\frac{h^3}{\eta}\Phi(\Lambda, N, h)\frac{\partial p}{\partial \varphi}\right) + \frac{\partial}{\partial z}\left(\frac{h^3}{\eta}\Phi(\Lambda, N, h)\frac{\partial p}{\partial z}\right) = 6\frac{dh}{d\varphi} \tag{9}$$

Φ(Λ,N,h) function in form (10) when in case of the Newtonian fluid it has a value 1 and the Reynolds equation (9) change into a non-Newtonian fluid equation.

$$\Phi(\Lambda, N, h) = 1 + 12\frac{\Lambda^2}{h^2} - 6\frac{N\Lambda}{h}\coth\left(\frac{Nh}{2\Lambda}\right) \tag{10}$$

Reynolds equation (9) can be presented in dimensionless form [1],[7] using the method of changing into this values:

$$\frac{\partial}{\partial \varphi}\left(\Phi_1(\Lambda_1, N, h_1)\frac{\partial p_1}{\partial \varphi}\right) + \frac{1}{L_1^2}\frac{\partial}{\partial z_1}\left(\Phi_1(\Lambda_1, N, h_1)\frac{\partial p_1}{\partial z_1}\right) = 6\frac{dh_1}{d\varphi} \tag{11}$$

for $\quad 0 \le \varphi \le \varphi_k; \;\; 0 \le r_1 \le h_1; \;\; -1 \le z_1 \le 1$

where: $$\Phi_1 = h_1^3 + 12\frac{h_1}{\Lambda_1^2} - 6\frac{Nh_1^2}{\Lambda_1}\coth\left(\frac{h_1 N\Lambda_1}{2}\right) \tag{12}$$

Below solutions (11) for infinity length bearing is presented. In this solution the Reynolds boundary conditions, applying to zeroing of pressure at the beginning ($\varphi=0$) and at the end ($\varphi=\varphi_k$) of the oil film and zeroing of the pressure derivative on the wrapping angle at the end of the film where fulfill. The pressure distribution function in case of the micropolar lubrication has a form:

$$p_1(\varphi) = 6\int_0^{\varphi} \frac{h_1 - h_{1k}}{\Phi_1(\Lambda_1, N, h_1)} d\varphi ; \qquad p_{1N}(\varphi) = 6\int_0^{\varphi} \frac{h_1 - h_{1k}}{h_1^3} d\varphi \tag{13}$$

where: $h_{1k}=h_1(\varphi_k)$ lubricating gap height at the end of the oil film.

In the boundary case of lubricating Newtonian fluid, pressure distribution function is a pressure $p_{1N}(\varphi)$. Example numerical calculation were made for the infinity length bearing with the relative eccentricity $\lambda=0,6$.

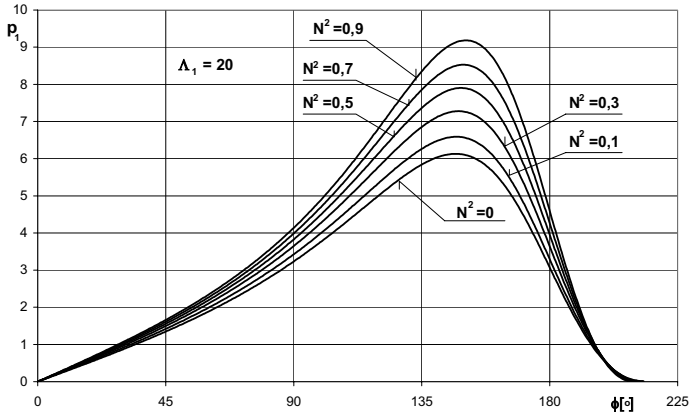

Fig.1 The dimensionless pressure distributions p_1 in direction φ in dependence on coupling number N^2 by micropolar ($N^2>0$) and Newtonian ($N^2=0$) lubrication for dimensionless eccentricity ratio $\lambda=0,6$ and characteristic dimensionless length of micropolar fluid $\Lambda_1=20$

Analyzing the influence of coupling number N^2 and the influence of dimensionless micropolar length Λ_1 on hydrodynamic pressure distribution in the bearing liner circuital direction. At the Fig.1 pressure distribution for individual coupling numbers at constant micropolar length $\Lambda_1=20$. The pressure increase effect is caused by oil dynamic viscosity efficiency increase as a result of coupling viscosity κ. At $N^2=0,5$, coupling viscosity is equal to shearing viscosity. Pressure graph in the Fig.1 for micropolar oil lubrication ($N^2>0$) find themselves above th e pressure graph at the

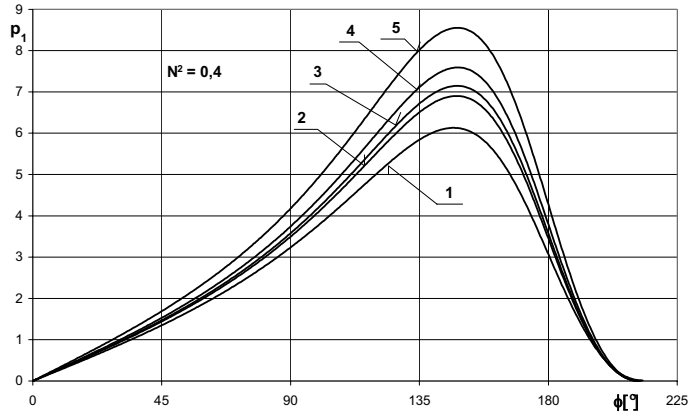

Fig.2 The dimensionless pressure distributions p_1 in direction φ in dependence on characteristic dimensionless length of micropolar fluid Λ_1: 1) Newtonian oil, 2) Λ_1=40, 3) Λ_1=30, 4) Λ_1=20, 5) Λ_1=10, for dimensionless eccentricity ratio λ=0,6 and coupling number N^2=0,4

Newtonian oil lubrication (N^2=0). Pressure distribution is higher for higher coupling number. It is caused by oil viscosity dynamic efficiency. In the Fig.2 the course of dimensionless pressure p_1 for few micropolar length quantity Λ_1 is shown: Decrease of this parameter determine the increase of micropolar oil rotational dynamic viscosity. Pressure distribution are presented at the constant coupling number N^2=0,4. Newtonian oil pressure in the co urse 1. Rotational viscosity increase determine the pressure distribution increase and is caused, because both the oil flow and microratation velocities are coupled. Quantities of coupling number N^2 and dimensionless micropolar length where taken from works [1],[2].

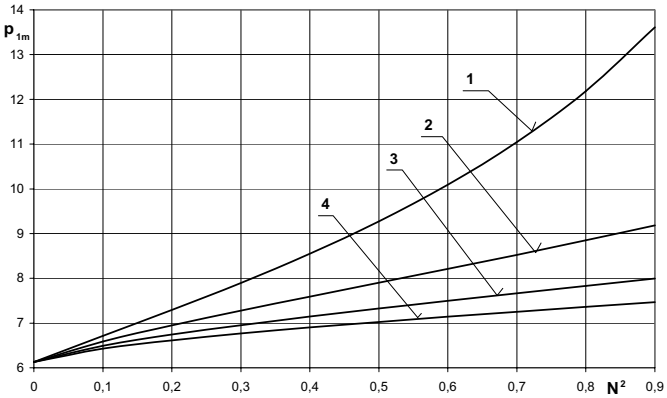

Fig.3 The dimensionless maximal pressure p_{1m} in dependence on coupling number N^2 for characteristic dimensionless length of micropolar fluid Λ_1:1) Λ_1=10, 2) Λ_1=20, 3) Λ_1=30, 4) Λ_1=40

Based on given hydrodynamic pressure distribution p_1 on wrapping angle of the bearing φ, the numerical quantities of maximal pressure p_{1m} and the angular coordinate φ_m (at the maximal position) were obtain. Quantities p_{1m} are presented in the Fig.3 in the coupling Number N^2 function for chosen micropolar length Λ_1. All lines are coming out from the maximal pressure point in case of Newtonian fluid flow. We observe maximal pressure increase when the coupling number N^2 increases (coupling viscosity increases κ) and the micropolar length decreases Λ_1 (rotational viscosity increases γ) . Full range of coupling number change, that covers the range [0,1), apply to coupling viscosity κ change from small to very high quantities. In most of the works, the hydrodynamic parameters of the bearing graphs are given in the function, which is

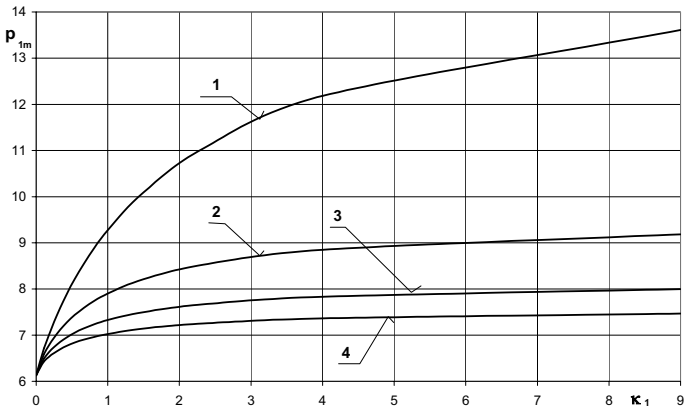

Fig.4 The dimensionless maximal pressure p_{1m} in dependence on dimensionless coupling viscosity κ_1 for characteristic dimensionless length of micropolar fluid Λ_1: 1) Λ_1=10, 2) Λ_1=20, 3) Λ_1=30, 4) Λ_1=40

nonlinear scale for coupling viscosity κ_1. In the Fig.4. the same graph is given in the dimensionless viscosity κ_1 function. Change range N^2 from the Fig.3 comply to κ_1 changes in the Fig.4. Maximal pressure courses presented in the Fig.4, can be more suitable for small quantities for parameter κ_1. In the Fig.5 presented maximal pressure p_{1m} courses in the dimensionless micropolar length function Λ_1 for a few coupling number N quantities.

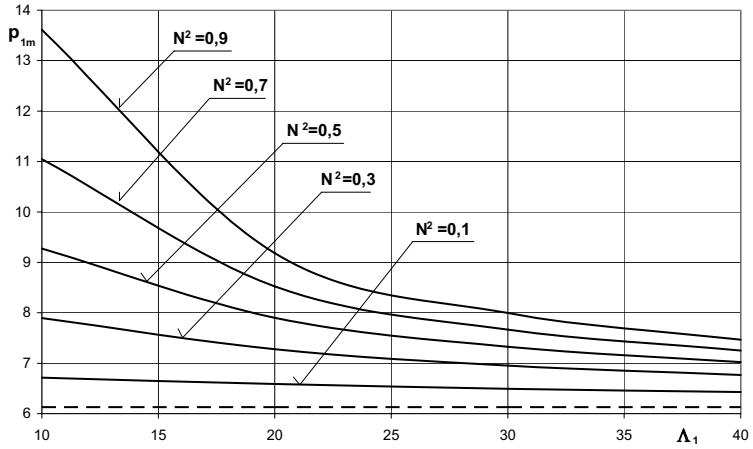

Fig.5 The dimensionless maximal pressure p_{1m} in dependence on characteristic dimensionless length of micropolar fluid Λ_1 for coupling number N^2 (---- Newtonian oil)

Broken line show the maximal pressure in case of Newtonian oil lubrication. All lines approach asymptoticly to the broken line when the micropolar length increases (rotational viscosity decreases γ). Together with coupling number increase, maximal pressure increases (coupling viscosity increases). Angular coordinate φ_m of maximal dimensionless pressure position p_{1m} in thesquare function of coupling number N^2 for chosen micropolar length Λ_1 were show in the Fig.6. All lines come out from the maximal pressure position point in case of Newtonian fluid flow. Increase of maximal pressure position angle φ_m is observed while the coupling number increases N^2 (coupling viscosity increases κ) and the micropolar length decreases Λ_1 (rotational viscosity increases γ). Graphs in the Fig.6 are described with nonlinear scale of dimensionless coupling viscosity κ_1 change.

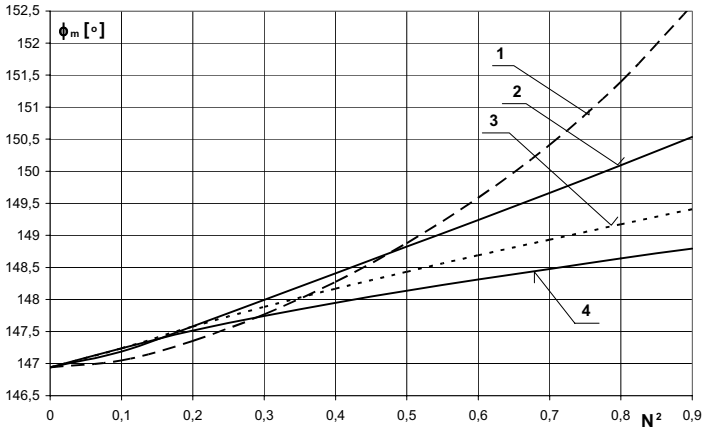

Fig.6 Angle φ_m situated maximal pressure p_{1m} in dependence on coupling number N^2 for characteristic dimensionless length of micropolar fluid Λ_1: 1) Λ_1=10, 2) Λ_1=20, 3) Λ_1=30, 4) Λ_1=40

In the Fig.7 the same graph is presented in the dimensionless coupling viscosity κ_1 (linear viscosity scale). N^2 change range from Fig.6 comply to change of κ_1 in the Fig.7.

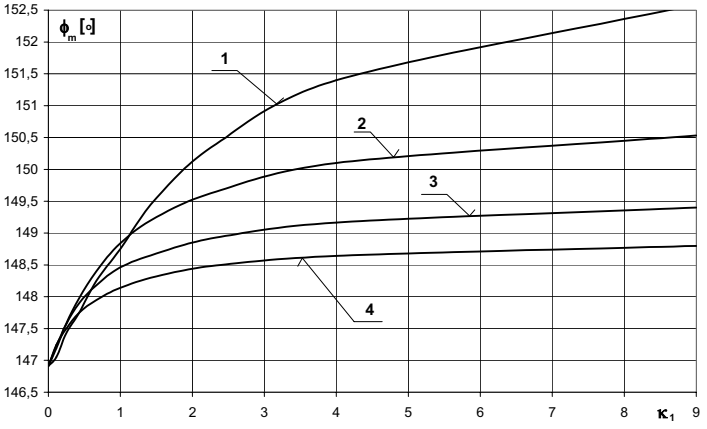

Fig.7 Angle φ_m situated maximal pressure p_{1m} in dependence on dimensionless coupling viscosity κ_1 for characteristic dimensionless length of micropolar fluid Λ_1:1) Λ_1=10, 2) Λ_1=20, 3) Λ_1=30, 4) Λ_1=40

Author claims that angular coordinate φ_m courses of maximal pressure position p_{1m} presented in the Fig.7 are more suitable for smaller quantities of parameter κ_1.

4. Conclusions

Presented example of the Reynolds equation solutions for steady laminar non-Newtonian lubricating oil flow with micropolar structure, enable the hydrodynamic pressure distribution introductory estimation as a basic exploitation parameter of slide bearing. Comparing Newtonian oil to oils with micropolar structure, can be used in order to increase hydrodynamic pressure and also to increase capacity load of bearing friction centre. Micropolar fluid usage has two sources of pressure increase in view of viscosity properties: increase of fluid efficient viscosity (coupling viscosity increase) and the rotational viscosity increase (characteristic length parameter Λ). Author realize that he made few simplified assumptions in the above bearing centre model and in

the constant parameter characterizing oil viscosity properties. Despite this calculation example apply to bearing with infinity length, received results can be usable in estimation of pressure distribution and of capacity force at laminar, steady lubrication of cylindrical slide bearing with infinity length. Presented results can be usable as a comparison quantities in case of numerical model laminar, unsteady flow Non-Newtonian fluids in the lubricating gaps of crosswise cylindrical slide bearings.

References

[1] Das S., Guha S.K., Chattopadhyay A.K., *Linear stability analysis of hydrodynamic jour nal bear ings under micropolar lubrication* - Tribology International 38 (2005), pp.500-507

[2] Krasowski P., *Stacjonarny, laminarny przepływ mikropolarnego czynnika smarującego w szczelinie smarnej poprzecznego łożyska ślizgowego* - Zeszyty Naukowe nr 49, pp. 72-90 , Akademia Morska, Gdynia 2003

[3] Łukaszewicz G., Micropolar Fluids. Theory and Aplications – Birkhäuser Boston 1999

[4] Walicka A., Reodynamika przepływu płynów nienewtonowskich w kana łach prostych i zakrzywionych – Uniwersytet Zielonogórski, Zielona Góra 2002

[5] Walicka A., *Inertia effects in the flow of a micropolar fluid in a slot between rotating sufrages of revolution* – International Journal of Mechanics and Engineering, 2001,vol.6, No. 3, pp. 731-790

[6] Wierzcholski K., *Mathematical methods in hydrodynamic theory of lubrication*- Technical University Press, Szczecin 1993.

[7] Xiao-Li Wang, Ke-Qin Zhu, *A study of the lubricating effectiveness of micropolar fluids in a dynamically loaded journal bearing* – Tribology International 37 (2004), pp.481-490

Notation

L_1 dimensionless bearing length $L_1 = b/R$
J microinertia constant (m^2)
N coupling number
R radius of the journal (m)
U peripheral journal velocity (m/s) $U = \omega R$
V_i components of oil velocity in co-ordinate $i = \varphi, r, z$ (m/s)
V_i $i = 1,2,3$ dimensionless components of oil velocity in co-ordinate φ, r, z
Λ characteristic length of micropolar fluid (m)
Λ_1 dimensionless characteristic length of micropolar fluid
Ω_i components of oil microrotation velocity in co-ordinate $i = \varphi, r, z$ (1/s)
Ω_i $i = 1,2,3$ dimensionless components of oil microrotation velocity in co-ordinate φ, r, z
b length of the journal (m)
h gap height (m)
h_1 dimensionless gap height $h = \varepsilon h_1$
p hydrodynamic pressure (Pa)
p_o characteristic value of pressure (Pa)
p_1 dimensionless hydrodynamic pressure $p_1 = p/p_0$
r co-ordinate in radial of the journal (m)
t time (s)
z co-ordinate in length of the journal (m)
z_1 dimensionless co-ordinate in length of the journal $z_1 = z/b$
α, β, γ micropolar rotational viscosities in co-ordinate φ, r, z (Pa s m^2)
ε radial clearance (m)
η dynamic oil viscosity (Pa s)

κ micropolar coupling viscosity (Pa s)
κ_1 dimensionless micropolar coupling viscosity
λ dimensionless eccentricity ratio
ρ oil density (kg/m^3)
φ the angular co-ordinate
φ_e the angular co-ordinate for the film end
ψ dimensionless radial clearance ($10^{-4} \le \psi \le 10^{-3}$) $\psi = \varepsilon/R$
ω angular journal velocity (1/s)

Journal of POLISH CIMAC

Faculty of Ocean Engineering & Ship Technology
GDAŃSK UNIVERSITY OF TECHNOLOGY

THE CONCEPTION OF UNCERTAINTY ANALYSIS OF RELIABILITY ASSESSMENT OF THE MC TYPE DIESEL ENGINE LUBRICATING OIL SYSTEM

Roman Liberacki

Gdansk University of Technology
ul. Narutowicza 11/12, 80-950 Gdańsk, Poland
tel.: +48 58 3471850, fax: +48 58 3472430
e-mail: romanl@pg.gda.pl

Abstract

In the article elements consisting on uncertainty of reliability assessment of the MC type diesel engine lubricating oil system have been discussed. The conception of uncertainty analysis of the system reliability assessment, on computational example, has been introduced. Moreover, the interpretation of the received result - burdened with large uncertainty, has been proposed.

Key words: *reliability, uncertainty, diesel engine, lubricating oil system*

1. Introduction

The key problem in making reliability analysis of systems, like lubricating oil system for diesel engine, is getting credible reliability data, which are the entrance data to created mathematical models. The probabilities of suitable technical elements failures are on generality these data, as well as the probabilities of the human errors (crew which exploits those technical devices).

Problem in this place appears - where from to draw these data. The sources of reliability data for technical structures can be: tests, data gathered with operation, experts' opinions. To estimate human errors probabilities the methods applied in nuclear energetic can be used, where they be led on wide scale. The description of these methods one can find in foreign literature [2, 8, 10, 12, 13, 14] as well as in national studies [3, 7].

We should remember, that reliability assessment of technical devices and energetic systems is always burdened with uncertainty, which we try to introduce as some numerical interval, including in our conviction marked value (reliability for given period of time). In this place we should underline clearly, that there is no certainty never, that appointed interval contains really in demand value. This is because of lack of full knowledge about system, his surroundings and influences inside the system and in relationship system - surroundings.

Applying the clean probabilistic approach to reliability assessment in such conditions is in the author's opinion inappropriate. The calculus of probability requires the possession of exactly definite data of relating random events. In practice, in the best case we can dispose with large number of empirical data, which will allow us to qualify the statistical rights (the distributions of random variables) relating to elements of considered system. However, it is proper to turn the attention, that the distribution of random empirical variable, used in statistics, it is not the same what the distribution of probability density function. We take into account fact this applying interval estimation in demand value, what simultaneously the uncertainty of reached result reflects.

In many situations we possess a small set of statistical data or we have outright to appeal to experts' opinions in aim gaining over reliability data. The use of possibility measure or fuzzy numbers seems to be reasonable solution in such case. They will allow us to estimate reliability of

considered system as well as uncertainty of this estimation. Naturally it is possible to join the statistical methods with the fuzzy set theory methods or with the possibility theory together.

2. Lubricating oil system for the MC – type diesel engine

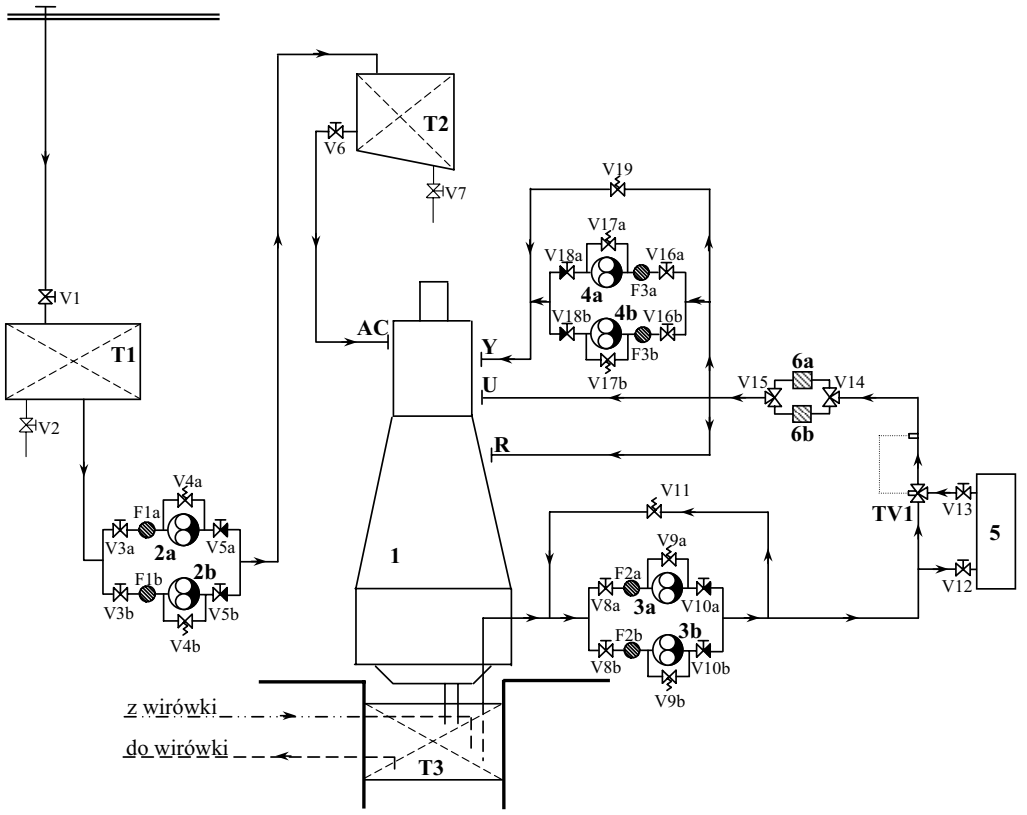

Fig. 1. Lubricating oil system for the MC – type diesel engine: 1 - diesel engine; 2a, 2b – cylinder lubricating oil transfer pumps; 3a, 3b - lubricating oil pumps; 4a, 4b – camshaft lubricating oil booster pumps; 5 – lubricating oil cooler; 6a, 6b – lubricating oil duplex filter; T1 – cylinder lubricating oil storage tank; T2 – cylinder lubricating oil service tank; T3 – lubricating oil bottom tank; TV1 – thermostatic valve; V… – valves; F… – suction filters

Lubricating oil system for the MC – type diesel engine is the object of considerations. The scheme of this system is shown in Fig. 1.

Building relative model of the system following assumptions have been made: stop the pumps can be the caused with lack of the power supply among different causes, the lubricating oil purifying system is fit, all stop valves and non return valves are in open position (except of valves V2 and V7), all tanks are equipped with signaling alarm of low level, duplex filter is equipped with signaling alarm of pressure drop to high, suction filters are equipped with signaling alarm of pressure drop to high, the critical leakage of oil from system requires immediate stop of engine.

The reliability of lubricating oil system, for considered period of time, means the probability, that in this period of time the work of engine will be possible. We by event of failure of lubricating oil system understand such event which extorts stop engine or causes stop engine directly.

3. Elements consisting on uncertainty of reliability assessment of the MC type diesel engine lubricating oil system

On uncertainty of reliability assessment of considered system consists:
- uncertainty of relative model,
- uncertainty of mathematical model based on the relative model,
- uncertainty resulting from possessed reliability data.

3.1. Uncertainty of relative model of system

Under notion of relative model of system one should understand a fault tree or reliability structure created for the system, which in graphic form reflect all sequences of basic events leading to appearing the event of failure of considered system.

The fault tree method found the wide use in reliability analyses of technical systems. The method is applied in nuclear energetic, chemical industry, aviation, land transportation. It is also commanded for shipping systems by developed under auspices of International Sea Organization (the IMO) Formal Safety Assessment method [11].

Uncertainty of relative model results from concern, or really sequences of basic events, recorded in form of fault tree or reliability structure, lead to appearing the event of failure of considered system or if any essential sequence of events was not skipped.

Verification of correctness of such model can be done using the experts' courts only. If experts will state, that all recorded in the fault tree sentences are true, as well as they will not be able to show different sequences of events, than these which were used already, then we can believe, that there are no bases to judge, that created model is inadequate.

We will attribute such a model plausibility measure 1(Pl =1). It means that we recognise our model for plausible. The plausibility measure 1, in distinction from probability measure 1, does not mark the hundred - percent certainty to adequacy of model (an additional expert would can find in the model mistake). The plausibility measure and the necessity measure were introduced by Shafer, how the authors write in [1].

It is obvious, that it is proper so long to consult with experts the correctness of model as well as to make possible corrections until we will can attribute the model plausibility measure 1.

3.2. Uncertainty of mathematical model

We build mathematical model with algebraical structure with support of fault tree, using the minimal cut sets method. We do not achieve in this case formula for reliability of the system, described with the fault tree, but formula for the lower boundary of reliability of this system. We can rebuild the fault tree on the success tree, then to solve the success tree using the minimal path sets method and to receive the formula for the upper boundary of reliability of this system. In the result we receive some area in which the demand function of reliability contains. We proceed so, because the exact delimitation the function of reliability of complex systems is in general very difficult.

In majority of reliability analyses we give up from marking the upper boundary of reliability. Only the lower boundary of reliability is marked. In this case we can say , that the reliability of system for considered interval of time is not lower than appointed value. Approach such is the working on principle of investigation of the worst case. It is obviously reasonable. Reliability of devices and technical systems influences on safety of those technical objects, men, natural environment as well as on achieved economic effects. Pessimistic approach to reliability assessment is therefore reasonable.

Simplifications used in the minimal cut sets and minimal path sets methods cause, that for considered period of time, we receive the result in the form of the interval, in which the reliability of system (modeled with the use of the fault tree and the success tree methods) contains.

To receive more precise results, we should abandon the fault tree and the success tree methods, than to try to model the reliability of the system with the help of the reliability structure method and to mark using this method exact formula on reliability of the system. However in practice it is very difficult, as it was said earlier. That is why the majority of system reliability analysts inclines to use only and the minimum cut sets method.

3.3. Uncertainty resulting from possessed reliability data

There are several situations possible with getting reliability data. We seek for such data for technical elements and for human as well.

When we have at our disposal a large statistical sample or a small statistical sample, but we know the statistical distribution of the time to failure for elements or we use the data given in reliability handbooks or guides, then we define the statistical distribution of the time to failure and parameters of the distribution on definite significance level (e.g. $\alpha = 0,1$), in compliance with laws of mathematical statistics.

Uncertainty of reliability assessment of the system for considered period of time is delimited then by numerical interval. We receive this interval by substituting the 5 % quantile and 95 % quantile of the statistical data to the formula describing reliability function of the system.

When we have at our disposal a small statistical sample and we do not know the statistical distribution of the time to failure for elements, then the problem can be solved using the possibility theory or the fuzzy sets theory. In case of using the possibility theory the uncertainty of estimation of reliability contains in numerical interval limited with measure of possibility and the measure of necessity [1].

The case in which we dispose no reliability data stays to consider. We have to reach the data in some way. We can try to find out these data in support of experts' opinions. Previous experiences show, that experts have difficulties with formulating their opinions in the form of numerical data. I propose so, to ask experts to formulate their opinion in the form of the linguistic probability terms like: probability, that the event of failure of given kind of element will happen in considered period of time is: very high, high, average, low, very low. We can transform the linguistic variables into the data in the form of the fuzzy numbers without experts' participation. The uncertainty of estimation of reliability is represented by the fuzzy number. Questions these became described wider by the author in [5, 6].

4. Reliability of the system with the uncertainty of the assessment taken into consideration

4.1. Uncertainty of relative model

The relative model, built for analysed system had the form of fault tree. In compliance with this what was written earlier (subentry 3.1.), the plausibility measure 1 was given for the fault tree. The structure of the fault tree is very complex, and that is why it was not introduced in this article. The fault tree structure the reader can find in study [6].

4.2. Uncertainty of mathematical model

The mathematical model was built with support of the fault tree, using the minimal cut sets method and the minimal path sets method. Moreover the reliability structure was built to avoid inaccuracies resulting from use of minimal cat sets and minimal path sets methods.

To illustrate uncertainty of the mathematical model the calculations of reliability of lubricating oil system were done:

a. using the reliability structure method (exact value of reliability)
b. using the minimal cut sets method (lower boundary of reliability)
c. using the minimal path sets method (upper boundary of reliability).

The reliability of the system was calculated for one year of service and for four years of service accepting, that the system at the beginning was new. Moreover, to show the uncertainty of mathematical model – a clean hypothetic assumption was taken, that the reliability data are certain.

The set of reliability data used in calculations, the fault tree and the reliability structure the reader can find in study [6]. Results of calculations were introduced in Tab. 1.

Tab. 1. Reliability of lubricating oil system for the MC type engines calculated using: the minimal path sets method, the exact method, the minimal cut sets method

Reliability of the system	1 year	4 years
Minimal path sets method	100 %	100 %
Exact method	92,7 %	65,3 %
Minimal cut sets method	92,1 %	51,3 %

Received results reflect the uncertainty of mathematical model, when we use the minimal cut sets and the minimal path sets methods. It was said in subsection 3.2., that the minimal cut sets method is the most often used method - as working on principle of the worst case. It is proper to turn attention, that in considered lubricating oil system case - the value of reliability calculated using the exact method is more approximate to this got using the minimal cut sets method, than these got with minimal path sets method.

Because it was possible to get exact formula for reliability of the system, therefore in more far considerations only this formula will be taken under attention. It will avoid us from received mathematical model uncertainty.

4.3. Uncertainty resulting from possessed reliability data

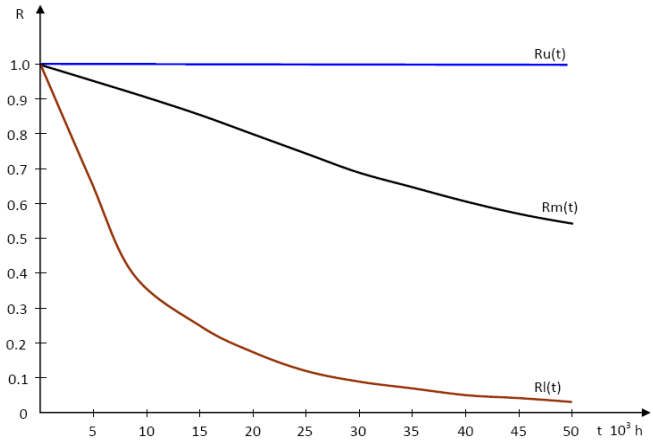

Fig. 2. The reliability function of the lubricating oil system for the MC – type diesel engine, considering the uncertainty of accomplished assessment; Rm(t) – reliability function appointed with the use of median values of reliability data, Rl(t) – lower boundary of reliability function, Ru(t) – upper boundary of reliability function

Reliability data for technical elements were taken from guide [9] as well as from study [4]. These data have a character of mean failure rate, what implies the use of the exponential distribution of time to failure for those technical elements. The ASEP – HRAP method was used to determine human error probabilities. Failure rate boundaries for technical elements were been delimited with the use of the 5 % quantile and 95 % quantile of lognormal distribution of the mean failure rate values. Similarly, the boundaries of human error probabilities were been delimited with the use of the 5 % quantile and 95 % quantile of lognormal distribution. Received results are shown in Fig. 2.

5. Proposal of interpretation of result with the large uncertainty

The reliability data used in calculations were burdened with large uncertainty, what was transferred on large uncertainty of reliability assessment of the lubricating oil system. Received results shown in Fig.2. tell us clearly, that it is very hard to assess reliability of our system. In support about such uncertainty results it is very hard to take the decision: to permit the system to work or to phase out the system from work. The decision is particularly hard for longer times of work.

It there is no possibility to define the reliability data more precisely - and the same to reduce the area of uncertainty, then we can try to analyse received results with the use of fuzzy numbers.

Let's accept, that we are interested in the reliability of the lubricating oil system for working time 4 years (35040 h) since the moment of putting this system to use. According to the author's model we can affirm, that for considered period of time: the upper boundary of reliability of the system equals 0.999; the median value of reliability of the system equals 0.653; the lower boundary of reliability of the system equals 0.068. We will demonstrate the received result in the form of fuzzy number A_R "about 0,653" in Fig. 3.

We can also affirm respectively, that for considered period of time: the lower boundary of unreliability of the system equals 0.001; the median value of unreliability of the system equals 0.347; the upper boundary of unreliability of the system equals 0.932. We will demonstrate the received result in the form of fuzzy number A_F "about 0,347" in Fig. 3.

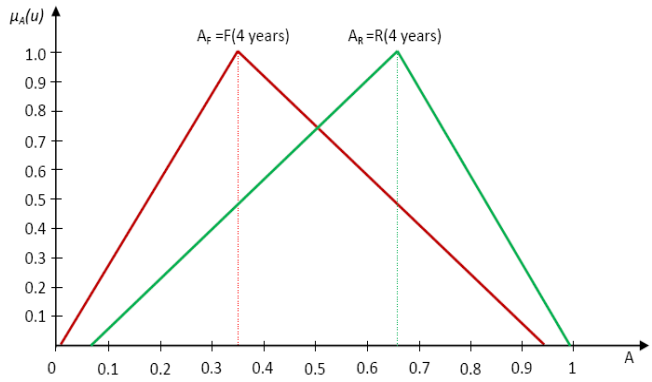

Fig. 3. The reliability value A_R and the unreliability value A_F of the lubricating oil system for the MC - type engine evaluated for working time 4 years, expressed in form of fuzzy numbers

Looking at Fig. 3. we can draw out following conclusions: 1) Generally, reliability of the system is higher then the unreliability. 2) The median value of probability, that system failure or system failures will occur in considered period of time equals 0.347. 3) The median value of probability, that no system failure will occur in considered period of time equals 0.653.

Let's try now to express the reliability of our system in terms of linguistic probability. To do this we will put in the same figure values of the linguistic reliabilities (established before) and the value of reliability of the system received in the form of fuzzy number A_R, for considered in our example period of time. The result is shown in Fig. 4. We can notice, that fuzzy value of reliability of our system belongs in different degree to every one from fuzzy numbers valuating linguistic reliability.

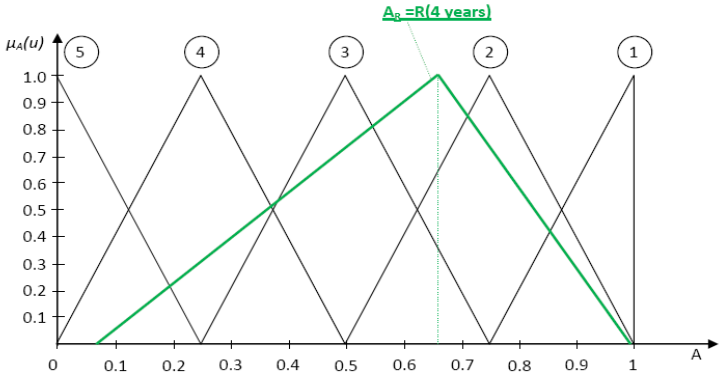

Fig. 4. Valuating the linguistic reliabilities
1 - very high reliability, 2 - high reliability, 3 - reliability about 50 %, 4 - low reliability, 5 - very low reliability, A_R - the reliability of considered system given in the form of fuzzy number

Let's accept the measure of possibility, that reliability of the system belongs to the valuating number A_i as: $\Pi_i = \max(\mu_{AR} \wedge \mu A_i)$. We will take down the results in Tab. 2. The sum total of possibility measures (in distinction from probability measures) according to the possibility theory can be greater then 1. In our case the sum is 2.81. Of course, we can transform these values to the form of percentages to give in total 100 %.

The results collected in Tab. 2. shows, that the highest possibility is that the reliability of lubricating oil system for the MC - type engines, in considered period of time is high – it means the reliability value contains in interval [0.5 - 1). Possibility this was estimated on 30% of all possibilities. The lowest possibility is that the reliability is very small – it means the reliability value contains in interval [0 – 0,25). Possibility that was estimated on 8% of all possibilities.

Tab. 2. The comparison of possibility measures, that reliability of lubricating oil system belongs to established fuzzy numbers valuating reliability

Linguistic values of reliability	Intervals of numerical values	Possibility measure Π_i that reliability of the system belongs to A_i
A_1 – reliability very high	[0,75 – 1)	Π_1=0,42 (15 %)
A_2 – reliability high	[0,5 –1)	Π_2=0,85 (30 %)
A_3 – reliability about 50 %	[0,25 – 0,75)	Π_3=0,81 (29 %)
A_4 – reliability low	[0 – 0,5)	Π_4=0,51 (18 %)
A_5 – reliability very low	[0 – 0,25)	Π_5=0,22 (8 %)

6. Final remarks

In the case of large uncertainty of estimated reliability of system, as in considered example (Fig. 2.) it is very hard to take rational decisions: to permit the system to work or to phase out the system from work, especially for longer time in service.

What should be done in such situation? First of all, we should try to gain over reliability data burdened with smaller uncertainty. If this is not possible, we can analyse received results using fuzzy numbers according to the author's proposal (Tab. 2.), what gives us enough good knowledge for undertaking the decision about more far exploitation of system.

The proposed method of reliability assessment with the large uncertainty has to bee improved.

The studies on appointment of numerical boundaries of estimations of linguistic reliabilities of diesel engines' systems in the closest time will be led. The boundaries not at all have to be and they should not be spread equably like it was shown in Fig. 4.

References

[1] Dubois, D., Prade, H., *Possibility Theory. An Approach to Computerised Processing of Uncertainty*, New York, 1988.

[2] Gertman, D.I., Blackman, H.S., *Human Reliability and Safety Analysis Data Handbook*, New York, 1994.

[3] Kosmowski, K.T., *Ocena niezawodności operatora w realizacji wybranych funkcji w procesie sterowania na przykładzie instalacji wytwarzania energii elektrycznej statków serii B 488*, Politechnika Gdańska, Gdańsk, 1997.

[4] Liberacki, R. Nowak, P., *Wyniki symulacji bezpieczeństwa napędowego statków serii B 488*, opracowanie wewnętrzne, Politechnika Gdańska, Gdańsk 1998.

[6] Liberacki, R., *Niepewność oszacowania niezawodności instalacji okrętowych*, XXVIII Sympozjum siłowni okrętowych, Gdynia, 2007.

[7] Liberacki, R., *Koncepcja szacowania danych niezawodnościowych dotyczących urządzeń energetycznych w przypadku uzyskania statystyk o małej liczności bądź braku danych niezawodnościowych dotyczących określonych urządzeń, opracowanie wewnętrzne*, Politechnika Gdańska, Gdańsk, 2007.

[8] Radkowski, S., *Podstawy bezpiecznej techniki*, Oficyna wydawnicza Politechniki Warszawskiej, Warszawa, 2003.

[9] Swain, A.D., Guttman, H.E., *Handbook of Human Reliability Analysis with Emphasis on Nuclear Power Plant Applications*, Final Report, prepared for U.S. Nuclear Regulatory Commission, August, 1983.

[10] DNV, *Offshore Reliability Data Handbook*, OREDA, 1998.

[11] IMO (MEPC 45/13), *Formal Safety Assessment Including Environmental Indexing of Ships*, 27 June 2000.

[12] IMO (MSC 66/INF.8), *A methodology for formal safety assessment of shipping*, London, 1996.

[13] Nuclear Energy Agency, Committee on the Safety of Nuclear Installations, *Critical Operator Actions, Human Reliability Modeling and Data Issue*, Final Task Report, OECD, 1998.

[14] Office of Nuclear Regulatory Research, US Department of Commerce, NUREG/CR – 2300, *PRA Procedures*

[15] *Guide, A Guide to the Performance of Probabilistic Risk Assessment for Nuclear Power Plants*, Final Report – Vol.1.,Washington DC., Jan 83.

[16] Safety and Reliability Directorate UK Atomic Energy Authority, *Human Reliability Assessors Guide*, October, 1988.

Journal of POLISH CIMAC

Faculty of Ocean Engineering & Ship Technology
GDAŃSK UNIVERSITY OF TECHNOLOGY

APPLICATION OF PROBABILISTIC DIAGNOSTIC MODELS IN DIAGNOSTIC SERVICE DECISIONS-AIDING SYSTEMS FOR SHIP MAIN PROPULSION ENGINE

Zbigniew Łosiewicz
Szczecin University of Technology
Al. Piastów 41, Szczecin, Poland
Tel.+48 600 275 871
e-mail: HORN.losiewicz@wp.pl

Abstract

The paper presents a relational diagnostic model of a ship main propulsion engine used in aiding the service decisions. Ship main engine has been identified as the diagnosed system, diagnostic parameters as well as inter-relations taking place between the main engine states and diagnostic parameters have been specified using appropriate mathematical apparatus.

Keywords*: ME probabilistic diagnostic model, ship main engine, technical condition of ship ME, diagnostic parameters, relational model, rational operation of a ship engine.*

1. Introduction

A high power combustion piston engine used for ship propulsion is a complex technical system designed following the design assumptions, according to which it is to ensure the execution of transport tasks, and to achieve its assumed parameters related to its service, reliability, safety and economy.

Depending on the application, it can be used directly for a direct drive of a screw propeller or in a diesel-electric system or diesel – electric – hydraulic system. Especially in case of a direct drive, the reliability of the main engine (ME) can be of essential importance for ship safety. Therefore it is essential to effect such operational policy that will aim at optimisation of the operational parameters (operation rates) of an engine, as well as at minimising the risk of any serious defect.

For this reason, arriving at reliable diagnosis essential for taking rational operational decisions is best based on the application of the engine diagnostics system.

A reliable diagnosis depends on the quality of the diagnostic process, including: correct identification of the object and its processes and phenomena, accurate selection of tested parameters measured in appropriate measuring points, and optimum use of diagnostic information obtained directly or as a result of information processing.

With regard to the above, in order to obtain a reliable and accurate diagnosis of a diesel engine condition an optimal diagnosis system should be built, consisting of a diagnosed system (object) and a diagnostics system (DS) specially built for a given type of the object.

2. Practical usefulness of currently applied diagnostics systems

Modern diagnostics systems being currently introduced into use are applied for specific types of diagnosed engines. These are systems of specific architectural solutions and their application needs special adaptation of the engines. Spare parts databases, maintenance planning and the procedures of ordering the original spare parts are very useful for an operator and form a very good data set useful for ship operator in his consultations with the technical support services of a shipowner, aiming at reduction of expenditures, but often without taking the required safety level into account.

Also the diagnostic information concerning the assessment of element wear during the execution of maintenance is very useful for the operator. The most troublesome are those diagnostic systems which are

designed to aid the operator's decisions during the engine operation. A lot of diagnostic information is calculated by the system, which provides correct results only if correct input data are entered, the verification of which is not always possible in practice. It is visible in the design of such systems which feature data transmission to the manufacturer's server and for the analysis of data by the manufacturer's experts. The knowledge and the experience of a ship engine operator not always allows him to properly interpret the information feedback of diagnostics system presented on its display screens.

There is a lack of data concerning discrete operation of MEs. Manufacturers normally determine the service lives and wear values for parts, subassemblies and systems on the basis of laboratory tests and experience in service. Also maintenance intervals are provided, after which preventative maintenance should be carried out, resulting from the number of hours of operation (apart from other cyclical maintenance provided for by the law). All these maintenance activities aim at renewal of engine's operational potential.

From the economical point of view, service life intervals for particular engine elements (their durability) should be set as multiplies of a common basic time interval, which would facilitate the execution of above-mentioned scheduled maintenance.

From the point of view of reliability and watt-hour efficiency of engine operation this can however cause the accumulation of negative factors often leading to serious disturbances in the engine operation or to its extensive damage and complete failure. Simultaneous progress of element wear in the engine can cause generation of ambiguous diagnostic signals.

With regard to the above, the manufacturers and operators of main engines collect their experiences over the whole time of operation and try to introduce changes aiming at increasing the reliability of main engines through the application of appropriate diagnostics systems for the determination of their technical condition [5,7].

Despite intense research and modernisation of both the diagnostics systems and the supervision procedures of service processes, extensive failures blamed on diagnostics still occur.

The reason for that is a continuous technical development and stricter and stricter requirements regarding economics, environment protection and service ease, forcing the increase of the main engine power with simultaneous reduction of their sizes. This leads to introduction of new technologies with simultaneous increase of loads on yet-untested elements and assemblies of main engines. Similar damages to parts and assemblies of main engines discovered in differing diagnostic conditions may be followed by differing results of their occurrence.

Modern diagnostics systems described in the papers [5,7,8] are examples of practically useful expert systems, however the modern methods of accurate, reliable collection of diagnostic information, including technical possibilities and costs of their operation onboard require high qualifications from the operator, the more so that the degree of the diagnostics system complexity increases very quickly, which is followed by a variety of possible irregularities in their functioning. Therefore along with the increase of operational requirements and development of engines as diagnosed systems, it is necessary to carry out works aiming at improvement of their diagnostics systems. Rational service of main engines – and thus, at the same time, also of ships being technical objects of enormous material value, depend on their diagnostics systems. Same applies to the ecological safety of the natural environment and the crew's health and lives.

3. The rationale for building of ME diagnostic models

Analysing the collected material it can be noticed that the building of diesel engine diagnostic models is strongly linked to the development of engines themselves being the diagnosed systems, as well as the development of science fields focusing on the research into phenomena and processes taking place in such engines.

Ship main propulsion engines are complex technical objects of large size and mass, and what follows, of large inertias in parameters characterising their energy transformations. They are also characterised by a variety of energy-related states, depending on their service state [1,2].

As a result of the above the phenomena and the processes taking place in the service of a marine diesel

engine have been mathematically modelled in a number of ways, including deterministic, pseudo-deterministic and probabilistic ones.
Various types of models are used simultaneously in modern diagnostic systems.
Deterministic models are most often used for operational control in conditions deemed to be normal.
The transitory or emergency conditions are modelled probabilistically, which better renders the actual conditions at sea. They provide information which facilitates rational decision-making by the operator. [1,2,3,4].

It should also be remembered in the quest for collection and analysis of a largest possible number of parameters that the crew selection process is also of stochastic nature, and that crews represent varying levels of technical training and competence (knowledge and experience).
Because of that, the information presented by a diagnostic system should be as accurate and trustworthy as possible.

Complex structure of a marine diesel engine and the numerous criteria for the evaluation of its service states make a relational model being one of possibilities.

As it has been proved in numerous publications [1,2] that the wear of engine elements and subassemblies often does not depend strictly on their total running hours, so the proposed relational model is based on a hypothesis that:

„it is possible to predict the state of a service process of main propulsion engines in $t + \Delta t$ moment when its state in t moment is only known, due to the fact that the condition in $t + \Delta t$ and its duration only depends on condition in t, and not on an earlier conditions and their duration" [1, 2, 8].
This hypothesis allows for the application in the decision-making process of the controlled semi-Markov process theory or a statistical theory of decision-making.
At the same time, a thesis is adopted that „the application of a probabilistic model for ship main propulsion engine should allow for a more rational decision-making and control of such engines' operation and service process [1, 2, 3, 4, 8].

4. Proposed diagnostic model

As a result of adopted assumptions, the process of building a ME diagnostics model required that the following problems are examined.

Identification of a ship main engine as an energy system, used, operated, diagnosed and controlled.
Identification of a main propulsion engine as a diagnostics system, and a determination of its technical and operational properties discovered its significant characteristics in the process of building a rational diagnostic model, which should consist of a diagnosed system (the engine), already adapted for diagnosing as dictated by identification results in the design phase, and a diagnosing system necessary for identification of its technical condition.
Determination of the influence that the load has on the wear rate and wear condition allows for calculating the probability of reaching parameter limit values which may lead to possible engine damage.
A basis assumption made during the building of a diagnostic model is not to establish the cause of past defects, but to take action which may lead to such decisions which would in turn enable prevention of engine damage, or at least limit significantly its consequences. Within such an activity, a particular importance is given to decision-based control of combustion engine service process, implemented within the automatic engine control system as presented in publications [1, 2, 3, 4].

Striving for full automation of engine control stems mostly from a need to reduce the influence of these engines' direct user on their operation, and to reduce the number of defects arising as a result of mistakes made in service.
Automatic control of combustion engine running (the engine is both a controlled and a diagnosed system) should be monitored by a diagnostics system integrated with a control system . Such an integration allows for controlling the engine in a way which could take into account the diagnosis generated by its diagnostics system, and then control the energy-related engine states following its changing technical condition and using

control signals adapted for this condition. Building such a diagnostics system requires first building the diagnostic model of the engine, which should include the requirements for the identification of both the technical conditions and energy-related states of a given engine, as well as the monitoring of engine control system and its running.

4.1 Identification of engine technical condition.

Technical condition of any engine is a set of technical properties of its structure, which allows it to operate (run) in accordance with its purpose for which it was designed and manufactured.
This condition in any moment t in its service life depends not only on this moment, but also on the technical condition of the engine at initial $t_0<t$ moment, and the flow of engine control during this time period.
Control has a definite influence on the change of engine technical condition, which depends on a number of factors after the conclusion of its manufacturing process, as described in literature [1,2].
What follows is that the process of changes of each engine technical condition is stochastic, but continuous in state flow and time. This means that there is an infinite number of engine technical conditions. Diagnosing all technical conditions of the engine is neither possible nor desirable due to both technical and economic reasons, which leads to a need to have this set divided into a limited number of classes (subsets) of technical conditions. Assuming a dividing criterion to be engine's readiness for service, the following classes of technical conditions can be distinguished, to be called directly the conditions [1,2,8]:

- the condition of full readiness (s_1), which allows the engine to be run in full range of loads, to which it was adapted in the design and manufacturing phase,
- the condition of reduced readiness (s_2), which allows the engine to be run in full range of loads, to which it was adapted in the design and manufacturing phase, but with a meaningfully reduced overall efficiency leading to increased fuel consumption or non-compliance with ecological standards.
- the condition of partial readiness (s_3), which allows for operating the engine in a reduced range of loads, narrower than the one for which the engine was designed in design and manufacturing phase.

the condition of being out of operation (s_4), which prevents the engine from any normal usage (due to e.g. damage, execution of maintenance works, etc.).

One important task is to build a model of engine technical condition changes. In case of any diesel engine the process of its technical condition change is a process where the periods of each of its conditions duration are stochastic variables. Particular implementations of these stochastic variables depend on many factors, including the wear of tribological systems of the engine, media quality and crew competences.

4.2 Identification of engine service conditions

Taking into account the knowledge contained in literature and the results of own empirical research it was assumed that the two-stroke low-speed diesel engine used as a main propulsor drive, may be in a number of service conditions, divided into classes (sets) of elementary states, presented in the work [8].
Diagnostic activity is carried out in each of mentioned state sets, with its scope depending on the capabilities of diagnostics systems used, as well as on time needed for the taking of rational service decision.
It is then necessary to identify impacts of particular elements/ subassemblies/ subsystems on the proper functioning of other elements, as well as the consequence of this impact on the quality of processes taking place in the engine. Due to this reason the physical and chemical properties of engine elements/subsystems having some influence on the quality of engine running and determining its technical condition class have been identified.
A main purpose of ME is to provide the energy for the propulsion of a ship during the execution of a given service task.
The readiness of the engine to enable task execution, its operational effectiveness and reliability in task execution as well as safety of operation depend on the quality of its service process.

Engine service includes its running and maintenance and these can be simultaneous [1]. The specifics of main engine service in marine conditions require forward planning of the processes outlined in [8]:
- normal ME operation, where efficiency attainable within environment protection limitations is the most important factor,
- emergency ME operation (complex, hazardous, defect or a disaster taking place), where priority is the ability to reach a location guaranteeing safety of ship and its crew,
- planned maintenance, during which there is no danger to crew lives and ship, and the purpose is to restore full readiness of ME,
- unplanned maintenance (necessary in case of defects), often at sea and in unfavourable conditions bringing dangers to crew lives and the ship itself, with the purpose being just to restore partial readiness of ME and to achieve a capability of reaching a safe destination.

During the process of formulating and defining the tasks for ME in its design phase, its service system is formed at the same time [1,2].

The conditions on modern market make the shipowners optimise the ME service system and press ME manufacturers in this direction – and any such action must be based on the appraisal of current ME condition.
As a result of the above, it was necessary to determine the ME service states and technical conditions, which allows for a rational service of ME, and facilitates the service-related decision-making also in emergency situations, where there is a reduced chance for making rational decisions due to stress and time pressure, as the emergency situations develop rather quickly.

The service process of any diesel engine is a compound process including the simultaneous changes of its technical condition and its service states, which has been presented in the literature in many forms such as graphs or matrices comprising probability distributions [1,2,8].

4.3 Determination of parameters identifying the technical and service conditions

The diagnosis process is greatly dependent on the information obtained via measurements fed into the diagnostics system.
It is thus necessary to define appropriate sets of diagnostic parameters which are going to provide a reliable representation of ME technical condition and its properties.
These may include the sets of : thermodynamic parameters, parameters related to vibration and acoustics, parameters related to physical and chemical properties of lubricants, and the geometric parameters defining the engine structure.
The parameter sets characterise the changes which are a result of various physical and chemical processes, often inter-related or derivative.
The values of parameters obtained during tests in manufacturer's laboratory (in known conditions) are adopted as benchmarks.
They are strictly connected with the technical and energy-related condition of the engine, and the properties of engine elements, subassemblies and subsystems are reflected in their values.
Attention should also be brought to the fact that the diagnosing system should not only help collect the information about engine condition, but also to help control it in such a way as to avoid any damage.
In both cases the result is to be a reduction in operating costs, and what follows, also a rise of service efficiency.
Due to the above, a main purpose in the building of diagnostic models is to search for and use such parameters whose changes should most readily indicate a change of engine technical condition, including its subsystems and elements.
Progress of engine structure wear should be signalled according to earlier adopted grading.

4.4 Determination of diagnostic relations between ME technical condition and diagnostic parameters used, taking into account the results of empirical research

Another important problem in diagnostic model building is the determination of mutual relations between factors influencing the correct running and durability of the engine and the diagnostic parameters which reflect its technical condition, while taking into account the operational priorities of particular ME service conditions. The relation sets have been defined following the ME readiness criteria [8]:
- diagnostic relations projecting the full readiness condition set into a set of diagnostic parameters,
- diagnostic relations projecting the reduced readiness condition set into a set of diagnostic parameters,
- diagnostic relations projecting the partial readiness condition set into a set of diagnostic parameters,
- diagnostic relations projecting the out-of-operation condition set into a set of diagnostic parameters.

4.5 Definition of a relation-based diagnostic model of ship ME

ME is a complex object and its model aimed at collection of diagnostic information may be a combination of various types of models, and may be presented in analytical, functional or topological form. Each model representation form has its research and educational value. The utilitarian value of a model of examined object depends on a number of factors, including a form used for the presentation of the results of analysis performed on data collected within the real-life diagnostic system.

Scientists tend to use forms of models different than those which could be easily understandable for ship crews which belong to a wide range of technical cultures and have highly varying levels of technical knowledge and psychological predispositions. In marine environment, the most suitable form of ME model seems to be a topological model containing the bidirectional relations between engine condition and diagnostic parameters. The drawing below presents the selected diagnostic relations projecting the condition of full readiness s_1 into a set diagnostic parameters k.

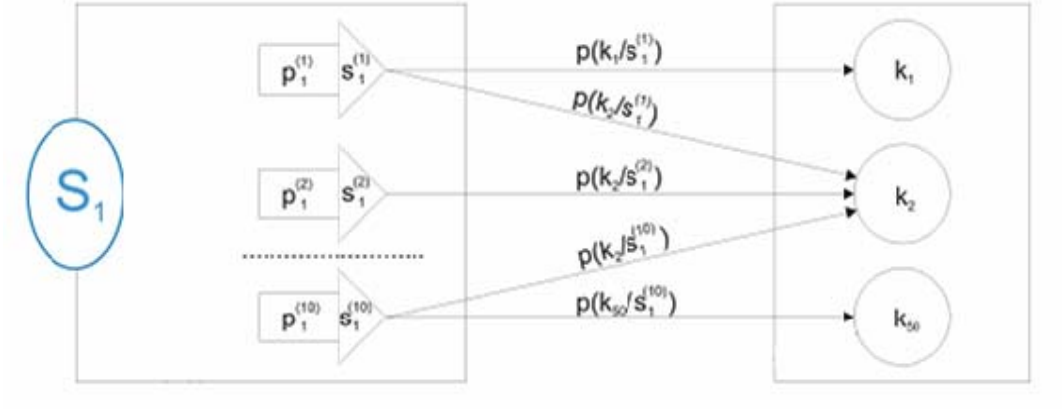

Fig.1 Selected diagnostic relations mapping the full readiness conditions set s1 into a diagnostic parameter set k[8].

Decision-based control of engine service process is the most important and most difficult problem in engine service, which follows from the fact that such a control is carried out in a stochastic situation with regard to decisions.

In such a situation, evaluation of statistical risk connected with making a wrong decision should be taken into account.

Such a wrong decision may be taken as a result of inability to precisely evaluate the unknown parameters of stochastic variable distributions, which are the conditions of engine service process, and also due to a lack of capability to obtain full and reliable diagnosis of engine technical condition.

Rational control of this process requires furthermore that statistical decision-making models are built for the purposes of control.

A theory of decision-based, controlled semi-Markov processes or a statistical theory of decision-making can both be used for the building of such models, being presented in detail in publications [1,2,3,4].

In case it is impossible to use objective probabilistic measure for the specification of diagnosis reliability which is the presented mathematic and logical probabilities, there is a need to frame the idea of diagnosis trueness in terms of subjective probability, also called a psychological one.

This probability refers to the degree the user of a diagnosis is convinced about chances of engine condition prognosis becoming true.

In this case, calling a diagnosis a reliable one is a subjective process, as it depends on the knowledge of a person preparing a diagnosis and his/her conviction about correct functioning of ME diagnostics system.

The above discussion can be based on calculations based on expert method [8].

On the basis of assigning appropriate diagnostic parameters to selected engine service states, which was presented in paper [8], a diagnostic model including relations shown in Fig.2 has been built, with the following concepts included: p_{ij} – probability of s_{ij} condition occurring, s_{ij} – engine service condition from the set S (s_1, s_2, s_3, s_4), $p(k_i/s_{ij})$ – probability of diagnostic parameter k_i occurring simultaneously with condition s_{ij}, k_i – diagnostic parameter, S_1, S_2, S_3, S_4 – classes of ME conditions.

5. Opportunities to implement the engine diagnostic model in service.

Main engine damage in real-life conditions is a random phenomenon. The results of each defect depend on:

- the time the change in ME condition leading to its damage is identified,
- accuracy of ME condition change identification,
- aptness of decisions taken as a result of ME condition change.

In sea conditions, where it should be assumed that the crew can count only on own skills and technical capabilities, possibly quick detection of ME partial readiness condition may contribute to saving the crew and cargo, as it allows the crew to ensure the safety of a ship.

Due to that it is so important to use diagnostic systems adapted for service needs resulting from the necessity that the decisions are made by the crew and the shipowner together. This also applies to diagnostic models which should be adapted for operation in real-life conditions. Many factors capable of interfering in diagnostics system operation need to be taken into account during their building, such as imperfections in ME structure and varying levels of crew competence [1,2,8].

Measurement relations should reflect the conditions of measurement and the accuracy of applied measurement methods, measurement equipment accuracy, physical properties and measured signals and their parameters, and the required accuracy of diagnostic measurement results.

The obtained set of results of a diagnostic examination is always charged with errors, sometimes significant ones, which may be a reason for obtaining a wrong (unreliable) diagnosis.

Due to this the examination results reflect the examined ME condition only to an approximate degree. This means that they do not inform the user of diagnosis about ME condition itself, but only about an approximate picture of this condition.

Therefore, what is important is to what degree the information about ME condition contained in its diagnosis is reliable, because it has to be processed to obtain diagnostic information about ME condition at further stages of deduction which are not immune to their own errors either.

It should be emphasized that the results which shall allow for a verification of a diagnostic model (in real-life service) or the aptness of decisions taken by human operator, are their real-life consequences.

The engineers operating the engine room and main engine propose the concepts of rational service actions to the shipowner. Quite often they are unable to convincingly justify the grounds for a specific preventive maintenance (as the diagnostic parameters do not exceed limit values) and are loathsome to take responsibility for any decision which generates substantial costs. These costs normally exceed the salary of a decision-maker by a dozen or a few dozens times, so their psychological impact is rather strong as none wants to be labelled as a source of such costs, which may lead to less than rational decisions being made.

At the same time the conditions of work in ship engine room, the daily changing of shifts, crew cultural multiplicity, random and varying work conditions (weather, sea states, emergencies, cargo shifts etc.) require constant attention and result in tiredness, loss of sensitivity to stimuli and paradoxically in a highly flux environment, a routine and mindless execution of duties, which also contributes to a loss of rationality in acting.

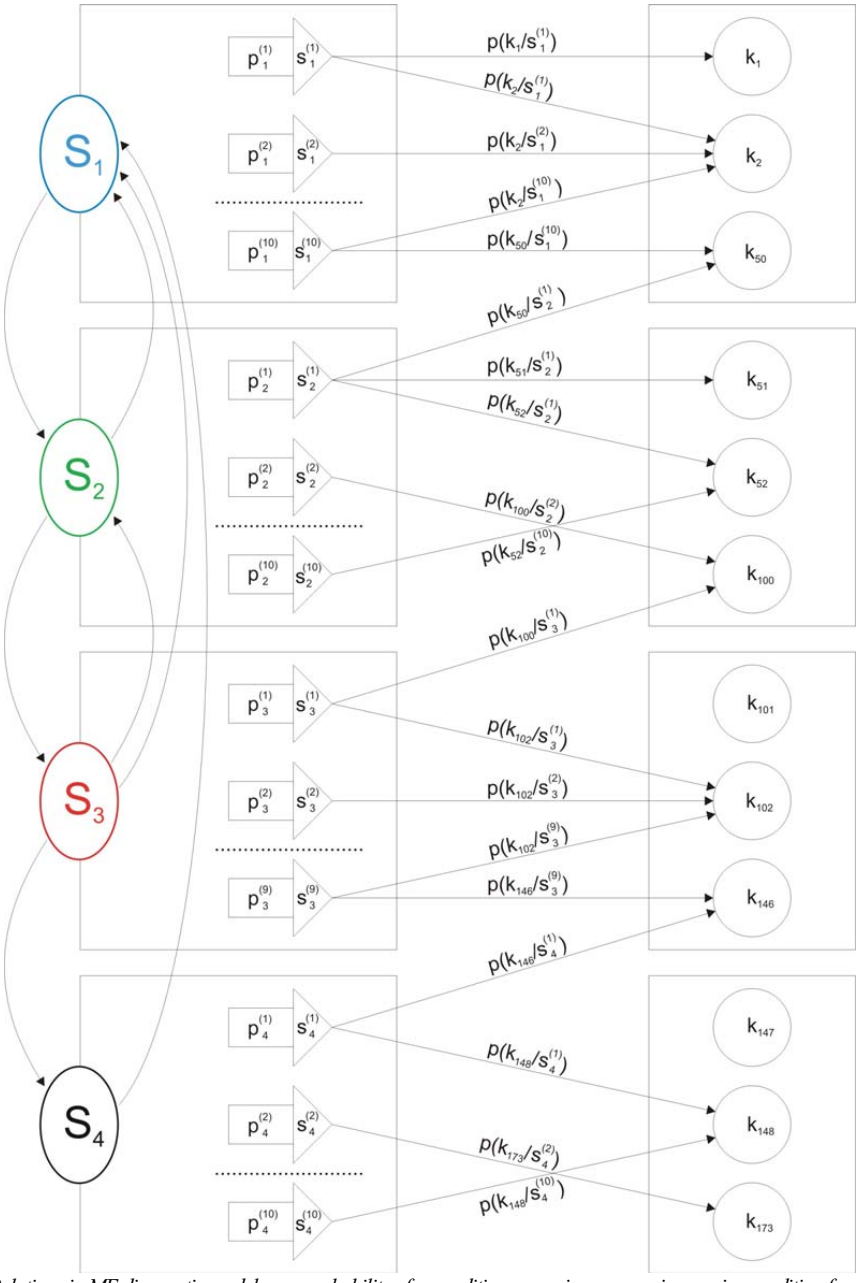

Fig.2 Relations in ME diagnostic model: p_{ij} – probability of s_{ij} condition occurring, s_{ij} – engine service condition from the set $S(s_1,s_2,s_3,s_4)$, $p(k_i/s_{ij})$ – probability of diagnostic parameter k_i occurring simultaneously with condition s_{ij}, k_i – diagnostic parameter, S_1,S_2, S_3, S_4 – classes of ME conditions

6. Summary

In order to make a correct service-related decision, its significance should be estimated first, i.e. its consequences should be predicted. In spite of complexity of this task some mathematical solutions have been proposed [1,2,3,4]. However, in real-life conditions, and particularly in random and variable conditions at sea, it is very difficult to predict the consequences of service decisions, and even more so that in addition to the above there are variable external conditions and the crew operating the ME also changes in a practically random fashion.

A relation-based diagnostic model of ship main engine has educational value and utilitarian value as well. In first case it is because the relations between discrete engine conditions and its signals have been identified, while in the latter it is because the model shall allow for an identification of real-life main engine technical condition and to predict its future conditions as well - through deduction.

Use of this model in practice may facilitate the decisions related to further engine operation or to any preventive maintenance aimed at restoration of its technical condition.

Broad competences of humans are clearly visible in modern diagnostics systems. Most modern decision-support systems on a ship are based on mutual co-operation between the ship engineer (operator), shipowner experts and manufacturer experts. This co-operation may bring about synergistic effect, but it is a ship engineer who has to make a service decision and bear responsibility for it.

Because of that and as a part of expert-evaluated data verification, in further research on the development of diagnostic models and real-life diagnostic systems efforts should be concentrated on the examination of statistical reliability of: engine elements, structural nodes, engine systems, engine as a whole, elements and subsystems of a diagnostics system as well as whole system, the ME – diagnostic system interface, and so the whole diagnosing systems.

References

[1] Girtler, J., *Diagnostyka jako warunek sterowania eksploatacją okrętowych silników spalinowych*, Studia Nr 28 WSM, Szczecin 1997.

[2] Girtler, J., Kuszmider S., Plewiński L., *Wybrane zagadnienia eksploatacji statków morskich w aspekcie bezpieczeństwa żeglugi*, WSM w Szczecinie, Szczecin 2003.

[3] Girtler, J., *Sami-Markovian model of the process of technical state changes of technical objects*, Polish Maritime Research Vol. 11, No 4(42), pp. 3-7, Gdańsk 2004.

[4] Girtler, J., *Physical aspects of application and usefulness of semi-Markovian processes for modeling the processes occurring in operational phase of technical objects*, Polish Maritime Research Vol. 11, No 3(41), pp. 25-30, Gdańsk 2004.

[5] Łosiewicz, Z., *Ocena możliwości podejmowania decyzji z zastosowaniem współczesnych systemów diagnozujących silników głównych*, Materiały konferencyjne III Międzynarodowej Konferencji Naukowo-Technicznej ”EXPLO-SHIP 2004”, AM w Szczecinie, Świnoujście-Kopenhaga 2004.

[6] Łosiewicz, Z., Pielka, D., *Możliwości zastosowania metod sztucznej inteligencji do diagnostyki okrętowego silnika spalinowego*, Zeszyty Naukowe nr 162 K/2, AMW w Gdyni, s. 261-266, AMW w Gdyni, Gdynia 2005.

[7] Łosiewicz, Z., *Walory eksploatacyjne współczesnych systemów diagnozujących dla okrętowych tłokowych silników spalinowych o zapłonie samoczynnym na przykładzie CoCoS i CBM*, Materiały XXVII Sympozjum Siłowni Okrętowych, s. 199-208, Politechnika Szczecińska, Szczecin 2006.

[8] Łosiewicz, Z., *Probabilistyczny model diagnostyczny okrętowego silnika napędu głównego statku*, Praca doktorska, Politechnika Gdańska, Gdańsk 2008.

Journal of POLISH CIMAC
Faculty of Ocean Engineering & Ship Technology
GDAŃSK UNIVERSITY OF TECHNOLOGY

INVESTIGATION OF THE OPERATIONAL MODAL ANALYSIS APPLICABILITY IN COMBUSTION ENGINE DIAGNOSTICS

Marcin Łukasiewicz

University of Technology and Life Science
ul. S. Kaliskiego 7, 85-789 Bydgoszcz, Poland
tel.: +48 52 3408262
e-mail:mlukas@utp.edu.pl

Abstract

The paper contains application of operational modal analysis in use of combustion engine chosen technical state identification. The combustion engine No. 138C.2.048 with 1.4l. swept capacity, power 55 kW, generally applied to Fiat was the investigation object. It makes possible to introduce generated vibration signals as well as the investigation of his adjustment influence on the combustion engine vibration signals change. Conducted researches of combustion engine depended on delimitations of vibroacoustics measures for fit engine and comparison of this measures, with measures appointed for damaged engine (e.g. damaged injector) and accomplishment the assessment of received results influence on engine state by operational modal analysis. The present research use vibration methods as Operational Modal Analysis to recognize the technical state of the system.

Keywords: *operational modal analysis, diagnostic inference, combustion engine*

1. Introduction

Owing to the complicated character of vibrations, technical diagnostics of combustion engines is very difficult and only a few of proposed methods of diagnosis can have a wider technical application. Application of the modal analysis as one of the vibroacoustics tools is the new approach to the technical analysis of the combustion engine. Following the changes of modal model parameters as a result of engine maladjustment, waste, damages or its failure is the main idea of operational modal analysis. The modal parameters are [4,5,6]:

- modal frequency,
- modal damping,
- mode shape.

Modal analysis is the process of determining the modal parameters of a structure for all modes in the frequency range of interest. The ultimate aim is to use these parameters to construct a modal model of the response.

Operational modal is the name for the technique to do modal analysis on operational data - cases where we do not excite the structure artificially but just allow the natural operating loads to excite the structure.

2. Operational modal analysis – LSCE method theory

In this paper Least Squares Complex Exponential method was used to determine the modal model parameters, by which the correlation function is approximated by the sum of exponentially decaying harmonic functions. This method, applied to impulse response of system is a well known method in modal analysis yielding global estimators of system poles – the root of the transfer function denominator. It can be proved that the cross correlation function can be used to identify modal system parameters in identical way as does the impulse response of the system. [4,5]

The dynamic equation of the system motion can be expressed by formula [4,5]:

$$M\ddot{x} + C\dot{x} + Kx = F(t), \tag{1}$$

where:

M,C,K – mass, damping and stiffness matrices,
$\ddot{x}, \dot{x}, x$ – acceleration, velocity and displacement vectors,
F(t) – vector of exciting forces.

The next step was transformation of formula (1) to principal coordinates applying the transformation expressed by the formula [4,5]:

$$x(t) = \Psi q(t) = \sum_{r=1}^{n} \Psi_r q_r(t), \tag{2}$$

where:

Ψ – matrix of modal vectors, the columns of which are eigenvectors corresponding to the given free vibration frequency,
q_r – principal (modal) coordinate,
n – number of vibration forms included in the model of vibration forms.

Assuming that damping is small and proportional, on substituting relation (2) into formula (1) and multiplying by Ψ^T, de-coupled equation set is obtained in the form [4,5]:

$$\ddot{q}_r(t) + 2\xi_r\omega_{nr}\dot{q}(t) + \omega_{nr}^2 q_r(t) = \frac{1}{m_r}\Psi_r^T f(t), \tag{3}$$

where:

ω_{nr} – is the r-th free vibration frequency,
ξ_r – is the modal damping coefficient for the r-th vibration form,
m_r – is the modal mass.

Assuming zero initial conditions for arbitrary excitation, the solution of equation (3) can be written in the form of convolution [4,5]:

$$q_r(t) = \int_{-\infty}^{t} \psi_r^T f(\tau) g_r(t-\tau) d\tau, \tag{4}$$

where:

$g_r(t) = 0 \quad \text{for} \quad t < 0,$

$g_r(t) = \frac{1}{m_r \omega_{rd}} \exp(-\xi_r \omega_{nr} t) \sin \omega_{nr} t \quad \text{for} \quad t \geq 0,$

$\omega_{rd} = \omega_{nr}(1-\xi_r^2)^{\frac{1}{2}}$ – is the frequency of damped free vibrations.

Making use of solution formula (4) for modal coordinates to determine the solution in generalised coordinates x(t), we obtain the formula [4,5]:

$$x(t) = \sum_{r=1}^{n} \psi_r \int_{-\infty}^{t} \psi_r^T f(\tau) g_r(t-\tau) d\tau , \tag{5}$$

where:

n – number of vibration forms taken into account in the solution.

Cross correlation function for two response signals at point i and j, resulting from an excitation applied at point k in the form of white noise has form [4,5]:

$$R_{ijk}(T) = E_o[x_{ik}(t+T) x_{ik}(t)], \tag{6}$$

where:

E_o – denotes the expected value operator.

If we know relation between cross correlation function, having the form of a sum of exponentially decaying harmonic functions and impulse transition function for direct application to do modal analysis tests, correlation function can be transformed to the form [4,5]:

$$R_{ij}(T) = \sum_{r=1}^{n} \frac{\psi_{ir} g_{jr}}{m_r \omega_{rd}} \exp(-\xi_r \omega_{nr} T) \sin(\omega_{rd} T + \vartheta_r), \tag{7}$$

where:

ϑ_r – the New phase angle,
G_{jr} – constant.

3. Model of diagnostics signal generation

The investigations object was a combustion engine no. 138C.2.048 applied to the Fiat and Lancia cars that is shown on figure 1. Basis on this system during investigations was created model of diagnostics signal generation [2,3]. The proposed model of combustion engine diagnostic signal generation is shown on figure 2.

The received signals in the any point of engine body are the sum of the answer at all elementary events $u_n(t, \Theta)$, outputs in individual partial dynamic arrangements with the pulse function of input $h_n(t, \Theta)$. These influences after passing by proper dynamic arrangements are sum up on the engine body, on chosen points was measured by the vibration transducers. As a result of conducted measurements output signals was used to estimation. By $n(t, \Theta)$ was marked accidental influence stepping out from presence of dynamic micro effects such as friction [2,3,6].

Conducted investigations of combustion engine depended on delimitations of vibroacoustics measures for fit engine and comparison them with measures appointed for damaged engine (eg. damaged injector) and accomplishment the assessment of received results influence on engine state by operational modal analysis methods.

Fig. 1. The investigation object – combustion engine No. 138C.2.048

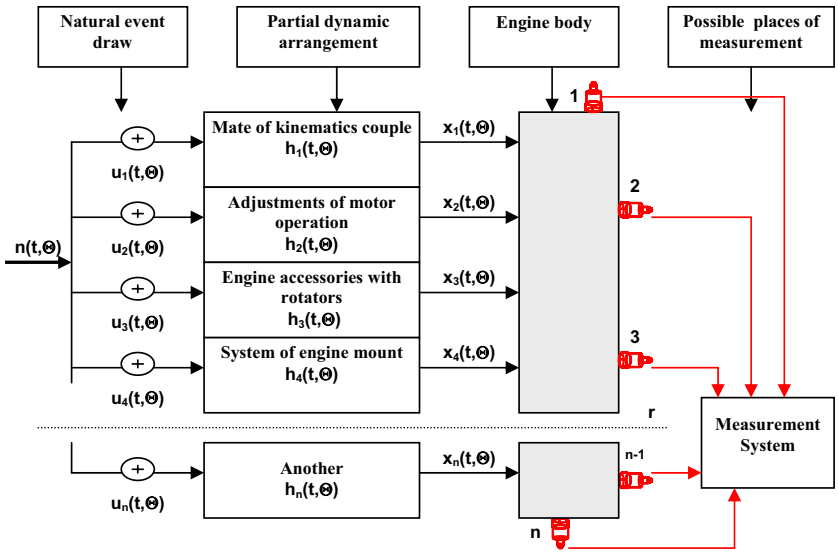

Fig.2. Combustion engine diagnostics signal generation model[2,3]

4. The investigations results

The modal model of combustion engine was created for put dynamic states on the basis of received measuring results. During investigations have been done vibroacoustics measures for fit engine and for engine with damaged injector and spark plug for each cylinder.

As a results of engine modal tests was created the stabilisation diagrams for each technical state. Basis on the stabilisation diagrams was created the modal model includes modal order, natural frequency and damping [2,4,5]. Figure 3 display the window with the stabilization diagram of engine in fit state. Table 1 present the results of modal investigations – modal model for put engine technical states. Basis on modal model parameters and estimators of vibroacoustics signal received during investigations in table 2 was shown the main observation matrix for engine performance. The final observation matrix of engine performance described 13 symptoms. The matrix have six modal symptoms (ω_1 - first natural frequency, rząd1 - modal order of first natural frequency, ξ_1 - modal damping coefficient of first natural frequency, ω_2 - second natural

frequency, rząd2 - modal order of second natural frequency, ξ_2 - modal damping coefficient of second natural frequency) and the last seven symptoms are vibration process (H(f) – real part of transfer function, H(f)L – imagine part of transfer function, γ^2_{xy} – coherence function, $A_{RMS(t)}$ – Root Mean Square in time domain, β_{kurt} – Kurtosis, C_s - Crest factor, I - Impulse factor).

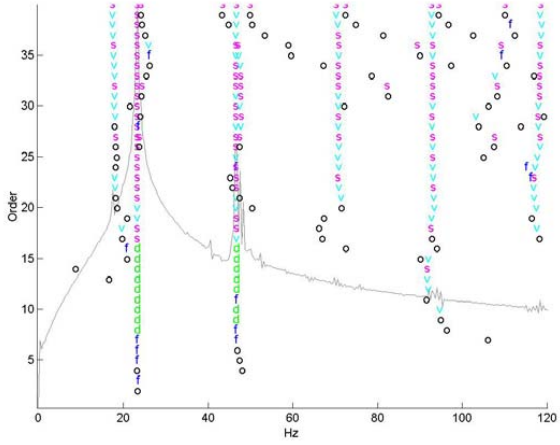

Fig. 3. Operational Modal Analysis stabilization diagram of investigated engine in fit technical state: s – stable pole, v – the frequency of vibration and modal vector is stabilized, d – the frequency of vibration and the stifling is stable, f – only the frequency of the vibration is stable, o – the pole is unstable

Table 1. Parameters of modal model received during investigations for put of 9 technical states of combustion engine: ω – is the free vibration frequency, Order – order of the model, ξ – is the modal damping coefficient

Technical state	Parameters of modal model						
1- fit engine	ω (Hz)	23,27	46,96				
	Order	18	17				
	ξ (%)	0,67	1,34				
2 - damaged injector on 4th cylinder	ω (Hz)	16,62	21,82	38,09			
	Order	20	19	20			
	ξ (%)	4,08	0,68	4,33			
3 - damaged injector on 3th cylinder	ω (Hz)	17,81	22,57	27,94	39,74		
	Order	19	17	28	18		
	ξ (%)	4,81	1,47	4,82	2,00		
4 - damaged injector on 2th cylinder	ω (Hz)	16,33	22,13	27,99	38,59	49,13	
	Order	29	18	31	17	23	
	ξ (%)	7,05	3,11	7,13	4,09	5,51	
5 - damaged injector on 1th cylinder	ω (Hz)	17,36	22,82	29,24	40,03	50,87	91,64
	Order	23	19	34	27	25	16
	ξ (%)	6,69	1,18	6,17	3,21	2,90	2,24
6 - damaged spark plug on 4th cylinder	ω (Hz)	20,13	22,05	39,08	49,60		
	Order	18	24	23	23		
	ξ (%)	1,93	7,93	6,98	4,80		
7 - damaged spark plug on 3th cylinder	ω (Hz)	16,52	20,70	25,51	41,43	47,43	
	Order	19	17	29	27	26	
	ξ (%)	10,11	2,48	6,73	4,61	4,07	
8 - damaged spark plug on 2th cylinder	ω (Hz)	16,50	21,89	37,74	46,34		
	Order	23	18	24	20		
	ξ (%)	11,47	1,21	6,33	1,78		
9 - damaged spark plug on 1th cylinder	ω (Hz)	17,59	23,58	45,93			
	Order	25	17	18			
	ξ (%)	3,83	0,71	1,27			

Table 2. The main observation matrix for engine performance

State	ω_1	rząd 1	ξ_1	ω_2	rząd 2	ξ_2	H(f)	H(f)L	γ^2_{xy}	$A_{RMS(t)}$	β_{kurt}	C_s	I
1	23,27	18	0,67	46,96	17	1,34	68,56	-2,18	108,18	0,2177	1,5567	1,7239	1,9268
2	21,82	19	0,68	38,09	20	4,33	47,08	30,59	100,22	0,1392	1,8989	2,1204	2,4456
3	22,57	17	1,47	39,74	18	2,00	36,42	8,84	104,40	0,2040	1,7532	1,8656	2,1198
4	22,13	18	3,11	38,59	17	4,09	31,34	-15,28	91,11	0,1769	1,9245	2,0762	2,3992
5	22,82	19	1,18	40,03	27	3,21	46,16	-75,94	101,15	0,2312	1,7148	2,0982	2,3673
6	20,13	18	1,93	39,08	23	6,98	42,24	-8,50	83,73	0,1702	2,5205	2,8157	3,3986
7	20,70	17	2,48	41,43	27	4,61	38,76	22,77	82,34	0,1363	2,2943	2,2926	2,7564
8	21,89	18	1,28	46,34	20	1,78	40,51	-19,29	83,29	0,1726	1,7401	2,0176	2,2929
9	23,58	17	0,71	45,93	18	1,27	19,45	-23,34	99,63	0,1904	1,6144	1,8260	2,0527

5. Results validation

As a results of investigation in this paper is shown presentation of singular value decomposition (SVD) method usage for combustion engine technical state results validation. The SVD method is the appropriate tool for analyzing a mapping from one vector space into another vector space, possibly with a different dimension [1]. The first step of SVD procedure is to centre and normalization all symptoms given in table two relative to the initial value of symptom vector. The observation matrix of transformate symptoms relative to the initial value is shown on figure 4.

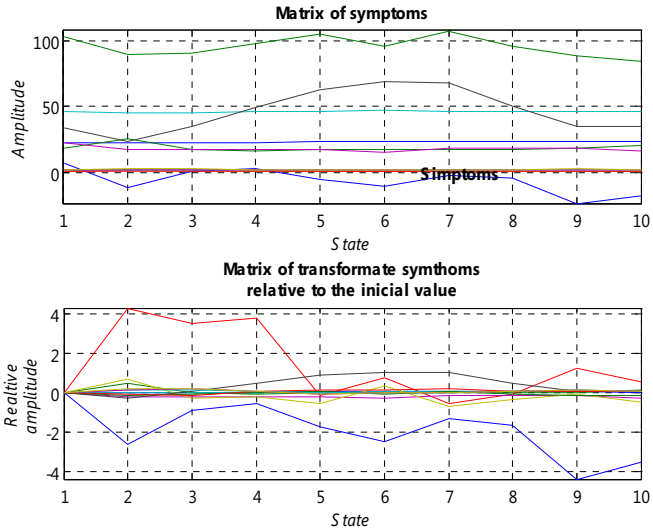

Fig.4. Matrix of symptoms before and after transformation

The second step of SVD procedure is to calculate the first generalized damage and evolution of damage. Graphical interpretation of this calculations is given in figure 5. Making data analysis in SVD method as a result we got the line up of symptoms together with the proportional description of given individual symptom of combustion engine technical state. Thanks to SVD methods we could decide which symptom given in observation matrix is the best to recognize a set of combustion engine technical state [1].

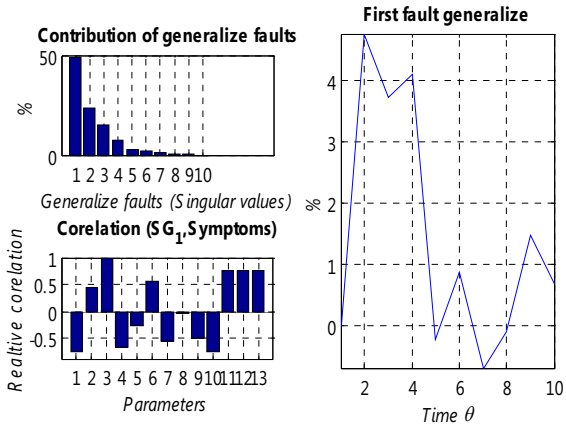

Fig.5. Graphical interpretation of first generalized damage and evolution of damage

In SVD procedure as a result we got a line up of five best symptoms given in table 3 that are most important in description of set technical state of combustion engine.

Table 3. Results of SVD method with five best symptoms for set of engine technical state

State	1 symptom	2 symptom	3 symptom	4 symptom	5 symptom
1	ξ_1	ω_1	$A_{RMS(t)}$	β_{kurt}	C_s
2	H(f)L	rząd 1	ξ_2	H(f)	γ^2_{xy}
3	ξ_1	H(f)L	rząd$_1$	ω_1	H(f)
4	rząd$_2$	H(f)L	ω_2	ξ_2	ξ_1
5	ξ_1	rząd$_1$	β_{kurt}	$A_{RMS(t)}$	γ^2_{xy}
6	H(f)L	ξ_1	$A_{RMS(t)}$	H(f)	rząd$_2$
7	ξ_1	C_s	I	rząd$_1$	γ^2_{xy}
8	H(f)L	ξ_1	ξ_2	γ^2_{xy}	ω_1
9	H(f)L	ξ_1	β_{kurt}	C_s	I

Relationships cause - consecutive expressing quantitative relation between studied variable symptoms results in this work were qualified using the function of the multiple regression. Basis on SVD results as a best symptoms in multiple regression were given: ω_1 – first natural frequency, ξ_1 - modal damping coefficient of first natural frequency, ξ_2 - modal damping coefficient of second natural frequency, H(f)L – imagine part of transfer function, γ^2_{xy} – coherence function. The equation of multiple regression is obtained in the form:

$$y = -1{,}44923\omega_1 - 0{,}61558\xi_1 - 0{,}35989\xi_2 - 0{,}06520H(f)L + 0{,}14424\gamma^2_{xy} + 35{,}9994, \quad (8)$$

Graphical interpretation of this calculations for first dependent variable ω_1 is given in figure 6. The red line present real data received during investigations, the blue line – estimated model for dependent variable.

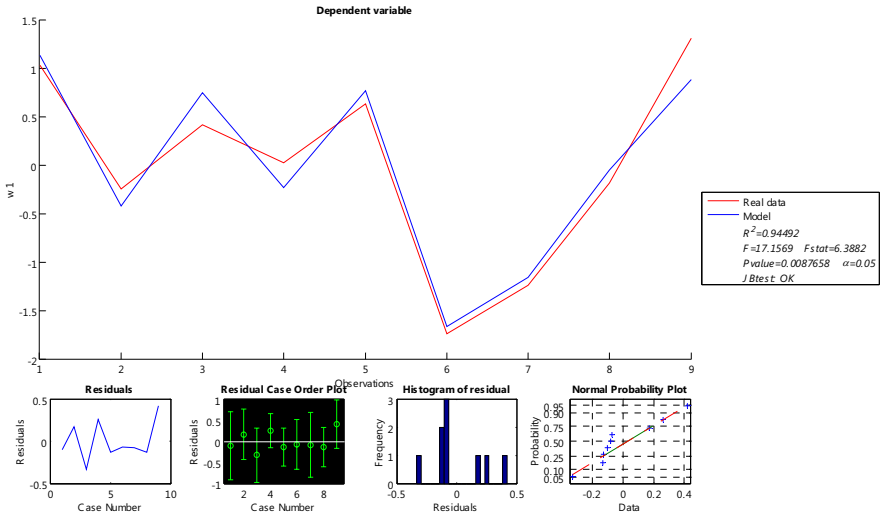

Fig. 6. Graphical interpretation of multiple regression for first dependent variable ω_1

6. Conclusion

Received in the experiment modal parameters and numerical estimators of vibroacoustics signal unambiguously show that the previously assumed conditions of the combustion engine's state reflect themselves in modal as well as other parameters characterising the vibrations and they are possible to be identified.

The use of the operational modal analysis in diagnostic investigations finds its use as one of many methods of marking the actual technical state of studied object. To complete the analysis process a SVD method and multiple regression were used. SVD methods marked most important symptom in description of engine technical state.

On the basis of the results, it is possible to determine the actual technical state of an object of the same type by means of comparison of the achieved results with the model ones and assigning them to the particular model's state, which answers to a particular damage, or its loss, in the object.

The introduced in paper results of investigations are the part of realized investigative project and they do not describe wholes of the investigative question, only chosen aspects.

References

[1] Cempel, Cz., *SVD Decomposition Of Symptom Observation Matrix As The Help In A Quality Assessment Of A Group Of Applications,* Diagnostyka v.35, PTDT Warszawa 2005.

[2] Łukasiewicz, M., *Próba odwzorowania modelu modalnego stanu technicznego silnika spalinowego w zastosowaniu do badań diagnostycznych,* Diagnostyka v.33, PTDT, Warszawa 2005.

[3] Łukasiewicz, M., *Badania napędu zasilania awaryjnego eksploatacyjną analizą modalną*, Inżynieria i Aparatura Chemiczna 1/2007, pp.83-84, Bydgoszcz 2007.

[4] Uhl, T., Lisowski, W., *Eksploatacyjna analiza modalna i jej zastosowanie,* AGH, Kraków 1999.

[5] Uhl, T., Kurowski P., *Vioma – instrukcja użytkownika*, AGH, Kraków 2002.

[6] Żółtowski, B., *Badania dynamiki maszyn,* ATR, Bydgoszcz, 2002.

Journal of POLISH CIMAC
Faculty of Ocean Engineering & Ship Technology
GDAŃSK UNIVERSITY OF TECHNOLOGY

ASSESSMENT OF OPERATION OF ENERGY SYSTEM OF SERIAL RELIABILITY STRUCTURE ON THE EXAMPLE OF SHIP MAIN PROPULSION SYSTEM

Jacek Rudnicki

Gdansk University of Technology
ul. Narutowicza 11/12, 80-950 Gdańsk, Poland
tel.: +48 58 3472973, fax: +48 58 3472430
e-mail:jacekrud@pg.gda.pl

Abstract

This paper presents a development of the known qualitative method for assessment of energy system operation, applied to ship main propulsion system as an example. According to this interpretation operation can be presented as a physical quantity. In this aspect , based on the selected functional system of the ship, was assessed usefulness of the quantity for description reliability features of the system. To the analysis was applied Poisson's uniform process which made it possible to elaborate a model of run of worsening the considered system's operation taken as a random process of identical independent decreases of energy efficiency within a given time interval.

Keywords: *reliability, operation, Poisson processes, ship power plant*

Introduction

During realization of a transport task by a ship to consider operation not only of particular elements of its propulsion system but also (and first of all) of full set of them which constitutes a functional entity, is necessary.

The existing publications [6, 7] pay special attention to main propulsion engine, other ones – to propeller and only a few – to the entire functional power plant subsystem.

High differentiation of contemporary ship propulsion systems makes it difficult to consider problems in this field generally, however an analysis of applied design solutions indicates that majority of solutions applied to typical transport ships (tankers, containerships, bulk carriers) still comprise only one driving unit (because of simplicity and lower investment and operational costs of such solution) which can be schematically presented as follows :

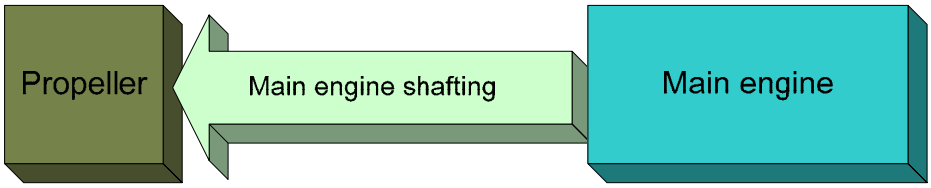

Fig.1. The functional structure of the typical solution of the ship propulsion

The solution shown in Fig. 1 constitutes a classical serial reliability structure of distinguished elements and this way role of each of them is very important in the aspect of realization of

objective function of the entire system. Therefore it seems justified to consider the entire structure apart from analyses which concern first of all its weakest elements.

Reliability assessment procedures of each device and system make it necessary to apply a valuation approach to the problem and to search for appropriate measures [3, 5, 9, 10].

Necessity of precise determination of a task requires to determine its duration time , apart from assuming conditions in which the task would be realized. The problem is this much important that specificity of sea shipping tasks is as a rule connected with necessity of functioning the crucial mechanisms and devices of ship for a long time.

Hence not only the problem of how large amount of energy can be deliver to the propeller but also that of duration time in which it can be delivered , becomes especially important.

Therefore it seems reasonable, apart from taking into acount commonly used reliability indices, to consider operation of propulsion system in such a way as it could be determined in function of energy and time simultaneously. The problems related to selected elements of ship power plant are described in [6, 7, 8], however publications presenting the above described approach to the entire propulsion system have been so far lacking (they are unknown to this author at least). In such case, operation of a given system (D) within the period [t_1, t_2] can be interpreted as a physical quantity determined by the product of the time-variable energy $E = f(t)$ and time, which can be generally described by the following relation, [6]:

$$D = \int_{t_1}^{t_2} E(\tau) d\tau \tag{1}$$

The so interpreted operation of a real technical object exposed to wear processes can be presented in the form of the diagram [6] shown in Fig.2a.

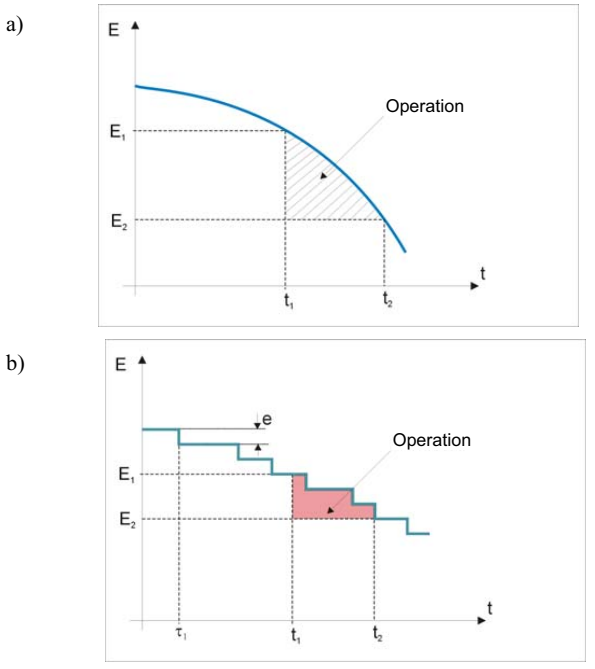

Fig.2. Operation by means of valuation. E – energy, t –time, e – elementary recordable constant value by which effective energy decreases in the random instants t_i. [6]

As the technical state change process is continuous with respect to time and states, the curve in Fig. 2a , which shows decreasing the effective energy E , is smooth. However in practice, as accuracy of measuring instruments is limited, its run will look like that shown in Fig. 2b.

Assessment of operation of main propulsion engine

In the case of analysis of operation of a self-ignition engine it can be consider that the energy released during fuel combustion in its cylinders makes it possible to develop torque by the engine. As a result of delivering the torque from the engine to the consumer the work L_e, is done, which can be determined from the relation:

$$L_e = M_o \cdot 2\pi\, n \cdot t \tag{2}$$

where:
L_e – effective work,
M_o – engine torque,
n – rotational speed of engine.

The product $M_o \cdot 2\pi\, n$ which appears in the relation (2) , is equivalent to value of the effective power N_e developed by the engine during realization of a given transport task, whose demanded value depends on a kind of task and can be determined , for an assumed ship speed , e.g. from the relation (3) which takes into account value of the thrust T developed by the propeller [11]:

$$N_e = \frac{T \cdot (1-\varphi) \cdot v}{\xi_K \cdot \eta_p \cdot \xi_{rot} \cdot \eta_{lw}} \tag{3}$$

where:
T – propeller thrust,
φ – thrust deduction factor,
v – ship speed,
η_{lw} – efficiency of shaft line,
η_p – efficiency of free propeller,
ξ_{rot} – relative rotative efficiency,
ξ_k – hull efficiency.

In such case, as results from the relations (1) and (2), the engine operation D_S can be determined by the formula (4), [6]:

$$D_S = 2\pi \int_{t_1}^{t_2} M_0\, n\, t\, dt \tag{4}$$

Further by introducing the following notions :

- the demanded operation D_W, i.e. that necessary for realization of a task , e.g. cargo shipping by sea within a given period, that is equivalent to maintaining a given average ship speed, hence also a relevant value of power developed by ship main propulsion engine (- s);
- the possible operation D_M, i.e. that can be realized by an engine being in a given technical state and given functioning conditions , and which can be obtained by checking the relation (5), [6]:

$$D_M \geq D_W \tag{5}$$

i.e. the serviceability assessment criterion whose detail interpretation is highlighted in [6, 7, 8].

Along with time of engine operation its total efficiency defined for instance as [2, 11]:

$$\eta_e = \frac{1}{g_e \cdot W_d} \tag{6}$$

where:

g_e – specific fuel oil consumption,

W_d – fuel lower calorific value,

decreases first of all due to the degradation resulting from wear processes [2, 11], which leads to changes with respect to the above defined value of the possible operation D_M.

The phenomenon can be graphically represented in the form of the diagram (Fig. 3) which has the following interpretation:

– the degradation processes which progress for the operation time between successive technical state restorations, result in occurrence of the successive recordable events S_1 which consist in the decreasing of value of the engine torque M_o at a maintained oil fuel consumption, or the events S' which consist in the increasing of oil fuel consumption in order to achieve the same value of the engine torque M_o.
– long-lasting use of the engine leads by itself to the worsening of its operational characteristics, that , because of a limited accuracy of measuring devices, can be represented by a sequence of the events appearing in the random instants t_i , which consist in either increasing the values B by the same increment $\Delta B' = b$ or decreasing the values M_o by the same decrement $\Delta M_o' = m_o$.

On assumptions on the stationarity , lack of consequences and singularity of flow of the above mentioned processes, the Poisson's homogeneous process can be applied to their description [1].

In the context of the above defined operation D , see the relation (1) , the process of decreasing the available work is of crucial practical importance. Hence, the occurrence , up to the instant t , of the number $U_{\Delta M}$ of the events S_1 , that results in the total decreasing of the value M_o by the value ΔM_o , can be represented as follows :

$$\Delta M_o = \Delta M_o' \cdot U_{\Delta M} = m_o \cdot U_{\Delta M} \tag{7}$$

and

$$\Delta L_e = m_o \cdot U_{\Delta M} \cdot 2\pi\, n \cdot t \tag{8}$$

where :

ΔM_o – the total decreasing of the value M_o after occurrence of $U_{\Delta M}$ number of the events S_1,

$\Delta M_o' = m_o$ – elementary recordable value of torque by which the value M_0 decreases,

and, the random variable $U_{\Delta M}$ has the following distribution [1]:

$$P(U_{\Delta M} = k) = \frac{(\lambda_M \cdot t)^k}{k} \exp(-\lambda_M t); \quad k = 1,2,...,n \tag{9}$$

where:

λ_M – a constant interpreted as the intensity of occurrence of the event S_1 (the decreasing of the value M_o by the elementary value m_o).

The process (on assumption of constant oil fuel charge) can be graphically illustrated in the way presented in Fig. 3. :

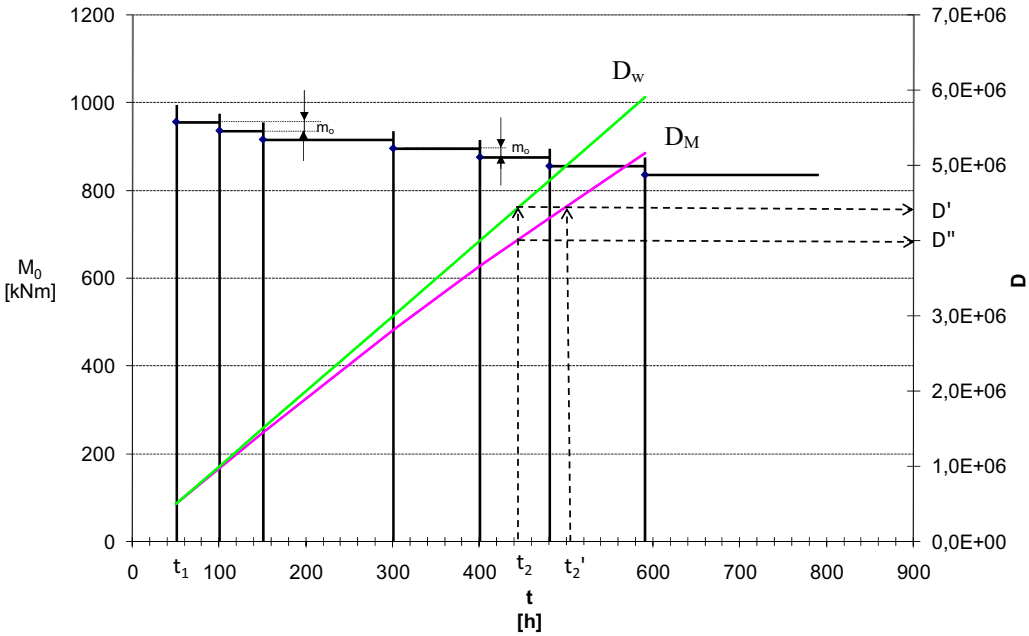

Fig.3.Main engine torque M_o and possible operation D_M decrease. D_w – demanded operation

As observed in Fig. 3, the difference between the demanded operation of the engine , D_w , and that possible one , D_M , is growing with time , that results in shifting the end of realization of transport task from the instant t_2 to t_2'.

Assessment of operation of power transmission line devices (shaft line)

As regards the power transmission line, the operation D_{LW} can be determined by the following relation:

$$D_{LW} = 2\pi \int_{t_1}^{t_2} Q\, n_S\, t\, dt \tag{10}$$

where:

Q – torque delivered to screw propeller,

n_S – rotational speed of screw propeller (for direct drive systems : $n_S = n$).

In the case of shaft line devices whose solution typical for aft ship power plant is schematically shown in Fig. 4a, the load-carrying (intermediate) bearings and stern tube bearings constitute the elements which potentially generate loss of power.

Also, as regards the objects in question, despite their relatively high efficiency (close to 100%), can be enumerated many processes leading to gradual change of their technical state and in consequence to occurrence , in random instants t , of the events S_2 which consist in decreasing the values of the transmitted torque Q by the same values $\Delta Q' = q$. The process is presented in Fig. 5b.

Therefore the occurrence , up to the instant *t* , of $U_{\Delta Q}$ number of the events which cause the total decreasing of the value Q by the value ΔQ , can be represented as follows:

$$\Delta Q = \Delta Q' \cdot U_{\Delta Q} = q \cdot U_{\Delta Q} \tag{11}$$

and consequently – the effective transmitted energy L_{e1} as :

$$\Delta L_{e1} = q \cdot U_{\Delta Q} \cdot 2\pi\, n \cdot t \tag{12}$$

where:

ΔQ – the total decreasing of the value Q after occurrence of $U_{\Delta Q}$ number of the events S_2,

$\Delta Q' = q$ – elementary recordable value of torque by which the value Q decreases,

where the random variable $U_{\Delta Q}$ has the following distribution, [1]:

$$P(U_{\Delta Q} = k) = \frac{(\lambda_Q \cdot t)^k}{k} \exp(-\lambda_Q t); \quad k = 1,2,..., n \tag{13}$$

and :

λ_Q – a constant interpreted as the intensity of occurrence of the event S_2 (the decreasing of the value Q by the elementary value q).

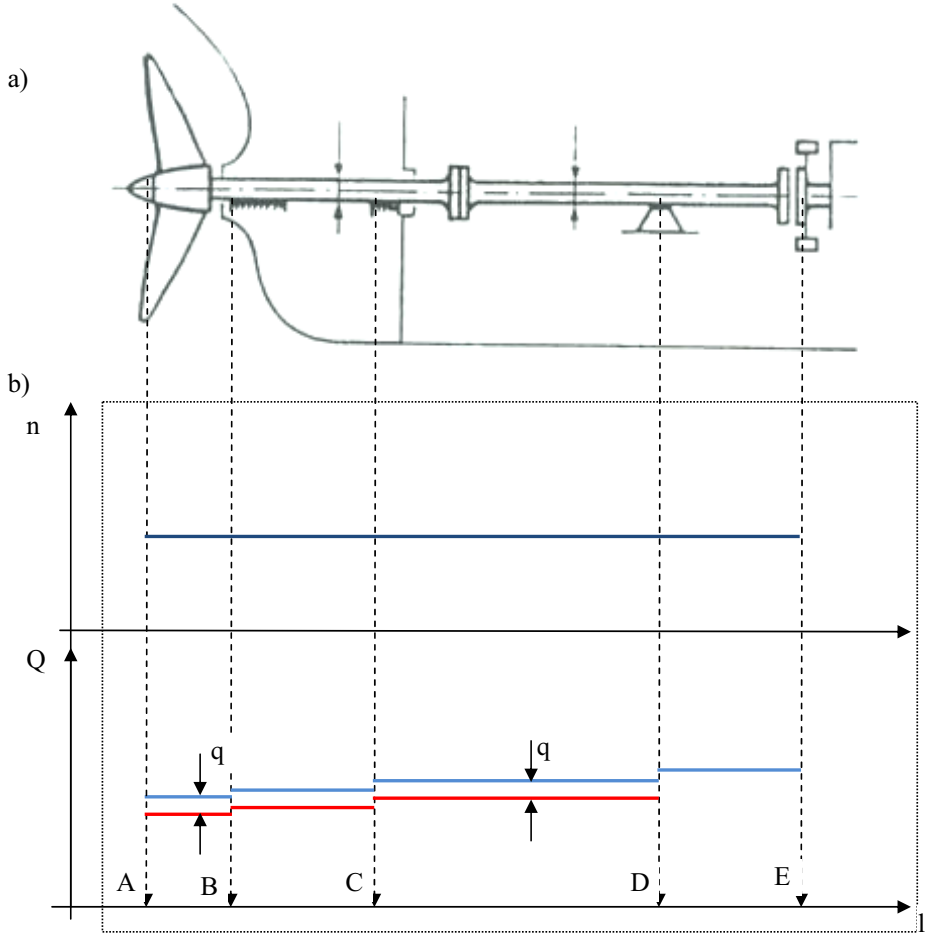

Fig.4. The single decreasing , by the elementary value q, of the torque in the power transmission line of ship propulsion system, resulting from wear and drop of efficiency of load-carrying bearings . A – screw propeller, B- aft stern tube bearing, C – fore stern tube bearing, D – load-carrying bearing, E – end terminal of engine power reception,

Assessment of operation of screw propeller

Similarly, an analysis of screw propeller operation leads to the conclusion that its operation D_P (in the sense of functioning) can be represented by the relation:

$$D_P = \int_{t_1}^{t_2} N_T \, t \, dt \tag{14}$$

where:

N_T – thrust horse - power [11],

$$N_T = 2\pi \cdot Q \cdot n \cdot \eta_P \cdot \xi_{rot} = T \cdot v \cdot (1 - w) \tag{15}$$

Q – torque delivered to screw propeller,

n – rotational speed of screw propeller,

η_P – efficiency of free propeller,

ξ_{rot} – relative rotative efficiency of propeller,

T – thrust,

v – ship speed,

w – wake coefficient.

The long-lasting use of screw propeller (time between successive repairs usually results from the ship dock overhaul schedule, i.e. every 3rd ÷5 th year, on average, [12]) is accompanied by many detrimental phenomena among which the following should be first of all numbered [4]:

- various modes of corrosion (electrochemical, of fatigue origin),
- erosion,
- cavitation,
- impact loads,
- transverse – torsional vibrations.

The phenomena contribute to degradation of technical state of screw propellers (as shown in Fig. 5) and the worsening of their serviceability characteristics, that results first of all from changes in hydrodynamical characteristics of screw propellers and their efficiency defined as follows, [2]:

$$\eta_p = \frac{J}{2 \cdot \pi} \cdot \frac{K_T}{K_Q} \tag{16}$$

where:

J – speed coefficient,

K_T – thrust coefficient,

K_Q – torque coefficient.

Fig.5. The examples of propeller wear and damages
(źródło: http://home.xtra.co.nz/hosts/henleyspropellers/prop_damage.htm)

Character of the above mentioned changes is presented in Fig. 6.

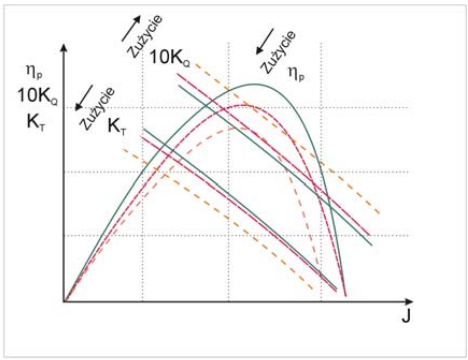

Fig. 6. Changes of hydrodynamical characteristics of screw propeller resulting from influence of wear processes [2]

As a result of the processes, propeller capability of transforming the delivered power N_D into designed value of the thrust T , diminishes. Hence on assumption of constant value of the power N_D and relatively constant ship sailing conditions (J = const) the screw propeller will produce smaller and smaller value of the thrust T and - in consequence - ship's speed will be also smaller at almost unchanged (or increased – see Fig. 17) engine load. Therefore also in relation to screw propeller, the process of occurrence, in random instants t , of the events S_3 which consist in decreasing values of produced thrust T by the constant values $\Delta T' = \delta$, can be considered.

Therefore the occurrence , up to the instant t , of $U_{\Delta T}$ number of the events causing the total decrease of the thrust value T by the value ΔT , can be expressed as follows:

$$\Delta T = \Delta T' \cdot U_{\Delta T} = \delta \cdot U_{\Delta T} \tag{17}$$

where:

ΔT – total decrease of the thrust value T after occurrence of $U_{\Delta T}$ number of the events S_3,

$\Delta T' = \delta$ – elementary recordable thrust value by which the thrust decreases, whereas the random variable $U_{\Delta T}$ has the following distribution [1]:

$$P\left(U_{\Delta T} = k\right) = \frac{\left(\lambda_T \cdot t\right)^k}{k} \exp\left(-\lambda_T t\right); \quad k = 1,2,...,n \tag{18}$$

where:

λ_T – a constant interpreted as the intensity of occurrence of the event S_3 (decreasing the thrust value T by the elementary value δ).

Operation of ship propulsion system as a serial reliability structure

As all main elements of ship propulsion system form a functional entity, a complex description of the entire system in the aspect of the defined operation seems to be necessary.

In the light of the considerations have been performed so far and as in accordance with the functional structure (Fig. 1) the output from every main component of the system in question constitutes the input to successive component , the occurring processes can be illustrated in the way shown in Fig. 7.

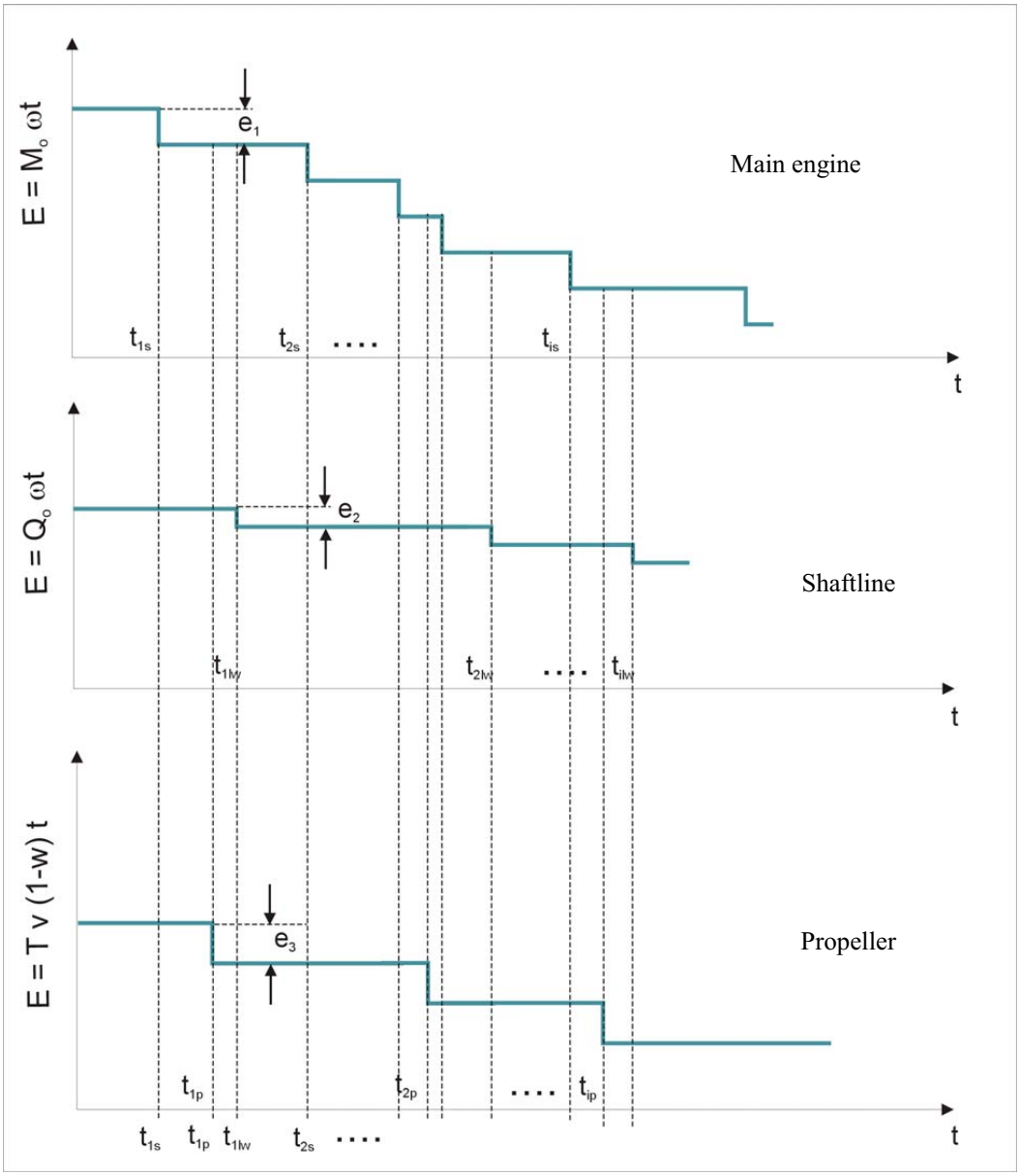

Fig.7. Operation of ship propulsion system as a serial reliability structure presented by means of valuation approach which takes into account the process of diminishing effective energy. e_1 – elementary recordable constant value by which effective energy of engine decreases in the random instants t_{is}, e_2 – elementary recordable constant value by which energy transmitted by shaftline decreases in the random instants t_{ilw}, e_3 – elementary recordable constant value by which energy transformed by screw propeller decreases in the random instants t_{ip}, i = 1, 2, ...

In the light of the considerations have been performed so far the Poisson homogeneous process can be applied as a model of the decreasing of propulsion system's effective energy.

If to assume that :

– the intensity of decreasing the effective energy in particular elements of the system by the value e_i , where : i = 1 (engine), 2 (shaftline), 3 (propeller), amounts to λ_i,

– the applied measuring instruments of similar accuracy make it possible to record the values e_1, e_2 and e_3 close to each other, i.e. to assume (without making a large error) that : $e_1 \approx e_2 \approx e_3 = e$,

then the process shown in Fig. 7 , can be represented, with the use of Poisson process features, by a new , summary one of the intensity λ_{UN} [2]:

(19)

in which the events S which consist in decreasing the effective energy by the constant value e, will occur in random instants (e.g. such as t_{1s}, t_{1p}, t_{1lw}, t_{2s} indicated in Fig. 8).

From practical point of view, determination of the values of e_i and λ_i becomes the crucial problem. The determination is possible in the case of satisfying the two complementary conditions :

– to have access to results of operational investigations carried out with application of standard control measuring instruments and diagnostic systems usually installed in ship power plants;

– to analyze technical documentation of the system's components and carry out simulation investigations in order to elaborate a mathematical model of influence of the occurring events S_i on parameters of ship motion in given, relatively constant, sailing conditions.

Summary

By assuming that for t = 0 the effective energy E(0) is equal to:

$$E(0) = L_{e\,max} \tag{20}$$

where:

$L_{e\,max}$ – new engine effective work,

and by determining the expected value and standard deviation of the decreasing of the energy in the instant t as :

$$E\left[\Delta L_e(t)\right] = e \cdot E\left(N_{\Delta E}\right) = e \cdot \lambda_{UN} \cdot t, \qquad \sigma_{Le} = e \cdot \sqrt{D^2\left(N_{\Delta E}\right)} = e \cdot \sqrt{\lambda_{UN} \cdot t} \tag{21}$$

where :

$N_{\Delta E}$ – random variable which describes cumulated number of the recorded, up to the instant t , events S , having the distribution [1, 6]:

$$P\left(N_{\Delta E} = k\right) = \frac{\left(\lambda_{UN} \cdot t\right)^k}{k} \exp\left(-\lambda_{UN} \cdot t\right); \quad k = 1,2,...,n \tag{22}$$

the relation which describes the decreasing of the energy L_e with time t, can be expressed as follows [6]:

$$L_e(t) = \begin{cases} L_{emax} & \text{dla} \quad t = 0 \\ L_{emax} - e \cdot \left(\lambda_{UN} \cdot t \pm e \cdot \sqrt{\lambda_{UN} \cdot t}\right) & \text{dla} \quad t > 0 \end{cases} \tag{23}$$

Making use of the relation (23) one can determine, for a given instant t , effective work (effective energy) which can be done by the entire propulsion system. Whereas, the relation (22) makes it possible to determine probability of occurrence of such number of the events S which would introduce additional limitations during realization of a given task (by making realization of a given ship speed impossible) or prevent it from realization at all. This way, value of the probability can be taken as a reliability index and used in the process of operational decision making.

The presented method seems to be a valuable supplement to the ways of description of reliability features of ship propulsion system , the crucial subsystem of ship power plant, which have been applied so far. Its basic advantage is the assessment of energy in function of time period during which a task is realized, that is very important in the case of realization of usually long-lasting tasks associated with cargo shipping by sea. An additional advantage is its versatility which makes that the method in question may be applied to reliability analysis of any device or energy subsystem of serial reliability structure, including those which are not machines, e.g. heat exchangers.

References

[1] Bielajew, J. K., Gniedenko, B. W., Sołowiew, A. D., *Metody matematyczne w teorii niezawodności*, Wydawnictwa Naukowo – Techniczne, Warszawa 1968.
[2] Chachulski, K., *Podstawy napędu okrętowego,* Wydawnictwo Morskie, Gdańsk 1988.
[3] DeGroot M. H., *Optymalne decyzje statystyczne,* PWN, Warszawa 1981.
[4] Kuliński, S., *Przyczyny i rodzaje uszkodzeń śrub napędowych występujące podczas eksploatacji statku,* Zeszyty Naukowe Politechniki Gdańskiej „Budownictwo Okrętowe nr 65", XXV Międzynarodowe Sympozjum Siłowni Okrętowych, Gdańsk 2004.
[5] Konieczny, J., *Sterowanie eksploatacją urządzeń*, PWN, Warszawa 1975.
[6] Girtler, J., Kuszmider, S., Plewiński, L., *Wybrane zagadnienia eksploatacji statków morskich w aspekcie bezpieczeństwa żeglugi*, Wyższa Szkoła Morska w Szczecinie, Szczecin 2003.
[7] Rudnicki, J., *Energy – Time Method for Assessment of Main Diesel Engine Operation,* Journal of KONES. Powertrain and Transport. - Vol. 14, nr 3 (2007), Warszawa 2007.
[8] Rudnicki J., *Ocena działania siłowni okrętowej w aspekcie energetyczno - czasowym* XXVIII Sympozjum Siłowni Okrętowych Gdynia 15-16 listopada 2007,Wydawnictwo Akademii Morskiej Gdynia 2007.
[9] Sadowski W., *Teoria podejmowania decyzji. Wstęp do badań operacyjnych,* Państwowe Wydawnictwo Ekonomiczne, Warszawa 1976.
[10] Smith D. J., *Reliability, Maintainability and Risk. Practical Methods for Engineers*, Butterworth –Heinemann Linacre House, Oxford 2001.
[11] Urbański, P., *Podstawy napędu statków,* Fundacja Rozwoju Akademii Morskiej w Gdyni, Gdynia 2005.
[12] Przepisy klasyfikacji i budowy statków morskich. Część I, Zasady klasyfikacji. Wyd. PRS, Gdańsk 2006.

Journal of POLISH CIMAC

Faculty of Ocean Engineering & Ship Technology
GDAŃSK UNIVERSITY OF TECHNOLOGY

DETERMINATION OF CRANKTRAIN FRICTIONAL RESISTANCE USING THE MOTORED ENGINE METHOD

Wojciech Serdecki

Institute of Combustion Engines and Transport
Poznań University of Technology
3, Piotrowo St., 60-965 Poznań
tel.+48 665 2243, fax: +48 6652204
e-mail: wojciech.serdecki@put.poznan.pl

Piotr Krzymień

Institute of Combustion Engines and Transport
Poznań University of Technology
3, Piotrowo St., 60-965 Poznań
tel.+48665 2239, fax: +48 6652204
e-mail: piotr.krzymien@put.poznan.pl

Abstract

Friction losses generated in engine kinematic nodes have an essential effect on its general efficiency. Measurement of these losses and indication of areas where they are generated can contribute to their minimization at the stage of engine design and during its operation as well. Most of the loss measurement methods requires an intervention in engine construction. The method of engine motoring does not require such intervention and at the same time offers possibility of precise measurement of engine resistance. The results obtained with the use of this method are considered hardly precise (among others because of different conditions during engine normal operation and its motoring), nevertheless they allow to estimate the influence of various effects on resistance observed on an engine.

This study presents the results of tests on the effect of certain quantities characteristic for engine operation as well as properties of lube oil applied on the course of instantaneous values of motored engine torque. Another achievement of the study is the recommendation of test conditions securing highest possible accuracy of engine resistance torque determination. The simulation tests were carried out on the 170A.000 engine.

Keywords: *piston-cylinder assembly, friction, friction loss assessment*

1. Introduction

Torque generated by the engine and transmitted to the power receiver results from following forces: gas force (decisive about torque course), inertia force and friction force (resulting in resistance torque reducing the gas force originated torque). In the case of multicylinder engine the resultant torque is a sum of torques generated in individual cylinders (see Fig. 1b for two-cylinder engine).

For a technically fit engine a typical course of torque instantaneous value corresponding to selected regimes of operation can be easily determined. Presence of any deviation can prove about irregularities that have occurred in operation of engine functional subassemblies (for instance about incorrect collaboration between elements of kinematic pairs). Recognition of interdependencies between the course of torque and engine technical condition and processes proceeding at its kinematic nodes and can be used for engine diagnostics.

Considerations on mutual relations between components of torque (relative to piston-cylinder assembly) have been carried out in [3, 4]. It was proved there that the component relative to the

gas force has the most significant effect on the torque while the other components have far lower effect (and could be omitted in typical, less accurate computations).

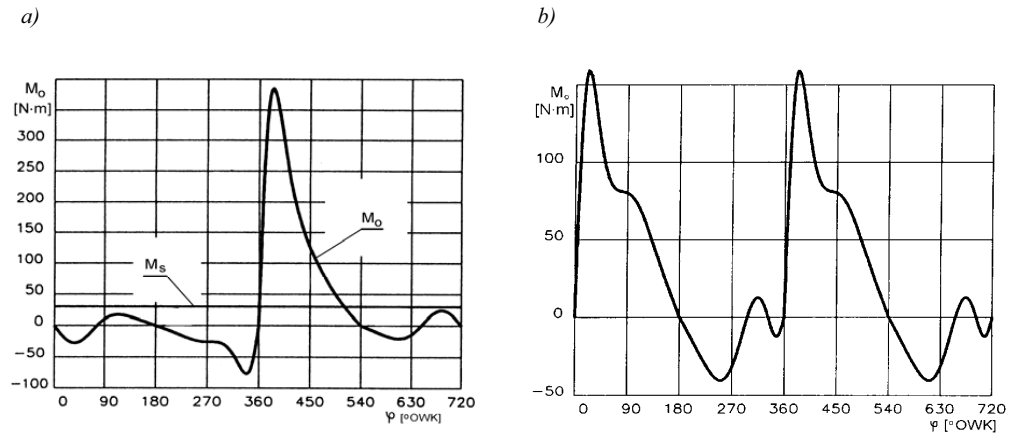

Fig. 1. Exemplary courses of 4-stroke engine torque instantaneous valueone-cylinder (a) and two-cylinder (b), M_s – mean torque [1]

As it can be noticed in Fig. 2, the torque component derived from friction force (important for presented analysis) is far lower than that produced by the gas force. This means that it is very difficult to detect changes in its value during measurement of torque transmitted from engine to the power receiver.

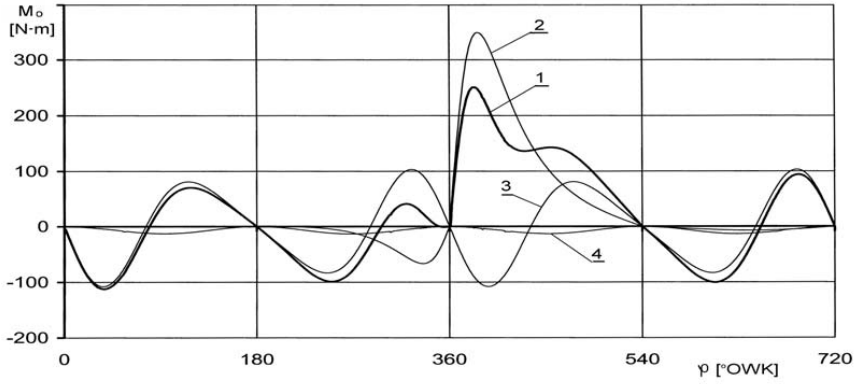

Fig. 2. Theoretical course of torque (1) and its components caused by following forces: 2 – gas force, 3 – inertia force, 4 – friction force, vs. crankshaft angle

An effective evaluation of the course of resistance torque caused by friction forces could be possible if the torque component relative to gas force (resulting from compression or combustion) was eliminated. Negligence of gas force means the need for tests on unfired engine which can happen when the engine is motored and does not generate the torque. Such method of investigation is called “engine motoring method”. This method consists in making unfired engine’s crankshaft rotate by the external drive. The drive train most often consists of electric motor, which can also operate as power generator and constitute the engine load. During the measurements a torque necessary for performing the rotation of driven engine crankshaft is being settled. The torque value can be find measuring the energy transmitted to the motoring electric motor or measuring the

moment of housing reaction. Although the results obtained using this method are considered less accurate (due to e.g. different conditions of fired and motored engine) still they allow to estimate the effect of various quantities on resistance to motion in engine individual subassemblies. The engine selected for tests should be deprived of fuel supply which means that there is no combustion and the pressure in cylinder corresponds to the compression pressure.

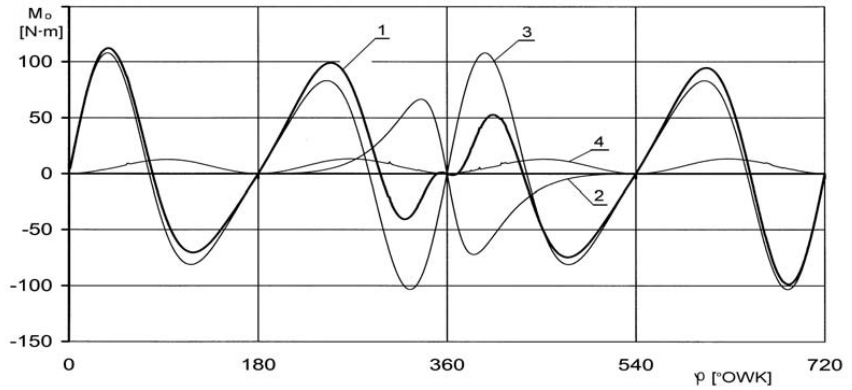

Fig. 3. Theoretical course of torque (1) and its components caused by following forces: 2 – gas force (no firing), 3 – inertia force, 4 – friction force, vs. crankshaft angle

However, the component relative to gas force is far lower for a case of unfired engine than for fired one it is still substantially higher than the component relative to friction force (see the course of resistance torque in Fig. 3). A complete exclusion of gas force is possible until after dismantling the cylinder head. Then the total resistance torque consists exclusively of components dependent on inertia and friction forces.

A further part of this study will present results of tests aimed at definition of the best conditions for carrying out the measurements of engine resistance to motion using the motoring method.

2. Course of measurement

Exemplary simulation tests presented in the further part of this study, have been carried out for the 170A.000 engine (Table 1) motored with a motor of adjustable rotational speed. Assumption on the lack of cylinder head made that the model takes into consideration only selected parameters that influence the changeable inertia and friction forces acting in piston-cylinder set. The synthetic oil of SAE 5W40 grade as well as semisynthetic SAE 10W40 and mineral SAE 15W40 ones have been selected for lubrication. Assumed temperature was 0°C, 20°C and 40°C while the rotational speed was limited to 100 rad/s.

Tab. 1. Basic technical data of the Cinquecento 170A.000 engine [6]

Parameter	Cinquecento ED 700
Engine swept volume, cm^3	704
Cylinder diameter, mm	80
Stroke, mm	70
Compression ratio	9
Max. torque (n = 3000 rpm), Nm	52
Max. power (n = 5000 rpm), kW	23
Number of cylinders	2 (in-line)

The assumption on temperature various values led to the need for definition of viscosity at those temperatures (oil viscosities defined according to [3] are collected in Table 2).

Tab. 2. Dynamic viscosity of the Elf lube oils at selected temperatures [5]

Rodzaj oleju	T = 0°C	T = 20°C	T = 40°C
SAE 5W/40 – synthetic	0.424	0.163	0.0717
SAE 10W/40 – semisynthetic	0.686	0.211	0.0822
SAE 15W/40 – mineral	0.979	0.262	0.0932

An analytical model of the piston-crank mechanism constructed for computations concerns the engine with dismantled cylinder head. The effect of following factors on collaboration of engine drive train elements, especially on changes in friction force and power has been taken into consideration during tests:

– changes in crankshaft speed,
– various types of lubricating oil
– fluctuations in oil temperature.

Masses of engine drive train elements performing the reciprocating motion like piston, rings, pin and connecting rod have been taken into account when calculating the inertia forces.

3. Results of resistance torque computations

Fig. 4 presents exemplary results of calculation of resistance torque and its components for selected crankshaft angular speeds and different lubrication oils (data of measurement conditions are presented in caption). An advantage of torque relative to friction force over that relative to inertia forces is easily noticeable for angular speed values selected for computations. For other input parameters these relations could be different. The analysis presented in [3] proves that inertia force connected with the operation of power train elements is proportional to the square of crankshaft angular speed while the friction force is proportional to the square root of this speed. However, this correlation should be treated merely as the approximation because only the wedge effect has been taken into account. It should be noted here that the presented results have been obtained using a complex model taking into consideration oil film phenomena of greater importance [2].

Variations in the course of resistance torque relate to the fluctuations of forces in engine power train. Fig. 5 presents a collective results of resistance torque calculations brought about for selected crankshaft speeds (at constant oil temperature) and courses obtained for different temperatures (at constant crankshaft speed).

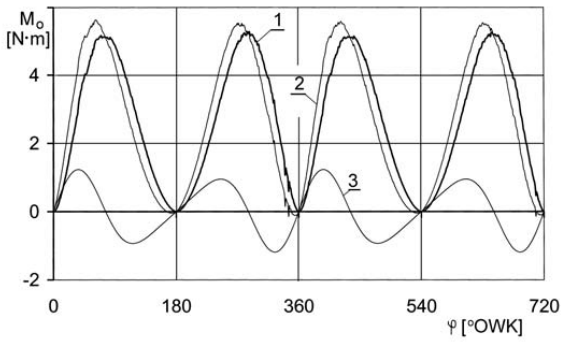

Fig. 4. Course of resistance torque (1) and its components relative to friction (2) and inertia (3) forces vs. crank angle, defined for SAE 5W40 grade lube oil; T = 20°C, ω = 50 rad/s

As expected, the resistance to motion increases with an increase in crankshaft speed and increase in oil viscosity while torque increase due to friction is slower than that due to inertia (what corresponds to presented previously dependencies). Courses presented in Fig. 5 show that for the analyzed range of input data inertia forces exceed the friction forces only on short sections of piston displacement and for the highest angular speed taken into account (total resistance torque is negative).

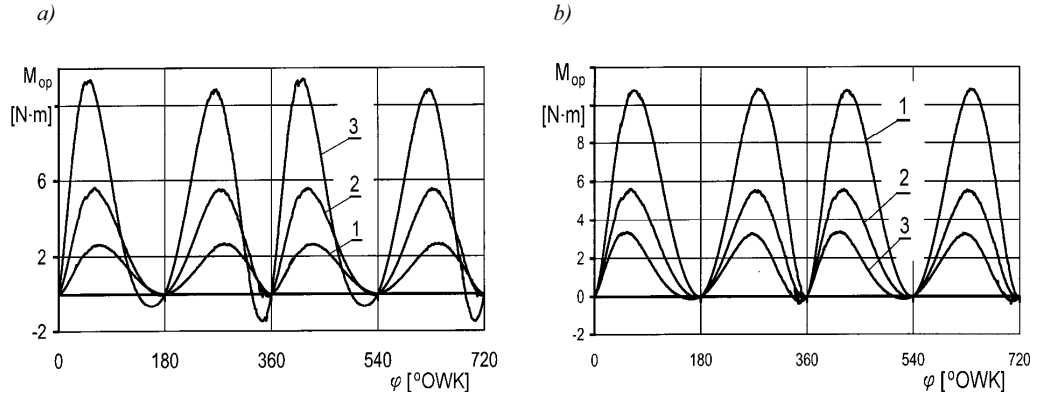

Fig. 5. Course of resistance torque vs. crank angle for selected angular speeds: 1 – 20 rad/s, 2 – 50 rad/s, 3 – 100 rad/s; for SAE 5W40 grade lube oil, t = 20°C (a), and different temperatures: 1 – 0°C , 2 – 20°C, 3 – 40°C;ω = 50 rad/s (b) [3]

Comparison of the course of resistance torque momentary value has a considerable diagnostic value but is not sufficiently precise for a global evaluation of individual factors contributing to motion resistance. Further part of this study compares not momentary values of torques but their mean values. Fig. 6 presents comparison of average values of motion resistance caused by friction (M_t) and inertia (M_b), for selected crankshaft speeds ω and oil temperature T. Computations were carried out for a synthetic oil of SAE 5W40 grade (Fig. 6a) and for mineral oil of SAE 15W40 grade (Fig. 6b). The results confirm earlier remarks on mutual proportions between these torques and about dependencies connecting those torques with crankshaft angular speed and lubricating oil viscosity.

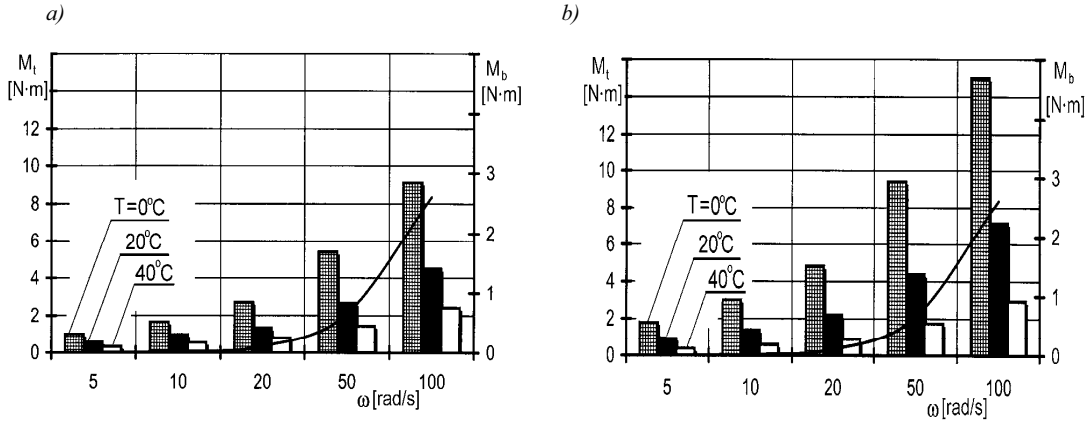

Fig. 6 . Arrangement of resistance torques mean values relative to friction M_t and inertia M_b (continuous line) for selected crankshaft angular speeds ω and oil temperature T: a –SAE 5W40 grade oil, b – SAE 15W40 grade oil

The measurement of friction torque would be more precise if the value of torque due to inertia was lower. In order to monitor mutual relations between those torques, a conception of AM factor has been introduced, that expresses relation of friction and inertia mean values. Higher value of this factor, more advantageous conditions for evaluation of friction torque.

When analyzing the course of A_M factor in Fig. 7 one can conclude that its value decreases with the increase in crankshaft angular speed regardless lube oil grade. This shows that the region of low crankshaft speeds is the most advantageous one for the foreseen investigations.

On the other hand, one should remember that with a drop in shaft speed conditions of collaboration between rings and cylinder liner deteriorate (an oil film rupture can happen and part of piston stroke in conditions of mixed lubrication extends). The quality of such collaboration can be described with relative displacement S expressed as the relation of stroke section covered in conditions of fluid friction (a sum of microunevennesses is smaller than the oil film thickness) to the entire stroke. As it outcomes from the hydrodynamic theory of lubrication, the length of this displacement increases with the increase in crankshaft speed and with drop in oil temperature (increase in oil viscosity).

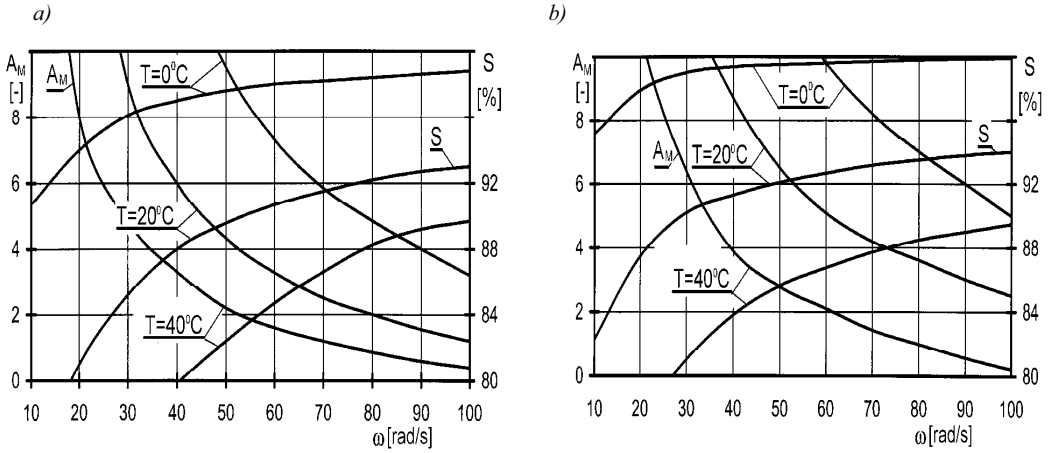

Fig. 7. Changes in A_M factor and S relative stroke vs. crankshaft angular velocity for selected temperatures of SAE 5W40 grade (a) and SAE 15W40 grade (b) lubricating oils

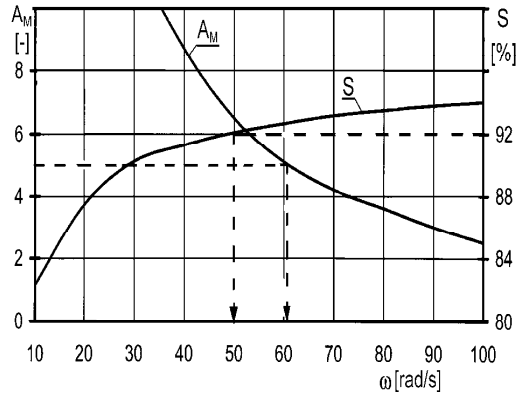

Fig. 8. Example of determination the crankshaft angular velocity corresponding to assumed input parameters of the test stand

Construction of diagrams presented in Fig. 7 is very time consuming (requires carrying out a number of simulation computations) but considerably eases a choice of best measurement conditions from the point of accuracy. A procedure of the choice has been presented in further example.

Assuming the input data as follows:

– measurement temperature: 20ºC,

– A_M factor: > 5,

– S displacement: > 92%

one can read from the graph in Fig. 8 that for the SAE 15W40 grade oil the crankshaft angular velocity satisfying these requirements lies within the limits of 50 and 61 rad/s.

These graphs could serve also as a tool for estimation of A_M and S parameters for introductory assumed values of crankshaft angular velocity.

4. Summary and conclusions

Most important conclusions from the presented investigations are as follows:

– gas forces relative to the processes performed in engine cylinder are far higher than other forces acting in engine power train; similar proportions are observed in the case of torques relative to the forces mentioned,

– decrease in crankshaft angular speed results in decrease in contribution of inertia related torque in total resistance torque,

– lowering the measurement temperature leads to the increase in oil viscosity and eventually to the increase in resistance torque relative to friction,

– drop in crankshaft speed results in longer distance covered by piston in conditions of mixed lubrication.

The analyses presented in this paper are based on analytical model investigations and the only way to verify them is to carry out tests on a test stand (including models of engine power train).

Literatura

[1] Iskra A., *Dynamika mechanizmów tłokowych silników spalinowych*, Wydawnictwo Politechniki Poznańskiej, Poznań 1995.

[2] Serdecki W., *Badania współpracy elementów układu tłokowo-cylindrowego silnika spalinowego*. Monografia, Wydawnictwo Politechniki Poznańskiej, Poznań 2002.

[3] Serdecki W., *Analiza zmienności momentu oporowego silnika spalinowego małej mocy*, Materiały konferencji KONMOT-AUTOPROGRES 2008 (w druku).

[4] Serdecki W., *Zmienność sił i momentów tarcia w układzie korbowo-tłokowym podczas rozruchu silnika spalinowego*. W: Eksploatacja Silników Samochodowych. Zeszyt nr 16, Polska Akademia Nauk – Oddział w Lublinie, Szczecin 2007.

[5] Materiały informacyjne firmy ELF.

[6] Materiały informacyjneFIAT.

Journal of POLISH CIMAC
Faculty of Ocean Engineering & Ship Technology
GDAŃSK UNIVERSITY OF TECHNOLOGY

TESTING OF REGENERATIVE THERMAL SPRAYING Ni-Al ALLOY COATINGS

Robert Starosta

Gdynia Maritime University, Faculty of Marine Engineering
ul. Morska 81-87,81-225 Gdynia
tel. +48 58 6901435
e-mail: starosta@am.gdynia.pl

Abstract

The article presents the results of testing of Ni-Al alloy coatings with different chemical constitution and phase composition, which might replace currently used electrolytic chromium coatings .Crust chromium coatings are suitable for reconditioning of machine parts because of their very good maintenance properties. However, due to toxicity of electrolylic chromium bath, their application tends to be restricted. Thermal flame and plasma spraying technologies were chosen for nickel aluminium coating application. Obtained coatings were distinguished by significant porosity of structure and surface roughness. The thickness of coatings ranged from 440 to 683 μm. Microhardness of coatings was not related to applied metal plating technology but to chemical constitution and phase composition. The more aluminium content in alloy coating the harder the coatings were. The hardness of coatings which resulted from NiAl phase was ca 250 HV 0.04. Flame spray coatings are distinguished by nearly 10 times bigger corrosion current density when compared with plasma spray coatings .The value of corrosion potential is influenced by structure and chemical constitution of coatings. The more aluminium content the lower E_{corr}.

Key words: *thermal spraying, regenerative coatings, nickel-aluminium coatings*

1. Introduction

Parts of devices and marine machines worn in operation can be reconditioned by coating application. Crust chromium coatings deposited from electrolytic baths Cr (VI) are commonly used in industry. They are resistant to tribologic wear, electrochemical and high-temperature corrosion. They are used to coat parts exposed to complex operating conditions, e.g. piston rings, cylinder liner sliding surfaces and other parts of heat engines and compressors. Despite wide range of applications, engineering chromium coatings have become less common in use due to the following [7 ÷ 9]:

- hydriding of basis
- big tension forces of own stress in chromium coating,
- electrolytic bath efficiency for chromium plating amounts only 10-15%,
- engineering chromium coatings are distinguished by big and heterogeneous thickness thus require grinding to size,
- electrolytic bath Cr (VI) is of high toxicity, environment-unfriendly, harmful and carcinogenic to human health,
- gas and chromium compounds (VI) emission pollute environment,
- growing insistence on environment protection in many countries resulted in increase of requirements referring to emission of Cr compounds (VI). For the time being in the European Union binding limit is 0.05 mg/ m^3 (MEL - maximum exposure limit), though the chrome

limit value (VI) (Cr_2O_3) mg/ m^3 proposed in the USA since 2004 is likely to be introduced by the European Union soon.

The reasons listed above will influence future designing and making of engineering superficial layers. For these reasons replacing electrolytic chromium coatings with nickel alloy coatings seems to be relevant. Nickel – chromium, titanium, iron and aluminium alloys are the most common.

Nickel–aluminium alloys form systems in which both solid solutions and ordered intermetallic phases can occur. Two-component system Ni-Al forms five intermetallic phases:
Ni_3Al, Ni_2Al_3, NiAl, Ni_5Al_3 and Ni_2Al. Alloys containing NiAl i Ni_3Al are the most common.
The alloys above are distinguished by the following [1÷6]:

- resistance to oxidation and carburizing in temperatures up to 1100ºC,
- good tensile, fatigue and creep strength in high temperature, very good abrasion resistance in high temperatures,
- transition from brittle to plastic state in the temperature range 300-600ºC.

The thesis presents selected properties of Ni-Al alloy coatings with various chemical constitution which were applied by two thermal spraying technologies i.e. flame and plasma spraying.

2. Preparation of samples

Flatbar 35 x 100 x 5 mm in size made of steel C45 served as basis metal. Before coating, the samples were degreased and prepared in vapour blasting to grade Sa3.

Tab. 1. Chemical constitution of ProXon 21021 by Castolin (mass fraction)

Component	%
Ni	93,45
Al	5
B	0,8
Fe	0,34
Cr	0,18
Si	0,15
C	0,08

Alloy coatings of constitution shown in table 1.should be distinguished by two-phase structure consisted of solid solution of aluminium in nickel and phase Ni_3Al. Coatings were applied by infrasound flame spraying and plasma spraying.

Intermetallic phase coatings NiAl (25 ÷ 35 per cent aluminium mass fraction) and Ni_3Al (ca 15 per cent aluminium mass fraction) were obtained by plasma spraying of powder of granulation 45 µm and 150 µm respectively by Alfa Aestar.
Infrasound flame spraying was performed by means of 'Roto-Teck' burner manufactured by Castolin. The parameters of technological process were as follows:

- acetylene pressure: 0.7 MPa,
- oxygen pressure: 0.04 MPa,
- burner feed rate: 25 m/min,
- distance between burner and sprayed surface: 150 mm,
- number of layers: 6.

Both alloy coatings as well as composite ones were applied by two methods: 'cold ' and 'hot '. 'Cold ' spraying involved preheating of steel basis with burner to the temperature ca 100 ºC. Then the coating was sprayed so as not to exceed the temperature of the sample 250 ºC. Before 'hot ' coating application, the processed surfaces were heated up to 250 ºC and then in the spraying process the temperature of an object was maintained between 500 ÷ 600 ºC.

Intermetals of nickel and coating material ProXon 21021 were thermally sprayed by plasma method by 'Plasma System' SA company. There were the following parameters of plasma spraying:

- current strength – 450A
- non-transferred arc voltage – 47V
- argon flow – 2000 [dm^3/h],
- hydrogen flow – 100 [dm^3/h],
- distance between nozzle and sample -70 mm

3. Testing methodology

Roughness of coatings and steel basis were measured with profile measurement gauge Hommel Tester T 1000. Measuring length was 4.8 mm, sample length 0.8 mm.

Microhardness was measured with hardness tester Vickers type by means of H type device mounted in a holder of metallographic microscope Vertival. Load used was 0.4 N in 10 sec in ambient temperature. Diagonal indentation lengths were measured with accuracy 0.2 μm.

The thickness of flame sprayed coatings was determined by microscopic method according to standards PN-EN ISO 2064 and PN-EN ISO 1463. An optical microscope Vertival with microhardness measurement instrumentation was used. The measurement was taken on sample cross-sections etched with nital to show the line between the basis and the coating. Five separate measurements along the microsection were taken determining local thicknesses of coating. Mean thickness was calculated from measurements of five randomly selected samples. Despite the measurement accuracy up to 0.4 μm , the values obtained were rounded to 1 μm due to standard recommendations PN-EN ISO 1463.

The thickness of plasma spray coatings was measured by means of an ultrameter Fischerscope MMS Permascope with EGAN probe.

Coating structures were assessed on cross-sections by means of metallographic optical microscope Zaiss Axio Vert 25.

Measurement of coatings corrosion resistance was taken by potenciodynamic method in three-electrode system. Degreased with acetone sample 1 cm^2 in size, an auxiliary electrode (polarizing) from platinized titanium and a reference electrode (saturated calomel electrode) were placed in a vessel filled with 500 ml 0.001 M H_2SO_4 solution of ambient temperature. The measurement was taken after 0.5 hour exposure of a sample in the electrolyte to stabilize corrosion potential. The electrolyte was being continuously stirred when measured.

Testing involved registering of polarization curves i=f(E) in range ± 150 mV from corrosion potential. Cathode curve was registered first , then anode curve. Potential change rate in all occurrences equaled 10 mV/min.

4. Results of testing

Tab. 2. Coatings roughness - R_a

Coating	Number of meas.	Average	Min.	Max.	Std dev.	Std.error
Ni-5%Al-"cold"	10	13	9,6	16,8	2,41	0,76
Ni-5%Al "hot"	10	13,6	11,3	15,7	1,48	0,47
Ni-5%Al plasma	10	8,9	7,4	10,1	0,84	0,26
Ni_3Al	10	12,9	11,2	16,2	1,47	0,46
NiAl	10	5,3	4,67	6,05	0,39	0,12

Coatings were distinguished by highly developed real surface which the results of roughness show table 2. The value of parameter R_a depending on chemical constitution and thermal spraying technology ranged from 5.3 μm for intermetallic phase NiAl coating to 13.6 μm for alloy coating with 5 % aluminium content obtained by 'hot ' flame method. High mean values R_a are probably related to porous and heterogenous, layered coating structure. Machine parts of so high roughness shouldn't operate in tribologic spots.
Coatings should be further treated in order to obtain better stereometric surface.

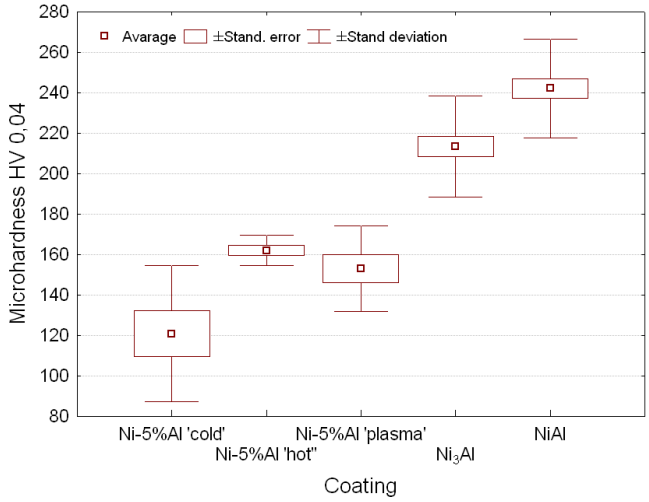

Fig. 1. Microhardness of thermal spray coatings

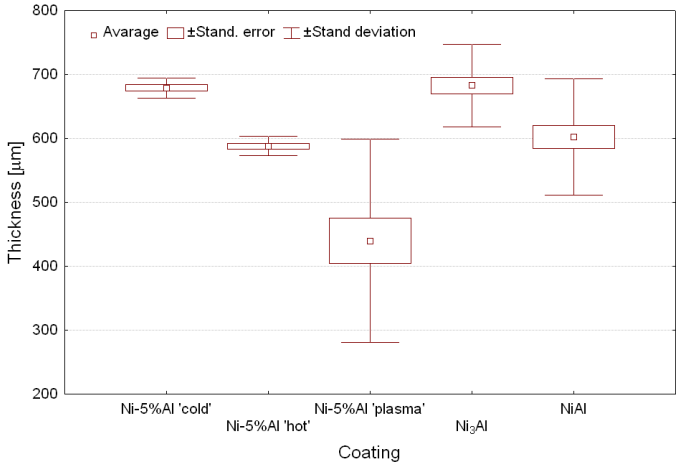

Fig. 2. Thickness of thermal spray coatings

Thermally spray alloy coatings Ni-5 %Al from powder material ProXon 21021 depending on applied technology had average microhardness from 121 HV 0.04 to 162 HV 0.04 (Fig. 1).The lowest average microhardness value was obtained in 'cold ' flame spraying technology occurrence. The average value was determined from 9 measurements. Obtained measurement results ranged between 70 to 158 HV 0.04. Measurement spread equalled 88 HV, standard deflection 32 HV, error of determining average value (standard error) 11.3 HV. Such a big spread of measurement

results was probably caused by high roughness of coatings. In some cases Vickers indenter could have met coating surface under which pores occurred.

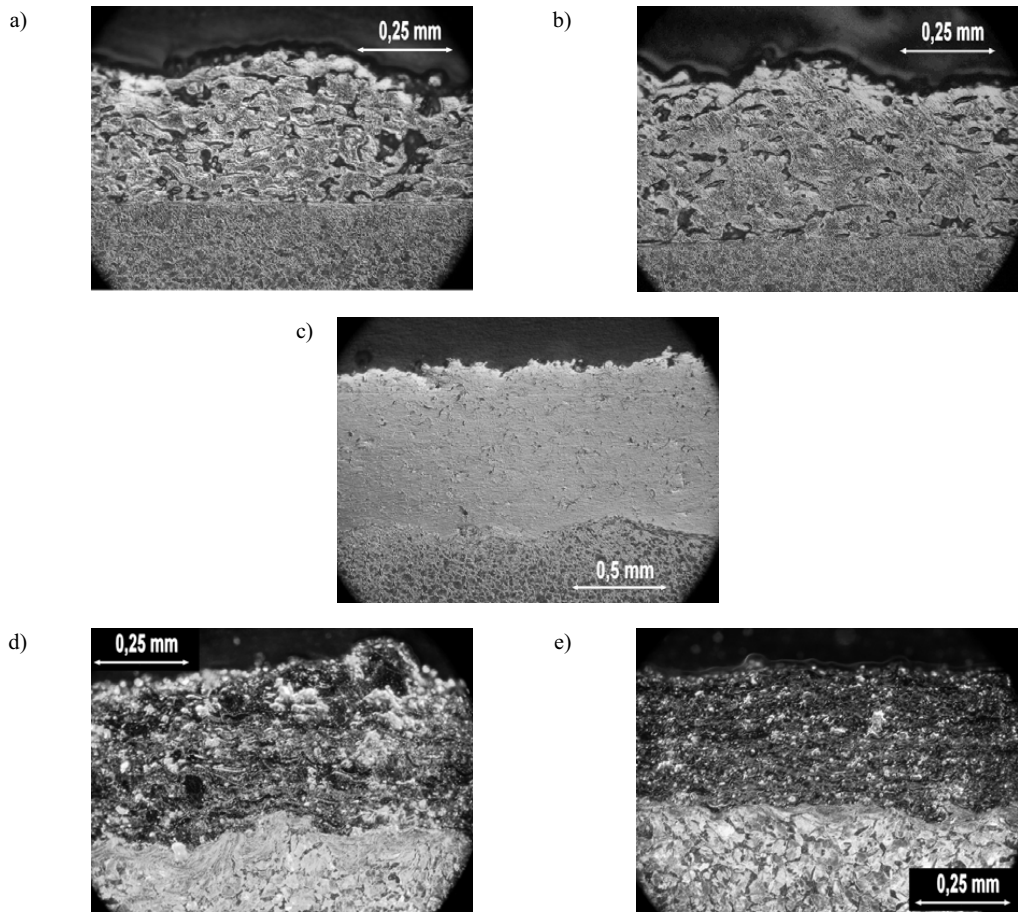

Fig. 3. Alloy coatings structure NiAl thermally sprayed.
a) 'Cold ' flame spray Ni-5%Al coating (bright field),
b) ' Hot' flame spray Ni-5%Al coating (bright field),
c) Plasma spray Ni-5%Al coating (bright field),
c) Plasma spray Ni_3Al coating (dark field),
d) Plasma spray NiAl coating (dark field)

Statistical analysis, Anova Kruskal-Walis test and median test for Ni-5%Al coatings at assumed relevance level α= 0,05 cannot exclude null hypothesis of no medians differences between variables. It can be mainained with 95% probability that applied technologies don't influence significantly the hardness of spraying alloy coatings with 5% aluminium mass fraction.

However, the hardness is affected by aluminium content in coating. In tested concentration range, growth in coatings hardness related to growing amount of aluminium content in a coating.

Tested coatings were applied in 6 layers. Depending on applied technology and chemical constitution, their average thickness varied from 440 to 683 μm (Fig. 2). Plasma spraying coatings in 'Plasma System SA' were distinguished by high spread range in obtained results of thickness

measurements, e.g. thickness of Ni-5%Al coating varied from 227 to 668 μm, which made standard deflection 159 μm. Such a considerable spread in measurement results was presumably caused by partial overlapping of beads while spraying flat surface. Coatings applied by ‘ hot ‘ flame spraying method were less thick than those treated by ‘ cold ‘ method.
Alloy coatings Ni-5%Al plasma sprayed were the least thick among coatings of such a chemical constitution. Higher temperature of the process and higher rate of spraying the coating material allow for reduction in coatings roughness, consequently reduction in their thickness.

The structure of alloy coating Ni-Al applied by flame and plasma spraying is shown in fig.3. The coatings obtained are considerably porous. The analysis of coatings structure in cross-sections proved that the number and size of pores are affected by coating technology and their chemical constitution. Coatings of this chemical constitution Ni-5%Al applied by ‘cold ‘ flame spraying were the most porous. The least number of pores was found in coatings obtained by plasma method.

Among coatings applied by plasma spraying, layers obtained in intermetallic phase Ni_3Al were considerably porous. It is probably connected with the change of structural constituent volume that occurs during phase changes in solid state. Nickel and aluminium alloy containing ca 85% Ni solidifies, forming mixture of eutectic type consisting of intermetallic phase NiAl and solid solution of aluminium in nickel.

Tab. 3. Corrosion current density and corrosion potential of thermal spray coatings

	Coating				
	Ni-5%Al ‘cold’	**Ni-5%Al ‘hot’**	**Ni-5%Al plasma**	**Ni_3Al**	**NiAl**
i_{corr} [μA/cm^2]	257	249	28	46	28
E_{corr} [mV]	-173	-188	-103	-166	-197

Coatings Ni-5% Al flame sprayed had around 10 times higher corrosion current density values (tab.3), thus they are several times less resistant to corrosive wear than coatings obtained by plasma method. This can be resulted from high roughness and porosity of these coatings, which is connected with highly developed real surface of tested samples. There is also probability of electrolyte penetration through pores to the steel basis surface. The influence of aluminium concentration on corrosion current density was not observed.

However, observed influence of aluminium content and phase structure on corrosion potential of plasma spray coating was significant. The bigger aluminium concentration the bigger corrosion potential. Presumably it is connected with much lower normal potential of aluminium when compared to that of nickel. Due to relatively high corrosion potential values of assessed coatings applied on steel basis, in case of electrolyte penetration through pores or mechanical damages, they will be cathodes. Steel basis will corrode. Technological process of applying these coatings must be assisted by their sealing by melting or impregnation with linseed oil.

5. Concusions

- Ni-Al alloy coatings applied by flame and plasma spraying are distinguished by considerable roughness of surface.
- Microhardness of coatings increases with aluminium content.
- Thermal spraying method doesn’t influence hardness significantly.
- Porosity of coatings is related to treatment technology and coatings composition. Flame spray coatings are more porous than coatings obtained by plasma technology. Increase of aluminium content increased porosity.
- Corrosion properties depend considerably on applied technology. Plasma coatings have very low corrosion current density values.

- In case of spray coatings, increase of aluminium concentration causes corrosion potential drop.
- Due to lower corrosion potential value of steel basis in comparison to Ni-Al alloy coatings the method which decreases their porosity needs to be worked out.

References

[1] Chang, J.T., Yeh, C.H., He, J.L, Chen, K.C., *Cavitation erosion and corrosion behavior of Ni–Al intermetallic coatings*, Wear no. 255, pp. 162–169, 2003.

[2] Chen, H., Xu C, ., Qu, J., Hutchings, I.M., Shipway, P.H., Liu, J., *Sliding wear behavior of laser clad coatings based upon a nickel-based self-fuxing alloy co-deposited with conventional and nanostructured tungsten carbide–cobalt hard metal,* Wear no 259, pp. 801–806, 2005.

[3] Deshpande, S., Sampath, S, Zhang, H., *Mechanisms of oxidation and its role in microstructural evolution of metallic thermal spray coatings—Case study for Ni–Al,* Surface & Coatings Technology, no 200, pp. 5395 – 5406, 2006.

[4] Duraiselvam, M., Galun, R., Siegmann, S., Wesling, V., Mordike, B. L., *Liquid impact erosion characteristics of martensitic stainless steel laser clad with Ni-based intermetallic composites and matrix composites,* Wear, no 261, pp. 1140–1149, 2006.

[5] Duraiselvam, M., Galun, R., Wesling, V., Mordike, B.L., Reiter R., Oligmüller J., *Cavitation erosion resistance of AISI 420 martensitic stainless steel laser-clad with nickel aluminide intermetallic composites and matrix composites with TiC reinforcement*, Surface & Coatings Technology, no 201, pp. 1289–1295, 2006.

[6] Starosta, R., Szczepaniak, P., Ocena odporności korozyjnej powłok z faz NiAl oraz Ni_3Al natryskiwanych plazmowo. Inżynieria Materiałowa, no 3, pp. 540-543, 2006.

[7] Starosta, R., Zieliński, A,. *Effect of chemical composition on corrosion and wear behaviour of the composite Ni-Fe-Al_2O_3 coatings*, Journal of Materials Processing Technology, no 157 – 158, pp. 434-441, 2004.

[8] Szeptycki, B., Elektroniczne powłoki kompozytowe z osnową niklową jako zamienniki powłok chromowych, Inżynieria Powierzchni, no 3, pp. 55-63, 2006.

[9] Sahraoui, T., Fenineche, N., Montavon, G., Coddet, C., *Alternative to chromium: characteristics and wear behavior of HVOF coatings for gas turbine shafts repair (heavy-duty)*. Journal of Materials Processing Technology, no 152, pp, 43–55, 2004.

Journal of POLISH CIMAC
Faculty of Ocean Engineering & Ship Technology
GDAŃSK UNIVERSITY OF TECHNOLOGY

REASONS OF A THRUST RING DAMAGE IN OIL-COOLED PISTON HEAD IN A DUAL FUEL CI ENGINE FUELLED WITH GAS AND DIESEL OIL

Zdzisław Stelmasiak, Jan Wencelis, Jerzy Larisch
Technical University of Bielsko-Biala, Internal Combustion Engines and Automobiles Branch
ul. Willowa 2, 43-300 Bielsko-Biała, Poland

Abstract

The paper presents a test results explaining reasons of thrust ring damage in piston head's cooling system of the Caterpillar 3516A engine run in dual fuel system. Task of the ring is to stop the oil injected by oil nozzles and to improve uniformity of piston head cooling. In the engine run on mine gas occurred two breakdowns in the piston-cylinder assembly; probably reason of these breakdowns was a fracture of the thrust ring. In connection with it, damaged rings were tested metallographicaly and dimensionally to find reasons of the fracture. Performed tests showed that the most probably reason of the breakdowns is wrong mounting of the ring in the piston head, causing its bending during engine operation by inertia forces and fatigue fracture in overstrained cross-section, in area of oil holes.

Keywords: *dual fuel, mine gas, piston, thrust ring, fatigue fracture of the ring, combustion process*

1. Introduction

In the 16 cylinder V-type Caterpillar 3516A engine the piston head is cooled by motor oil sprinkled from two nozzles located in channel of lubricating system. The oil gets the channel formed by recess at internal side of the piston head and closes channel of the thrust ring, what is shown in the Fig.1. The thrust ring consists of two half-rings with oval holes located opposite the nozzles of oil injectors, Fig. 2. During full cycle of engine operation, oil channel in the piston head is fed intensively with oil in time when the piston is near BDC position only. Objective of the ring is to prolong time when the oil is in contact with the piston head, and to improve uniformity of its cooling. The half-rings are mounted with interference fit to the piston head, whereas elastic forces should protect it against falling out during engine operation.

a) b)

Fig. 1. The piston of the Caterpillar 3516A engine: a) the view of the piston ; b) the scheme of ring mount in the

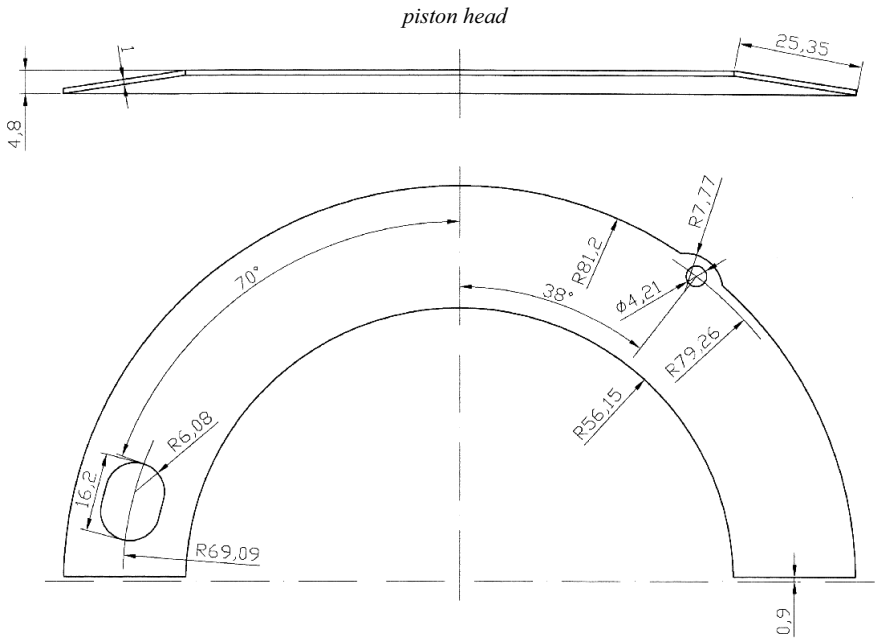

Fig 2. The drawing of oil ring

Version of the 3516A engine adapted to operation in dual fuel system is discussed in the present paper. The engine runs on mine gas as the main source of energy and Diesel oil which initiates combustion of the mine gas. View of the engine is shown in the Fig. 3; its technical specification is listed in the Table 1.

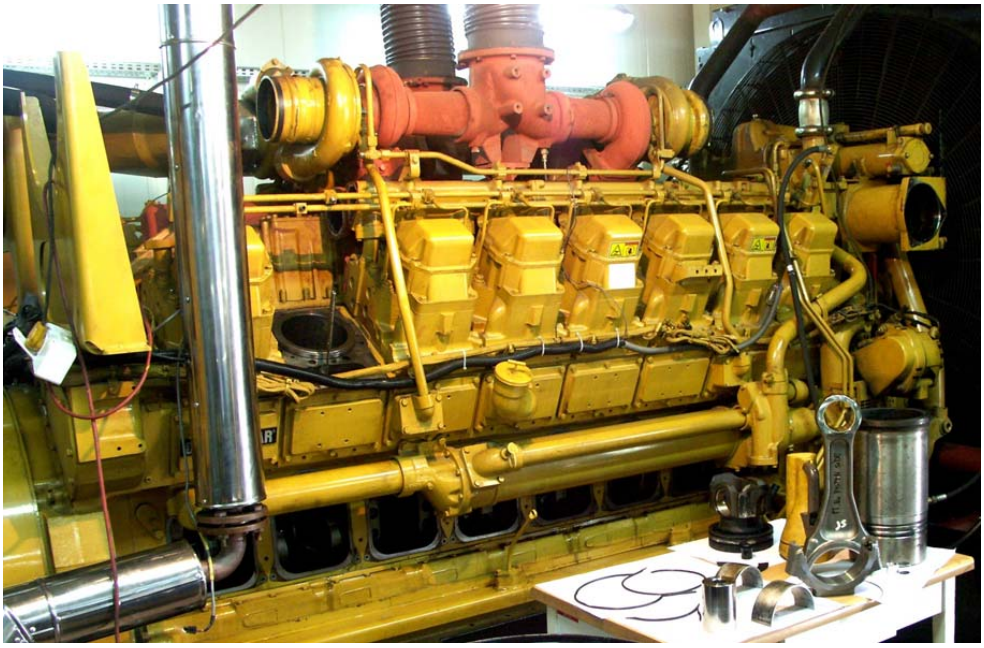

Fig. 3. View of a Caterpillar 3516A engine

Table 1. Engine Specification

Engine type	3516A
Number of cylinders	16,V type 60^{o}
Bore	170 mm
Stroke	190 mm
Displacement volume	69,1 dm^{3}
Compression ratio	13:1
Effective output power	1100 kW when fuelled with gas
Rotational speed	1500 rpm
Combustion chamber	direct injection to chamber in piston crown
Diesel oil injection system	mechanical united injector in each cylinder
Natural gas feeding system	mixer-type
Supercharging	4 turbocompressors

After about 5000h of engine operation, in the 7th cylinder from LH side of the engine a breakdown in piston-cylinder system occurred, seen as non-uniform and noisy operation. After dismantling of the crankshaft assembly there was confirmed a seizure of the piston skirt in its bearing part, partial jamming of the 1st and 2nd sealing ring, and fracture of the thrust ring in cooling system of the piston head, shown in the Fig. 2.

Conditions of the piston and its components are shown in the Fig. 4. It was found a breakage and lack of a considerable part of the thrust ring, Figs. 4a and 4b. Some broken elements were found in the sump, whereas some file dust got at between piston's skirt in bearing part of the piston and the cylinder, bringing about its damage and carving a deep scratches, what is seen in the Fig. 4e. Traces of scuffing are distinctly visible in the Figs. 4c and 4d. Simultaneously, however, there weren't confirmed any unequivocal symptoms of anomaly of combustion process, what would effect in local melting of upper edge of the piston head, or local partial melting of the combustion chamber. That fact enabled to presume, that possible primary reason of the damage was a fracture and falling out of a considerable part of the thrust ring, Fig. 4b, what resulted in worsened cooling of the piston head, and as consequence its overheating.

The second damage of the same engine occurred after about 8000h of operation in 8th cylinder from LH side of the engine (cylinder adjacent to the one discussed above). The damage consisted in a slight leak of coolant due to failure of rubber ring which seals the fluid channel in metal spacer between cylinder and cylinder head, Fig. 5a. Because the cylinders touch each other, damage of the thrust ring could not arise in result of overheating of the second cylinder. It should be supposed, that the damage was of a random character and wasn't connected with faulty engine operation. At the opportunity of repair of that damage, piston-con rod assembly of the 8th cylinder was also disassembled to perform its verification.

a)

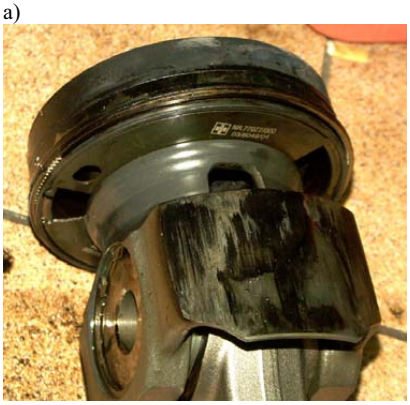

b)

c)

d)

e)

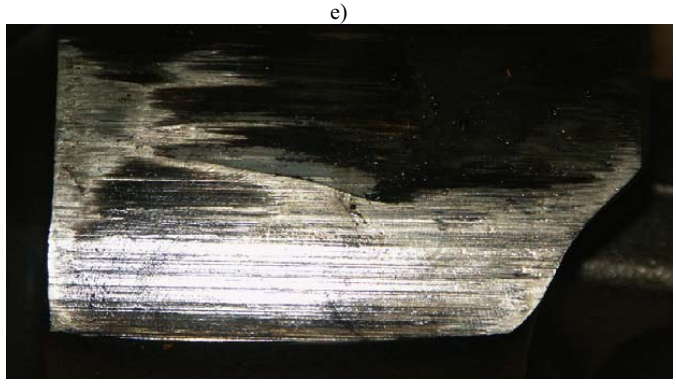

Fig.4. View of the piston, damaged after about 5000h of engine operation: a) piston with fragments of the ring in the seat; b) fragment of the ring after removal from the piston (visible loss); c) and d) bearing surfaces of the piston with visible traces of scuffing; e) bearing surface of the piston with visible, deep scratches arisen due to penetration of fragments of broken ring to the cylinder.

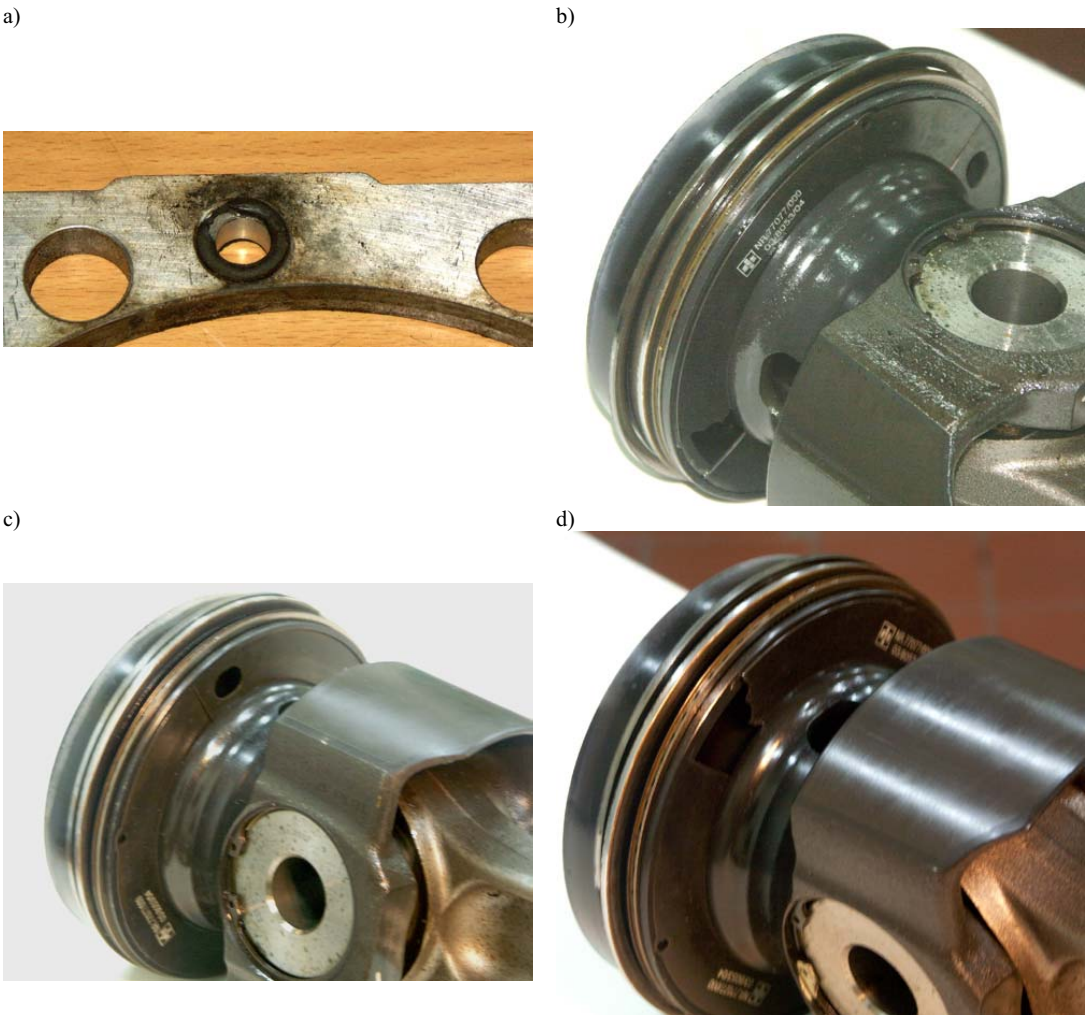

Fig. 5. A view of the piston after failure on the 8th cylinder

In result of visual inspection of the piston it was found a fracture and breakage of a fragment of the ring in area of the oil hole, Figs. 5b and 5d. Simultaneously, however, both the piston and the cylinder liner did not show any traces of non correct mating. There existed visible traces of honing operation on the cylinder liner, whereas on mating surface with the piston there weren't any scratches or any durable traces of mating. Also on bearing elements of the piston were visible distinct traces of mechanical working and lack of wear, Figs. 5c and 5d. All piston rings were movable and did not show any traces of non correct mating and excessive wear. With respect to a slight loss of the piston, Fig. 5b and 7a, one can suppose that the damage did not significantly deteriorate conditions of the piston head cooling and did not lead to its seizure. These facts allow to assuming that accidentally detected damage of the thrust ring was not connected with thermal problems of the piston, and could effect from defective manufacturing of the ring or its non correct assembly.

The problems presented above induced the authors to carry out tests aimed at explanation of a reason which could cause defects of the rings and to take actions to avoid failure in other cylinders of the engine.

2. Results of the tests

Scope of the performed tests applied to:

- determination of chemical constitution of material of the ring;
- determination of hardness;
- determination of microstructure of the material;
- investigation of possible reasons of damage of the ring.

Chemical constitution tests of the material were performed with use of spectrometer, obtained results are shown in the Table 2. From analysis of the chemical constitution is evident that the tested material belongs to brand of spring steel, equivalent to C75S grade according to PN-EN 10132-4: 2000 standard (old marking as 75 according to PN-74/H-84032 standard).

Table 2. Chemical analysis of the ring

Elementary substance	**Measured contents [%]**	**U_{Amean}**
Al	**0,01**	-
Cr	**0,03**	-
Mn	**0,64**	0,01
Ni	**0,03**	-
P	**0,017**	0,004
Si	**0,24**	0,01
Ti	**0,004**	-
W	**0,01**	0,001
C	**0,74**	0,02
S	**<0,005**	-
U_{Amean} – extended uncertainty of mean value (from 3 measurements, category A, at confidence level of p=0,95		

The hardness was measured with use of Vickers method according to PN EN ISO 6507-1:2006(U) standard with use of metallographic specimen - test piece cut out perpendicularly to surface of the ring. Results are put together in the Table No.3.

Table 3. Results of hardness measurements of the thrust ring material

HV10 Hardness					**Mean**
480	473	470	478	483	477
U_{Amean} = 7 HV (extended uncertainty of the mean value, category A, at confidence level of p = 0,95					

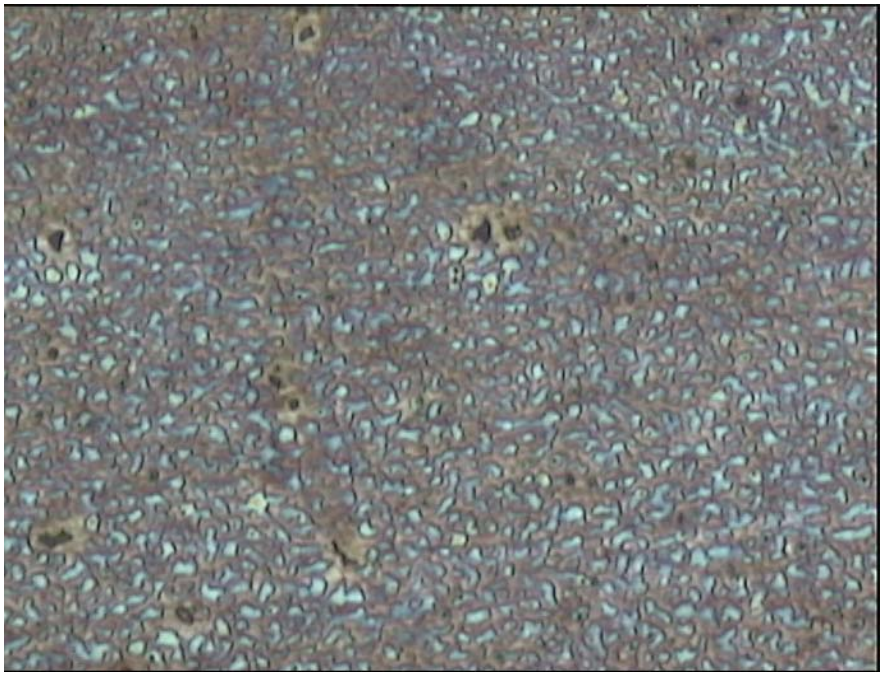

Fig. 6 Microstructure of thrust ring material in quenched and tempered state: bainitic-sorbitic structure; etched with nital, magnification 500x

Measured hardness and microstructure is typical of the tested material in quenched and tempered state. Simultaneously, in material shown in the Fig. 6 are visible numerous non-metallic inclusions having considerable size, which could constitute the reason initiating commencement of fatigue fracture.

Magnifications of cross-section of the fracture shown in the Fig. 7 confirmed that fatigue fracture was the root cause of damage of the ring. Brightening shown in the Figs. 7b and 7c is typical of the fatigue fracture. Simultaneously, brightening shown in the Fig. 7f and obtained at high magnification indicates that the fatigue fractures could be initiated by non-metallic inclusions in material of the ring.

Visual checks and tests of the ring show that the rings were manufactured by die shearing in press, and next were heat treated. Method of die shearing of the rings with use of a press-forming die effects adversely on their fatigue strength. Sharp edges and scratches left after the processing are probably the beginning of the fatigue fracture. Accurate visual check of mating surface of the ring with its seat enabled to state that the ring was supported at the ends and in its middle part, Fig. 8. Due to radial clearance, the ring was bended during its operation by inertia forces having variable value and direction. The highest bending moment occurred near the ends of ring, i.e. in points of its support. Especially high values of bending stress occurred in vicinity of oil holes, and just in these points where cracking of the ring occurred.

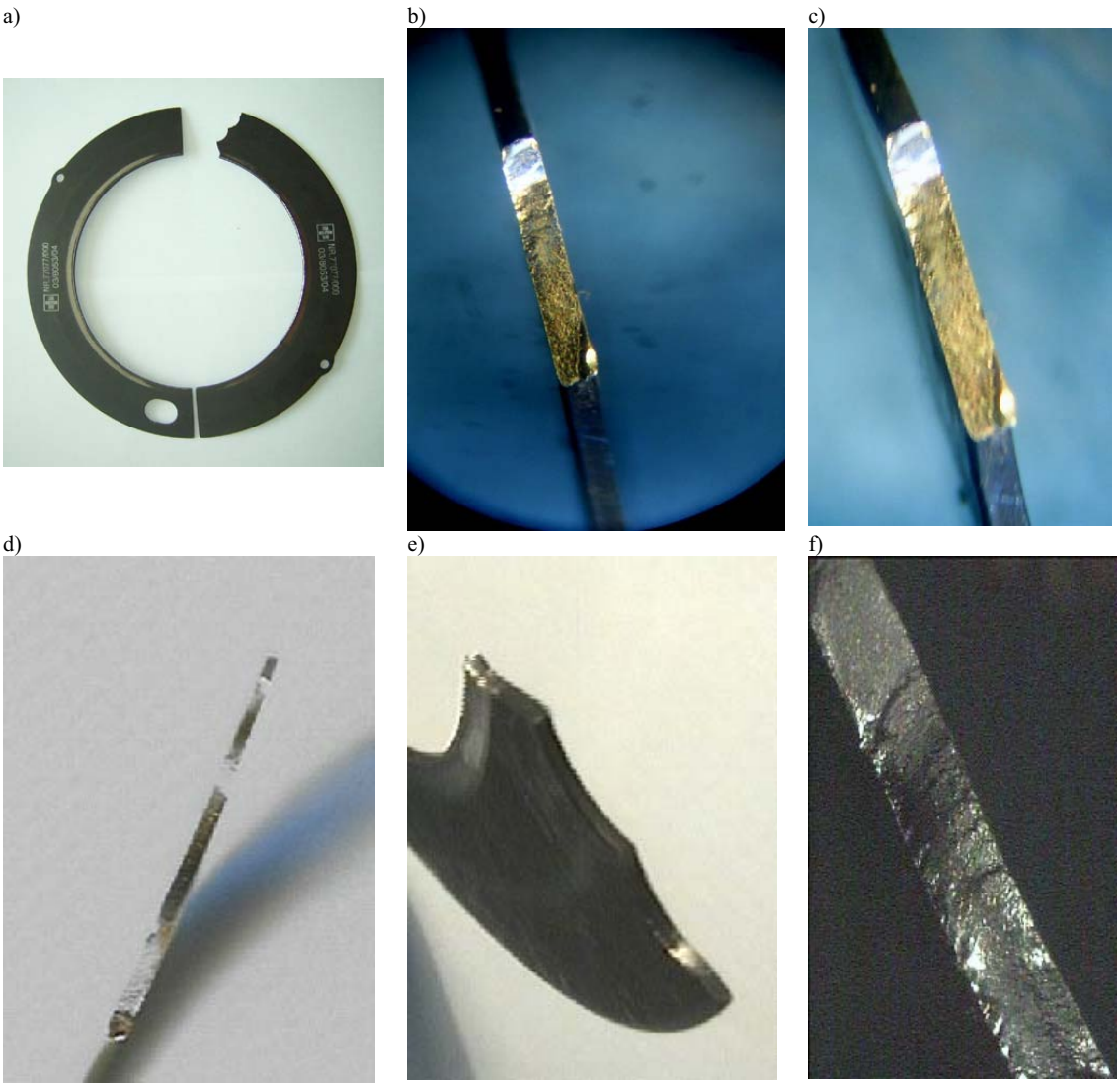

Fig. 7. Magnifications of cross-section of the ring's fracture

Disadvantageous contact of the ring with the seat results from its deformation arisen probably during the heat treatment. Seems that during the heat treatment, to prevent its deformation, the ring should be kept in a special swage.

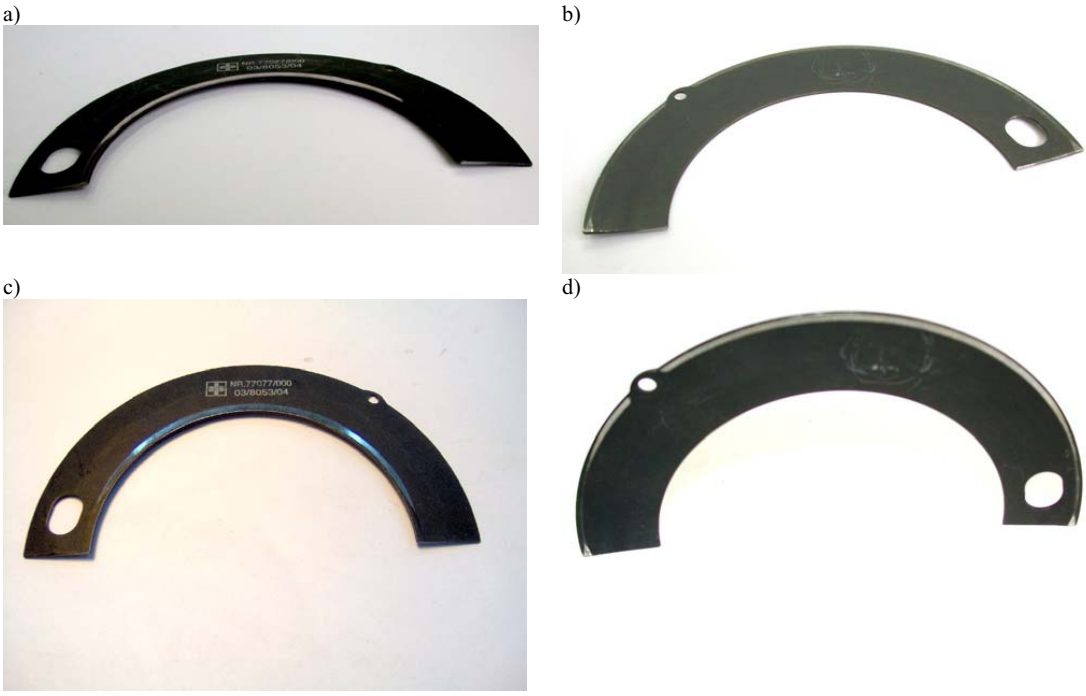

Fig. 8. View of the half-ring with visible contact surface (brightening)

4. **Summary**

On base of the performed tests one can formulate the following conclusions:

1. Cracking of the thrust ring in oil-type cooling of the piston head was the most probably root cause of damage of the 3516A engine.
2. Both material used to production of the ring, corresponding to spring steel grade, and its heat treatment were correctly selected to the task which needed to be performed by the ring.
3. It was confirmed, that fracture of the ring is of fatigue character and could be caused by:
   - mechanical working of the ring: punching from blanking die, what generates a scratches initiating fatigue fracture;
   - shape of the ring deformed during heat treatment, what effected in not correct contact of the ring with the seat, and in case of backlash, bending of the ring on its ends;
   - wrong radial clearance during assembly of the ring in the seat, what after heating up of the piston results in excessive clearance, favorable for displacement of the ring with respect to the piston.
4. It is recommended to perform a periodical check of conditions of the rings in all cylinders during engine operation. Such action will enable early detection of abnormalities and protection against failure of the engine. It is recommended to perform such check every 2000h of engine operation.
5. It is recommended to change production technology of the rings. In particular, it concerns punching operation and heat treatment which should be performed in a swage, disabling deformation of the ring's shape. Moreover, fit of the ring in the seat should be verified to

disable displacement of the ring during engine operation. Simultaneously it seems, however, that circumferential backlash of the half-rings should be slightly increased, what would have favorable impact on conditions of its operation.

References

[1] Borman G.L., Ragland K.W.: *Combustion Engineering.* McGraw-Hill, New York 1998.
[2] Friedemann Z.: *Gasmotoren.* Vogel Buchverlag Wurzburg, 2001.
[3] Hebda M., Janecki J.: *Tarcie, smarowanie i zużycie części maszyn.* WNT W-wa 1972.
[4] Jezierski J.: *Technologia tłokowych silników wysokoprężnych.* WNT W-wa 1999.
[5] Kozaczewski W.: *Konstrukcja grupy tłokowo-cylindrowej silników spalinowych.* WKiŁ W-wa 2004.
[6] Pflaum W., Mollenhauer K.: *Wärmeübergang in der Verbrennungskraftmaschine*. Verlag New York Wien, 1977.
[7] Stelmasiak Z.: *Analysis of Combustion Phenomena in Dual Fuel Engine Fed With Natural Gas (CNG).* Fisita 2002 World Automotive Congress, Paper No. F02 V030, 2002.
[8] Stone R.: *Introduction to Internal Combustion Engines.* 3rd Edition, Palgrave, London 1999.
[9] Stauba Fr.: Atlas mikrostruktur stali. Wydawnictwo Śląski, Katowice 1970.
[10] Wajand J.A., Wajand J.T.: *Tłokowe silniki spalinowe średnio- i szybkoobrotowe.* WNT W-wa 2005.
[11] Wajand J.A.: *Uszkodzenia trakcyjnych silników spalinowych.* WNT W-wa 1969.

Journal of POLISH CIMAC

Faculty of Ocean Engineering & Ship Technology
GDAŃSK UNIVERSITY OF TECHNOLOGY

THE NEW GENERATION OF ENGINE ROOM SIMULATORS WITH APPLICATION OF 3D VISUALIZATION

Leonard Tomczak

Gdynia Maritime University
Marine Propulsion Plant Department
Morska Street 81-87, 81-225 Gdynia, Poland

Abstract

Nowadays, tremendous changes are taking place in computing, information technology and simulation. Maritime education and training is not isolated from such changes and ought to benefit from these tendencies, specially taking into account the possible improvements for safety of ship operation. The present development of personal computers, modern processors and graphical cards allows for an easy application of 3D simulation techniques and for this reason manufacturers of engine room simulators begin to apply tri-dimensional graphical system's layout presentation.

Their aim is to provide machinery simulation as close as possible to reality. As a result, following the training, trainees are far better prepared to deal with real life operation of machinery.

The experiences in the application of virtual visualisation, the benefits and advantages of the use of engine room simulators in the educational process of engine room officers are equally presented in this paper. This paper describes an example of application of new generation of engine room simulators with 3D visualization, based on modern - computer controlled engine room with medium speed main engine, applied on a container ship.

The simulator described in the paper provides for a new approach to navigation through the different system's elements, allowing for an easy and quick access to basic engine room operation (valve opening/closing, setting position of switches, push-buttons etc.). This has been possible due the application of state-of-the art 3D visualisation with zoom techniques.

Keywords: 3D computer simulation, marine engine room simulators.

1 Introduction

Engine room simulators are used in maritime academies as a valuable asset for the educational process for more than 30 years [1]. The application of engine room simulators is also recommended by STCW 95 IMO Convention [2].

Marine engine simulators allow for operation of emergency situations that are not permissible under normal exploitation conditions due to safety limitations [3]. Simulator's software includes also assessment features that enable the objective review of the capacities acquired by trainees. During simulator exercise the instructor is able to apply various exercise set-ups (initial conditions) and scenarios that include different fault finding tasks.

It is worthwhile mentioning that marine engine room simulators used until now represented also some basic disadvantages. Namely, they include lots of simplifications, abbreviations and schematic presentation of machinery systems as a result of the fact that they are presented only in 2D visualization. Hence, the trainee with perfect knowledge of simulator operation can experience serious problems with real ship power plant operation, because the

graphical presentation and operating procedures of the simulator are distinct from the reality.

For this reason, manufacturers started to apply 3D graphical system's layout presentation in in new generation of engine room simulators, in order to provide a machinery configuration as close as possible to reality.

The main problem in creation of 3D simulators is to provide for proper navigation through the system's elements [4,5,6]. Engine room is a complex, multi level and complicated set of sub-systems, equipment and machinery and this requirement constitutes a new challenge for entities creating such kind of simulators.

It is also necessary to allow for an easy and quick access to basic engine room operation (valve opening/closing, setting position of switches, push-buttons etc.). It is possible to achieve this feature by applying zoom techniques for selected elements of the system. Users of 3D simulators should also be able to observe the system's elements from pre-select specific parts of the engine room.

Based on the author's experiences with the application of different types of simulators, a better solution consists in navigation by mouse cursor and zooming facilities.

The application of new 3D simulation techniques in marine engineering education shall be analysed on the examples of full mission, hardware type engine room simulator with medium speed main engine type MED3DH.

A new technique of navigation through the system's elements has been applied in this virtual reality simulator, providing for a solution of the main problem in creation of 3D visualisation. The latest development includes also a combination of 3D and 2D diagram presentation, which enables to follow how a certain device really functions and provides a complete picture of its structure. The presented solutions have improved considerably the level of simulator fidelity in relation to real machinery. In consequence, it was possible to eliminate the disadvantages of the engine room simulator with typical 2D presentation consisting in a schematic and simplified presentation of machinery systems.

The application of virtual simulation in teaching the operation of complex marine machinery leads to a better understanding of the functioning principles of both the equipment and the systems in comparison with traditional educational methods. As a result, trainees are far better prepared to deal with real life operation of machinery, thus increasing in a considerable manner the standards of safety of ship operation. It has been observed during many years of application of engine room simulators in Gdynia Maritime University that trainees have a very different approach to exercises conducted with hardware type of simulator in comparison with training conducted only with software. The trainee's attitude to exercises conducted only with software is very similar to the approach adopted to computer games and the trainee often does not consider these as serious experience that reflects reality. If the exercise is conducted with the application of hardware, the trainees have the impression to conduct real life operations and in consequence, their aptitude to perform such operations in reality increases. On the other hand, software, due to its features enables the trainee to repeat in an unlimited number of times the required operations, thus to achieve the necessary preparedness level.

The engine room simulator based on the medium speed engine room simulator is one of the first simulators which uses hardware and software type of consoles combined with 3D visualization.

This simulator specially enhances the operational procedures related to emergency situations, like electrical black-down, emergency manual operation of the main engine with propulsion system as well as auxiliary machinery in case of remote control failure. As it has been said before, these procedures may not be trained in real life conditions due to safety constraints. From didactic point of view the best solution is to combine hardware version of engine room simulator with 3D visualization. Such combination improves in a considerable

manner the safe operation of marine engine room, as the crew members have previously been trained in relation to various fault scenarios.

2 MED3H Medium speed engine room simulator's description

The basic role of this simulator is the familiarization with different operational modes.

This simulator is designated for training students of maritime academies as well as for different types of marine vocational training centres. The simulator has universal features and may be used both for training merchant and navy fleet crew.

The MED3DH is a full mission, hardware type Engine Simulator and has been based on very modern solutions, being presently used in medium-sized, computer controlled, engine rooms (one four-stroke type main engines with reduction gear and controllable pitch propeller). This kind of computer controlled engine room is a typical configuration applied on modern container ships. The main purpose of the MED3DH simulator is the practical preparation of the trainee for engine room operation, and more particularly:

- familiarization with the basic engine room installation (compressed air system, fresh and sea water cooling system, lubricating, fuel oil system etc.), specially taking into account training on the base of modern, computer controlled engine room;
- acknowledgment with main engine and auxiliary equipment exploitation procedures;
- propulsion system manoeuvring (main engine – reduction gear – CPP);

The simulator has been developed in compliance with:

- STCW Code: Section A-1/12 and Section B-1/12.
- ISM Code: Section 6 and Section 8.

The MED3DH simulator has been equipped with a hardware consoles and panels that enable main engines, gear, CPP, auxiliary machinery and electric system's operation and control.

MED3DH simulator consists of three main parts (Fig. 1):

- Engine Control Room ECR with main engine control console and main electric switchboard,
- Engine Room with two PC projectors and control console for 3D visualization combined with diagram presentation,
- Instructor's Room.

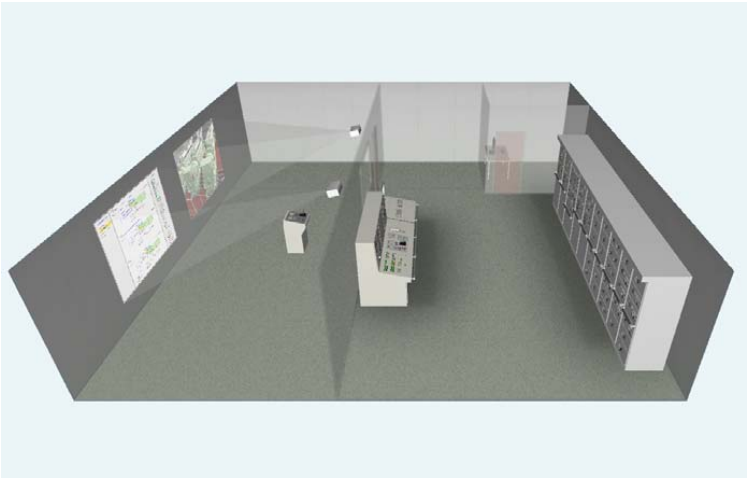

Fig. 1 General view of Full Mission Engine Room Simulator – MED3DH

The MED3DH simulator room's panels and consoles have been presented on Fig. 2 and 3.

Fig. 2 MED3DH Engine Room Simulator – Switchboard panels

Fig. 3 MED3DH Engine Room Simulator - Main engine's control consoles

The basic operation with auxiliary sub-systems, identically as in real modern ship, is performed by "mouse clicking" operation on the PC monitors screen (Fig. 3). On the PC's screen diagrams related to specific installation like fuel oil, compressed air system, cooling

system, lubricating system, steam system, etc. are presented. For security reasons and in the same way that in real engine room, the Engine Control Room is equipped with two identical PCs with monitors. In case of one PC failure, the second one takes over the systems' control automatically. On the monitor screen by "mouse clicking" it this possible to start/stop the pumps, compressors and open/close the valves which are remote controlled. On fig. 4 an example of compressed air diagram for remote control from PC screen is shown.

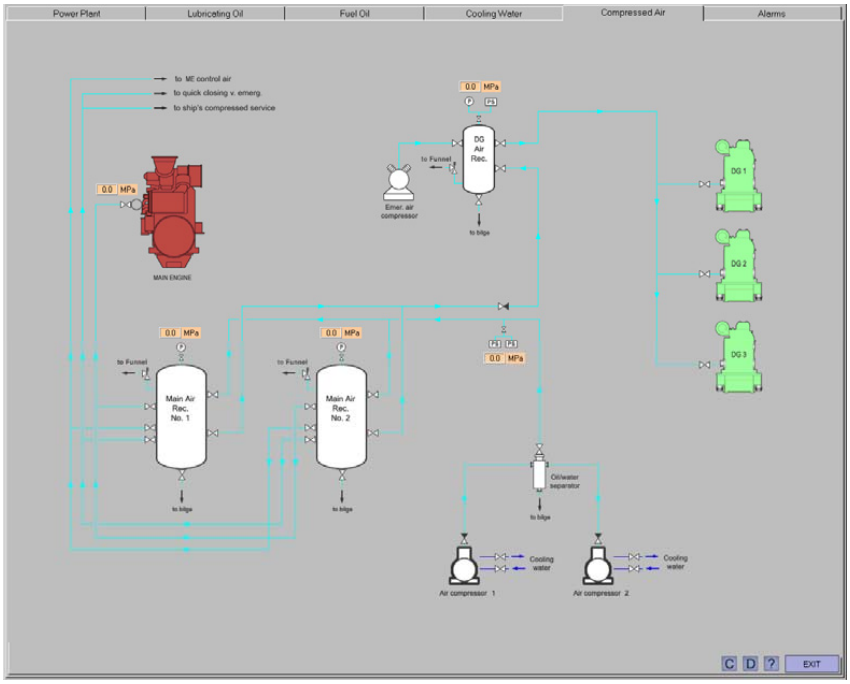

Fig. 4 MED3DH Engine Room Simulator - Example of compressed air diagram (remote control from PC screen)

All operating procedures which are necessary to be performed in engine rooms (outside of Engine Control Room) are effectuated is a separate room equipped with two projector screens

One screen presents engine room elements is 3D visualization and another one presents in form of a diagram related to specific and selected compartments or system of engine rooms, for example auxiliary generators' room, emergency generator's room, compressed system room etc. On fig. 5 two screens visualization of main engine is presented. Selection of engine room's elements that are important from the point of view of exploitation is performed by zoom techniques.

The software allows for the simulation of opening/closing of basic valves and auxiliary equipment operation in engine room. The software also generates the main engine room's sound.

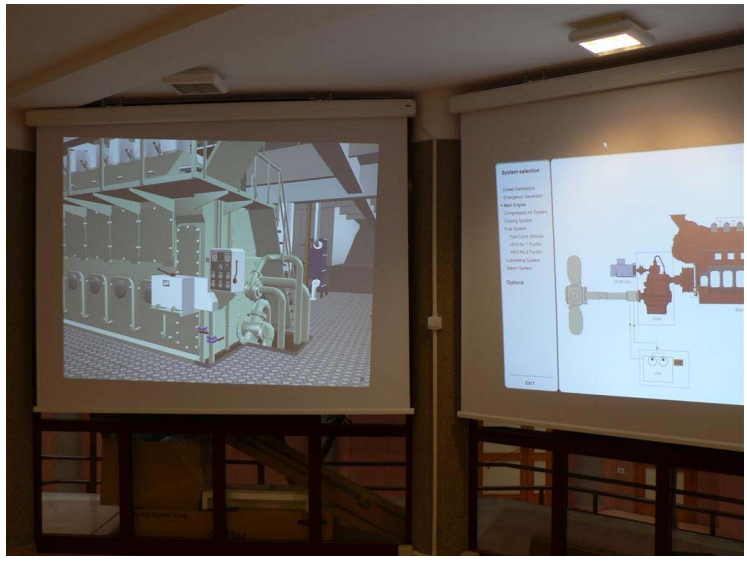

Fig. 5 MED3DH Engine Room Simulator - Two screen presentation in engine room

The MED3DH virtual reality simulator provides for a new approach to navigation through the different system's elements, allowing for an easy and quick access to basic engine room operation (valve opening/closing, setting position of switches, push-buttons etc.). This has been possible due the application of state-of-the art 3D visualisation with zoom techniques. The latest development includes also a combination of 3D and 2D diagram presentation, which enables to follow how a certain device really functions and gives a complete picture of its structure. The presented solutions have improved considerably the level of simulator fidelity in relation to real machinery. In consequence, it was possible to eliminate the disadvantages of the engine room simulator with typical 2D presentation consisting in a schematic and simplified presentation of machinery systems.

On fig. 6 – 9 selected part of engine room machinery with 3D visualization are shown.

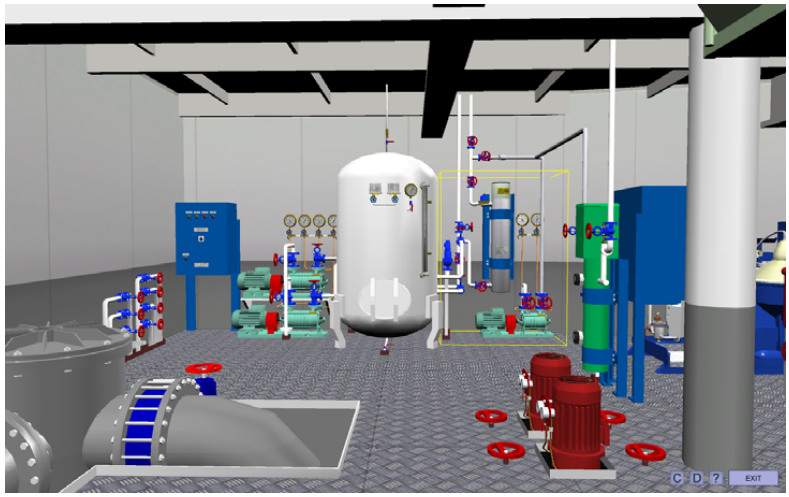

Fig. 6 MED3DH Engine Room Simulator - Hydrophore installation

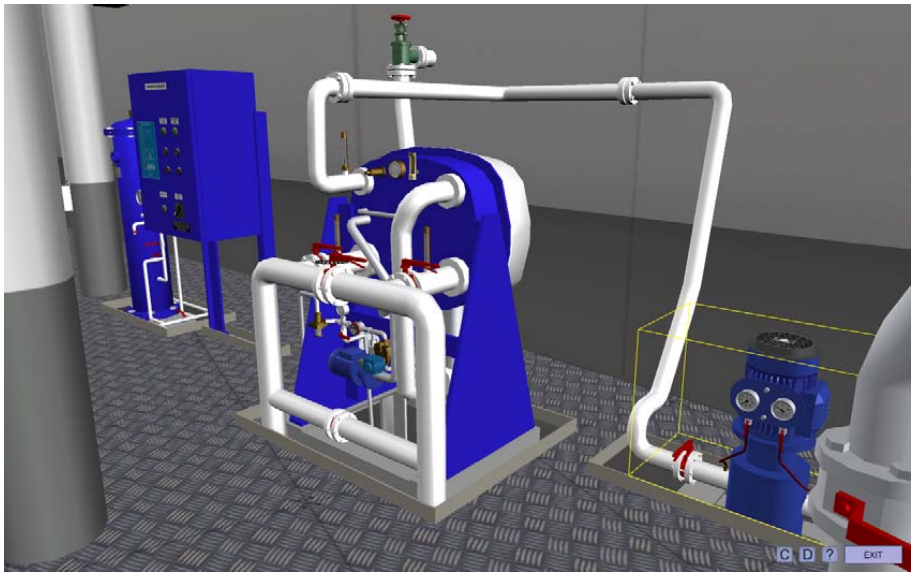

Fig. 7 MED3DH Engine Room Simulator – Fresh water generator installation

Fig. 8 MED3DH Engine Room Simulator – fuel separator module

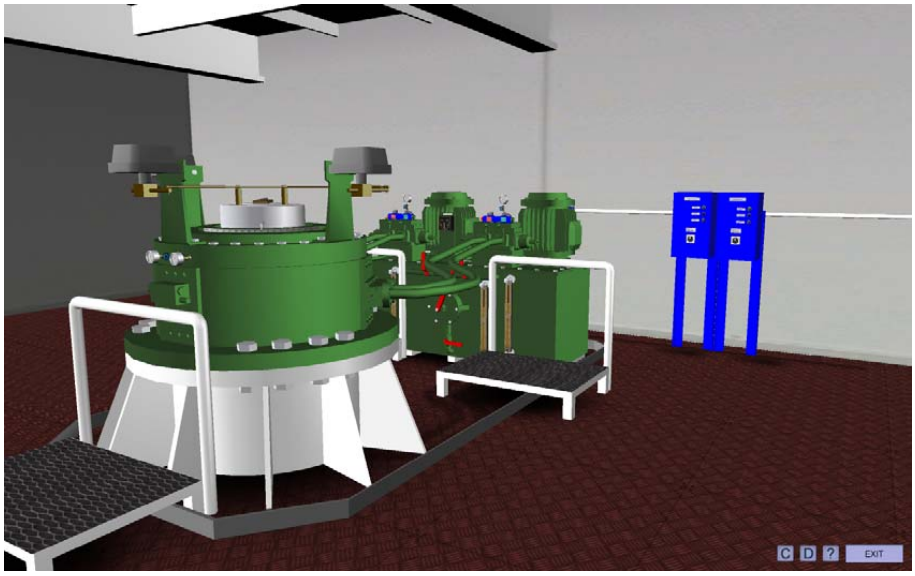

Fig. 9 MED3DH Engine Room Simulator – Rotary vane steering gear installation

3 Conclusion

As it has been mentioned above, the new generation of engine room simulator combining hardware with 3D visualization improves in a considerable manner the safety of operation of marine engines as it enables the trainee to achieve high level of emergency preparedness. The didactic purposes are achieved through training involving various fault scenarios and the simulator also enables proper navigation through its elements. The new concepts of view selection, zooming features of elements and operation by cursor and mouse clicking, as applied in the simulator that has been described in this paper, appears to be very effective and easily adaptable by trainees in practice.

Due to the specificity of operating marine equipment in real life conditions, the didactic goals in marine education are directly linked with achieving preparedness for emergency situations. Such preparedness may only be achieved if the trainee is familiar with both the equipment and its operating modes, including emergency situations. If the trainee has been trained only on simulators that are far from real machinery environment, his state of preparadness for emergencies on board is not satisfactory and safety is put at risk.

3D visualisation reduces the gap between operating marine machinery in simulation conditions and in real life. In the near future, this type of 3D solutions should be applied more and more often in engine room simulators design. The presented simulators are related to marine machinery, but the concept of composition and navigation through the system's elements can be easily applied for the purposes of any type of technical equipment.

To summarize, the application of a new generation of engine room simulators with 3D visualization improves the safety of operation of marine equipment on board as it reduces the level of human error in the operation and maintenance of these devices.

References

[1] R.Cwilewicz, L.Tomczak, Z.J. Pudlowski, *Effective application of engine room simulators in marine engineering education*, *Proc. 3rd Global Conference on Engineering Education,* Glasgow, Scotland, United Kingdom, 2002, pp. 316-318.

[2] *STCW - Standards of Training, Certification and Watchkeeping for Seafarers 78/95 Convention International Maritime Organization*, London, 1996

[3] R. Cwilewicz, L. Tomczak, *The role of computer simulation programs for marine engineers in hazard prevention by reducing the risk of human error in the operation of marine machinery*, *Proc. 4th International Conference on Computer Simulation in Risk Analysis and Hazard Mitigation* - Risk Analysis IV, 2004, pp. 245-249

[4] L. Tomczak, *Practical aspects of 3D graphical applications in marine Engineering Education*, *Global Journal of Engineering Education, 9(2)*, 2005, pp.137-142.

[5] L. Tomczak, *Application of 3D visualization in marine engine room simulators*, *Proc. 7th International Conference on Engine Room Simulators (ICERS7) ,* Portoroz, Slovenia, 2005, pp. 232-240.

[6] L. Tomczak, *The latest developments of 3D visualization in marine engine room simulators*, *Proc. 8th International Conference on Engine Room Simulators (ICERS8), Manila, Philippines, 2007, pp40-42.*

Journal of POLISH CIMAC
Faculty of Ocean Engineering & Ship Technology
GDAŃSK UNIVERSITY OF TECHNOLOGY

CHANGES OF TOXIC COMPOUNS OF EXHAUSTES DURING THE RUNNING-IN OF ENGINE

Ryszard Zadrąg

The Polish Naval Academy
Ul. Śmidowicza 69, 81-103 Gdynia, Poland
Tel.: +48 58 626 23 82

Abstract

Reliability and durability are the most important features of the combustion engines. The significant influence on these features has construction, production technology, and proper selection of materials. Regardless of precise producing the cooperative elements of the engine should undergo the running-in process. This process has great influence on durability of elements and normal time of exploitation. If it is properly selected and conducted, it will extend the time of future engine operation by decreasing initial value of wear of its friction pairs and giving proper values to the outer layers.

During the running-in process, beside giving proper shape to the outer layers of individual elements of engine, parameters of the toxic compounds emission changes. The paper presents results of researches, which were aimed at describing the values of toxic compounds emission changes during the running-in process of engine.

1. Introduction

The main factor, which determinate reliability and durability of the engines, beside the common applied modern technologies of production using the most recent materials, still remains the running-in process, understood as a process of conscious forming the outer layers of elements by the technological transformation of outer layers (which appeared at the stage of production) into exploitative outer layer. It occurs under influence of forces such as: pressure, temperature, engine rotational speed at presence of the active compounds of lubricating factor.

As it was mentioned, the period of normal exploitation is strictly determined by the conditions and the course of running-in process at the beginning of associated friction pair. When this process will be correctly conducted, surfaces will reciprocally form and also changes of the outer layer properties occur, in comparison to the initial properties, given during obtaining the elements. These changes will result in the increase of resistance of associated friction pair on wear.

Along with this change of properties of outer layers of running-in engine elements, also broad understood working parameters of the combustion engine will change, including parameters describing the combustion process, among them parameters of the toxic compounds emission.

The information on the subject of exhausts toxicity changes during the running-in process in the available professional literature are poor, yet using obvious relation between structure parameters and directly related to them parameters of the combustion process could be make an attempt of conclusion the correctness of running-in process. It seems that suggested solution could be used with success to observe and conclude the correctness of running-in process course of engine in the place, where it is installed, which means the shipping power

station, but very often service do not have specialist laboratory devices to register the parameters of running-in process.

2. The running-in process of marine combustion engine

There are great discrepancies in the running-in process worked out by producers of engines. Often these programs have been worked out on the basis of existing, verified in practice programs of the running-in process for other engines. Additionally, significant standards of similarity of the engines have not been taken under consideration, what is a condition of such action. Therefore, with high probability can be concluded that in many cases running-in process was not correctly performed.

Running-in is performed depending on the engine types, its repair and test place. Running-in program should assure realization of the typical engine load characteristic, in case of the marine engine of main propulsion it is a propeller characteristic. The optimal running-in program and related technology should be such worked out to obtain the lowest values of wear required durability of the elements – properties of outer layers – at the minimal time of the engine operation.

General conditions of optimal running-in, which enables obtaining best condition of outer layer, amounts to such engine load during the running-in process, where unit pressure on these surfaces will approach to the plasticity limit of material, but it will not be exceeded and when slide speed will assure good condition of forming lubricating wedge and its upper limit will not evoke the increase of temperature, which violate durability of the protective layers, absorbed on the friction surfaces [1,16].

To assess the quality of the running-in are applied factors of different type such as: temperature of associated elements, friction coefficient, mechanical vibrations, tightness of the cylinders, noise etc. The most convenient quality factor of the running-in process of engine is its internal resistance, which change during the running-in process. The thing is about resistance, which includes: friction resistance, hydraulic resistance, load compression resistance and spring resistance. As a result of the running-in process the friction resistance decreases while load compression resistance increases as an effect of the increase of tightness of the piston rings and cylinder set. Changes and then stabilization of the friction resistance could be used as a quality index. Friction coefficient intensively changes at the beginning of the running-in process till its stabilization, which in the further stage of running-in remains invariable. These changes depend not only on speed applied at the time of running-in, but unit and lubrication pressure.

What concerns the temperature, the increase of crankshaft rotational speed and also load are caused by the stroke temperature increase of the elements. When running-in conditions change, every time the change of temperature occurs stabilizes after some time till the next change of engine operating conditions.

Among others running-in quality indexes could be numbered: effective power and torque, unit fuel consumption, tightness of the cylinders, which is assessed by the measurement of compression pressure, vibrations, which are measured as acoustic pressure.

As it was mentioned before, the running-in of marine engine occurs according to the propeller characteristic and it could be performed during the tests in engine test stand or on the marine ship. In all tests the control parameters of the running-in process have been engine rotational speed and power reached by the engine. Because of the fact, that the running-in process occurs in terms of the resilient deformations of mircoirregular protrusions, the initial engine load should be such selected to fulfill the conditions.

In practice, the first stage of load responds to the engine operating at the idling run [1]. Then the optimal conditions for unit pressure are not fulfilled. If engine can not work at the

idling run, the running-in process begins at the possibly lowest load, when engine operation is the most stable. Then this condition would be the first stage of the running-in. The second stage is realized at the load, which is a result of the minimal performance according to the propeller characteristic. Course of the running-in occurs at the load increase index within 1,2 – 1,3

Above is presented the methodology of working out the running-in program according to [1,2]:

1. Initial data:
   N_z –nominated engine power;
   n_z – nominated engine rotational speed;
   n_{min} – the lowest engine rotational speed, when the loaded engine works stable;
   n_l – engine rotational speed at idling run;
   $\varphi = 1,3$ – power increase coefficient at the consecutive stages of load.

2. Initial, lowest running-in power of the test engine, which the lowest running-in power is equal to the minimal engine rotational speed, calculated from the general propeller characteristic of power.

$$N_1^* = 0,634 \cdot (n_{\min}^*)^3 + 0,0213 + 0,343 \cdot (n_{\min}^*)^4 \tag{1}$$

3. Number of running-in stages at load

$$k = \frac{\ln(\frac{N_2^*}{N_1^*} \cdot \varphi)}{\ln \varphi} \tag{2}$$

4. Number of running-in stages, considering the engine operation without load (at the laid-back run)

$$k' = k + 1 \tag{3}$$

5. Conditions of the engine load at the first stage of running-in

$$N^* = 0 \tag{4}$$

$$n^* = n_1^* \tag{5}$$

$$M_o^* = 0 \tag{6}$$

6. Values of power, engine rotational speed and torque at consecutive stages of running-in

$$N_i^* = N_1^* \cdot \varphi^{i-1}\ , \tag{7}$$

$$n_i^* = [1020\sqrt[3]{N_i^*} - 19,5 \cdot (N_i^*)^3 - 0,013 \cdot (N_i^*)^{-3}] \cdot 10^{-3}, \tag{8}$$

$$M_{0i}^{*} = \frac{N_i^{*}}{n_i^{*}}, \qquad \text{i=1,2,3…,k.} \tag{9}$$

7. General running-in time, depending on the value of nominated engine rotational speed n_n

$$\Sigma t = 200(1366 \cdot \frac{1}{n^{n}} + 1{,}177 - 0{,}0655 \cdot \sqrt[3]{n_n}) \tag{10}$$

8. Running-in time at particular stages of load

$$t = \frac{\Sigma t}{k+1} \tag{11}$$

The running-in process of cooperating surfaces of engine elements is always accompanied by the friction phenomenon and wear, which is evoked by friction. The influence on the intensity of wear of friction pair in the time of normal exploitation have properties of outer layer, which are given to the surfaces, cooperating in the running-in process. So running-in process should be proceeded in conditions possibly the closest to the real exploitation conditions. Applied programs in many cases do not take under consideration these requirements, in particular the manners of realization loads. If it concerns the marine engines of main propulsion, running-in should be bared on the progressively increase of loads according to the propeller characteristic.

The running-in process should be a continual process, which means if halt time of engine does not exceed the time, necessary to conduct the survey, remove the hitches and improve the regulation condition of working continual is not fulfilled, running-in should be conducted again. The surveys should be conducted again as well. The first should be conducted after the realization I stage and next after the realization 1/3 of working time on particular stages of the running-in process. After the end of running-in process the final survey is performed.

Oil filters should be checked and cleaned, also temperature of the crankshaft-bearing and the smooth surfaces of cylinder sleeve should be checked after every survey. During the surveys the location of friction surfaces must not be violated.

Engine load during the transitions from one stage of the running-in to another and after the working break caused by survey should be fluent. Transitions time to the other stages should be determined by the thermal condition of the engine. It is recommended, that the time of increasing load was 1 min for the engine of main propulsion and 0,5 min for the engines of current generating and auxiliary set [1].

The control of the running-in process lies in the analysis of the measured parameters, which characterize engine operation and the comparison of its values, given by the producer of engine.

Running-in is assumed as correct if:

- the running-in process is fluently realized
- engine reaches nominated value of effective power at nominated values of fuel setting and engine rotational speed

3. Engine tests

At one stage of the research project 4T12D 05 529 were performed tests, which were aimed to carry out analysis of process, which occurs in the piston-ring-cylinder set of combustion engine ZS during the running-in process and also assessment of the influence of

P-R-C set tightness on energy parameters of engine and toxic compounds emission in exhausts [5,6].

Tests have been conducted in the laboratory stand of 1SB test engine in the Exploitation Laboratory of Shipping Power Stations in the Naval Academy of Gdynia.

The running-in program of 1SB engine has been worked out according to the above presented methodology.

Comparison of particular parameters of the plan is included in table 1 and graphic is presented in Fig. 1.

Table 1. Table of parameters of the running-in program on the test engine

The running-in stage	Efficient power [kW]	Engine rotatonal speed [rpm]	Torque [kN·m]	Running-in time at the particular stage [min]	General running-in time [min]
I	3,489	796	41	46	46
II	4,535	869	49	46	92
III	5,896	948	59	46	138
IV	7,665	1032	71	46	184
V	9,964	1120	85	46	230

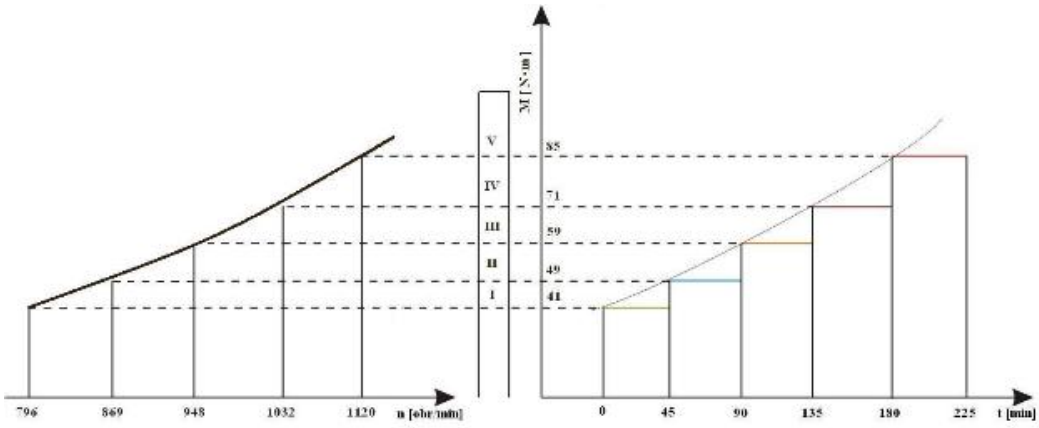

Fig.1. Graphic of the measured running-in process according to [2]

To interchangeably describe the parameters of running-in process, engine has been loaded by torque. It was possible thanks to/because of applying the electrowhirl break AMX type of Automex Company, which is characterized by great precision in the maintenance of given load. Additionally, according to the program, after establishing load and engine rotational speed the fuel stick was blocked to establish the dose of fuel. Applied engine load system has allowed to interchangeably determining the end of running-in at particular stages of approved running-in program. As is such combination should be expected, the engine rotational speed changes in case of mechanic efficiency improvement.

During the running-in process on the measure stand were registered and then analyzed above others such indexes/factors of engine as: engine rotational speed n [rpm], torque M_o [N·m], unit fuel consumption g_e [g/kW·h], exhausts temperature in the exhaust pipe T_{g2} [^oC], mean indicated pressure p_i [MPa], mean effective pressure p_e [MPa].

As it is given in the literature, first and foremost influence on the toxic compounds concentration has the course of combustion process. Significant influence on this process have unstable conditions and accompanying transitional process, which among others thing/inter alia brings into power changes i.e. change of coefficient λ. It results in throwing the cylinder off the thermodynamic equilibrium. Return to the relative equilibrium takes relatively long time (in case of CO it is the longest among/of all analyzed compounds, but its character is the same for every ZT).

The return process of cylinder to the thermodynamic equilibrium could be divided into 2 periods. The first period is relatively short, when after bringing into new load the changes of the CO concentration are greatest and the second period, when changes are relatively stabilized and they asymptotically decrease. For the reason, that participation of the first period in the time of whole process is little and in the considered case we have to deal with comparatively long period of registration the stage of running-in (i.e. 45 min) it was decided to pass over/omit this stage in the subsequent analysis. According to Fig. 2 registered course of CO changes were divided into 5 periods, which correspond to the consecutive stages of running-in.

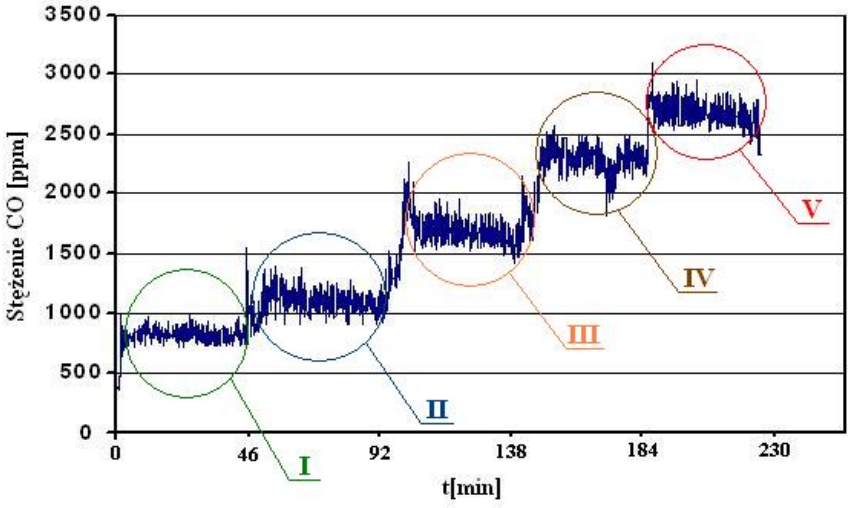

Fig. 2. Change of the CO concentration in exhausts during the running-in process, where: I-V – stages of the running-in process

As it could be noticed, along with the load increase, CO concentration increases. It is connected with the decreasing air-exceed coefficient λ. Above course is typical for the unsupercharged engine. Difference of the Co concentration between I and II stages is 300 ppm, between II and III – 50 ppm, between III and IV – 700 ppm. However, in case of transition from IV to V, this difference is 400 ppm. Probably it is connected with the

insignificant change of air-exceed coefficient λ (in comparison to previous stages). Similar character has the course of change of NO_x concentration

Somewhat differently forms the course of NO_x concentration change. Analyzing this course in the context of λ change it is noticeable, that the NO_x concentration increases, despite the decrease of air-exceed coefficient λ. increase at the consecutive stages of running-in is admittedly low, but significant. It occurs, probably because of the fact, that despite the smaller amount of oxygen, which is necessary to form the NO_x, the change of combustion temperature occurs, which is the second factor responsible for the NO_x appearance [22,23]. Time of nitrogen oxides' stabilization after introducing the unstable condition, caused by the changeable extend of running-in process, is definitely shorter than in case of CO and HC. As in case of CO, which change of running-in extend ex. from 2 to 3 is 15 min, so the same change of load causes shorten reaction for NO_x, which is about 7 min.

In order to generalize the changes of particular toxic compounds' concentration observed during the process of running-in, the initial and final concentrations of different stages were compared. The time of process was also registered, considering the moment of the engine's rotation speed stabilisation as the end of running-in (on the given stage). The results of the analysis are presented with relative values (Fig. 3 and 4).

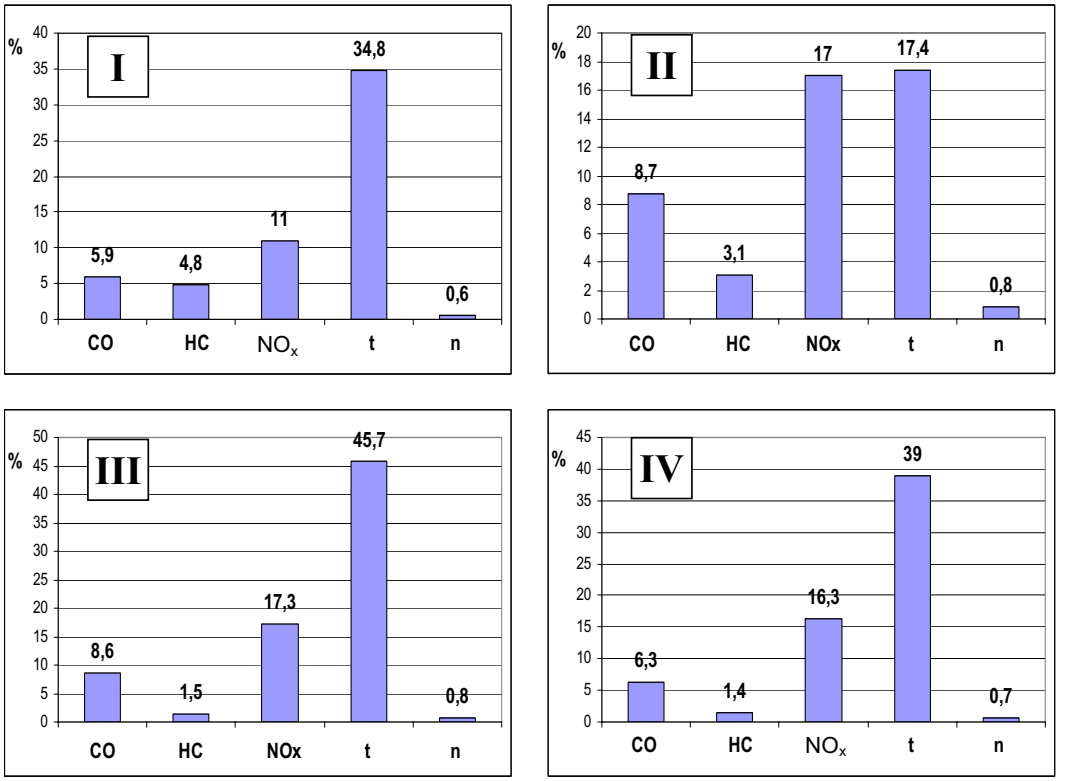

Fig. 3. Changes of the parameters of running-in process, where: I, II,..., IV – extend of the running-in process, t – time of the running-in process realization, n – engine rotational speed

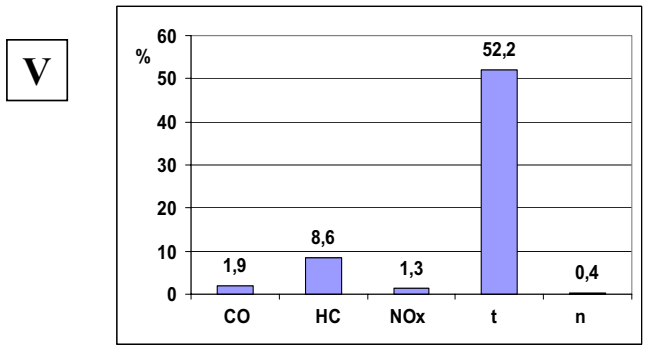

Fig. 4. Changes of the parameters of running-in process, where: V – extend of the running-in process, t – time of the running-in process realization, n – engine rotational speed

4. Conclusions

Presented above material does not fully extend considered subject, this presented experiment has confirmed obvious relation between the running-in process and processes, which occur in the engine cylinder, despite the values of parameters of structure of piston-ring-cylinder set, used in the experiment, were not significant.

The greatest changes of exhausts concentration indexes during the running-in process can be remarked for the HC and, in lower extend, for CO. Changes of index values in the HC and CO concentration are the more significant at comparison their values to changes of the basic index, which described the correctness of the running-in process course, namely engine rotational speed. Changes of this index is an order of 0,4 – 0,8% at11 – 17% of change of the HC concentration.

Considering the fact that most of the running-in programs have general character (do not consider the specificity of individual engines, as well as the differences, which come out of the tolerance of particular copies assembly).It is apparently in Fig. 3 and 4, where only at the second running-in stage time decreased for 8 min, which results in 17,4% economy of time at II running-in stage. In other cases economies are definitely greater and adequately are: I – 34,8%, III – 45,7%, IV – 39% i V – 52,2%. In this situation, when we have to deal with appreciable costs of fuel, such economy is not indifferent

Literature:

[1] Piaseczny L., *Technologia naprawy okrętowych silników spalinowych*. Gdańsk 1992.
[2] Bergier T., *Programowanie optymalnego procesu docierania średniobieżnych okrętowych silników o zapłonie samoczynnym.* Rozprawa doktorska Łódź 1980.
[3] Bielaczek P., Merkisz J., Pielucha J., *Stan cieplny silnika spalinowego a emisja związków szkodliwych.* Wydawnictwo Politechniki Poznańskiej 2001.
[4] Merkisz J., *Ekologiczne problemy silników spalinowych*. Wydawnictwo Politechniki Poznańskiej. Poznań 1999.
[5] Piaseczny L.,Zadrąg R., *Programowanie obciążeń w czasie badań silników*. Materiały konferencyjne KONSSPAL'98. Wrocław 1998.
[6] Piaseczny L., Zadrąg R., *Badania symulacyjne zmian emisji związków toksycznych silników spalinowych spowodowanych dławieniem spalin*. PAN, Teka Komisji Naukowo-Problemowej Motoryzacji. Kraków 2001.

Journal of POLISH CIMAC
Faculty of Ocean Engineering & Ship Technology
GDAŃSK UNIVERSITY OF TECHNOLOGY

MULTIPLE INVESTIGATIONS OF FUME EMISSIONS OF ENGINES WITH AUTOMATIC IGNITION

Bogdan Żółtowski

University of Technology and Life Science, BYDGOSZCZ
bogzol@utp.edu.pl

Abstract

The results of the investigations of the post and exploitation emissions of the harmful components of the fumes of diesel engines were introduced in the work. Obtained results were subjected to a statistical study according to new computer procedures. Qualitative and quantitative reports were established for the level and kind of emission in reference to the changes of the state of studied engines.

Keywords: combustion engines, toxic fume components, environmental protection

1. Introduction

The assumption for researches of this work was the performance of the analysis of the influence of starting phase and engine warming on the harmful emission at these states of engine's work, especially concerning climate conditions in Poland. In the range of researches, the analysis of the emission of harmful compounds was performed during the first few minutes after the start-up of a cold and warmed up engine in the neutral gear at different temperatures of the environment. The contribution of harmful components of fumes of diesel engines into total atmosphere pollution is as follows: there are mostly solid particles (PM) and nitro oxides (NOx) in fumes, whilst in smaller amounts there is carbon oxide (CO) and not burned hydrocarbons (HC).

The results of realized laboratory tests on a chosen group of diesel engines allow determine practically and cognitively important premises in the field of toxic effects of diesel engines on the environment.

2. Research objects

The researches of his work, in the field of recognizing toxic components generated by diesel engines for different modeled technical states and changeable external temperature, were performed on a stationary engine S-359 in the laboratory UTP (fig.1).

Fig. 1 General view of test stations

The object of research in this work was S-359 engine with self-acting fusion whose basic technical data is presented in Tab.1. It is an engine of a wide practical application, and characterized by small unitary fuel use, good dynamic characteristics and small damageability.

Tab.1. Basic technical data of the engine S- 359 [105]

Cylinder formation	row, vertical
Number of cylinders	6
Cylinder diameter	110 mm
Piston stroke	120 mm
Swept capacity	6,842 dm^3
Compression degree	17
Order of cylinder work	1-5-3-6-2-4
Maximum Power	110 KW with 2800 min^{-1}
Maximum turning moment	438Nm with 1800-2100min^{-1}
Minimum unitary fuel use	224 g/kWh
Statistical angle of pumping beginning	$18,5^0$OWK before GMP
Injection system	Direct
Injection pump	P-76G10
Injection pressure	22MPa

The engine is a running unit for trucks: Star 200 – street, Star 266 – cross-country, produced in Factory on Starachowice (at present: Star Trucks Sp.z o.o). These cars are widely used in the national industry, as well as military service.

The tested combustion engines belong to the group of exploitation objects, used in difficult training conditions of military service. Large and changeable loads of engines implied by inexperienced drivers diversified their technical state, which for the researches of his work posed a challenge in the range of preparing the experiment, its proper realization, and careful concluding and statistical work.

3. Testing stations

Stationary tests were performed in a laboratory of combustion engines located inside laboratory rooms, in order to obtain natural environment conditions. It mattered considering the acquisition of different temperatures, in which the engine S-359 was thermally stabilized, and considering the temperature of the air used for running the engine.

Before proceeding with the tests, the following were checked and regulated:

a. technical state of the engine,
b. injection pump at the probing station type PW-8, predestined for testing fuel equipment of high-pressure engines with regard to dosage, performing, according to BN-88/1301-16 velocity characteristics of fuel injection,
c. injectors used for the tests were checked and regulated on an injector probe type PRW-3, performing the evaluation of pressure of the injector's opening, tightness and trickling of the sprayer, and the correctness of fuel spraying,
d. suction and exhaustion valves – according to the manufacturer's suggestions,
e. during the test, the following were registered:
   - multi component composition of exhausted fumes of the engine,
   - smoking of fumes with a smoke-meter AVL.

Fume tests with respect to the quantity of toxic substances were performer with the use of a multi-component analyzer of fumes LANCOM, whose general image is presented on the Fig.2.

The analyzer LANCOM enables the measurements of: CO, CH, NO_x, SO_2, fumes temperature and environment temperature.

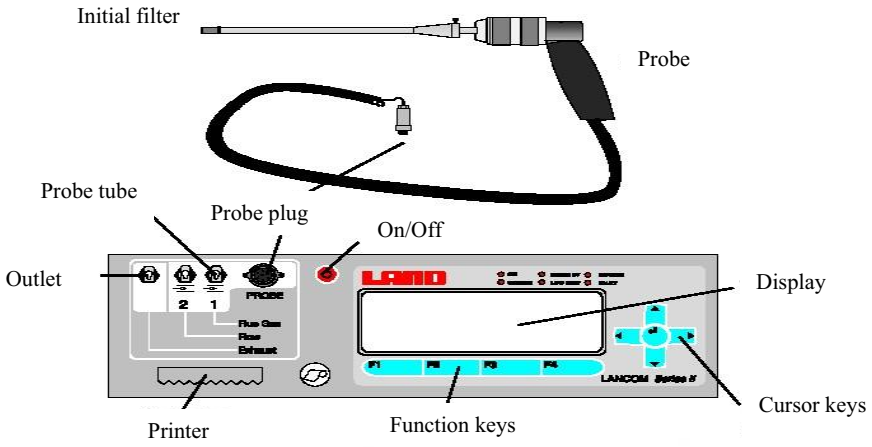

Fig.2. General image of fume analyzer LANCOM with fume acquisition probe

The measurements of smoking degree of fumes of diesel engines were performer with the use of a smoke-meter AVL-4000 for the need of further statistical processing the measured values were saved in a sheet (Excel).

4. Testing conditions

In order to obtain a wide range of temperatures of engine start-up, the tests were being performed throughout a dozen of months, taking into account summer and winter months. The engine, before each test, was subjected to thermal stabilization, thanks to which all elements of the engine and exploitation liquids and exhaust system had the same temperature equal to the environment temperature. Environment temperature and motor oil temperature were measured directly prior to each measurement, and if the temperature differences did not exceed 1°C, the measurement began. Also performed were tests in the conditions of a hot start-up. i.e. during a start-up of an engine beforehand warmed up to a normal temperature (oil temp. 80°C) in certain environment conditions. During the measurement, registered were (LANCOM, AVL) the contents of carbon oxides (CO), hydrocarbons (HC), nitro oxides (NO_x) in fumes, motor oil temperature, rotational speed of the crankshaft, environment temperature, and fumes smoking.

Considering the aim of the work, stationary researches were performed in the conditions of cold and hot start-up of the engine for the recognized seven states:

1. apt engine (with regulation settings suggested by the manufacturer),
2. values of the advance angle of fuel injection of 10°OWK (delayed injection – nominal advance angle of fuel injection advance has 18,5°OWK),
3. values of the advance angle of fuel injection of 24°OWK (advance injection),
4. for the pressure of injection processes beginning in cylinders: first 20MPa, fifth 18MPa and third 16MPa (nominal injection pressure – 22MPa),
5. for the pressure of injection processes beginning In cylinders: sixth 23MPa, second 24MPa and fourth 25MPa (in the other cylinders nominal injection pressure – 22MPa),
6. for inlet valves clearings in cylinders: first, fifth and third 0.15mm each,

7. for inlet valves clearings in cylinders: first, fifth and third 0,45mm each (nominal inlet valves clearing – 0.3mm).

The tests were performer for two variants of the engine's thermal states: cold and hot start-up on environment temperatures of 5°C, 10°C and 20°C. During the tests constant registration of fumes emissions during work in neutral wear from the moment of starting for the first 6 minutes of the engine's work.

5. Stationary tests results

The measurements of emissions of fumes toxic components and smoking of the engine with self-acting fuse S-359 in the laboratory were realized for specified states, at slow rotations of the crankshaft for three environment temperatures (5°C, 10°C, 20°C), with cold and hot start-up.

The results of stationary tests in the range of estimating toxic components emissions (*NOx, CO, HC*) o fan apt engine for cold and hot start-up at environment temperatures: 5, 10 and 20°C. The coefficient of fumes smoking (*k*) for the examined conditions is given of Fig. 3.

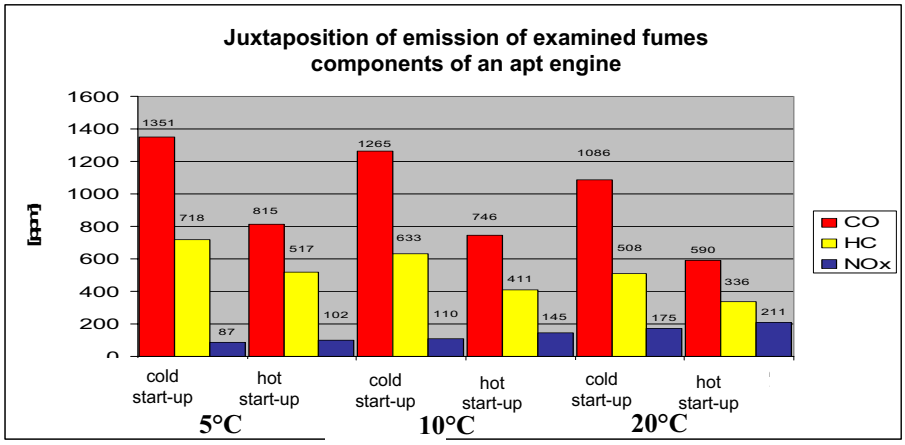

Fig. 3. Juxtaposition of emission of examined fumes components of an apt engine

Research results of smoking of an apt engine in a cold and hot start-up are presented the Fig. 4.

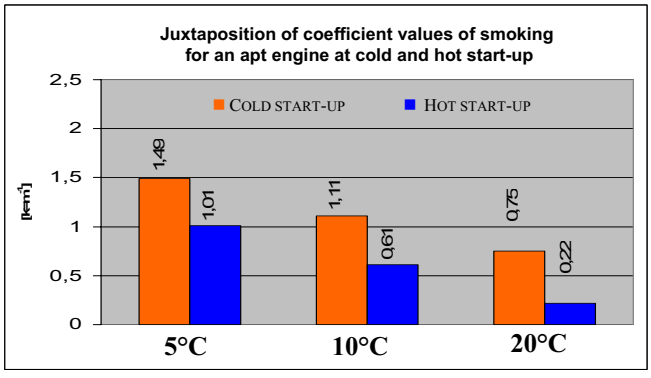

Fig. 4. Juxtaposition of coefficient values of smoking for an apt engine at cold and hot start-up

The volume of separate components of fumes and smoking for the start-up of a cold and hot engine, with a specified angle of injection advance 10°OWK was shown in the Fig. 5.

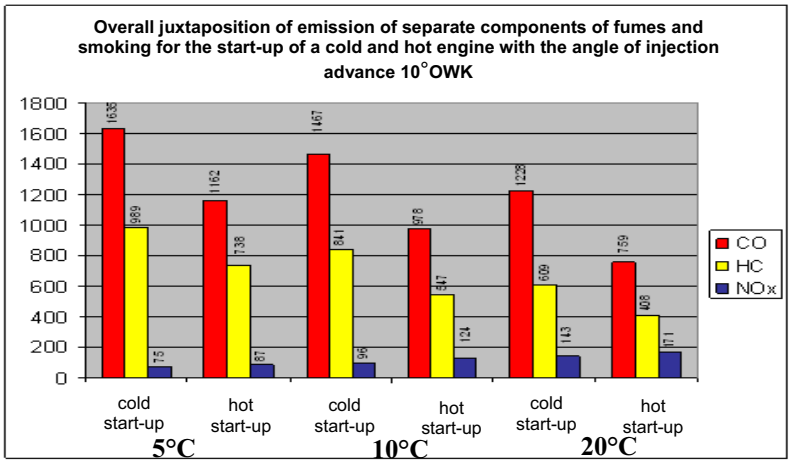

Fig.5. Overall juxtaposition of emission of separate components of fumes and smoking for the start-up of a cold and hot engine with the angle of injection advance 10°OWK

In the Fig. 6 shown below, research results of smoking of the engine for the start-up of a cold and hot engine with the angle of injection advance 10°OWK are shown.

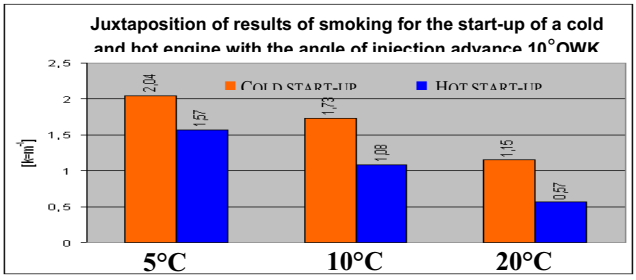

Fig.6. Juxtaposition of results of smoking for the start-up of a cold and hot engine with the angle of injection advance 10°OWK

Quantity comparison of the emission of toxic components: CO, HC, NOx and smoking, during cold and hot start-up of the engine for the angle of injection advance 24^{O}OWK – accelerated (nominal $18{,}5^{O}$OWK) is presented in the Fig.7.

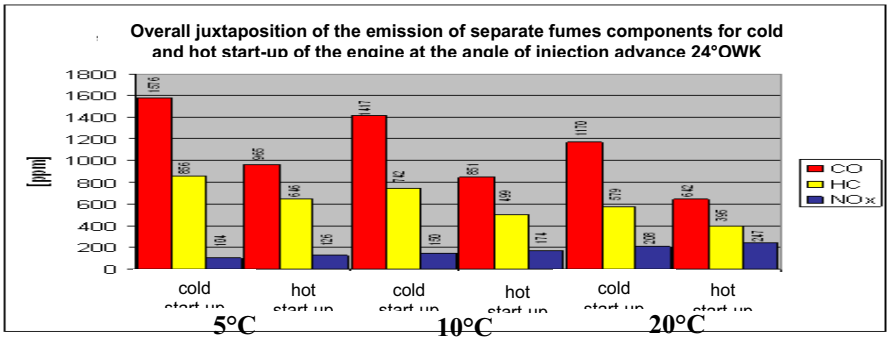

Fig.7. Overall juxtaposition of the emission of separate fumes components for cold and hot start-up of the engine at the angle of injection advance 24°OWK

Next Fig. 8 presents research results of smoking of the engine for cold and hot start-up At different environment temperatures (5°, 10°, 20°C), at the angle of injection advance of 24°OWK.

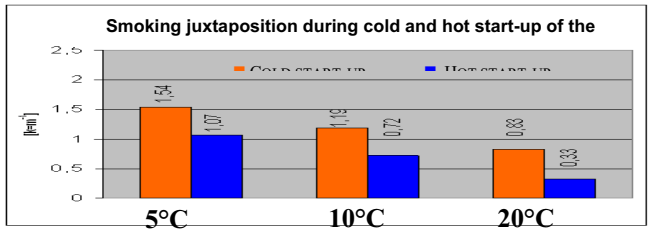

Fig.8. Smoking juxtaposition during cold and hot start-up of the engine for the angle of injection advance 24°OWK

The volume of the emission of separate fume components at the start-up of a cold and hot engine for the injection pressure of 20MPa, 18MPa, 16MPa in cylinders 1, 5, 3, with sustaining nominal values of pressure (nominal 22MPa) in the other cylinders, is shown in the Fig. 9.

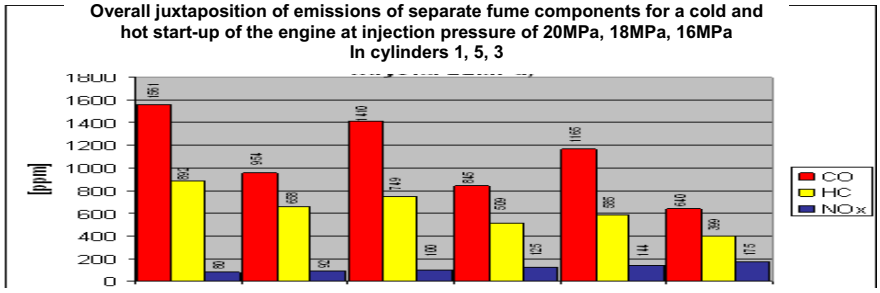

Fig. 9. Overall juxtaposition of emissions of separate fume components for a cold and hot start-up of the engine at injection pressure of 20MPa, 18MPa, 16MPa In cylinders 1, 5, 3

Overall juxtaposition of results of smoking tests of the engine at cold and hot start-up at different temperatures of the environment for modeled injection pressures in cylinders 1, 3, 5 is shown in the Fig. 10.

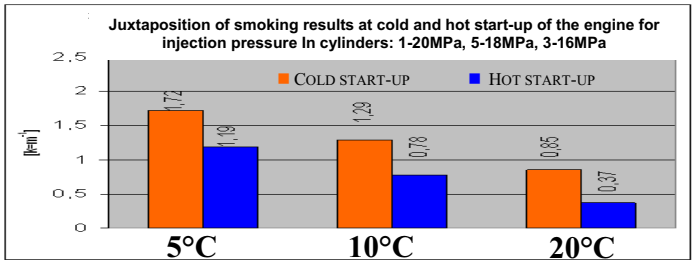

Fig. 10. Juxtaposition of smoking results at cold and hot start-up of the engine for injection pressure in cylinders: 1-20MPa, 5-18MPa, 3-16MPa

The contents of separate fume components and smoking at the start-up of a cold and hot engine at injection pressure of 23MPa, 24MPa, 25MPa in cylinders 6, 2, 4 (in the other cylinders nominal 22MPa) is shown in the Fig. 11.

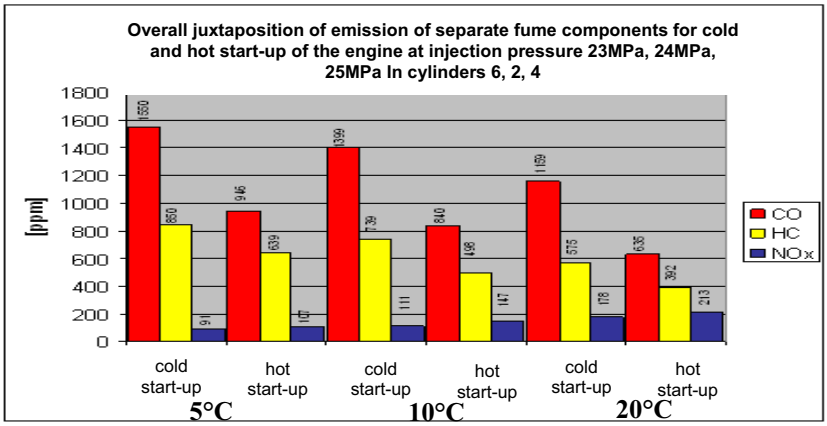

Fig. 11. Overall juxtaposition of emission of separate fume components for cold and hot start-up of the engine at injection pressure 23MPa, 24MPa, 25MPa In cylinders 6, 2, 4

The values of fume smoking at cold and hot start-up of the engine for modeled injection pressures in cylinders: 6, 2, 4 at different temperatures of the environment, is shown in the Fig. 12.

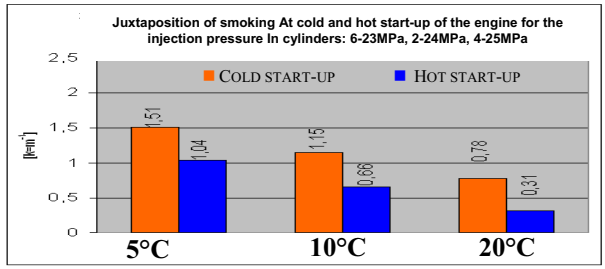

Fig. 12. Juxtaposition of smoking At cold and hot start-up of the engine for the injection pressure In cylinders: 6-23MPa, 2-24MPa, 4-25MPa

The contents of emissions of separate fume components and smoking at the start-up of a cold and hot engine for clearing of inlet valves of 0.15mm in cylinders 1, 5, 3 (nominal clearing 0.3mm) at different temperatures of the environment, is shown in the Fig. 13.

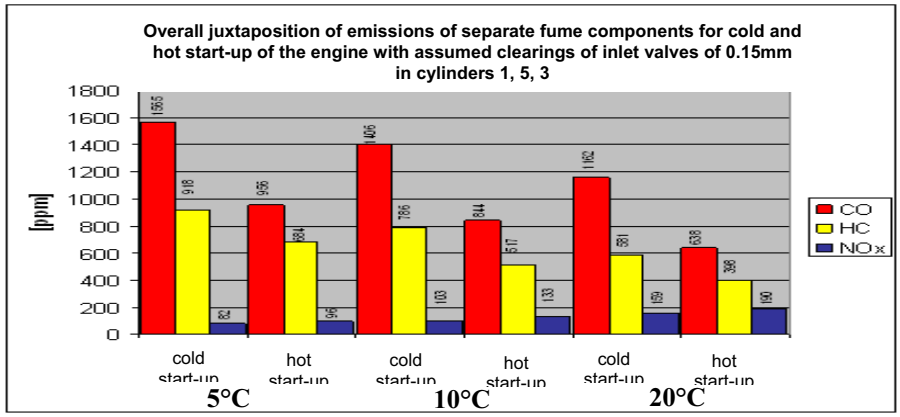

Fig. 13. Overall juxtaposition of emissions of separate fume components for cold and hot start-up of the engine with assumed clearings of inlet valves of 0.15mm in cylinders 1, 5, 3

The values of fume smoking at cold and hot start-up of the engine for modeled valve clearings in cylinders: 1, 5, 3 at different environment temperatures is shown in the Fig. 14.

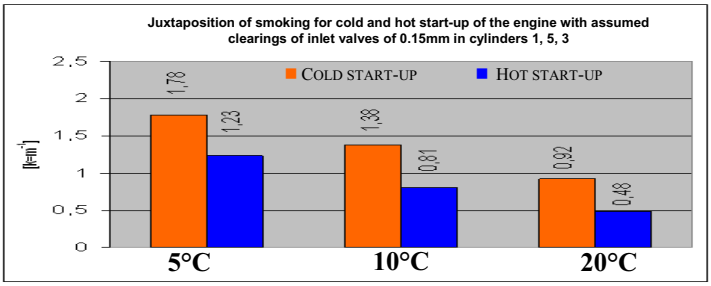

Fig.14. Juxtaposition of smoking for cold and hot start-up of the engine with assumed clearings of inlet valves of 0.15mm in cylinders 1, 5, 3

The contents of emissions of separate fume components and smoking at the start-up of a cold and hot engine for clearing of inlet valves 0.45mm in cylinders 1, 5, 3 (nominal clearing 0.3mm) at different environment temperatures is shown in the Fig. 15.

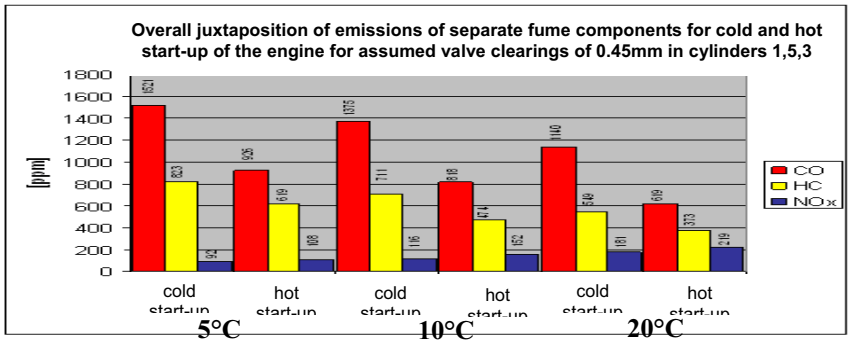

Fig. 15. Overall juxtaposition of emissions of separate fume components for cold and hot start-up of the engine for assumed valve clearings of 0.45mm in cylinders 1,5,3

The results of engine smoking tests at cold and hot start-up for different environment temperatures with modeled values of valve clearings is show in the Fig. 16.

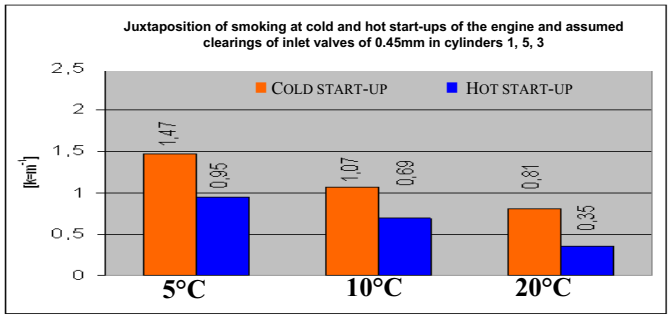

Fig. 16. Juxtaposition of smoking at cold and hot start-ups of the engine and assumed clearings of inlet valves of 0.45mm in cylinders 1, 5, 3

From the examined maladjustments, the highest influence on the increase of emissions of toxic fume components compared to an apt engine has the delayed angle of injection advance $\alpha_{ww} = 10^0 C$ before ZZ (nominal $\alpha_{ww} = 18{,}5^0 C$ before ZZ).

The second, deciding on the number of the volume of emitted toxic substances in fumes, is a maladjustment consisting in the acceleration of the injection advance angle ($\alpha_{ww} = 24^0 C$ before ZZ). More toxic compounds in fumes are emitted at a delayed angle of injection advance ($\alpha_{ww} = 10^0 C$ before ZZ) regardless the kind of the engine start-up and environment temperature.

Another maladjustment considerably affecting the volume of emitted toxic fume components is the decrease of clearing of 3 inlet valves from 0.3mm to 0.15mm. The analysis of separate periods of the engine's work showed that a considerable role for a cold and hot start-up of the engine is played by the first 60-70 seconds of work, in which maximum quantities of CO, HC, NO_x and smoking are emitted.

6. Summary

The presented results were submitted to statistical analysis, where the methods OPTIMUM and SVD were used, as well as correlation and regression methods. It gave the possibility of quality and quantity comparison of results of fumes contents from stationary tests and exploitation researches. The results of this research allow a model (mathematical relations) determination of relations between smoking and the quantity of toxic fume components of a high-pressure engine.

The performed tests and analyses in his work's researches indicate to the conclusions:

1. In the engine of self-acting fuse (ZS), the emission of carbon oxide (CO), hydrocarbons (HC) and smoking are considerable, especially during start-up and engine warming.
2. Along with the decrease of environment temperature, the emission of CO, HC and smoking increase, whilst the quantity of NOx goes down providing premises confirming the specified regulations of forming dangers on the side of engine fumes emission.
3. The phases of start-up and warming up of the ZS engine are characterized by increased fuel usage and increased emission of carbon oxide – CO, giving information and sensitizing vehicle users to these harmful for the engine working conditions.
4. The influence of environment temperature on the emission and smoking of fumes during hot start-ups is weaker than during cold start-ups.

References

[1] Kwiatkowski K., Żółtowski B.: *Manners of regeneration of solid particles filters* (in Polish). Materiały Konferencji Regeneracja. Bydgoszcz 2002.

[2] Kwiatkowski K., Żółtowski B.: *Ecological aspects of high-pressure engines affecting* (in Polish). Diagnostyka, vol.26, 2002.

[3] Kwiatkowski K., Żółtowski B.: *Combustion engines – environmental menace*. Teka Komisji Motoryzacji i Energetyki Rolnictwa, PAN, tom III, Lublin 2003.

[4] Kwiatkowski K., Żółtowski B.: *Combustion engines as the source of harmful fumes components* (in Polish). Diagnostyka, vol. 32, 2004.

[5] Kwiatkowski K., Żółtowski B.: *Measurements of fumes composition of combustion engines* (in Polish). Akademia Morska w Szczecinie, ZN nr 5(77), 2005.

[6] Merkisz J.: *Ecological problem of combustion engines*. Vol. 1 (in Polish). PP, Poznań 1999.

[7] Żółtowski B.: *High-pressure engine diagnosis* (in Polish). ITE, Radom 1995 (s.171).

[8] Żółtowski B., Cempel C. (red.): *Machine diagnostics engineering* (in Polish). ITE Radom, 2004 (s.1109).